APPENDIX F
AIR QUALITY CALCULATIONS

(This page intentionally left blank)

TAB A. EMISSIONS SUMMARY

Table 1. Construction for Proposed Action: Institutional Support Projects

YEAR	Area	VOC T/yr	CO T/yr	NOx T/yr	SO2 T/yr	PM10 T/yr	PM2.5 T/yr	CO2e MT/yr
TBD	Main Base Construction	1.01	4.85	14.62	0.20	14.54	2.14	1,291
	Mainland and Island	0.12	0.54	1.60	0.02	6.70	0.74	140
	TBD Construction Total	**1.13**	**5.39**	**16.22**	**0.22**	**21.24**	**2.88**	**1,431**
TBD	Main Base Demo	0.11	0.73	1.28	0.03	13.34	1.43	157
	Mainland and Island	0.01	0.10	0.15	0.00	0.27	0.04	19
	TBD Demo Total	**0.12**	**0.83**	**1.42**	**0.03**	**13.61**	**1.47**	**176**
2019	Main Base	0.02	0.13	0.21	0.00	0.12	0.03	25
	Mainland and Island	0.47	2.92	11.30	1.73	0.37	0.35	2,518
	2019 Total	**0.49**	**3.05**	**11.50**	**1.73**	**0.49**	**0.38**	**2543**
2020	Main Base	0.07	0.37	1.05	0.02	0.11	0.06	94
	Mainland and Island	0.48	3.03	11.48	1.73	0.88	0.42	2,540
	2020 Total	**0.56**	**3.39**	**12.53**	**1.75**	**0.99**	**0.48**	**2,634**
2021	Mainland and Island	0.47	2.91	11.28	1.73	0.36	0.35	2,515
2022	Main Base	0.01	0.09	0.13	0.00	0.98	0.11	17
	Mainland and Island	0.47	2.91	11.28	1.73	0.36	0.35	2,515
	2022 Total	**0.48**	**2.99**	**11.41**	**1.73**	**1.34**	**0.46**	**2,532**
2023	Mainland and Island	**0.78**	**5.15**	**21.04**	**2.14**	**0.72**	**0.69**	**3,148**

Table 2. Potential Annual Operations for Proposed Action

Year	Activity	VOC T/yr	CO T/yr	NOx T/yr	SO_2 T/yr	PM_{10} T/yr	$PM_{2.5}$ T/yr	CO2e MT/yr
2019-2025	3-MW Generators	1.43	12.50	2.39	ND	0.36	0.36	2,350
2019-2025	new launch envelope	0.00	68.13	7.20	ND	152.19	152.19	5,253
2019-2025	Annual UAS Operations	0.35	2.20	2.37	0.19	0.09	0.09	101.25
	2019 – 2025 Annual Total	**1.78**	**82.83**	**11.96**	**0.19**	**152.64**	**152.64**	**7,704**

Table 3. Comparison of Current Envelope Launch Vehicle (Antares + LMLV-3) Emissions to Proposed Envelope Launch Vehicle (LSLB + Falcon 9) Emissions

Launch Vehicle	CO T/yr	NOx T/yr	(PM) T/yr	HCL T/yr	CO2 MT/yr
current envelope	184.1	0.0	153.6	125	646
new envelope	68.1	7.2	154.6	107.0	5,253
Change:	**-116.0**	**7.2**	**1.0**	**-18.1**	**4,607**

Table 4. Comparison of Total Operational Emissions for UAS and Launch Vehicles

UAV + Launch Operations	CO T/yr	NOx T/yr	CO2 MT/yr
current envelopes	184.3	0.4	655
new envelopes	70.3	9.6	5,354
Change:	**-114.0**	**9.2**	**4,699**

TAB B. CONSTRUCTION EMISSIONS - PROPOSED ACTION INSTITUTIONAL SUPPORT PROJECTS

Basic Conversions

453.59	grams per pound
43,560	Conversion from Acre to SF
0.03704	Cubic feet to Cubic Yards
0.1111	Square Feet to Square Yards
1.4	tons/CY for Gravel
80,000	lbs/Truck Load for Delivery
1.66	CY for each CY of asphalt/concrete demo
0.50	asphalt thickness for demolition
0.50	asphalt thickness for pavement
2000	pounds per ton
145	lb/ft^3 density of Hot Mix Asphalt
0.67	asphalt thickness for pavement on runways

TBD CONSTRUCTION

Table 1. Clearing - TBD

2.0 Acres

Vehicle Trips = 11

				Emission Factors						
				VOC	**CO**	**NOx**	**SO_2**	**PM_{10}**	**$PM_{2.5}$**	**CO_2**
Off-road Equipment	**Cumulative Hours of Operation**	**Engine HP**	**Load Factor**	g/hp-hr	g/hp-hr	g/hp-hr	g/hp-hr	g/hp-hr	g/hp-hr	g/hp-hr
Dozer	24	145	0.58	0.38	1.41	4.17	0.12	0.30	0.29	535.69
Loader w/ integral Backhoe	24	87	0.21	1.43	7.35	6.35	0.15	1.06	1.03	691.66
Small backhoe	24	55	0.21	1.43	7.35	6.35	0.15	1.06	1.03	691.66
				VOC	**CO**	**NOx**	**SO_2**	**PM_{10}**	**$PM_{2.5}$**	**CO_2**
On-road Equipment	**Cumulative Hours of Operation**	**Engine HP**	**Productivity based Speed (miles/hour)**	lb/mile	lb/mile	lb/mile	lb/mile	lb/mile	lb/mile	lb/mile
Dump Truck	11	230	16	0.00166	0.00858	0.03922	0.00002	0.00169	0.00164	3.38

	Annual Emissions						
	VOC	**CO**	**NOx**	**SO_2**	**PM_{10}**	**$PM_{2.5}$**	**CO_2**
	lb	lb	lb	lb	lb	lb	lb
	1.64	6.17	18.20	0.50	1.29	1.25	2,336
	1.36	6.96	6.01	0.14	1.01	0.98	655
	0.86	4.40	3.80	0.09	0.64	0.62	414
	VOC	**CO**	**NOx**	**SO_2**	**PM_{10}**	**$PM_{2.5}$**	**CO_2**
	lb	lb	lb	lb	lb	lb	lb
	0.30	1.54	7.02	0.00	0.30	0.29	605
Subtotal (lbs):	**4**	**19**	**35**	**1**	**3**	**3**	**4,011**
Clearing Grand Total in Tons	**0.00**	**0.01**	**0.02**	**0.00**	**0.00**	**0.00**	
Clearing Grand Total in Metric Tons							**2**

Vehicle Trips = 11

Table 2. Site Work - TBD

Site Prep - Excavate/Fill (CY)	50,858 CY		
Trenching (LF)	2,500 LF	Assume 3' deep,1 ' wide	
Grading (SY)	26,944 SY	Assume compact 0.5 feet (0.166 yards)	4,473 CY compacted

Off-road Equipment	Hours	Engine HP	Load Factor	VOC g/hp-hr	CO g/hp-hr	NOx g/hp-hr	SO_2 g/hp-hr	PM10 g/hp-hr	PM2.5 g/hp-hr	CO_2 g/hp-hr
Excavator	170	243	0.59	0.34	1.21	4.03	0.12	0.22	0.22	536
Skid Steer Loader	203	160	0.23	0.38	1.47	4.34	0.12	0.31	0.30	536
Dozer (Rubber Tired)	184	145	0.59	0.38	1.41	4.17	0.12	0.30	0.29	536
Compactor	21	103	0.58	0.40	1.57	4.57	0.12	0.32	0.31	536
Grader	10	285	0.58	0.34	1.21	4.07	0.12	0.23	0.22	536
Backhoe/Loader	4	87	0.59	0.35	1.25	4.23	0.12	0.24	0.23	536

	VOC lb	CO lb	NOx lb	SO2 lb	PM lb	PM2.5 lb	CO_2 lb
Excavator	18.43	64.80	215.92	6.18	11.94	11.58	28,709.57
Skid Steer Loader	6.33	24.26	71.60	1.90	5.04	4.89	8,840.99
Dozer (Rubber Tired)	13.09	49.15	145.05	4.00	10.29	9.98	18,617.45
Compactor	1.08	4.28	12.45	0.31	0.87	0.84	1,460.81
Grader	1.20	4.21	14.19	0.40	0.79	0.76	1,868.27
Backhoe/loader	0.16	0.57	1.92	0.05	0.11	0.10	242.52

On-road Equipment	Hours	MPH	Engine HP	VOC lb/mile	CO lb/mile	NOx lb/mile	SO_2 lb/mile	PM10 lb/mile	PM2.5 lb/mile	CO_2 lb/mile
Dump Truck	170	5	230	0.0015	0.0080	0.0361	0.0000	0.0015	0.0015	3.4385

	VOC lb	CO lb	NOx lb	SO2 lb	PM lb	PM2.5 lb	CO_2 lb
Dump Truck	1.29	6.82	30.57	0.02	1.28	1.24	2,915
Subtotal in lb:	**42**	**154**	**492**	**13**	**30**	**29**	**62,654**
Site Prep Grand Total in Tons	**0.02**	**0.08**	**0.25**	**0.01**	**0.02**	**0.01**	
Site Prep Grand Total in Metric Tons							**28**

Vehicle Trips = 92

Table 3. RBR Demo - TBD

71,040 SF — 3,552 Estimated CY of debris based on 20 SF/CY

Off-road Equipment	Hours of Operation	Engine HP	Load Factor	Emission Factors: VOC g/hp-hr	CO g/hp-hr	NOx g/hp-hr	SO_2 g/hp-hr	PM_{10} g/hp-hr	$PM_{2.5}$ g/hp-hr	CO_2 g/hp-hr
Hydraulic excavator	592	86	0.59	0.23	2.57	2.68	0.11	0.40	0.39	595.46
Wheel Loader w/ integral Backhoe	592	87	0.23	1.07	6.13	5.02	0.14	0.95	0.92	692.77
Wheel mounted air compressor	592	49	0.59	0.26	1.41	3.51	0.11	0.23	0.22	536.20

	Annual Emissions: VOC lb	CO lb	NOx lb	SO_2 lb	PM_{10} lb	$PM_{2.5}$ lb	CO_2 lb
Hydraulic excavator	15.16	170.21	177.51	7.53	26.69	25.88	39,433.37
Wheel Loader w/ integral Backhoe	27.86	160.03	131.14	3.69	24.78	24.04	18,092.25
Wheel mounted air compressor	9.90	53.16	132.37	4.07	8.75	8.49	20,231.58
Subtotal (lbs):	52.93	383.40	441.02	15.29	60.21	58.41	77757.20

On-road Equipment	Hours of Operation	Engine HP	Speed (mph)	VOC lb/mile	CO lb/mile	NOx lb/mile	SO_2 lb/mile	PM_{10} lb/mile	$PM_{2.5}$ lb/mile	CO_2 lb/mile
Dump Truck (12 CY Capacity)	326	230	27	0.001521	0.008042	0.036070	1.80E-05	0.001504	0.001458	3.438541

	VOC lb	CO lb	NOx lb	SO_2 lb	PM_{10} lb	$PM_{2.5}$ lb	CO_2 lb
Dump Truck (12 CY Capacity)	13.39	70.79	317.49	0.16	13.24	12.83	30,266
Subtotal (lbs):	66.32	454.19	758.51	15.45	73.46	71.24	108,023.23
Building Demo Grand Total in Tons	**0.033**	**0.227**	**0.379**	**0.008**	**0.037**	**0.036**	
Building Demo Grand Total in Metric Tons							**49.00**

Vehicle Trips = 278

Table 4. Demo Asphalt Concrete RBR - TBD

72,604 SF   2,232 CY

Off-road Equipment	Hours of Operation	Engine HP	Load Factor	VOC g/hp-hr	CO g/hp-hr	NOx g/hp-hr	SO_2 g/hp-hr	PM_{10} g/hp-hr	$PM_{2.5}$ g/hp-hr	CO_2 g/hp-hr
				Emission Factors						
Crawler Dozer w/attachments	263	125	0.58	0.34	1.21	4.08	0.12	0.23	0.22	535.79
Air Compressor	263	49	0.59	0.33	2.54	4.53	0.13	0.54	0.53	595.16
Excavator	61	380	0.59	0.31	2.50	4.51	0.13	0.55	0.54	595.21
				Annual Emissions						
				VOC lb	CO lb	NOx lb	SO_2 lb	PM_{10} lb	$PM_{2.5}$ lb	CO_2 lb
Crawler Dozer w/attachments				14.48	50.84	171.82	4.85	9.52	9.23	22562.78
Wheel mounted air compressor				5.50	42.68	76.02	2.15	9.10	8.83	9994.14
Excavator				9.34	74.67	134.78	3.83	16.51	16.01	17800.11

On-road Equipment	Hours of Operation	Engine HP	Speed (mph)	VOC lb/mile	CO lb/mile	NOx lb/mile	SO_2 lb/mile	PM_{10} lb/mile	$PM_{2.5}$ lb/mile	CO_2 lb/mile
Dump Truck	205	230	27	0.0015	0.0080	0.0361	0.0000	0.0015	0.0015	3.4385
				VOC lb	CO lb	NOx lb	SO_2 lb	PM_{10} lb	$PM_{2.5}$ lb	CO_2 lb
Dump Truck				8.42	44.51	199.65	0.10	8.33	8.07	19,032
Subtotal (lbs):				**38**	**213**	**582**	**11**	**43**	**42**	**69,389**
Asphalt Demo Grand Total in Tons				**0.02**	**0.11**	**0.29**	**0.01**	**0.02**	**0.02**	
Asphalt Demo Grand Total in Metric Tons										**31**

Vehicle Trips = 92

Table 5. Building Construction

120,000 SF Foundation
120,000 SF Total

Off-road Equipment	Hours of Operation	Engine HP	Load Factor	VOC g/hp-hr	CO g/hp-hr	NOx g/hp-hr	SO_2 g/hp-hr	PM10 g/hp-hr	PM2.5 g/hp-hr	CO_2 g/hp-hr
				Emission Factors						
Crane	600	330	0.58	0.25	1.22	5.26	0.11	0.21	0.20	530
Concrete Truck	600	300	0.43	0.19	1.45	4.32	0.12	0.21	0.20	536
Diesel Generator	480	40	0.43	0.26	1.41	3.51	0.11	0.23	0.22	536
Telehandler	1,200	99	0.59	0.51	3.94	4.93	0.13	0.52	0.51	595
Scissors Lift	960	83	0.59	0.51	3.94	4.93	0.13	0.52	0.51	595
Skid Steer Loader	600	67	0.59	1.69	7.97	6.70	0.15	1.19	1.15	691
Pile Driver	6,188	260	0.43	0.46	1.55	5.90	0.11	0.31	0.30	530
All Terrain Forklift	24	84	0.59	0.51	3.94	4.93	0.13	0.52	0.51	595
				Annual Emissions						
				VOC lb	CO lb	NOx lb	SO2 lb	PM lb	PM2.5 lb	CO_2 lb
Crane				62.21	308.75	1331.67	28.88	52.59	51.01	134,261
Concrete Truck				32.01	248.20	737.28	19.68	35.85	34.77	91,507
Diesel Generator				4.78	25.64	63.85	1.96	4.22	4.09	9,760
Telehandler				78.74	608.80	761.66	19.76	80.53	78.11	91,884
Scissors Lift				52.81	408.32	510.85	13.26	54.01	52.39	61,627
Skid Steer Loader				88.49	416.63	350.23	7.77	62.18	60.31	36,125
Pile Driver				707.73	2366.77	9001.43	173.76	478.69	464.33	807,780
All Terrain Forklift				1.34	10.33	12.93	0.34	1.37	1.33	1,559

On-road Equipment	Hours of Operation	Engine HP	Speed (mph)	VOC lb/mile	CO lb/mile	NOx lb/mile	SO2 lb/mile	PM lb/mile	PM2.5 lb/mile	CO_2 lb/mile
Delivery Truck	2,880	265	45	0.0015	0.0080	0.0361	0.0000	0.0015	0.0015	3.4385
				VOC lb	CO lb	NOx lb	SO2 lb	PM lb	PM2.5 lb	CO_2 lb
Delivery Truck				197.16	1042.24	4674.68	2.34	194.98	188.93	445,635
Subtotal (lbs):				**1225**	**5436**	**17445**	**268**	**964**	**935**	**1680139**
Building Construction Grand Total in Tons				**0.61**	**2.72**	**8.72**	**0.13**	**0.48**	**0.47**	
Building Construction Grand Total in Metric Tons										**762**

Vehicle Trips = 1664

Table 6. Gravel Work - TBD

23,389 CY — 1,671 trips — 147,017 total miles

Off-road Equipment	Hours	Engine HP	Load Factor	VOC g/hp-hr	CO g/hp-hr	NOx g/hp-hr	SO_2 g/hp-hr	PM_{10} g/hp-hr	$PM_{2.5}$ g/hp-hr	CO_2 g/hp-hr
Dozer	234	185	0.59	0.34	1.21	4.08	0.12	0.23	0.22	536
Wheel Loader for Spreading	292	87	0.59	0.35	1.25	4.23	0.12	0.24	0.23	536
Compactor	645	103	0.43	0.36	1.34	4.45	0.12	0.26	0.25	536
				VOC lb	CO lb	NOx lb	SO2 lb	PM10 lb	PM2.5 lb	CO_2 lb
Dozer				19.35	67.95	229.64	6.49	12.72	12.34	30155.48
Wheel Loader for Spreading				11.54	41.30	140.06	3.81	7.90	7.66	17726.03
Compactor				22.65	84.32	280.39	7.26	16.19	15.71	33743.76

On-road Equipment	Miles	Engine HP	VOC lb/mile	CO lb/mile	NOx lb/mile	SO_2 lb/mile	PM_{10} lb/mile	$PM_{2.5}$ lb/mile	CO_2 lb/mile
Dump Truck	147,017	230	0.0015	0.0080	0.0361	0.0000	0.0015	0.0015	3.4385
			VOC lb	CO lb	NOx lb	SO2 lb	PM10 lb	PM2.5 lb	CO_2 lb
Dump Truck			223.66	1182.30	5302.90	2.65	221.18	214.31	505,523
Subtotal (lbs):			**277**	**1,376**	**5,953**	**20**	**258**	**250**	**587,148**
Gravel Work Grand Total in Tons			**0.14**	**0.69**	**2.98**	**0.01**	**0.13**	**0.13**	
Gravel Work Grand Total in Metric Tons									**266**

Vehicle Trips = 183

Table 7. Concrete Work - TBD

Foundation Work 17,778 CY
Sidewalks, etc. 74 CY
Total 17,852 CY

Note: Assume all excavated soil is accounted for in Excavate/Fill and Trenching

Off-road Equipment	Hours of Operation	Engine HP	Load Factor	Emission Factors VOC g/hp-hr	CO g/hp-hr	NOx g/hp-hr	SO_2 g/hp-hr	PM10 g/hp-hr	PM2.5 g/hp-hr	CO_2 g/hp-hr
Concrete Mixer	940	3.5	0.43	0.69	3.04	6.17	0.13	0.54	0.52	588
Concrete Truck	850	300	0.43	0.38	1.75	6.18	0.11	0.27	0.26	530
				Annual Emissions						
				VOC lb	CO lb	NOx lb	SO2 lb	PM lb	PM2.5 lb	CO_2 lb
Concrete Mixer				2.14	9.49	19.25	0.39	1.69	1.64	1,834.95
Concrete Truck				91.77	422.06	1,494.69	27.56	64.96	63.01	128,109.75
Subtotal (lbs):				**94**	**432**	**1,514**	**28**	**67**	**65**	**129,945**
Concrete Work Grand Total in Tons				**0.05**	**0.22**	**0.76**	**0.01**	**0.03**	**0.03**	
Concrete Work Grand Total in Metric Tons										**59**

Vehicle Trips = 280

Table 8. Paving - TBD

Pavement - Surface Area 12,000 SF — 222 CY
Paving - HMA 4,000 CF

Off-road Equipment	Hours of Operation	Engine HP	Load Factor	VOC g/hp-hr	CO g/hp-hr	NOx g/hp-hr	SO2 g/hp-hr	PM g/hp-hr	PM2.5 g/hp-hr	CO_2 g/hp-hr
Grader	37	145	0.59	0.38	1.41	4.16	0.12	0.30	0.29	536
Roller	55	401	0.59	0.34	2.46	5.53	0.12	0.34	0.33	536
Paving Machine	74	164	0.59	0.38	1.44	4.25	0.12	0.30	0.29	536
Asphalt Curbing Machine	7	130	0.59	0.40	1.57	4.57	0.12	0.32	0.31	536
				VOC lb	CO lb	NOx lb	SO2 lb	PM lb	PM2.5 lb	CO_2 lb
Grader				2.61	9.79	28.84	0.80	2.05	1.99	3,713.03
Roller				9.81	70.81	159.14	3.31	9.74	9.45	15,405.71
Paving Machine				5.96	22.62	66.67	1.81	4.70	4.56	8,398.95
Asphalt Curbing Machine				0.49	1.95	5.67	0.14	0.40	0.38	665.71

On-road Equipment	Hours of Operation	Engine HP	Productivity based Speed (miles/hour)	VOC lb/mile	CO lb/mile	NOx lb/mile	SO2 lb/mile	PM lb/mile	PM2.5 lb/mile	CO_2 lb/mile
Dump Truck	44	230	17	0.001521	0.008042	0.036070	1.80E-05	0.001504	0.001458	3.438541
Water Truck	1	230	10	0.001521	0.008042	0.036070	1.80E-05	0.001504	0.001458	3.438541
				VOC lb	**CO** lb	**NOx** lb	**SO2** lb	**PM** lb	**PM2.5** lb	**CO_2** lb
			Dump Truck	1.15	6.06	27.19	0.01	1.13	1.10	2,592
			Water Truck	0.02	0.09	0.42	0.00	0.02	0.02	40

Hot Mix Asphalt (HMA)	Volume of HMA (ft^3)	Weight of HMA (tons)	VOC lb/ton of asphalt	VOC lb	CO lb	NOx lb	SO2 lb	PM10 lb	PM2.5 lb	CO_2 lb
Standard Hot Mix Asphalt	4,000	0	0.04	0.00	-	-	-	-	-	-
			Subtotal (lbs):	**20**	**111**	**288**	**6**	**18**	**17**	**30,815**
			Paving Grand Total in Tons	**0.01**	**0.06**	**0.14**	**0.00**	**0.01**	**0.01**	
			Paving Grand Total in Metric Tons							**14**

Vehicle Trips = 7

Table 9. Runway Construction

Concrete Surface	187,500 SF	4.3	acres
	20,831 SY	1.83	yards thick

[1]Off-road Equipment	[2]Cumulative Hours of Operation	[3]Engine HP	[4]Load Factor	[6,7]Emission Factors VOC g/hp-hr	CO g/hp-hr	NOx g/hp-hr	SO_2 g/hp-hr	PM10 g/hp-hr	PM2.5 g/hp-hr	CO_2 g/hp-hr
Grader (CAT 120M2 or similar)	29	150	0.61	1.06	3.52	8.24	0.06	0.47	0.47	568
Steel drum roller/soil compactor	290	401	0.56	0.70	3.18	7.20	0.05	0.28	0.28	568
Paving/Concrete Machine	290	164	0.53	1.14	3.71	8.87	0.49	0.49	0.49	568
Curbing Machine	14	130	0.59	1.14	3.71	8.87	0.49	0.49	0.49	568
Cement and Motar Mixer 1	290	9	0.56	0.92	2.64	5.41	0.07	0.35	0.35	568
Cement and Motar Mixer 2	290	9	0.56	0.92	2.64	5.41	0.07	0.35	0.35	568
Cement and Motar Mixer 3	290	9	0.56	0.92	2.64	5.41	0.07	0.35	0.35	568
Tractor/Loader/Backhoe	290	75	0.55	1.50	4.22	8.33	0.06	0.80	0.80	568
[1]On-road Equipment	**[2]Cumulative Hours of Operation**	**[3]Engine HP**	**[5]Speed (miles/hour)**	**VOC** lb/mile	**CO** lb/mile	**NOx** lb/mile	**SO2** lb/mile	**PM10** lb/mile	**PM2.5** lb/mile	**CO2** lb/mile
Cement Truck	290	230	20	0.001521	0.008042	0.036070	1.80E-05	0.001504	0.001458	3.438541
Water Truck/Oil truck	29	230	10	0.001521	0.008042	0.036070	1.80E-05	0.001504	0.001458	3.438541

	Annual Emissions VOC lb	CO lb	NOx lb	SO2 lb	PM lb	PM2.5 lb	CO_2 lb
	6.21	20.58	48.15	0.33	2.74	2.74	3,321.35
	99.97	456.55	1,032.14	7.17	40.45	40.45	81,512.80
	63.01	205.70	492.61	27.43	27.43	27.43	31,551.00
	2.78	9.08	21.73	1.21	1.21	1.21	1,392.06
	2.96	8.51	17.42	0.21	1.12	1.12	1,829.46
	2.96	8.51	17.42	0.21	1.12	1.12	1,829.46
	2.96	8.51	17.42	0.21	1.12	1.12	1,829.46
	39.50	111.19	219.34	1.58	21.13	21.13	14,973.30
	VOC lb	**CO** lb	**NOx** lb	**SO2** lb	**PM** lb	**PM2.5** lb	**CO_2** lb
	8.82	46.60	209.01	0.10	8.72	8.45	19,924
	0.44	2.33	10.45	0.01	0.44	0.42	996
Runway Construction Grand Total in Tons	**0.11**	**0.44**	**1.04**	**0.02**	**0.05**	**0.05**	
Runway Construction Grand Total in Metric Tons							**72**

Vehicle Trips = 278

TBD - DEMO

Table 10. Demo Site Work - TBD

Site Prep - Excavate/Fill (CY)	33,692	CY
Trenching (LF)	0	LF
Grading (SY)	7,590	SY

Assume compact 0.5 feet (0.166 yards) 1,260 CY compacted

Off-road Equipment	Hours	Engine HP	Load Factor	VOC g/hp-hr	CO g/hp-hr	NOx g/hp-hr	SO_2 g/hp-hr	PM10 g/hp-hr	PM2.5 g/hp-hr	CO_2 g/hp-hr
Excavator	112	243	0.59	0.34	1.21	4.03	0.12	0.22	0.22	536
Skid Steer Loader	135	160	0.23	0.38	1.47	4.34	0.12	0.31	0.30	536
Dozer (Rubber Tired)	122	145	0.59	0.38	1.41	4.17	0.12	0.30	0.29	536
Compactor	6	103	0.58	0.40	1.57	4.57	0.12	0.32	0.31	536
Grader	3	285	0.58	0.34	1.21	4.07	0.12	0.23	0.22	536

	VOC lb	CO lb	NOx lb	SO2 lb	PM lb	PM2.5 lb	CO_2 lb
Excavator	12.21	42.92	143.04	4.09	7.91	7.67	19,019.29
Skid Steer Loader	4.19	16.07	47.44	1.26	3.34	3.24	5,856.91
Dozer (Rubber Tired)	8.67	32.56	96.09	2.65	6.81	6.61	12,333.54
Compactor	0.30	1.21	3.51	0.09	0.25	0.24	411.50
Grader	0.34	1.19	4.00	0.11	0.22	0.21	526.27

On-road Equipment	Hours	MPH	Engine HP	VOC lb/mile	CO lb/mile	NOx lb/mile	SO_2 lb/mile	PM10 lb/mile	PM2.5 lb/mile	CO_2 lb/mile
Dump Truck	112	5	230	0.0015	0.0080	0.0361	0.0000	0.0015	0.0015	3.4385

	VOC lb	CO lb	NOx lb	SO2 lb	PM lb	PM2.5 lb	CO_2 lb
Dump Truck	0.85	4.52	20.25	0.01	0.84	0.82	1,931
Subtotal in lb:	**27**	**98**	**314**	**8**	**19**	**19**	**40,078**
Site Prep Grand Total in Tons	**0.01**	**0.05**	**0.16**	**0.00**	**0.01**	**0.01**	
Site Prep Grand Total in Metric Tons							**18**

Vehicle Trips = 59

Table 11. Demo Bldgs - TBD

153,102 SF 7,655 Estimated CY of debris based on 20 SF/CY

Off-road Equipment	Hours of Operation	Engine HP	Load Factor	Emission Factors VOC g/hp-hr	CO g/hp-hr	NOx g/hp-hr	SO_2 g/hp-hr	PM_{10} g/hp-hr	$PM_{2.5}$ g/hp-hr	CO_2 g/hp-hr
Hydraulic excavator	1,276	86	0.59	0.23	2.57	2.68	0.11	0.40	0.39	595.46
Wheel Loader w/ integral Backhoe	1,276	87	0.23	1.07	6.13	5.02	0.14	0.95	0.92	692.77
Wheel mounted air compressor	1,276	49	0.59	0.26	1.41	3.51	0.11	0.23	0.22	536.20

	Annual Emissions VOC lb	CO lb	NOx lb	SO_2 lb	PM_{10} lb	$PM_{2.5}$ lb	CO_2 lb
Hydraulic excavator	32.68	366.84	382.56	16.22	57.51	55.79	84,984.91
Wheel Loader w/ integral Backhoe	60.05	344.89	282.62	7.96	53.40	51.80	38,991.55
Wheel mounted air compressor	21.35	114.56	285.28	8.78	18.86	18.29	43,602.12
Subtotal (lbs):	114.08	826.29	950.46	32.96	129.77	125.88	167578.58

On-road Equipment	Hours of Operation	Engine HP	Speed (mph)	VOC lb/mile	CO lb/mile	NOx lb/mile	SO_2 lb/mile	PM_{10} lb/mile	$PM_{2.5}$ lb/mile	CO_2 lb/mile
Dump Truck (12 CY Capacity)	702	230	27	0.001521	0.008042	0.036070	1.80E-05	0.001504	0.001458	3.438541

	VOC lb	CO lb	NOx lb	SO_2 lb	PM_{10} lb	$PM_{2.5}$ lb	CO_2 lb
Dump Truck (12 CY Capacity)	28.84	152.43	683.67	0.34	28.52	27.63	65,174
Subtotal (lbs):	142.91	978.72	1,634.13	33.30	158.29	153.51	232,752.68
Building Demo Grand Total in Tons	**0.071**	**0.489**	**0.817**	**0.017**	**0.079**	**0.077**	
Building Demo Grand Total in Metric Tons							**105.57**

Vehicle Trips = 598

Table 12. Demo Asphalt Concrete - TBD

15,358 SF 472 CY

Off-road Equipment	Hours of Operation	Engine HP	Load Factor	Emission Factors VOC g/hp-hr	CO g/hp-hr	NOx g/hp-hr	SO_2 g/hp-hr	PM_{10} g/hp-hr	$PM_{2.5}$ g/hp-hr	CO_2 g/hp-hr
Crawler Dozer w/attachments	263	125	0.58	0.34	1.21	4.08	0.12	0.23	0.22	535.79
Air Compressor	263	49	0.59	0.33	2.54	4.53	0.13	0.54	0.53	595.16
Excavator	61	380	0.59	0.31	2.50	4.51	0.13	0.55	0.54	595.21
				Annual Emissions						
				VOC lb	CO lb	NOx lb	SO_2 lb	PM_{10} lb	$PM_{2.5}$ lb	CO_2 lb
Crawler Dozer w/attachments				14.48	50.84	171.82	4.85	9.52	9.23	22562.78
Wheel mounted air compressor				5.50	42.68	76.02	2.15	9.10	8.83	9994.14
Excavator				9.34	74.67	134.78	3.83	16.51	16.01	17800.11

On-road Equipment	Hours of Operation	Engine HP	Speed (mph)	VOC lb/mile	CO lb/mile	NOx lb/mile	SO_2 lb/mile	PM_{10} lb/mile	$PM_{2.5}$ lb/mile	CO_2 lb/mile
Dump Truck	205	230	27	0.0015	0.0080	0.0361	0.0000	0.0015	0.0015	3.4385
				VOC lb	CO lb	NOx lb	SO_2 lb	PM_{10} lb	$PM_{2.5}$ lb	CO_2 lb
Dump Truck				8.42	44.51	199.65	0.10	8.33	8.07	19,032
Subtotal (lbs):				**38**	**213**	**582**	**11**	**43**	**42**	**69,389**
Asphalt Demo Grand Total in Tons				**0.02**	**0.11**	**0.29**	**0.01**	**0.02**	**0.02**	
Asphalt Demo Grand Total in Metric Tons										**31**

Vehicle Trips = 92

2019

Table 13. Building Demo - 2019

153,102 SF 7,655 Estimated CY of debris based on 20 SF/CY

Off-road Equipment	Cumulative Hours of Operation	Engine HP	Load Factor	Emission Factors VOC g/hp-hr	CO g/hp-hr	NOx g/hp-hr	SO_2 g/hp-hr	PM_{10} g/hp-hr	$PM_{2.5}$ g/hp-hr	CO_2 g/hp-hr
Hydraulic excavator with breakers and jackhammer bits	287	86	0.59	0.23	2.57	2.68	0.11	0.40	0.39	595.46
Wheel Loader w/ integral Backhoe	287	87	0.23	1.07	6.13	5.02	0.14	0.95	0.92	692.77
Wheel mounted air compressor	287	49	0.59	0.26	1.41	3.51	0.11	0.23	0.22	536.20
On-road Equipment	**Cumulative Hours of Operation**	**Engine HP**	**Productivity based Speed (miles/hour)**	**VOC** lb/mile	**CO** lb/mile	**NOx** lb/mile	**SO_2** lb/mile	**PM_{10}** lb/mile	**$PM_{2.5}$** lb/mile	**CO_2** lb/mile
Dump Truck (12 CY Capacity)	158	230	27	0.00166	0.00858	0.03922	0.00002	0.00169	0.00164	3.38

	Annual Emissions VOC lb	CO lb	NOx lb	SO_2 lb	PM_{10} lb	$PM_{2.5}$ lb	CO_2 lb
	7.36	82.59	86.13	3.65	12.95	12.56	19,134
	13.52	77.65	63.63	1.79	12.02	11.66	8,779
	4.81	25.79	64.23	1.98	4.25	4.12	9,817
	VOC lb	CO lb	NOx lb	SO_2 lb	PM_{10} lb	$PM_{2.5}$ lb	CO_2 lb
	7.15	36.97	169.00	0.08	7.29	7.08	14,575
Subtotal (lbs):	**33**	**223**	**383**	**7**	**37**	**35**	**52,306**
Building Demo Grand Total in Tons	**0.016**	**0.112**	**0.192**	**0.004**	**0.018**	**0.018**	
Building Demo Grand Total in Metric Tons							**23.73**

Vehicle Trips = 135

Table 14. Demo Asphalt and Concrete- 2019

15,358 SF 94 CY

Off-road Equipment	Cumulative Hours of Operation	Engine HP	Load Factor	Emission Factors VOC g/hp-hr	CO g/hp-hr	NOx g/hp-hr	SO_2 g/hp-hr	PM_{10} g/hp-hr	$PM_{2.5}$ g/hp-hr	CO_2 g/hp-hr
Crawler Dozer w/attachments	11	125	0.58	0.34	1.21	4.08	0.12	0.23	0.22	535.79
Air Compressor	11	49	0.59	0.33	2.54	4.53	0.13	0.54	0.53	595.16
Excavator	3	380	0.59	0.31	2.50	4.51	0.13	0.55	0.54	595.21
On-road Equipment	**Cumulative Hours of Operation**	**Engine HP**	**Productivity based Speed (miles/hour)**	**VOC lb/mile**	**CO lb/mile**	**NOx lb/mile**	**SO_2 lb/mile**	**PM_{10} lb/mile**	**$PM_{2.5}$ lb/mile**	**CO_2 lb/mile**
Dump Truck	9	230	27	0.00166	0.00858	0.03922	0.00002	0.00169	0.00164	3.38

	Annual Emissions VOC lb	CO lb	NOx lb	SO_2 lb	PM_{10} lb	$PM_{2.5}$ lb	CO_2 lb
	0.60	2.12	7.17	0.20	0.40	0.39	942
	0.23	1.78	3.17	0.09	0.38	0.37	417
	0.39	3.14	5.67	0.16	0.69	0.67	748
	VOC lb	**CO lb**	**NOx lb**	**SO_2 lb**	**PM_{10} lb**	**$PM_{2.5}$ lb**	**CO_2 lb**
	0.41	2.11	9.63	0.00	0.42	0.40	830
Subtotal (lbs):	**2**	**9**	**26**	**0**	**2**	**2**	**2,938**
Asphalt Demo Grand Total in Tons	**0.00**	**0.00**	**0.01**	**0.00**	**0.00**	**0.00**	
Asphalt Demo Grand Total in Metric Tons							**1**

Vehicle Trips = 4

2020

Table 15. Building Demo - 2020

12,000 SF — 600 Estimated CY of debris based on 20 SF/CY

Off-road Equipment	Cumulative Hours of Operation	Engine HP	Load Factor	VOC g/hp-hr	CO g/hp-hr	NOx g/hp-hr	SO_2 g/hp-hr	PM_{10} g/hp-hr	$PM_{2.5}$ g/hp-hr	CO_2 g/hp-hr
				Emission Factors						
Hydraulic excavator with breakers and jackhammer bits	100	86	0.59	0.23	2.57	2.68	0.11	0.40	0.39	595.46
Wheel Loader w/ integral Backhoe	100	87	0.23	1.07	6.13	5.02	0.14	0.95	0.92	692.77
Wheel mounted air compressor	100	49	0.59	0.26	1.41	3.51	0.11	0.23	0.22	536.20
On-road Equipment	**Cumulative Hours of Operation**	**Engine HP**	**Productivity based Speed (miles/hour)**	**VOC** lb/mile	**CO** lb/mile	**NOx** lb/mile	**SO_2** lb/mile	**PM_{10}** lb/mile	**$PM_{2.5}$** lb/mile	**CO_2** lb/mile
Dump Truck (12 CY Capacity)	55	230	27	0.00166	0.00858	0.03922	0.00002	0.00169	0.00164	3.38

	VOC lb	CO lb	NOx lb	SO_2 lb	PM_{10} lb	$PM_{2.5}$ lb	CO_2 lb
	Annual Emissions						
	2.56	28.75	29.98	1.27	4.51	4.37	6,661
	4.71	27.03	22.15	0.62	4.19	4.06	3,056
	1.67	8.98	22.36	0.69	1.48	1.43	3,417
	VOC lb	**CO** lb	**NOx** lb	**SO_2** lb	**PM_{10}** lb	**$PM_{2.5}$** lb	**CO_2** lb
	2.49	12.87	58.83	0.03	2.54	2.46	5,074
Subtotal (lbs):	**11**	**78**	**133**	**3**	**13**	**12**	**18,208**
Building Demo Grand Total in Tons	**0.006**	**0.039**	**0.067**	**0.001**	**0.006**	**0.006**	
Building Demo Grand Total in Metric Tons							**8.26**

Vehicle Trips = 47

Table 16. Building Construction-2020

12,000 SF Foundation
12,000 SF Total

Off-road Equipment	Hours of Operation	Engine HP	Load Factor	VOC g/hp-hr	CO g/hp-hr	NOx g/hp-hr	SO_2 g/hp-hr	PM10 g/hp-hr	PM2.5 g/hp-hr	CO_2 g/hp-hr
				Emission Factors						
Crane	60	330	0.58	0.25	1.22	5.26	0.11	0.21	0.20	530
Concrete Truck	60	300	0.43	0.19	1.45	4.32	0.12	0.21	0.20	536
Diesel Generator	48	40	0.43	0.26	1.41	3.51	0.11	0.23	0.22	536
Telehandler	120	99	0.59	0.51	3.94	4.93	0.13	0.52	0.51	595
Scissors Lift	96	83	0.59	0.51	3.94	4.93	0.13	0.52	0.51	595
Skid Steer Loader	60	67	0.59	1.69	7.97	6.70	0.15	1.19	1.15	691
Pile Driver	619	260	0.43	0.46	1.55	5.90	0.11	0.31	0.30	530
All Terrain Forklift	2	84	0.59	0.51	3.94	4.93	0.13	0.52	0.51	595

	VOC lb	CO lb	NOx lb	SO2 lb	PM lb	PM2.5 lb	CO_2 lb
	Annual Emissions						
Crane	6.22	30.88	133.17	2.89	5.26	5.10	13426.11
Concrete Truck	3.20	24.82	73.73	1.97	3.58	3.48	9150.71
Diesel Generator	0.48	2.56	6.39	0.20	0.42	0.41	975.95
Telehandler	7.87	60.88	76.17	1.98	8.05	7.81	9188.40
Scissors Lift	5.28	40.83	51.09	1.33	5.40	5.24	6162.72
Skid Steer Loader	8.85	41.66	35.02	0.78	6.22	6.03	3612.54
Pile Driver	70.77	236.68	900.14	17.38	47.87	46.43	80778.00
All Terrain Forklift	0.13	1.03	1.29	0.03	0.14	0.13	155.92

On-road Equipment	Hours of Operation	Engine HP	Speed (mph)	VOC lb/mile	CO lb/mile	NOx lb/mile	SO2 lb/mile	PM lb/mile	PM2.5 lb/mile	CO_2 lb/mile
Delivery Truck	288	265	45	0.0015	0.0080	0.0361	0.0000	0.0015	0.0015	3.4385
				VOC lb	CO lb	NOx lb	SO2 lb	PM lb	PM2.5 lb	CO_2 lb
			Delivery Truck	19.72	104.22	467.47	0.23	19.50	18.89	44,563
			Subtotal (lbs):	**123**	**544**	**1744**	**27**	**96**	**94**	**168014**
			Building Construction Grand Total in Tons	**0.06**	**0.27**	**0.87**	**0.01**	**0.05**	**0.05**	
			Building Construction Grand Total in Metric Tons							**76**

Vehicle Trips = 166

Table 17. Gravel Work-2020

244 CY   17 trips   1,534 total miles

Off-road Equipment	Hours	Engine HP	Load Factor	VOC g/hp-hr	CO g/hp-hr	NOx g/hp-hr	SO_2 g/hp-hr	PM_{10} g/hp-hr	$PM_{2.5}$ g/hp-hr	CO_2 g/hp-hr
Dozer	2	185	0.59	0.34	1.21	4.08	0.12	0.23	0.22	536
Wheel Loader for Spreading	3	87	0.59	0.35	1.25	4.23	0.12	0.24	0.23	536
Compactor	7	103	0.43	0.36	1.34	4.45	0.12	0.26	0.25	536
				VOC lb	CO lb	NOx lb	SO2 lb	PM10 lb	PM2.5 lb	CO_2 lb
			Dozer	0.17	0.58	1.96	0.06	0.11	0.11	257.86
			Wheel Loader for Spreading	0.12	0.42	1.44	0.04	0.08	0.08	181.89
			Compactor	0.25	0.92	3.04	0.08	0.18	0.17	366.18

On-road Equipment	Miles	Engine HP	VOC lb/mile	CO lb/mile	NOx lb/mile	SO_2 lb/mile	PM_{10} lb/mile	$PM_{2.5}$ lb/mile	CO_2 lb/mile
Dump Truck	1,534	230	0.0015	0.0080	0.0361	0.0000	0.0015	0.0015	3.4385
			VOC lb	CO lb	NOx lb	SO2 lb	PM10 lb	PM2.5 lb	CO_2 lb
		Dump Truck	2.33	12.33	55.32	0.03	2.31	2.24	5,274
		Subtotal (lbs):	**3**	**14**	**62**	**0**	**3**	**3**	**6,080**
		Gravel Work Grand Total in Tons	**0.00**	**0.01**	**0.03**	**0.00**	**0.00**	**0.00**	
		Gravel Work Grand Total in Metric Tons							**3**

Vehicle Trips = 2

Table 18. Concrete Work - 2020

Foundation Work 1,778 CY
Sidewalks, etc. 7 CY
Total 1,785 CY

Note: Assume all excavated soil is accounted for in Excavate/Fill and Trenching

Off-road Equipment	Hours of Operation	Engine HP	Load Factor	**Emission Factors** VOC g/hp-hr	CO g/hp-hr	NOx g/hp-hr	SO_2 g/hp-hr	PM10 g/hp-hr	PM2.5 g/hp-hr	CO_2 g/hp-hr
Concrete Mixer	94	3.5	0.43	0.69	3.04	6.17	0.13	0.54	0.52	588
Concrete Truck	85	300	0.43	0.38	1.75	6.18	0.11	0.27	0.26	530
				Annual Emissions VOC lb	CO lb	NOx lb	SO2 lb	PM lb	PM2.5 lb	CO_2 lb
			Concrete Mixer	0.21	0.95	1.92	0.04	0.17	0.16	183.48
			Concrete Truck	9.18	42.20	149.45	2.76	6.50	6.30	12,809.54
			Subtotal (lbs):	**9**	**43**	**151**	**3**	**7**	**6**	**12,993**
			Concrete Work Grand Total in Tons	**0.00**	**0.02**	**0.08**	**0.00**	**0.00**	**0.00**	
			Concrete Work Grand Total in Metric Tons							**6**

Vehicle Trips = 28

2022

Table 19. Building Demo - 2022

22,337 SF | 1,117 Estimated CY of debris based on 20 SF/CY

Off-road Equipment	Cumulative Hours of Operation	Engine HP	Load Factor	VOC g/hp-hr	CO g/hp-hr	NOx g/hp-hr	SO_2 g/hp-hr	PM_{10} g/hp-hr	$PM_{2.5}$ g/hp-hr	CO_2 g/hp-hr
Hydraulic excavator with breakers and jackhammer bits	186	86	0.59	0.23	2.57	2.68	0.11	0.40	0.39	595.46
Wheel Loader w/ integral Backhoe	186	87	0.23	1.07	6.13	5.02	0.14	0.95	0.92	692.77
Wheel mounted air compressor	186	49	0.59	0.26	1.41	3.51	0.11	0.23	0.22	536.20
On-road Equipment	**Cumulative Hours of Operation**	**Engine HP**	**Productivity based Speed (miles/hour)**	**VOC** lb/mile	**CO** lb/mile	**NOx** lb/mile	**SO_2** lb/mile	**PM_{10}** lb/mile	**$PM_{2.5}$** lb/mile	**CO_2** lb/mile
Dump Truck (12 CY Capacity)	102	230	27	0.00166	0.00858	0.03922	0.00002	0.00169	0.00164	3.38

Annual Emissions

	VOC lb	CO lb	NOx lb	SO_2 lb	PM_{10} lb	$PM_{2.5}$ lb	CO_2 lb
	4.76	53.48	55.77	2.37	8.38	8.13	12,390
	8.75	50.28	41.20	1.16	7.79	7.55	5,684
	3.11	16.70	41.59	1.28	2.75	2.67	6,357
	VOC lb	**CO** lb	**NOx** lb	**SO_2** lb	**PM_{10}** lb	**$PM_{2.5}$** lb	**CO_2** lb
	4.62	23.87	109.10	0.05	4.70	4.57	9,409
Subtotal (lbs):	**21**	**144**	**248**	**5**	**24**	**23**	**33,840**
Building Demo Grand Total in Tons	**0.011**	**0.072**	**0.124**	**0.002**	**0.012**	**0.011**	
Building Demo Grand Total in Metric Tons							**15.35**

Vehicle Trips = 87

Table 20. Demo Asphalt and Concrete- 2022

2,234 SF | 69 CY

Off-road Equipment	Cumulative Hours of Operation	Engine HP	Load Factor	VOC g/hp-hr	CO g/hp-hr	NOx g/hp-hr	SO_2 g/hp-hr	PM_{10} g/hp-hr	$PM_{2.5}$ g/hp-hr	CO_2 g/hp-hr
D-6K Crawler Dozer with attachments	8	125	0.58	0.34	1.21	4.08	0.12	0.23	0.22	535.79
Wheel mounted air compressor	8	49	0.59	0.33	2.54	4.53	0.13	0.54	0.53	595.16
Pneumatic Paving Breaker and jackhammer on excavator (CAT 345D L or similar)	2	380	0.59	0.31	2.50	4.51	0.13	0.55	0.54	595.21
On-road Equipment	**Cumulative Hours of Operation**	**Engine HP**	**Productivity based Speed (miles/hour)**	**VOC** lb/mile	**CO** lb/mile	**NOx** lb/mile	**SO_2** lb/mile	**PM_{10}** lb/mile	**$PM_{2.5}$** lb/mile	**CO_2** lb/mile
Dump Truck	6	230	27	0.00166	0.00858	0.03922	0.00002	0.00169	0.00164	3.38

Annual Emissions

	VOC lb	CO lb	NOx lb	SO_2 lb	PM_{10} lb	$PM_{2.5}$ lb	CO_2 lb
	0.44	1.54	5.22	0.15	0.29	0.28	685
	0.17	1.30	2.31	0.07	0.28	0.27	303
	0.31	2.47	4.46	0.13	0.55	0.53	588
	VOC lb	**CO** lb	**NOx** lb	**SO_2** lb	**PM_{10}** lb	**$PM_{2.5}$** lb	**CO_2** lb
	0.27	1.40	6.42	0.00	0.28	0.27	553
Subtotal (lbs):	**1**	**7**	**18**	**0**	**1**	**1**	**2,130**
Asphalt Demo Grand Total in Tons	**0.00**	**0.00**	**0.01**	**0.00**	**0.00**	**0.00**	
Asphalt Demo Grand Total in Metric Tons							**1**

Vehicle Trips = 3

Table 21. Fugitive Dust

Year	PM_{10} tons/acre/mo	acres	days of disturbance	PM_{10} Total (tons)	$PM_{2.5}/PM_{10}$ Ratio	$PM_{2.5}$ Total (tons)
TBD - Construction	0.42	7.28	90	13.8	0.1	1.4
TBD - Demo	0.42	3.5	180	13.2	0.1	1.3
2019	0.42	0.2	30	0.1	0.1	0.0
2020	0.42	0.3	9	0.1	0.1	0.0
2022	0.42	0.5	90	1.0	0.1	0.1

Table 22. Annual Construction Worker POVs - 2019 - TBD

Year	Vehicle Trips	mile/trip	VOCs lb/mi	CO lb/mi	NOx lb/mi	SO_2 lb/mi	PM_{10} lb/mi	$PM_{2.5}$ lb/mi	CO_2 g/mi	CH_4 g/mi	N_2O g/mi
TBD - Construction	2,885	6	0.00129	0.03681	0.00510	0.00001	0.00021	0.00019	364.00	0.031	0.032
TBD - Demo	749	6	0.00129	0.03681	0.00510	0.00001	0.00021	0.00019	364.00	0.031	0.032
2019	138	6	0.00129	0.03681	0.00510	0.00001	0.00021	0.00019	364.00	0.031	0.032
2020	243	6	0.00129	0.03681	0.00510	0.00001	0.00021	0.00019	364.00	0.031	0.032
2022	90	6	0.00129	0.03681	0.00510	0.00001	0.00021	0.00019	364.00	0.031	0.032

VOCs ton/year	CO ton/year	NOx ton/year	SO_2 ton/year	PM_{10} ton/year	$PM_{2.5}$ ton/year	CO_2e metric ton/year
0.011	0.319	0.044	0.000	0.002	0.002	6.5
0.003	0.083	0.011	0.000	0.000	0.000	1.7
0.001	0.015	0.002	0.000	0.000	0.000	0.3
0.001	0.027	0.004	0.000	0.000	0.000	0.5
0.000	0.010	0.001	0.000	0.000	0.000	0.2

Table 23. Wallops Main Base Area Construction Summary

YEAR	VOC T/yr	CO T/yr	NOx T/yr	SO_2 T/yr	PM_{10} T/yr	$PM_{2.5}$ T/yr	CO_2 MT/yr
TBD - Construction	1.01	4.85	14.62	0.20	14.54	2.14	1,291
TBD - Demo	0.11	0.73	1.28	0.03	13.34	1.43	157
2019	0.02	0.13	0.21	0.00	0.12	0.03	25
2020	0.07	0.37	1.05	0.02	0.11	0.06	94
2022	0.01	0.09	0.13	0.00	0.98	0.11	17

TAB C. CONSTRUCTION EMISSIONS - CONTROL CENTER AREA

Basic Conversions

453.59	grams per pound
43,560	Conversion from Acre to SF
0.03704	Cubic feet to Cubic Yards
0.1111	Square Feet to Square Yards
1.4	tons/CY for Gravel
80,000	lbs/Truck Load for Delivery
1.66	CY for each CY of asphalt/concrete demo
0.333333333	asphalt thickness for demolition
0.333333333	asphalt thickness for pavement
2000	pounds per ton
145	lb/ft^3 density of Hot Mix Asphalt
0.666666667	asphalt thickness for pavement on runways

TBD Construction

Table 1. Clearing - TBD

3.5 Acres

Vehicle Trips = 19

Off-road Equipment	Cumulative Hours of Operation	Engine HP	Load Factor	Emission Factors VOC g/hp-hr	CO g/hp-hr	NOx g/hp-hr	SO_2 g/hp-hr	PM_{10} g/hp-hr	$PM_{2.5}$ g/hp-hr	CO_2 g/hp-hr
Dozer	41	145	0.58	0.38	1.41	4.17	0.12	0.30	0.29	535.69
Loader w/ integral Backhoe	41	87	0.21	1.43	7.35	6.35	0.15	1.06	1.03	691.66
Small backhoe	41	55	0.21	1.43	7.35	6.35	0.15	1.06	1.03	691.66
On-road Equipment	**Cumulative Hours of Operation**	**Engine HP**	**Productivity based Speed (miles/hour)**	**VOC** lb/mile	**CO** lb/mile	**NOx** lb/mile	**SO_2** lb/mile	**PM_{10}** lb/mile	**$PM_{2.5}$** lb/mile	**CO_2** lb/mile
Dump Truck	19	230	16	0.00166	0.00858	0.03922	0.00002	0.00169	0.00164	3.38

	Annual Emissions VOC lb	CO lb	NOx lb	SO_2 lb	PM_{10} lb	$PM_{2.5}$ lb	CO_2 lb
	2.86	10.75	31.73	0.88	2.25	2.18	4,072.21
	2.36	12.14	10.48	0.25	1.76	1.70	1,142.23
	1.49	7.67	6.63	0.16	1.11	1.08	722.10
	VOC lb	**CO** lb	**NOx** lb	**SO_2** lb	**PM_{10}** lb	**$PM_{2.5}$** lb	**CO_2** lb
	0.51	2.64	12.08	0.01	0.52	0.51	1,042
Subtotal (lbs):	**7**	**33**	**61**	**1**	**6**	**5**	**6,979**
Clearing Grand Total in Tons	**0.00**	**0.02**	**0.03**	**0.00**	**0.00**	**0.00**	
Clearing Grand Total in Metric Tons							**3**

Vehicle Trips = 19

Table 2. Site Prep

Site Prep - Excavate/Fill (CY)	14,442 CY		
Trenching (LF)	3,300 LF	Assume 3' deep,1 ' wide	
Grading (SY)	32,263 SY	Assume compact 0.5 feet (0.166 yards)	5,356 CY compacted

Off-road Equipment	Hours	Engine HP	Load Factor	VOC g/hp-hr	CO g/hp-hr	NOx g/hp-hr	SO_2 g/hp-hr	PM10 g/hp-hr	PM2.5 g/hp-hr	CO_2 g/hp-hr
Excavator	48	243	0.59	0.34	1.21	4.03	0.12	0.22	0.22	536
Skid Steer Loader	58	160	0.23	0.38	1.47	4.34	0.12	0.31	0.30	536
Dozer (Rubber Tired)	52	145	0.59	0.38	1.41	4.17	0.12	0.30	0.29	536
Compactor	25	103	0.58	0.40	1.57	4.57	0.12	0.32	0.31	536
Grader	11	285	0.58	0.34	1.21	4.07	0.12	0.23	0.22	536
Backhoe/Loader	5	87	0.59	0.35	1.25	4.23	0.12	0.24	0.23	536

	VOC lb	CO lb	NOx lb	SO2 lb	PM lb	PM2.5 lb	CO_2 lb
Excavator	5.23	18.40	61.31	1.75	3.39	3.29	8,152.57
Skid Steer Loader	1.80	6.89	20.33	0.54	1.43	1.39	2,510.55
Dozer (Rubber Tired)	3.72	13.96	41.19	1.14	2.92	2.83	5,286.74
Compactor	1.29	5.13	14.91	0.38	1.04	1.01	1,749.16
Grader	1.44	5.04	16.99	0.48	0.94	0.91	2,237.05
Backhoe/loader	0.21	0.74	2.51	0.07	0.14	0.14	317.59

On-road Equipment	Hours	MPH	Engine HP	VOC lb/mile	CO lb/mile	NOx lb/mile	SO_2 lb/mile	PM10 lb/mile	PM2.5 lb/mile	CO_2 lb/mile
Dump Truck	48	5	230	0.0015	0.0080	0.0361	0.0000	0.0015	0.0015	3.4385
				VOC lb	CO lb	NOx lb	SO2 lb	PM lb	PM2.5 lb	CO_2 lb
			Dump Truck	0.37	1.94	8.68	0.00	0.36	0.35	828
			Subtotal in lb:	**14**	**52**	**166**	**4**	**10**	**10**	**21,081**
			Site Prep Grand Total in Tons	**0.01**	**0.03**	**0.08**	**0.00**	**0.01**	**0.00**	
			Site Prep Grand Total in Metric Tons							**10**

Vehicle Trips = 31

Table 3. Building Construction

12,000 SF Foundation
12,000 SF Total

Off-road Equipment	Hours of Operation	Engine HP	Load Factor	Emission Factors VOC g/hp-hr	CO g/hp-hr	NOx g/hp-hr	SO_2 g/hp-hr	PM10 g/hp-hr	PM2.5 g/hp-hr	CO_2 g/hp-hr
Crane	60	330	0.58	0.25	1.22	5.26	0.11	0.21	0.20	530
Concrete Truck	60	300	0.43	0.19	1.45	4.32	0.12	0.21	0.20	536
Diesel Generator	48	40	0.43	0.26	1.41	3.51	0.11	0.23	0.22	536
Telehandler	120	99	0.59	0.51	3.94	4.93	0.13	0.52	0.51	595
Scissors Lift	96	83	0.59	0.51	3.94	4.93	0.13	0.52	0.51	595
Skid Steer Loader	60	67	0.59	1.69	7.97	6.70	0.15	1.19	1.15	691
Pile Driver	619	260	0.43	0.46	1.55	5.90	0.11	0.31	0.30	530
All Terrain Forklift	2	84	0.59	0.51	3.94	4.93	0.13	0.52	0.51	595
				Annual Emissions VOC lb	CO lb	NOx lb	SO2 lb	PM lb	PM2.5 lb	CO_2 lb
			Crane	6.22	30.88	133.17	2.89	5.26	5.10	13426.11
			Concrete Truck	3.20	24.82	73.73	1.97	3.58	3.48	9150.71
			Diesel Generator	0.48	2.56	6.39	0.20	0.42	0.41	975.95
			Telehandler	7.87	60.88	76.17	1.98	8.05	7.81	9188.40
			Scissors Lift	5.28	40.83	51.09	1.33	5.40	5.24	6162.72
			Skid Steer Loader	8.85	41.66	35.02	0.78	6.22	6.03	3612.54
			Pile Driver	70.77	236.68	900.14	17.38	47.87	46.43	80778.00
			All Terrain Forklift	0.13	1.03	1.29	0.03	0.14	0.13	155.92

On-road Equipment	Hours of Operation	Engine HP	Speed (mph)	VOC lb/mile	CO lb/mile	NOx lb/mile	SO2 lb/mile	PM lb/mile	PM2.5 lb/mile	CO_2 lb/mile
Delivery Truck	288	265	45	0.0015	0.0080	0.0361	0.0000	0.0015	0.0015	3.4385
				VOC lb	CO lb	NOx lb	SO2 lb	PM lb	PM2.5 lb	CO_2 lb
			Delivery Truck	19.72	104.22	467.47	0.23	19.50	18.89	44,563
			Subtotal (lbs):	**123**	**544**	**1744**	**27**	**96**	**94**	**168014**
			Building Construction Grand Total in Tons	**0.06**	**0.27**	**0.87**	**0.01**	**0.05**	**0.05**	
			Building Construction Grand Total in Metric Tons							**76**

Vehicle Trips = 166

Table 4. Gravel Work

2,761 CY 197 trips 17,355 total miles

Off-road Equipment	Hours	Engine HP	Load Factor	VOC g/hp-hr	CO g/hp-hr	NOx g/hp-hr	SO_2 g/hp-hr	PM_{10} g/hp-hr	$PM_{2.5}$ g/hp-hr	CO_2 g/hp-hr
Dozer	28	185	0.59	0.34	1.21	4.08	0.12	0.23	0.22	536
Wheel Loader for Spreading	35	87	0.59	0.35	1.25	4.23	0.12	0.24	0.23	536
Compactor	76	103	0.43	0.36	1.34	4.45	0.12	0.26	0.25	536
				VOC lb	CO lb	NOx lb	SO2 lb	PM10 lb	PM2.5 lb	CO_2 lb
			Dozer	2.28	8.02	27.11	0.77	1.50	1.46	3559.76
			Wheel Loader for Spreading	1.36	4.88	16.53	0.45	0.93	0.90	2092.50
			Compactor	2.67	9.95	33.10	0.86	1.91	1.85	3983.35

On-road Equipment	Miles	Engine HP	VOC lb/mile	CO lb/mile	NOx lb/mile	SO_2 lb/mile	PM_{10} lb/mile	$PM_{2.5}$ lb/mile	CO_2 lb/mile
Dump Truck	17,355	230	0.0015	0.0080	0.0361	0.0000	0.0015	0.0015	3.4385
			VOC lb	**CO** lb	**NOx** lb	**SO2** lb	**PM10** lb	**PM2.5** lb	**CO_2** lb
		Dump Truck	26.40	139.57	625.99	0.31	26.11	25.30	59,675
		Subtotal (lbs):	**33**	**162**	**703**	**2**	**30**	**30**	**69,311**
		Gravel Work Grand Total in Tons	**0.02**	**0.08**	**0.35**	**0.00**	**0.02**	**0.01**	
		Gravel Work Grand Total in Metric Tons							**31**

Vehicle Trips = 22

Table 5. Concrete Work

Concrete Surface SF

4,690 SY 1.83 yards thick

[1]Off-road Equipment	[2]Cumulative Hours of Operation	[3]Engine HP	[4]Load Factor	[6,7]Emission Factors VOC g/hp-hr	CO g/hp-hr	NOx g/hp-hr	SO_2 g/hp-hr	PM10 g/hp-hr	PM2.5 g/hp-hr	CO_2 g/hp-hr
Grader (CAT 120M2 or similar)	7	150	0.61	1.06	3.52	8.24	0.06	0.47	0.47	568
Steel drum roller/soil compactor	65	401	0.56	0.70	3.18	7.20	0.05	0.28	0.28	568
Paving/Concrete Machine	65	164	0.53	1.14	3.71	8.87	0.49	0.49	0.49	568
Curbing Machine	3	130	0.59	1.14	3.71	8.87	0.49	0.49	0.49	568
Cement and Motar Mixer 1	65	9	0.56	0.92	2.64	5.41	0.07	0.35	0.35	568
Cement and Motar Mixer 2	65	9	0.56	0.92	2.64	5.41	0.07	0.35	0.35	568
Cement and Motar Mixer 3	65	9	0.56	0.92	2.64	5.41	0.07	0.35	0.35	568
Tractor/Loader/Backhoe	65	75	0.55	1.50	4.22	8.33	0.06	0.80	0.80	568
[1]On-road Equipment	**[2]Cumulative Hours of Operation**	**[3]Engine HP**	**[5]Speed (miles/hour)**	**VOC** lb/mile	**CO** lb/mile	**NOx** lb/mile	**SO2** lb/mile	**PM10** lb/mile	**PM2.5** lb/mile	**CO2** lb/mile
Cement Truck	65	230	20	0.001521	0.008042	0.036070	1.80E-05	0.001504	0.001458	3.438541
Water Truck/Oil truck	7	230	10	0.001521	0.008042	0.036070	1.80E-05	0.001504	0.001458	3.438541

	Annual Emissions VOC lb	CO lb	NOx lb	SO2 lb	PM lb	PM2.5 lb	CO_2 lb
	1.40	4.63	10.84	0.08	0.62	0.62	747.78
	22.51	102.79	232.38	1.61	9.11	9.11	18,352.00
	14.19	46.31	110.91	6.17	6.17	6.17	7,103.47
	0.63	2.04	4.89	0.27	0.27	0.27	313.41
	0.67	1.91	3.92	0.05	0.25	0.25	411.89
	0.67	1.91	3.92	0.05	0.25	0.25	411.89
	0.67	1.91	3.92	0.05	0.25	0.25	411.89
	8.89	25.03	49.38	0.36	4.76	4.76	3,371.13
	VOC lb	**CO** lb	**NOx** lb	**SO2** lb	**PM** lb	**PM2.5** lb	**CO_2** lb
	1.98	10.49	47.06	0.02	1.96	1.90	4,486
	0.10	0.52	2.35	0.00	0.10	0.10	224
Runway Construction Grand Total in Tons	**0.03**	**0.10**	**0.23**	**0.00**	**0.01**	**0.01**	
Runway Construction Grand Total in Metric Tons							**16**

Vehicle Trips = 63

Table 6. Paving

Pavement - Surface Area 2,400 SF 30 CY

Paving - HMA 800 CF

Off-road Equipment	Hours of Operation	Engine HP	Load Factor	VOC g/hp-hr	CO g/hp-hr	NOx g/hp-hr	SO2 g/hp-hr	PM g/hp-hr	PM2.5 g/hp-hr	CO_2 g/hp-hr
Grader	7	145	0.59	0.38	1.41	4.16	0.12	0.30	0.29	536
Roller	11	401	0.59	0.34	2.46	5.53	0.12	0.34	0.33	536
Paving Machine	15	164	0.59	0.38	1.44	4.25	0.12	0.30	0.29	536
Asphalt Curbing Machine	1	130	0.59	0.40	1.57	4.57	0.12	0.32	0.31	536
				VOC lb	**CO** lb	**NOx** lb	**SO2** lb	**PM** lb	**PM2.5** lb	**CO_2** lb
			Grader	0.50	1.86	5.49	0.15	0.39	0.38	707.24
			Roller	1.96	14.13	31.76	0.66	1.94	1.88	3,074.15
			Paving Machine	1.22	4.62	13.61	0.37	0.96	0.93	1,714.07
			Asphalt Curbing Machine	0.07	0.27	0.77	0.02	0.05	0.05	90.57

On-road Equipment	Hours of Operation	Engine HP	Productivity based Speed (miles/hour)	VOC lb/mile	CO lb/mile	NOx lb/mile	SO2 lb/mile	PM lb/mile	PM2.5 lb/mile	CO_2 lb/mile
Dump Truck	6	230	17	0.001521	0.008042	0.036070	1.80E-05	0.001504	0.001458	3.438541
Water Truck	0	230	10	0.001521	0.008042	0.036070	1.80E-05	0.001504	0.001458	3.438541
				VOC lb	CO lb	NOx lb	SO2 lb	PM lb	PM2.5 lb	CO_2 lb
			Dump Truck	0.16	0.82	3.68	0.00	0.15	0.15	351
			Water Truck	0.00	0.00	0.00	0.00	0.00	0.00	0

Hot Mix Asphalt (HMA)	Volume of HMA (ft^3)	Weight of HMA (tons)	VOC lb/ton of asphalt	VOC lb	CO lb	NOx lb	SO2 lb	PM10 lb	PM2.5 lb	CO_2 lb
Standard Hot Mix Asphalt	800	58	0.04	2.32	-	-	-	-	-	-
			Subtotal (lbs):	**6**	**22**	**55**	**1**	**4**	**3**	**5,937**
			Paving Grand Total in Tons	**0.00**	**0.01**	**0.03**	**0.00**	**0.00**	**0.00**	
			Paving Grand Total in Metric Tons							**3**

Vehicle Trips = 1

TBD Demo

Table 7. Building Demo - TBD

27,094 SF 1,355 Estimated CY of debris based on 20 SF/CY

Off-road Equipment	Hours of Operation	Engine HP	Load Factor	Emission Factors VOC g/hp-hr	CO g/hp-hr	NOx g/hp-hr	SO_2 g/hp-hr	PM_{10} g/hp-hr	$PM_{2.5}$ g/hp-hr	CO_2 g/hp-hr
Hydraulic excavator	226	86	0.59	0.23	2.57	2.68	0.11	0.40	0.39	595.46
Wheel Loader w/ integral Backhoe	226	87	0.23	1.07	6.13	5.02	0.14	0.95	0.92	692.77
Wheel mounted air compressor	226	49	0.59	0.26	1.41	3.51	0.11	0.23	0.22	536.20
				Annual Emissions						
				VOC lb	CO lb	NOx lb	SO_2 lb	PM_{10} lb	$PM_{2.5}$ lb	CO_2 lb
			Hydraulic excavator	5.79	64.98	67.76	2.87	10.19	9.88	15,053.96
			Wheel Loader w/ integral Backhoe	10.64	61.09	50.06	1.41	9.46	9.18	6,906.84
			Wheel mounted air compressor	3.78	20.29	50.53	1.55	3.34	3.24	7,723.54
			Subtotal (lbs):	20.21	146.37	168.36	5.84	22.99	22.30	29684.33

On-road Equipment	Hours of Operation	Engine HP	Speed (mph)	VOC lb/mile	CO lb/mile	NOx lb/mile	SO_2 lb/mile	PM_{10} lb/mile	$PM_{2.5}$ lb/mile	CO_2 lb/mile
Dump Truck	124	230	27	0.001521	0.008042	0.036070	1.80E-05	0.001504	0.001458	3.438541
				VOC lb	CO lb	NOx lb	SO_2 lb	PM_{10} lb	$PM_{2.5}$ lb	CO_2 lb
			Dump Truck (12 CY Capacity)	5.09	26.92	120.76	0.06	5.04	4.88	11,512
			Subtotal (lbs):	25.30	173.29	289.12	5.90	28.02	27.18	41,196.57
			Building Demo Grand Total in Tons	**0.013**	**0.087**	**0.145**	**0.003**	**0.014**	**0.014**	
			Building Demo Grand Total in Metric Tons							**18.69**

Vehicle Trips = 106

2019

Table 8. Building Demo - 2019

3,705 SF 185 Estimated CY of debris based on 20 SF/CY

Off-road Equipment	Cumulative Hours of Operation	Engine HP	Load Factor	Emission Factors VOC g/hp-hr	CO g/hp-hr	NOx g/hp-hr	SO_2 g/hp-hr	PM_{10} g/hp-hr	$PM_{2.5}$ g/hp-hr	CO_2 g/hp-hr
Hydraulic excavator with breakers and jackhammer bits	31	86	0.59	0.23	2.57	2.68	0.11	0.40	0.39	595.46
Wheel Loader w/ integral Backhoe	31	87	0.23	1.07	6.13	5.02	0.14	0.95	0.92	692.77
Wheel mounted air compressor	31	49	0.59	0.26	1.41	3.51	0.11	0.23	0.22	536.20
On-road Equipment	**Cumulative Hours of Operation**	**Engine HP**	**Productivity based Speed (miles/hour)**	**VOC** lb/mile	**CO** lb/mile	**NOx** lb/mile	**SO_2** lb/mile	**PM_{10}** lb/mile	**$PM_{2.5}$** lb/mile	**CO_2** lb/mile
Dump Truck	17	230	27	0.00166	0.00858	0.03922	0.00002	0.00169	0.00164	3.38

	Annual Emissions						
	VOC	CO	NOx	SO_2	PM_{10}	$PM_{2.5}$	CO_2
	lb	lb	lb	lb	lb	lb	lb
	0.79	8.88	9.26	0.39	1.39	1.35	2,057
	1.45	8.35	6.84	0.19	1.29	1.25	944
	0.52	2.77	6.90	0.21	0.46	0.44	1,055
	VOC	CO	NOx	SO_2	PM_{10}	$PM_{2.5}$	CO_2
	lb	lb	lb	lb	lb	lb	lb
	0.77	3.98	18.18	0.01	0.78	0.76	1,568
Subtotal (lbs):	4	24	41	1	4	4	5,624
Building Demo Grand Total in Tons	**0.002**	**0.012**	**0.021**	**0.000**	**0.002**	**0.002**	
Building Demo Grand Total in Metric Tons							**2.55**

Vehicle Trips = 10

2020

Table 9. Building Demo - 2020

36,106 SF

1,805 Estimated CY of debris based on 20 SF/CY

				Emission Factors						
Off-road Equipment	**Cumulative Hours of Operation**	**Engine HP**	**Load Factor**	**VOC** g/hp-hr	**CO** g/hp-hr	**NOx** g/hp-hr	**SO_2** g/hp-hr	**PM_{10}** g/hp-hr	**$PM_{2.5}$** g/hp-hr	**CO_2** g/hp-hr
Hydraulic excavator with breakers and jackhammer bits	301	86	0.59	0.23	2.57	2.68	0.11	0.40	0.39	595.46
Wheel Loader w/ integral Backhoe	301	87	0.23	1.07	6.13	5.02	0.14	0.95	0.92	692.77
Wheel mounted air compressor	301	49	0.59	0.26	1.41	3.51	0.11	0.23	0.22	536.20
On-road Equipment	**Cumulative Hours of Operation**	**Engine HP**	**Productivity based Speed (miles/hour)**	**VOC** lb/mile	**CO** lb/mile	**NOx** lb/mile	**SO_2** lb/mile	**PM_{10}** lb/mile	**$PM_{2.5}$** lb/mile	**CO_2** lb/mile
Dump Truck	165	230	27	0.00166	0.00858	0.03922	0.00002	0.00169	0.00164	3.38

	Annual Emissions						
	VOC	CO	NOx	SO_2	PM_{10}	$PM_{2.5}$	CO_2
	lb	lb	lb	lb	lb	lb	lb
	7.71	86.54	90.25	3.83	13.57	13.16	20,050
	14.17	81.37	66.68	1.88	12.60	12.22	9,199
	5.04	27.03	67.30	2.07	4.45	4.32	10,287
	VOC	CO	NOx	SO_2	PM_{10}	$PM_{2.5}$	CO_2
	lb	lb	lb	lb	lb	lb	lb
	7.47	38.61	176.49	0.08	7.61	7.39	15,221
Subtotal (lbs):	34	234	401	8	38	37	54,756
Building Demo Grand Total in Tons	**0.017**	**0.117**	**0.200**	**0.004**	**0.019**	**0.019**	
Building Demo Grand Total in Metric Tons							**24.84**

Vehicle Trips = 94

Table 10. Fugitive Dust

Year	**PM_{10} tons/acre/mo**	**acres**	**days of disturbance**	**PM_{10}** Total (tons)	**$PM_{2.5}/PM_{10}$** Ratio	**$PM_{2.5}$** Total (tons)
TBD - Construction	0.42	3.5	90	6.6	0.1	0.7
TBD - Demo	0.42	0.6	20	0.3	0.1	0.0
2019	0.42	0.1	5	0.0	0.1	0.0
2020	0.42	0.8	30	0.5	0.1	0.1

Table 11. Annual Construction Worker POVs - 2019 - TBD

Year	Vehicle Trips	mile/trip	**VOCs** lb/mi	**CO** lb/mi	**NOx** lb/mi	**SO_2** lb/mi	**PM_{10}** lb/mi	**$PM_{2.5}$** lb/mi	**CO_2** g/mi	**CH_4** g/mi	**N_2O** g/mi
TBD - Construction	302	6	0.00129	0.03681	0.00510	0.00001	0.00021	0.00019	364.00	0.031	0.032
TBD - Demo	106	6	0.00129	0.03681	0.00510	0.00001	0.00021	0.00019	364.00	0.031	0.032
2019	10	6	0.00129	0.03681	0.00510	0.00001	0.00021	0.00019	364.00	0.031	0.032
2020	94	6	0.00129	0.03681	0.00510	0.00001	0.00021	0.00019	364.00	0.031	0.032

VOCs ton/year	**CO** ton/year	**NOx** ton/year	**SO_2** ton/year	**PM_{10}** ton/year	**$PM_{2.5}$** ton/year	**CO_2e** metric ton/year
0.001	0.033	0.005	0.000	0.000	0.000	0.7
0.000	0.012	0.002	0.000	0.000	0.000	0.2
0.000	0.001	0.000	0.000	0.000	0.000	0.0
0.000	0.010	0.001	0.000	0.000	0.000	0.2

Table 12. Wallops Mainland and Island Area Construction Summary

YEAR	VOC T/yr	CO T/yr	NOx T/yr	SO_2 T/yr	PM_{10} T/yr	$PM_{2.5}$ T/yr	CO_2 MT/yr
TBD - Construction	0.12	0.54	1.60	0.02	6.70	0.74	140
TBD - Demo	0.01	0.10	0.15	0.00	0.27	0.04	19
2019	0.00	0.01	0.02	0.00	0.01	0.00	3
2020	0.02	0.12	0.20	0.00	0.52	0.07	25

TAB D. CONSTRUCTION EMISSIONS - Dredging and Bridge Construction

Basic Conversions

453.59	grams per pound
43,560	Conversion from Acre to SF
0.03704	Cubic feet to Cubic Yards
0.1111	Square Feet to Square Yards
1.4	tons/CY for Gravel
80,000	lbs/Truck Load for Delivery
1.66	CY for each CY of asphalt/concrete demo
0.333333333	asphalt thickness for demolition
0.333333333	asphalt thickness for pavement
2000	pounds per ton
145	lb/ft^3 density of Hot Mix Asphalt
0.666666667	asphalt thickness for pavement on runways

Dredging

Table 1. Mechanical Dredge 2019-2023

500,000 CY

					Emission Factors						
Off-road Equipment	**Cumulative Hours of Operation**	**Engine HP**	**Engine KW**	**Load Factor**	**VOC** g/hp-hr	**CO** g/hp-hr	**NOx** g/hp-hr	**SO_2** g/hp-hr	**PM_{10}** g/hp-hr	**$PM_{2.5}$** g/hp-hr	**CO_2** g/hp-hr
Mechanical Dredge- main	1,529	1,800	1,342	0.40	0.52	1.92	7.41	0.11	0.32	0.31	529.46
Mechanical Dredge- auxiliary	1,529	200	149	0.30	0.46	1.55	5.90	0.11	0.31	0.30	529.64
Marine Vessel Equipment	**Cumulative Hours of Operation**	**Engine HP**	**Engine KW**	**Load Factor**	**VOC** g/kw-hr	**CO** g/kw-hr	**NOx** g/kw-hr	**SO_2** g/kw-hr	**PM_{10}** g/kw-hr	**$PM_{2.5}$** g/kw-hr	**CO_2** g/kw-hr
Tender Boat - main	1,529	300	224	0.40	0.27	1.5	10	0.63	0.3	0.291	758.85
Tender Boat- auxiliary	1,529	35	26	0.40	0.27	2	11	0.63	0.9	0.873	758.85
Survey Vessel	510	100	75	0.40	0.27	1.7	10	0.63	0.4	0.388	758.85

	Annual Emissions						
	VOC lb	**CO** lb	**NOx** lb	**SO_2** lb	**PM_{10}** lb	**$PM_{2.5}$** lb	**CO_2** lb
	1,268.98	4,662.79	17,975.90	276.42	782.01	758.55	1,285,061
	93.86	313.87	1,193.73	23.04	63.48	61.58	107,124
	VOC lb	**CO** lb	**NOx** lb	**SO_2** lb	**PM_{10}** lb	**$PM_{2.5}$** lb	**CO_2** lb
	81.45	452.48	3,016.51	190.04	90.50	87.78	228,908
	9.50	70.39	387.12	22.17	31.67	30.72	26,706
	9.05	56.98	335.17	21.12	13.41	13.00	25,434
Subtotal (lbs):	**1,463**	**5,557**	**22,908**	**533**	**981**	**952**	**1,673,233**
Dredging Total in Tons	**0.73**	**2.78**	**11.45**	**0.27**	**0.49**	**0.48**	
Dredging Total in Metric Tons							**759**

Table 2. Materials Handling post dredge 2019-2023

500,000 CY

					Emission Factors						
Off-road Equipment	**Cumulative Hours of Operation**	**Engine HP**	**Engine KW**	**Load Factor**	**VOC** g/hp-hr	**CO** g/hp-hr	**NOx** g/hp-hr	**SO_2** g/hp-hr	**PM_{10}** g/hp-hr	**$PM_{2.5}$** g/hp-hr	**CO_2** g/hp-hr
Loader w/ integral Backhoe	2,500	87	65	0.21	1.43	7.35	6.35	0.15	1.06	1.03	691.66
On-road Equipment	**Cumulative Hours of Operation**	**Engine HP**	**Productivity based Speed (miles/hour)**		**VOC** lb/mile	**CO** lb/mile	**NOx** lb/mile	**SO_2** lb/mile	**PM_{10}** lb/mile	**$PM_{2.5}$** lb/mile	**CO_2** lb/mile
Dump Truck	8,929	230	16		0.00166	0.00858	0.03922	0.00002	0.00169	0.00164	3.38

	Annual Emissions						
	VOC lb	**CO** lb	**NOx** lb	**SO_2** lb	**PM_{10}** lb	**$PM_{2.5}$** lb	**CO_2** lb
	144.18	740.10	639.30	14.98	107.06	103.85	69,648
	VOC lb	**CO** lb	**NOx** lb	**SO_2** lb	**PM_{10}** lb	**$PM_{2.5}$** lb	**CO_2** lb
	240.28	1,242.19	5,678.63	2.64	244.84	237.76	489,735
Subtotal (lbs):	**384**	**1,982**	**6,318**	**18**	**352**	**342**	**559,383**
Materials Handling Total in Tons	**0.19**	**0.99**	**3.16**	**0.01**	**0.18**	**0.17**	
Materials Handling Total in Metric Tons							**254**

Table 3. Annual Emissions from Dredging

YEAR	VOC T/yr	CO T/yr	NOx T/yr	SO_2 T/yr	PM_{10} T/yr	$PM_{2.5}$ T/yr	CO_2 MT/yr
Annually	0.18	0.75	2.92	0.06	0.13	0.13	203

Bridge

Table 4. Site Prep - Excavate/Fill - Trenching - Grading - 2019-2022

Site Prep - Excavate/Fill (CY)	12,963 CY	Assume 100% hauled in or out	12,963 CY hauled				
Trenching (LF)	0 LF	Assume 2 ft deep trench, 2 feet wide	0 CY	Assume 100% hauled in or out	0 CY hauled		
Grading (SY)	1,556 SF	Convert	173 SY	Assume compact 0.5 feet (0.166 yards)	29 CY compacted		

Off-road Equipment	Cumulative Hours of Operation	Engine HP	Load Factor	Emission Factors VOC g/hp-hr	CO g/hp-hr	NOx g/hp-hr	SO_2 g/hp-hr	PM_{10} g/hp-hr	$PM_{2.5}$ g/hp-hr	CO_2 g/hp-hr
Backhoe Excavator	43	243	0.59	0.34	1.21	4.03	0.12	0.22	0.22	535.79
Skid Steer Loader	52	160	0.23	0.38	1.47	4.34	0.12	0.31	0.30	535.67
Dozer	47	145	0.59	0.38	1.41	4.17	0.12	0.30	0.29	535.69
Scraper Hauler Excavator	47	365	0.58	0.38	1.42	4.19	0.12	0.30	0.29	535.69
Compactor	15	103	0.58	0.40	1.57	4.57	0.12	0.32	0.31	535.63
Grader	6	285	0.58	0.34	1.21	4.07	0.12	0.23	0.22	535.79
Trenching with backhoe loader	3	87	0.59	0.35	1.25	4.23	0.12	0.24	0.23	535.77
On-road Equipment	**Cumulative Hours of Operation**	**Engine HP**	**Productivity based Speed (miles/hour)**	**VOC** lb/mile	**CO** lb/mile	**NOx** lb/mile	**SO_2** lb/mile	**PM_{10}** lb/mile	**$PM_{2.5}$** lb/mile	**CO_2** lb/mile
Dump Truck (12 CY capacity)	926	230	16	0.00166	0.00858	0.03922	0.00002	0.00169	0.00164	3.38
Delivery Truck	4	365	45	0.00166	0.00858	0.03922	0.00002	0.00169	0.00164	3.38

	Annual Emissions VOC lb	CO lb	NOx lb	SO_2 lb	PM_{10} lb	$PM_{2.5}$ lb	CO_2 lb
	4.70	16.52	55.03	1.57	3.04	2.95	7,318
	1.61	6.18	18.25	0.48	1.28	1.25	2,253
	3.34	12.53	36.97	1.02	2.62	2.54	4,745
	8.27	31.11	91.78	2.53	6.50	6.30	11,742
	0.80	3.18	9.23	0.23	0.65	0.63	1,083
	0.76	2.67	8.99	0.25	0.50	0.48	1,183
	0.12	0.42	1.42	0.04	0.08	0.08	180
	VOC lb	**CO** lb	**NOx** lb	**SO_2** lb	**PM_{10}** lb	**$PM_{2.5}$** lb	**CO_2** lb
	24.92	128.82	588.90	0.27	25.39	24.66	50,787
	0.26	1.35	6.18	0.00	0.27	0.26	533
Subtotal (lbs):	**45**	**203**	**817**	**6**	**40**	**39**	**79,825**
Site Prep Grand Total in Tons	**0.02**	**0.10**	**0.41**	**0.00**	**0.02**	**0.02**	
Site Prep Grand Total in Metric Tons							**36**

Vehicle Trips (per year)	6

Table 5. Construct bridge base (Cofferdams, Piers)

1400 Feet of Bridge 4466 CY Concete

Off-road Equipment	Cumulative Hours of Operation	Engine HP	Engine KW	Load Factor	Emission Factors VOC g/hp-hr	CO g/hp-hr	NOx g/hp-hr	SO_2 g/hp-hr	PM_{10} g/hp-hr	$PM_{2.5}$ g/hp-hr	CO_2 g/hp-hr
Crane	2240	330	246	0.21	0.25	1.22	5.26	0.11	0.21	0.20	530.30
Backhoe/loader	622	98	73	0.21	0.35	1.25	4.23	0.12	0.24	0.23	535.77
Small generator	2489	10	7	0.43	0.26	1.41	3.51	0.11	0.23	0.22	536.20
Concrete Truck	213	300	224	0.43	0.19	1.45	4.32	0.12	0.21	0.20	536.26
Pile Driver	2,240	260	194	0.43	0.46	1.55	5.90	0.11	0.31	0.30	529.64
Marine Vessel Equipment	**Cumulative Hours of Operation**	**Engine HP**	**Engine KW**	**Load Factor**	**VOC** g/kw-hr	**CO** g/kw-hr	**NOx** g/kw-hr	**SO_2** g/kw-hr	**PM_{10}** g/kw-hr	**$PM_{2.5}$** g/kw-hr	**CO_2** g/kw-hr
Tugboat - main	2,240	2,000	1491	0.6	0.27	2.50	13.00	0.63	0.30	0.29	722.10
Tugboat - auxiliary	2,240	200	149	0.4	0.27	1.50	10.00	0.63	0.40	0.39	758.85
Work Boat	2,240	200	149	0.4	0.27	1.50	10.00	0.63	0.40	0.39	758.85
On-road Equipment	**Cumulative Hours of Operation**	**Engine HP**	**Productivity based Speed (miles/hour)**		**VOC** lb/mile	**CO** lb/mile	**NOx** lb/mile	**SO_2** lb/mile	**PM_{10}** lb/mile	**$PM_{2.5}$** lb/mile	**CO_2** lb/mile
Delivery truck	388	180	40		0.00166	0.00858	0.03922	0.00002	0.00169	0.00164	3.38

	Annual Emissions VOC lb	CO lb	NOx lb	SO_2 lb	PM_{10} lb	$PM_{2.5}$ lb	CO_2 lb
	84.09	417.35	1,800.06	39.04	71.09	68.96	181,484
	9.84	35.24	119.50	3.25	6.74	6.54	15,124
	6.19	33.24	82.77	2.55	5.47	5.31	12,651
	11.36	88.11	261.73	6.99	12.73	12.34	32,485
	256.20	856.78	3,258.54	62.90	173.29	168.09	292,419
	VOC lb	**CO** lb	**NOx** lb	**SO_2** lb	**PM_{10}** lb	**$PM_{2.5}$** lb	**CO_2** lb
	1,193.15	11,047.65	57,447.79	2,784.01	1,325.72	1,286	3,191,004
	79.54	441.91	2,946.04	185.60	117.84	114	223,560
	79.54	441.91	2,946.04	185.60	117.84	114	223,560
	VOC lb	**CO** lb	**NOx** lb	**SO_2** lb	**PM_{10}** lb	**$PM_{2.5}$** lb	**CO_2** lb
	25.78	133.26	609.18	0.28	26.27	25.51	52,537
Subtotal (lbs):	**1,746**	**13,495**	**69,472**	**3,270**	**1,857**	**1,801**	**4,224,824**
Bridge Construction Total in Tons	**0.87**	**6.75**	**34.74**	**1.64**	**0.93**	**0.90**	
Bridge Construction Total in Metric Tons							**1916**

Vehicle Trips (per year) 378

Table 6. Construct superstructure, final roadway approaches (concrete)

26 Prestress Bridge Section Approaches 40,000 SF

Pavement - Surface Area 40,000 SF 494 CY

					Emission Factors						
Off-road Equipment	**Cumulative Hours of Operation**	**Engine HP**	**Engine KW**	**Load Factor**	**VOC** g/hp-hr	**CO** g/hp-hr	**NOx** g/hp-hr	**SO_2** g/hp-hr	**PM_{10}** g/hp-hr	**$PM_{2.5}$** g/hp-hr	**CO_2** g/hp-hr
Crane	416	170	127	0.21	0.25	1.22	5.26	0.11	0.21	0.20	530.30
Grader	184	150	112	0.59	1.06	3.52	8.24	0.06	0.47	0.47	568.30
Roller	184	30	22	0.59	0.70	3.18	7.20	0.05	0.28	0.28	568.30
Paving/Concrete Machine	245	164	122	0.53	1.14	3.71	8.87	0.49	0.49	0.49	568.30
Small diesel engines	245	25	19	0.43	0.26	1.41	3.51	0.11	0.23	0.22	536.20
Concrete Truck	155	300	224	0.43	0.19	1.45	4.32	0.12	0.21	0.20	536.26
Marine Vessel Equipment	**Cumulative Hours of Operation**	**Engine HP**	**Engine KW**	**Load Factor**	**VOC** g/kw-hr	**CO** g/kw-hr	**NOx** g/kw-hr	**SO_2** g/kw-hr	**PM_{10}** g/kw-hr	**$PM_{2.5}$** g/kw-hr	**CO_2** g/kw-hr
Tugboat - main	416	2,000	1491	0.6	0.27	2.5	13	0.63	0.3	0.29	722.10
Tugboat - auxiliary	416	200	149	0.4	0.27	1.5	10	0.63	0.4	0.39	758.85
Work Boat	416	200	149	0.4	0.27	1.5	10	0.63	0.4	0.39	758.85
On-road Equipment	**Cumulative Hours of Operation**	**Engine HP**	**Productivity based Speed (miles/hour)**		**VOC** lb/mile	**CO** lb/mile	**NOx** lb/mile	**SO_2** lb/mile	**PM_{10}** lb/mile	**$PM_{2.5}$** lb/mile	**CO_2** lb/mile
Delivery truck	150	180	40		0.00166	0.00858	0.03922	0.00002	0.00169	0.00164	3.38

	Annual Emissions						
	VOC lb	**CO** lb	**NOx** lb	**SO_2** lb	**PM_{10}** lb	**$PM_{2.5}$** lb	**CO_2** lb
	8.04	39.93	172.21	3.73	6.80	6.60	17,363
	38.07	126.27	295.34	2.04	16.81	16.81	20,374
	5.00	22.82	51.60	0.36	2.02	2.02	4,075
	53.29	173.94	416.57	23.19	23.19	23.19	26,681
	1.52	8.18	20.37	0.63	1.35	1.31	3,113
	8.28	64.21	190.73	5.09	9.27	8.99	23,672
	VOC lb	**CO** lb	**NOx** lb	**SO_2** lb	**PM_{10}** lb	**$PM_{2.5}$** lb	**CO_2** lb
	221.58	2,051.71	10,668.87	517.03	246.20	239	592,615
	14.77	82.07	547.12	34.47	21.88	21	41,518
	14.77	82.07	547.12	34.47	21.88	21	41,518
	VOC lb	**CO** lb	**NOx** lb	**SO_2** lb	**PM_{10}** lb	**$PM_{2.5}$** lb	**CO_2** lb
	9.97	51.52	235.52	0.11	10.15	9.86	20,312
Subtotal (lbs):	**375**	**2,703**	**13,145**	**621**	**360**	**350**	**791,242**
Superstructure Construction Total in Tons	**0.19**	**1.35**	**6.57**	**0.31**	**0.18**	**0.18**	
Superstructure Construction Total in Metric Tons							**359**

Vehicle Trips (per year) 70

Table 7. Demo Asphalt/Concrete- 2023

20,000 CY

					Emission Factors						
Off-road Equipment	Cumulative Hours of Operation	Engine HP	Enging KW	Load Factor	VOC g/hp-hr	CO g/hp-hr	NOx g/hp-hr	SO2 g/hp-hr	PM10 g/hp-hr	PM2.5 g/hp-hr	CO2 g/hp-hr
D-6K Crawler Dozer with attachments	2,125	125	93	0.58	0.34	1.21	4.08	0.12	0.23	0.22	535.79
Wheel mounted air compressor	2,125	49	37	0.59	0.33	2.54	4.53	0.13	0.54	0.53	595.16
excavator (CAT 345D L or similar)	445	380	283	0.59	0.31	2.50	4.51	0.13	0.55	0.54	595.21
Marine Vessel Equipment	Cumulative Hours of Operation	Engine HP	Engine KW	Load Factor	VOC g/kw-hr	CO g/kw-hr	NOx g/kw-hr	SO_2 g/kw-hr	PM_{10} g/kw-hr	$PM_{2.5}$ g/kw-hr	CO_2 g/kw-hr
Tugboat - main	523	2,000	1491	0.6	0.27	2.5	13	0.63	0.3	0.29	722.10
Tugboat - auxiliary	523	200	149	0.4	0.27	1.5	10	0.63	0.4	0.39	758.85
Work Boat	523	200	149	0.4	0.27	1.5	10	0.63	0.4	0.39	758.85
On-road Equipment	Cumulative Hours of Operation	Engine HP	Productivity based Speed (miles/hour)		VOC lb/mile	CO lb/mile	NOx lb/mile	SO2 lb/mile	PM10 lb/mile	PM2.5 lb/mile	CO2 lb/mile
Dump Truck	1,650	230	27		0.00166	0.00858	0.03922	0.00002	0.00169	0.00164	3.38

	Annual Emissions						
	VOC lb	CO lb	NOx lb	SO2 lb	PM10 lb	PM2.5 lb	CO2 lb
	116.73	410.00	1385.57	39.14	76.77	74.47	181,947
	44.38	344.13	613.06	17.34	73.39	71.19	80,593
	68.64	548.82	990.58	28.14	121.31	117.67	130,827
	VOC lb	CO lb	NOx lb	SO_2 lb	PM_{10} lb	$PM_{2.5}$ lb	CO_2 lb
	278.31	2,576.98	13,400.29	649.40	309.24	300	744,335
	18.55	103.08	687.19	43.29	27.49	27	52,148
	18.55	103.08	687.19	43.29	27.49	27	52,148
	VOC lb	CO lb	NOx lb	SO_2 lb	PM_{10} lb	$PM_{2.5}$ lb	CO_2 lb
	74.68	386.06	1,764.88	0.82	76.09	73.89	152,206
Subtotal (lbs):	**619.84**	**4472.15**	**19528.78**	**821.42**	**711.78**	**690.51**	**1,394,203**
Demo Asphalt/Concrete Total in Tons	**0.31**	**2.24**	**9.76**	**0.41**	**0.36**	**0.35**	
Demo Asphalt/Concrete Total in Metric Tons							**632**

Vehicle Trips (per year) 163

Table 9. Bridge POV 2019- 2023

Year	Vehicle Trips	mile/trip	VOCs lb/mi	CO lb/mi	NOx lb/mi	SO_2 lb/mi	PM_{10} lb/mi	$PM_{2.5}$ lb/mi	CO_2 g/mi	CH_4 g/mi	N_2O g/mi
Any year 2019 - 2023	617	6	0.00128593	0.03681076	0.00509876	0.00001339	0.00020844	0.00019220	364.00	0.031	0.032

VOCs ton/year	CO ton/year	NOx ton/year	SO_2 ton/year	PM_{10} ton/year	$PM_{2.5}$ ton/year	CO_2e metric ton/year
2.38E-03	6.81E-02	9.43E-03	2.48E-05	3.86E-04	3.55E-04	1

Table 10. Wallops Causeway Bridge Totals

YEAR	VOC T/yr	CO T/yr	NOx T/yr	SO_2 T/yr	PM_{10} T/yr	$PM_{2.5}$ T/yr	CO_2 MT/yr
2019	0.28	2.16	8.35	1.67	0.23	0.22	2,313
2020	0.28	2.16	8.35	1.67	0.23	0.22	2,313
2021	0.28	2.16	8.35	1.67	0.23	0.22	2,313
2022	0.28	2.16	8.35	1.67	0.23	0.22	2,313
2023	0.59	4.39	18.12	2.08	0.58	0.56	2,945

Table 11. Causeway, Bridge and Dredging Totals

YEAR	VOC T/yr	CO T/yr	NOx T/yr	SO_2 T/yr	PM_{10} T/yr	$PM_{2.5}$ T/yr	CO_2 MT/yr
2019	0.47	2.91	11.28	1.73	0.36	0.35	2,515
2020	0.47	2.91	11.28	1.73	0.36	0.35	2,515
2021	0.47	2.91	11.28	1.73	0.36	0.35	2,515
2022	0.47	2.91	11.28	1.73	0.36	0.35	2,515
2023	0.78	5.15	21.04	2.14	0.72	0.69	3,148

Project Name	Building Number	Type (Renov or Const)	Year	FootPrint (AC)	Clearing (AC)	Grading (sf)	Demo Bldgs (SF)	Demo asphalt/ concrete (SF)	Site Prep - Excavate/Fill (CY)	Trenching (LF)	Building Construction - Total Size (sf)	Building Construction foundation footprint (sf)	# Stories	Paving - Surface area (SF)	Pavement type, vehicle or aircraft	Paving - HMA (CF)	Sidewalks (sf)	Gravel Work (CY)	Concrete Work - sidewalks, etc (CY)	Concrete Work - foundation (CY)	Runway Construction (Concrete and Asphalt) (SF)	Concrete Pilings Required	Building Square Footage (original for Renovation)
Main Base																							
Commercial Space Terminal	N/A	New	TBD	0.80	-	35,000			1,296	-	35,000	35,000	1	3,500		1,167	1,750	745	22	5,185			
Runway 04/22 Extension	N/A	New	TBD	4.30	-	187,500			20,833	2,500	-	-	-		Aircraft			20,833			187,500		
Sounding Rocket Program Facility	E-107	New	TBD	0.46	0.25	20,000	6,040	604	1,329	-	20,000	20,000	1	2,000	Vehicle	667	1,000	426	12	2,963	-	-	
Range and Project Management Facility	N/A	RBR	TBD	1.72	1.72	-	65,000	72,000	27,400	-	65,000	65,000	1	6,500	Vehicle	2,167	3,250	1,384	40	9,630	-	-	
Totals TBD				**7.28**	**2.0**	**242,500**	**71,040**	**72,604**	**50,858**	**2,500**	**120,000**	**120,000**	**-**	**12,000**	**-**	**4,000**	**6,000**	**23,389**	**74**	**17,778**	**187,500**	**-**	
Packing and Crating Facility	D-049	Demo	TBD	0.08	-	-	3,200	320	704	-	-	-	-	-	-	-	-	-	-	-	-		
ATC Tower	A-001	Demo	TBD	0.10	-	4,232	4,232	423	931	-	-	-	-	-	-	-	-	-	-	-			
Source Evaluation Board Building	A-131	Demo	TBD	0.02	-	882	882	88	194	-	-	-	-	-	-	-	-	-	-	-			
Air Support	C-015	Demo	TBD	0.12	-	5,097	5,097	510	1,121	-	-	-	-	-	-	-	-	-	-	-			
Groundwater Remediation Facility	E-010	Demo	TBD	0.09	-	3,909	3,909	391	860	-	-	-	-	-	-	-	-	-	-	-			
Management Education Center	E-104	Demo	TBD	0.80	-	35,000	35,000	3,500	7,700	-	-	-	-	-	-	-	-	-	-	-			
Reproduction Facility	F-001	Demo	TBD	0.14	-	5,940	5,940	594	1,307	-	-	-	-	-	-	-	-	-	-	-			
Telecommunications Facility	F-002	Demo	TBD	0.15	-	6,495	6,495	650	1,429	-	-	-	-	-	-	-	-	-	-	-			
Visitors Center	J-017	Demo	TBD	0.09	-	3,728	3,728	373	820	-	-	-	-	-	-	-	-	-	-	-			
Garage	H-030	Demo	TBD	0.05	-	2,068	2,068	207	455	-	-	-	1	-	-	-	-	-	-	-			
Empty Drum Storage	F-014	Demo	TBD	0.02	-	960	960	96	211	-	-	-	1	-	-	-	-	-	-	-			
WFF Administration	F-006	Demo	TBD	0.34	-	-	14,613	1,461	3,215	-	-	-	1	-	-	-	-	-	-	-			
Compressed Air Distribution Facility	F-021	Demo	TBD	-	-	-	110	11	24	-	-	-	1	-	-	-	-	-	-	-	-	-	-
Rain Simulator Shelter	F-162	Demo	TBD	0.06	-	-	2,500	250	550	-	-	-	1	-	-	-	-	-	-	-	-	-	-
Supply Warehouse	F-019	Demo	TBD	0.51	-	-	22,400	2,240	4,928	-	-	-	-	-	-	-	-	-	-	-			
Optical Lab	D-101	Demo	TBD	0.05	-	-	2,100	210	462	-	-	-	1	-	-	-	-	-	-	-			
Post Office	E-007	Demo	TBD	0.18	-	-	7,902	790	1,738	-	-	-	1	-	-	-	-	-	-	-	-	-	-
Credit Union	N-133	Demo	TBD	0.03	-	-	1,446	192	328	-	-	-	1	-	-	-	-	-	-	-			
Cafeteria/Photo Lab/Gift Shop	E-002	Demo	TBD	0.70	-	-	30,520	3,052	6,714	-	-	-	1	-	-	-	-	-	-	-			
Totals TBD				**3.52**		**68,311**	**153,102**	**15,358**	**33,692**	**0**	**0**	**0**	**-**	**0**	**-**	**0**	**0**	**0**	**0**	**0**	**0**	**-**	**0**
Central Heating Plant	D-008	Demo	2019	0.16	-	0	7,137	714	1,570														
Totals 2019				**0.16**	**-**	**7,137**	**7,137**	**714**	**71**														
Consolidated Laboratories	N/A	RBR	2020	0.28		12000	12000	1,200			12,000	12,000	1	600	Vehicle		600	244	7	1,778			
Totals 2020				**0.28**	**-**	**12,000**	**12,000**	**1,200**		**-**	**12,000**	**12,000**	**1**	**600**	**Vehicle**		**600**	**244**	**7**	**1,778**	**-**	**-**	**-**
Health/Quality Verification Lab	F-160	Demo	2022	0.51			22,337	2,234	4,914														
Totals 2022				**0.51**		**-**	**22,337**	**2,234**	**4,914**	**-**			**-**		**-**						**-**	**-**	**-**
Project Name	**Building Number**	**Type (Renov or Const)**	**Year**	**FootPrint (AC)**	**Clearing (AC)**	**Grading (sy)**	**Demo Bldgs (SF)**	**Demo asphalt/ concrete (SF)**	**Site Prep - Excavate/Fill (CY)**	**Trenching (LF)**	**Building Construction - Total Size (sf)**	**Building Construction foundation footprint (sf)**	**# Stories**	**Paving - Surface area (SF)**	**Pavement type, vehicle or aircraft**	**Paving - HMA (CF)**	**Sidewalks (sf)**	**Gravel Work (CY)**	**Concrete Work - sidewalks, etc (CY)**	**Concrete Work - foundation (CY)**	**Runway Construction (Concrete and Asphalt) (CY)**	**Concrete Pilings Required**	**Building Square Footage (original for Renovation)**
Mainland and Wallops Island																							
ELV Launch Pad 0-C		Infrastructure - New	TBD	3.18	3.18	15,389	-	-	6,840	500			1			-	-	0	-		0	10	
DoD SM-3 Vertical Launch System Pad		New	TBD	0.00	0.00	12	-	-	47	500				-		-		5	-		23	4	
ESSM Launch System Pad and Blockhouse		New	TBD			2,222	-	-	6,667	500	-	-	-	-		-		2,222	-		4,444		
Radar and Computer Facility (AEGIS)		New	TBD	0.34	0.34	14,640	-	-	889	1,800	12,000	12,000	1	2,400	Vehicle	800	240	533	3	222	-	-	
Totals TBD				**3.52**	**3.5**	**32,263**			**14,442**	**3,300**	**12,000**	**12,000**	**-**	**2,400**	**-**	**800**	**240**	**2,761**	**3**	**222**	**4,468**	**-**	
Block House 3		Demo	TBD	0.48			20872																
Terminal Cubicle		Demo	TBD	0.00			97																
Cable Terminal		Demo	TBD	0.01			541																
Fuel Storage Magazine		Demo	TBD	0.04			1681																
Island Radar Control Building		Demo	TBD	0.08			3503																
Camera Stand		Demo	TBD	0.01			400																
Totals TBD				**0.6**			**27,094**								**-**							**-**	
AN FSP Radar	Y-055	Demo	2019	0.08	-	-	3,510		-	-	-	-	1	-	-	-	-	-	-	-	-	-	-
Sewer Ejector Station	Y-061	Demo	2019	0.00	-	-	195		-	-	-	-	1	-	-	-	-	-	-	-	-	-	-
Totals 2019				**0.09**	**-**	**-**	**3,705**		**-**	**-**	**-**	**-**	**-**	**-**	**-**	**-**	**-**	**-**	**-**	**-**	**-**	**-**	**-**
Former Coast Guard Station		Demo	2020	0.10			4,140																
Rocket Motor Storage Facility		Demo	2020	0.19			8,200																
Fire Department Support Building		Demo	2020	0.02			1,024																
Paint Shop		Demo	2020	0.06			2,410																
Paint Shop Storage		Demo	2020	0.01			422																
Electrical Storage Building		Demo	2020	0.02			1,000																
NSEC Performance Test Building		Demo	2020	0.27			11,617																
Block House 1		Demo	2020	0.08			3,300																
Movable Launch Shelter Building		Demo	2020	0.04			1,890																
Launch Control Building		Demo	2020	0.01			240																
Rocket Flight Hardware Storage	Y-050	Demo	2020	0.02	-	-	955		-	-	-	-	1	-	-	-	-	-	-	-	-	-	-
Fire Pump House	X-091	Demo	2020	0.01	-	-	235		-	-	-	-	1	-	-	-	-	-	-	-	-	-	
Relocation of Radar 3 (Relocated to Mainland)		Relocation	2020	0.01	-		625		-	-	625	625	1	-	-	-	-	12	-	93	-	-	-
Storm Drainage Pump	Y-046	Demo	2020	0.00	-	-	48		-	-	-	-	1	-	-	-	-	-	-	-	-	-	
Totals 2020				**0.83**	**-**	**0**	**36,106**	**0**	**-**	**-**	**625**	**625**	**-**	**-**	**-**	**-**	**-**	**12**	**-**	**93**	**-**	**-**	**-**
Project Name	**Building Number**	**Type (Renov or Const)**	**Year**	**FootPrint (AC)**	**Clearing (AC)**	**Grading (sf)**	**Demo Bldgs (SF)**	**Demo asphalt/ concrete (CY)**	**Site Prep - Excavate/Fill (CY)**	**Trenching (LF)**	**Building Construction - Total Size (sf)**	**Building Construction foundation footprint (sf)**	**# Stories**	**Paving - Surface area (SF)**	**Pavement type, vehicle or aircraft**	**Paving - HMA (CF)**	**Sidewalks (sf)**	**Gravel Work (CY)**	**Concrete Work - sidewalks, etc (CY)**	**Concrete Work - foundation (CY)**	**Runway Construction (Concrete and Asphalt) (SF)**	**Concrete Pilings Required**	**Dredging (CY)**
Causeway																							
Causeway Bridge			2019-2023	0.30	-	14,000	-	-	12,963		-	-	-	70,000	Vehicle - Concrete	-	-	-	-	-	-	Yes	
Causeway Bridge Demolition			2023		-	-	-	20,000	-	-	-	-	-	-	-	-	-	-	-	-	-	no	
Dredging			2019-2023	-	-	-	-	-	-	-	-	-	-	-	-	-	-	-	-	-	-	-	500,000

20,000 tons construction debris
20,000 CY
based on 2000 lb/cy

TAB F. OPERATIONAL EMISSIONS

Table 1. [1]Antares Launch Exhaust Emissions

Burn Rate:	2,414 lbm/sec	Fuel (RP-1):	142,735 x 1 =		142,735 lbm
Time to 10,000 ft	45 sec	Oxidizer (LOX):	390,779 x 1 =		390,779 lbm
Time to 3,000 feet	13.50 sec			Sum:	533,514 lbm

Compound	Mole Fractions	Molecular Weight	Weight (g/gmole)	Weight Fraction	Total Mass (lbm)	Per-launch Mass (tons)	6 launches per year total (tons)	Below 3000 ft AGL Mixing Height (tons)	Total in Metric Tons
CO	0.23932	28.01000	6.7033532	0.254385863	135,718	67.86	407.16	**24.87**	**22.19**
CO2	0.26632	44.01000	11.7207432	0.44479103	237,302	118.65	**711.91**		**646**
H	0.00144	1.00800	0.00145152	5.50838E-05	29	0.01	0.09		
H2	0.07231	0.32204	0.023286712	0.000883709	471	0.24	1.41		
H2O	0.41938	18.01500	7.5551307	0.286710007	152,964	76.48	458.89		
O	0.00002	15.99900	0.00031998	1.21429E-05	6	0.00	0.02		
OH	0.00118	17.00700	0.02006826	0.000761571	406	0.20	1.22		
O2	0.00004	31.9988	0.001279952	4.8573E-05	26	0.01	0.08		
SUM:	0.99999		26.35112	1.00000	533,514	266.76	1,600.54		

Source: Evaluation of Taurus II Static Test Firing and Normal Launch Rocket Plume Emissions, ACTA 2009

Current Envelope					
	CO	**CO2**	**NOx**	**PM**	**HCl**
Antares	24.87	646			
LMLV-3	159			154	125
Total	**184**	**646**	**0**	**154**	**125**
New Envelope					
Castor 1200 Beast	68.13	92.87		154.56	107.03
Falcon 9		5,160	7.2		
Total	**68**	**5,253**	**7**	**155**	**107**
Net change	**-116.0**	**4,607.4**	**7.2**	**1.0**	**-18.1**

Table 2. LMLV-3 Launch Exhaust Emissions[1]

Burn Rate 1 for Castor IV:	4,436 lb/sec	Fuel (NH4ClO4 in HTPB):		293,479 lb total
	for 60 sec	Total fuel burned in 60 sec:		88,720 lb
Burn Rate 2 for Castor IV:	1,367 lb/sec	Burn duration:	80 sec	
	for 20 sec	Total fuel burned in 20 sec:		27,340 lb
Time to 3,000 feet	20 sec	Total fuel burned in 80 sec:		116,060 lb

Compound	Below 3000 ft AGL Mixing Height (lbs)	Below 3000 ft AGL Mixing Height (tons)	Total for 12 Launches	Total in Metric Tons
Al2O3	25,596	13	154	139
CO	26,544	13	159	144
HCl	20,856	10	125	114

[1]Data from Environmental Assessment for Range Operations Expansion at the NASA Goddard Space Flight Center. 1997.

Table 3. Total Existing Launch Envelope Emissions

	Al2O3	HCl	CO	CO2
Total in Tons	154	125	184	712
Total in Metric Tons	139	114	167	646

Note: CO2 is also emitted from solid rocket fuel combustion, but at much lower concentrations - around an order of magnitude lower compared to Al2O3 and HCl (ATK-EELV Program 1996). This would amount to less than 10 tons for the entire fuel-burning trajectory in 12 launches.

Table 4. Large Space Launch Booster Emissions - with Castor 1200 solid rocket motors - 12 launches annually

1,114,115 lb mass of the TP-1148 propellent per motor

Chemical	ACTA Weight Fraction[1]	Approx. lbs per launch	Approx. tons per launch (metric tons for CO2)	12 launches annually T/yr except CO2 (MT/yr)
Al_2O_3	0.16797	187,138	12.68	152.19
CO	0.07519	83,770	5.68	68.13
CO_2	0.11299	125,884	7.74	92.87
Cl	0.00052	579	0.04	0.47
HCl	0.11813	131,610	8.92	107.03
H	0.00001	11	0.00	0.01
OH	0.00007	78	0.01	0.06
H_2	0.00333	3,710	0.25	3.02
H_2O	0.12725	141,771	9.61	115.30
NO	0.00001	11	0.00	0.01
N_2	0.38621	430,282	29.16	349.93
$FeCl_2$	0.00261	2,908	0.20	2.36

Castor 1200 burn time =	132.8	s
Time to reach 10,000 FT AGL =	20	s
Time to reach 3,000 FT AGL =	18	s
13.55%	of total time	

[1]ACTA 2012. Evaluation of Toxic Emissions for a Large Solid Propellent Launch Vehicle at Wallops Flight Facility, Table 5-1, page 35.

Table 5. Falcon 9 Launch Emissions - 6 Launches Annually Including RTLS

Launch Vehicle	Max # launches/yr	RP-1 Use gal/launch	RP-1 MMBtu/gal	[1]NOx Tons/launch	NOx Annual Tons	[2]CO2 EF (kg/gal)	CO2 Metric Tons
Falcon 9	6	35,000	0.135	1.2	7.2	9.76	2,050

[1] From Table 4.5-1 of Environmental Assessment for the Operation and Launch of the Falcon 1 and Falcon 9 Space Vehicles at CCAFS, FL 2007

[2] From Environmental Assessment Falcon 9 and Falcon 9 Heavy Launch Vehicle Programs from SLC-4E, Vandenberg AFB 2011.

Vehicle	Max # RTLS/yr	Vertical Landing sec	[1]CO2 Exhaust lb/sec	Total CO2 exhaust MT/yr
Falcon 9 - RTLS	6	17	1,121	3,111

[1] From Table 4.5-1 of Environmental Assessment for the Operation and Launch of the Falcon 1 and Falcon 9 Space Vehicles at CCAFS, FL 2007

Table 6. Generator Operations

Wallops Island

Two 3 -MW Caterpillar 175 emergency power generator

Meets EPA Interim Tier 4 emission requirements

		Emission Factors						Emissions					
Hours/yr	Fuel Flow Rate L/Hr @ 100%	[1]g/kW-hr VOCs	[1]g/kW-hr CO	[1]g/kW-hr NOx	[1]g/kW-hr PM10	[1]g/kW-hr PM2.5	[2]kg/l CO2	**T/yr VOCs**	**T/yr CO**	**T/yr NOx**	**T/yr PM10**	**T/yr PM2.5**	**MT/yr CO2**
360	807	0.4	3.5	0.67	0.1	0.1	2.70	**0.952**	**8.334**	**1.595**	**0.238**	**0.238**	**1,567**

[1]USEPA Interim Tier 4 emission standards.

[2]Federal GHG Accounting and Reporting Guidance Technical Document, Appendix D, Table D-2. 2010.

Main Base

One 3 -MW Caterpillar 175 emergency power generator

		Emission Factors						Emissions					
Hours/yr	Fuel Flow Rate L/Hr @ 60%	[1]g/kW-hr VOCs	[1]g/kW-hr CO	[1]g/kW-hr NOx	[1]g/kW-hr PM10	[1]g/kW-hr PM2.5	[2]kg/l CO2	**T/yr VOCs**	**T/yr CO**	**T/yr NOx**	**T/yr PM10**	**T/yr PM2.5**	**MT/yr CO2**
144	484	0.4	3.5	0.67	0.1	0.1	2.70	**0.476**	**4.167**	**0.798**	**0.119**	**0.119**	**783**

[1]USEPA Interim Tier 4 emission standards.

[2]Federal GHG Accounting and Reporting Guidance Technical Document, Appendix D, Table D-2. 2010.

UAS

Table 1. Operation of Viking UAS

Model	HP	annual # flights	flight time (hr)	BSFC lb/hp-hr	VOC lb/hp-hr	CO lb/hp-hr	NOx lb/hp-hr	PM lb/hp-hr	CO2 g/hp-hr	VOC Tons	CO Tons	NOx Tons	PM Tons	CO2 Metric Tons
Viking 300	25	1,950	11	0.408	0.000966	0.004764	0.0097884	0.000588	188	0.11	0.52	1.07	0.06	101

Table 2. Operation of MQ-4C

Engine is Rolls-Royce/Allison AE3007H

Number Type of Operation	Number of Operations per Year	Power Setting	Fuel Flowrate (lb/hr)	Time in Mode	Total Fuel Used	Emission Factor (lb/1000 lb)						
						VOCs	**CO**	**NOx**	**SO_2**	**PM_{10}**	**$PM_{2.5}$**	**CO2**
Taxi/Idle-out	1,950	Idle	427.65	0.1083	46.33	2.39	17.31	3.82	1.2	0.15	0.14	3.1
Takeoff	1,950	Military	3021.05	0.0067	20.14	0.26	0.83	20.5	1.2	0.27	0.24	3.1
Climbout	1,950	Intermediate	2531.72	0.0083	21.10	0.26	0.83	17.43	1.2	0.24	0.22	3.1
Approach	1,950	Approach	946.85	0.0267	25.25	0.61	3.27	7.77	1.2	0.22	0.2	3.1
Taxi/Idle-In	1,950	Idle	427.65	0.1083	46.33	2.39	17.31	3.82	1.2	0.15	0.14	3.1
						Total Emission in pounds						
						VOCs	**CO**	**NOx**	**SO_2**	**PM_{10}**	**$PM_{2.5}$**	**CO2**
						215.9	1,563.8	345.1	108.4	13.6	12.6	280
						10.2	32.6	805.1	47.1	10.6	9.4	122
						10.7	34.1	717.1	49.4	9.9	9.1	128
						30.0	161.0	382.6	59.1	10.8	9.8	153
						215.9	1,563.8	345.1	108.4	13.6	12.6	280
					Annual emissions (tons/year)	**0.24**	**1.68**	**1.30**	**0.19**	**0.03**	**0.03**	
					Annual Emission (metric ton/year)							**0.44**

Table 3. Net Change Based on Total Representative Annual UAS Operations

Operations	**VOCs**	**CO**	**NOx**	**SO_2**	**PM_{10}**	**$PM_{2.5}$**	**CO2**
Original Envelope	0.03	0.2	0.4	NA	0.05	0.05	9.6
New Envelope	0.35	2.20	2.37	0.19	0.09	0.09	101
Net Change	**0.32**	**2.00**	**1.97**	**NA**	**0.04**	**0.04**	**91.7**

Report No. 09-640/5-01

Evaluation of Taurus II Static Test Firing and Normal Launch Rocket Plume Emissions

Subcontract No.
Prime Contract No.
Task No. *5*

Prepared by

Randolph L. Nyman

2790 Skypark Dr Ste 310
Torrance, CA 90505

Prepared for

National Aeronautics and Space Administration
Wallops Flight Facility, Environmental Office
Code 250
Wallops Island, VA 23337

Under Subcontract to:

Computer Sciences Corporation
7700 Hubble Drive
Lanham-Seabrook, MD 20706

March 18, 2009

TABLE OF CONTENTS

LIST OF FIGURES

LIST OF TABLES

1. INTRODUCTION

The Taurus II launch vehicle is being designed and built by Orbital Sciences Corporation with the objective of launching missions from Wallops Flight Facility (WFF) to service the International Space Station. This report presents the findings of rocket exhaust plume emission and atmospheric dispersion analyses performed for the Taurus II first stage using a large archive of WFF weather balloon soundings. The report also explains the development of input data, describes the basic features of the modeling tools and identifies the assumptions made to support the analyses.

The Taurus II first stage uses liquid propellants commonly found in other modern U.S. built rockets. The first stage fuel is a refined form of kerosene known as RP-1 and the oxidizer is liquid oxygen (LOX). Although these propellants are burned in a fuel rich mixture the exhaust products can be considered environmentally friendly compared to solid propellant exhaust. The use of RP-1/LOX also avoids handling and spill toxic hazards associated with liquid hypergolic propellants. Consequently, the primary chemical exhaust constituent of concern from a toxicity standpoint is carbon monoxide (CO). The hazard associated with exposure to CO can be associated with several industry standard exposure criteria. Since rocket emissions from static test firings or rocket launches are relatively short duration events that only occur a few times a year over the course of the program, short duration or emergency exposure standards are more appropriate than long duration exposure standards designed for work place environments. One such emergency exposure standard is the National Institute for Occupational Safety and Health (NIOSH) definition of the Immediately Dangerous to Life or Health (IDLH) exposure threshold for an airborne chemical. The IDLH is intended to be used in conjunction with workers wearing respirators in contaminated areas, such that if the respirator fails the person could escape the contaminated area without being incapacitated given a maximum exposure of 30 minutes. Perhaps a more appropriate set of exposure guidelines are the Acute Exposure Guideline Levels (AEGLs) that are supported by the EPA. The development of Acute Exposure Guideline Levels (AEGLs) is a collaborative effort of the public and private sectors worldwide. AEGLs are intended to describe the risk to humans resulting from once-in-a-lifetime, or rare, exposure to airborne chemicals. The National Advisory Committee for the Development of Acute Exposure Guideline Levels for Hazardous Substances (AEGL Committee) is involved in developing these guidelines to help both national and local authorities, as well as private companies, deal with emergencies involving spills, or other catastrophic exposures. The recommended interim AEGLs for carbon monoxide are listed in Table 1-1.

Table 1-1: Interim Acute Exposure Guideline Levels (AEGLs) for Carbon Monoxide.

AEGL Level	10 min Exposure [ppm]	30 min Exposure [ppm]	60 min Exposure [ppm]	4 hr Exposure [ppm]
AEGL 1	NR	NR	NR	NR
AEGL 2	420	150	83	33
AEGL 3	1700	600	330	150

NR = No exposure level recommended due to insufficient or inconclusive data.

Definitions of the AEGL levels are as follows:

AEGL-1 is the airborne concentration, expressed as parts per million or milligrams per cubic meter (ppm or mg/m3) of a substance above which it is predicted that the general population, including susceptible individuals, could experience notable discomfort, irritation, or certain asymptomatic nonsensory effects. However, the effects are not disabling and are transient and reversible upon cessation of exposure.

AEGL-2 is the airborne concentration (expressed as ppm or mg/m3) of a substance above which it is predicted that the general population, including susceptible individuals, could experience irreversible or other serious, long-lasting adverse health effects or an impaired ability to escape.

AEGL-3 is the airborne concentration (expressed as ppm or mg/m3) of a substance above which it is predicted that the general population, including susceptible individuals, could experience life-threatening health effects or death.

The time duration that a receptor is exposed to a rocket exhaust plume emission depends upon the cloud transport wind speed and the size of the cloud. The cloud or plume grows in size as it transports downwind. Typical exposure durations are estimated to be in the 10 to 30 minute range but may approach one hour under very light wind conditions.

The report authors do not have toxicological expertise regarding hazardous CO thresholds for flora and fauna that may be of environmental concern. The selection of the most appropriate exposure level to apply to exposed flora and fauna is left to the judgment of others. It is however noted here that the vast majority of emission scenarios evaluated in this study predict far field maximum ground level CO concentrations below 10 parts per million (ppm), which is quite benign relative to all published human hazardous thresholds.

There are two emission scenarios of concern for the Taurus II environmental assessment:

1. Static test firing of the first stage while the stacked vehicle is held stationary on the launch pad. In this scenario the two first stage engines are both ignited and are run through a 52 second thrust profile that ramps the engines up to full performance (112.9%) and back down. Exhaust from the rocket engine nozzles is directed downward into a flame trench and deflected through the flame duct such that the exhaust gases are diverted away from the launch vehicle and nearby facilities. The exhaust plume exits the flame duct at supersonic velocity and the flow is approximately parallel to and slightly above the ground.

2. Normal launch of the Taurus II vehicle. In this scenario a fully configured launch vehicle with payload is ignited on the launch pad at time T-0. The vehicle is held on the pad for approximately 2 seconds as the first stage engines build thrust and then hold-downs are released allowing the vehicle to begin ascent to orbit. During ascent the vehicle velocity steadily increases resulting in a time and altitude varying exhaust product emission rate. Initially the rocket engine exhaust is largely directed into and through the flame duct. As the vehicle lifts off from the pad and clears the launch tower, a portion of the exhaust plume impinges on the pad structure and is directed radially around the launch pad stand. The portion of the rocket plume that interacts with the launch pad and flame trench is referred to as the "ground cloud". As the vehicle climbs to several hundred feet above the pad, the rocket plume reaches a point where the gases no longer interact with the ground surface and the exhaust plume is referred to as the "contrail cloud".

The concepts of the ground and contrail clouds are illustrated in Figure 1-1 using a Titan IV launch from Cape Canaveral as an example. For atmospheric dispersion analyses of rocket emissions that could affect receptors on the ground, it has been standard practice at the Federal Ranges (Cape Canaveral and Vandenberg Air Force Base) to simulate the emissions from the ascending launch vehicle from the ground to a vehicle altitude of approximately 3000 meters. The operational toxic dispersion analysis tool used by the Federal Ranges for launch support and public risk assessment is Version 7.13 of the Rocket Exhaust Effluent Diffusion Model (REEDM). This same computer program was used to perform the dispersion analyses for the Taurus II emission scenarios. The features of REEDM pertinent to this study are discussed in the next section.

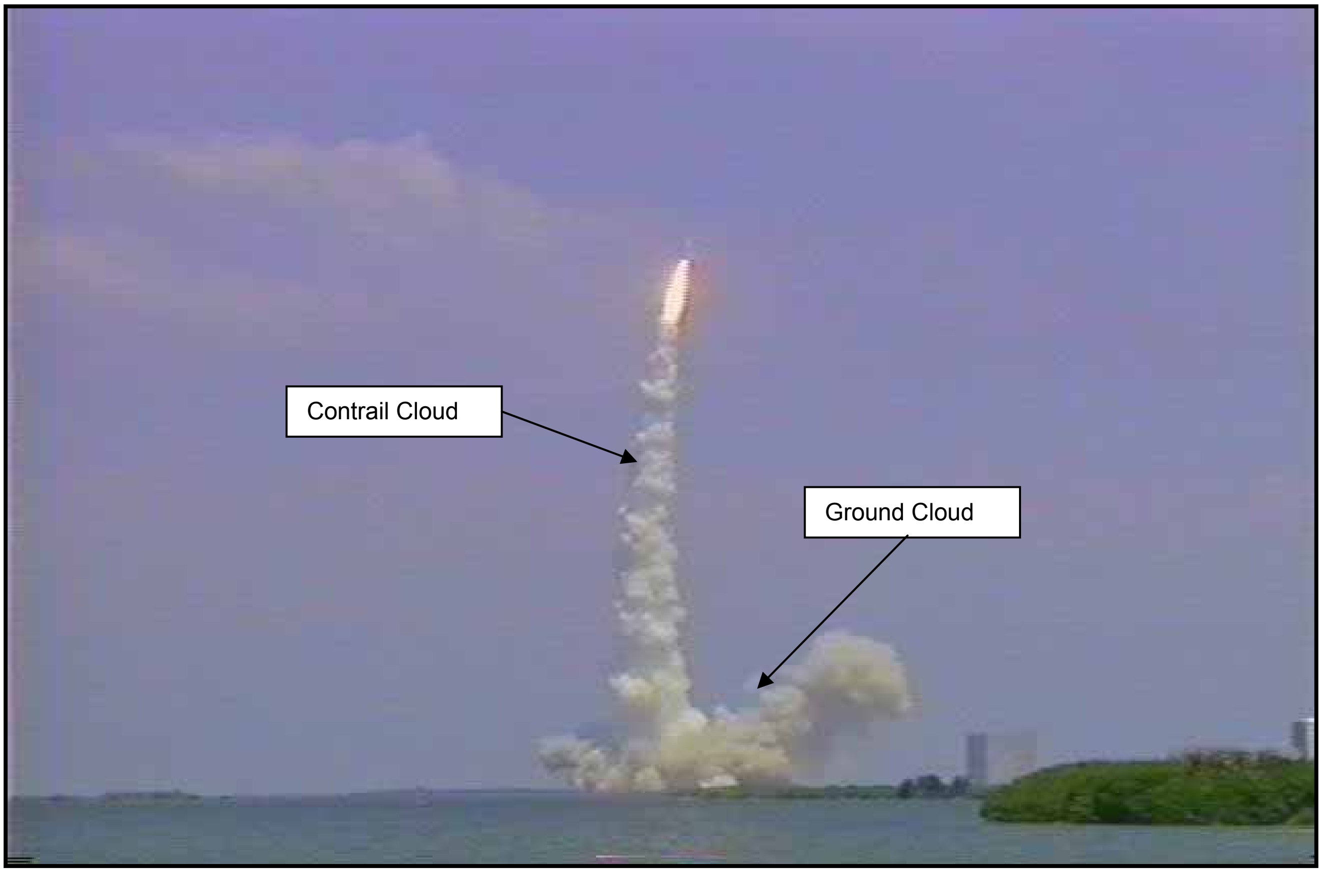

Figure 1-1. Illustration of the Ground Cloud and Contrail Cloud Portions of a Titan IV Rocket Emission Plume Associated With Normal Vehicle Launch.

2. THE ROCKET EXHAUST EFFLUENT DISPERSION MODEL (REEDM)

REEDM is a toxic dispersion model specifically tailored to address the large buoyant source clouds generated by rocket launches, test firings and catastrophic launch vehicle explosions. Under ongoing Air Force support, REEDM evolved from the NASA Multi-Layer Diffusion Model, which was written initially to evaluate environmental effects associated with the Space Shuttle, and has been generalized to handle a wide variety of launch vehicle types and propellant combinations. REEDM falls in the category of "Gaussian puff" atmospheric dispersion models in that the initial mass distribution of toxic materials within the cloud at the time the cloud reaches thermal stabilization height in the atmosphere is assumed to be normally distributed. By making the Gaussian mass distribution assumption, the differential equation defining mass diffusion can be solved in closed form using exponential functions and may be readily implemented in a fast running computer program. Gaussian puff models are still widely used by the EPA for environmental and permitting studies, by Homeland Security and the Defense Threat Reduction Agency for assessment of chemical, biological and radiological materials, and by the petrochemical industry for accidental releases of industrial chemicals.

REEDM processing of an emission event can be partitioned into the following basic steps:

1. Acquire and process vehicle related data from an input vehicle database file.

2. Acquire and process meteorological data, which in this study is a combination of archived weather balloon soundings used in conjunction with an internal REEDM climatological turbulence algorithm.

3. Acquire the chemical composition and thermodynamic properties of the rocket exhaust emissions and define the initial size, shape, location and heat content of the exhaust cloud (herein referred to as the "source term" or "source cloud"). REEDM has an internal propellant equilibrium combustion model that is used to compute these terms for vehicle catastrophic failure modes but for normal launch and static test firing scenarios this data is calculated external to REEDM and placed in the vehicle database file read by REEDM.

4. Iteratively calculate the buoyant cloud rise rate and cloud growth rate to achieve a converged estimate of the cloud stabilization height above ground, size and downwind position. The cloud rise equations evaluate both cloud thermodynamic state as well as the local atmospheric stability, which is defined by the potential temperature lapse rate.

5. Partition the stabilized cloud into disks and mark whether or not part of the stabilized cloud is above a capping atmospheric temperature inversion. Inversions (or other sufficiently stable air masses) act as a barrier to gaseous mixing and are treated in REEDM as reflective boundaries.

6. Transport the cloud disks downwind and grow the disk size using climatologic model estimates of atmospheric turbulence intensity. Turbulence intensity is a function of wind speed and solar radiation intensity. Turbulence varies with time of day and cloud cover conditions because these influence the solar radiation intensity.

7. Calculate concentrations at ground receptor points and determine the plume or cloud track "centerline" that defines the peak concentration as a function of downwind distance. Concentration at any given receptor point is computed as the sum of exposure contributions from each cloud disk. Concentration is solved using the closed form Gaussian dispersion equation and accounts for the effect of ground and capping inversion reflections.

8. Report concentration centerline values in table format as a function of distance from the source origin (e.g. launch pad)

There are other features and submodels of REEDM that are more fully described in the REEDM technical description manual and will not be reviewed in this report.

There are several important assumptions made in REEDM that have a bearing on this Environmental Assessment study. REEDM was designed to primarily predict hazard conditions downwind from the stabilized exhaust cloud. REEDM does not directly calculate or report cloud concentrations during the buoyant cloud rise phase, however, advanced model users can extract sufficient pertinent cloud data from internal calculations to derive concentration estimates during the cloud rise phase manually. One assumption that REEDM makes about the nature and behavior of a rocket exhaust cloud is that it can be initially defined as a single cloud entity that grows and moves but remains as a single cloud during the formation and cloud rise phases. A consequence of this assumption is that once the cloud lifts off the ground during the buoyant cloud rise phase, there will be no predicted cloud chemical concentration on the ground immediately below the cloud. Ground level concentrations will be predicted to remain at zero ppm until the some of the elevated cloud material is eventually brought back down to ground level by mixing due to atmospheric turbulence. This concept is illustrated in Figure 2-1 and it is noted that REEDM is designed to report concentrations downwind from the stabilized cloud position. The region downwind from the stabilized exhaust cloud is referred to as the "far field". It is also noted here that the most concentrated part of these rocket exhaust clouds remains at an altitude well above the ground level. REEDM is not able to model stochastic uncertainty in the source cloud and atmospheric flow such that if a gust of wind, small turbulence eddy or nuance of the launch pad flame duct structure causes a small portion of the main exhaust cloud to detach from the main cloud, the model will not correctly predict the transport, dispersion or concentration contribution from the detached cloud material. Likewise if there are strong atmospheric updrafts or down drafts, such as associated with development of thunderstorm cells or towering cumulus clouds, REEDM will not correctly model strong vertical displacements of the entire exhaust cloud or strong shearing forces that may completely breakup the cloud under such conditions (these are not favorable conditions for launch either and a planned launch would never be conducted with strong thunderstorm and cloud development activity in the launch area).

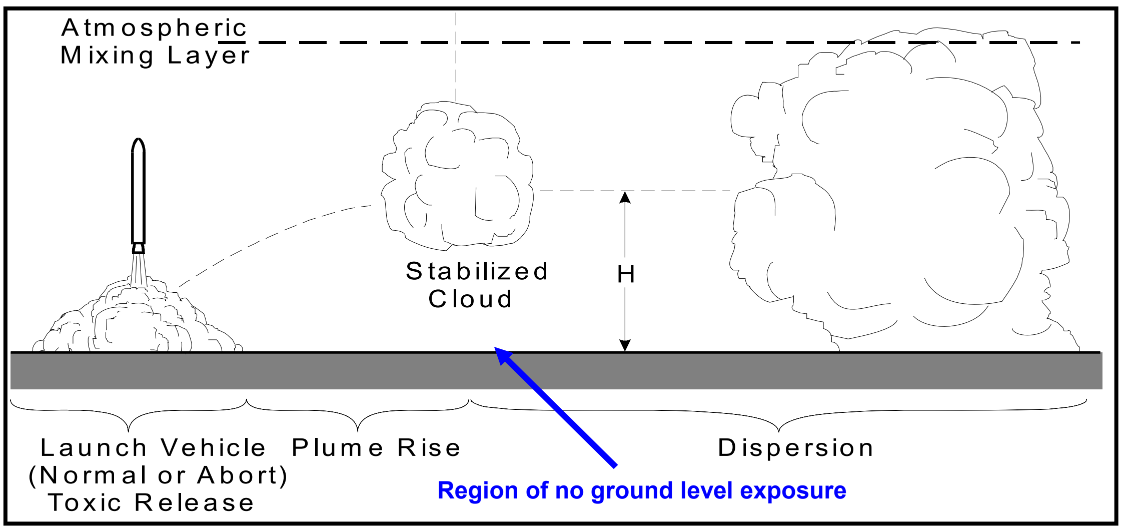

Figure 2-1. Conceptual Illustration of Rocket Exhaust Source Cloud Formation, Cloud Rise and Cloud Atmospheric Dispersion.

REEDM is also somewhat constrained by the Gaussian assumptions inherent in the model that require a single average transport wind speed and direction. The portion of the atmosphere selected for averaging the transport winds has been improved over the years of operational use at the Air Force ranges. Old versions of REEDM averaged the winds over the entire boundary layer, which in the absence of a capping inversion, was treated as being 3000 meters deep. The modern version of REEDM now selects the appropriate atmospheric layer based on the stabilization height of the cloud, the top of the cloud and the location of the reflective boundary layers. Comparison of REEDM predicted rocket exhaust cloud transport direction and speed with Doppler weather radar tracks of rocket exhaust clouds has indicated that the modern version of REEDM performs very satisfactorily in predicting the correct average cloud transport direction and speed. The "multi-layer" aspect of REEDM is still retained from its early development and refers to the partitioning of the stabilized rocket exhaust cloud into "disks" of cloud material assigned to meteorological levels at different altitudes. The altitude bands are typically 20 to 50 meters in depth. REEDM models the initial formation of a rocket exhaust cloud as either an ellipsoid or a sphere and predicts the buoyant could rise of the source as a single cloud entity. Once the cloud is predicted to have achieved a condition of thermal stability in the atmosphere, the cloud is partitioned into disks. The placement of each disk relative to the source origin (e.g. the launch pad) is determined based on the rise time of the cloud through a sequence of meteorological layers that are defined using the measurement levels obtained from a mandatory weather balloon input data file. Each meteorological layer may have a unique wind speed and direction that displaces the cloud disk in the down wind direction. The initial placement of cloud disks that are associated with the lower portion of the overall source cloud are not influenced by winds above their stabilized altitude level whereas disks near the top of the stabilized cloud will be displaced by the winds all the way from the ground level to the disk stabilization altitude. Thus the vertical stack of cloud disks can be displaced relative to each other due to the influence of wind speed and direction shears. The concept of the stabilized cloud partition into disks is illustrated in Figure 2-2.

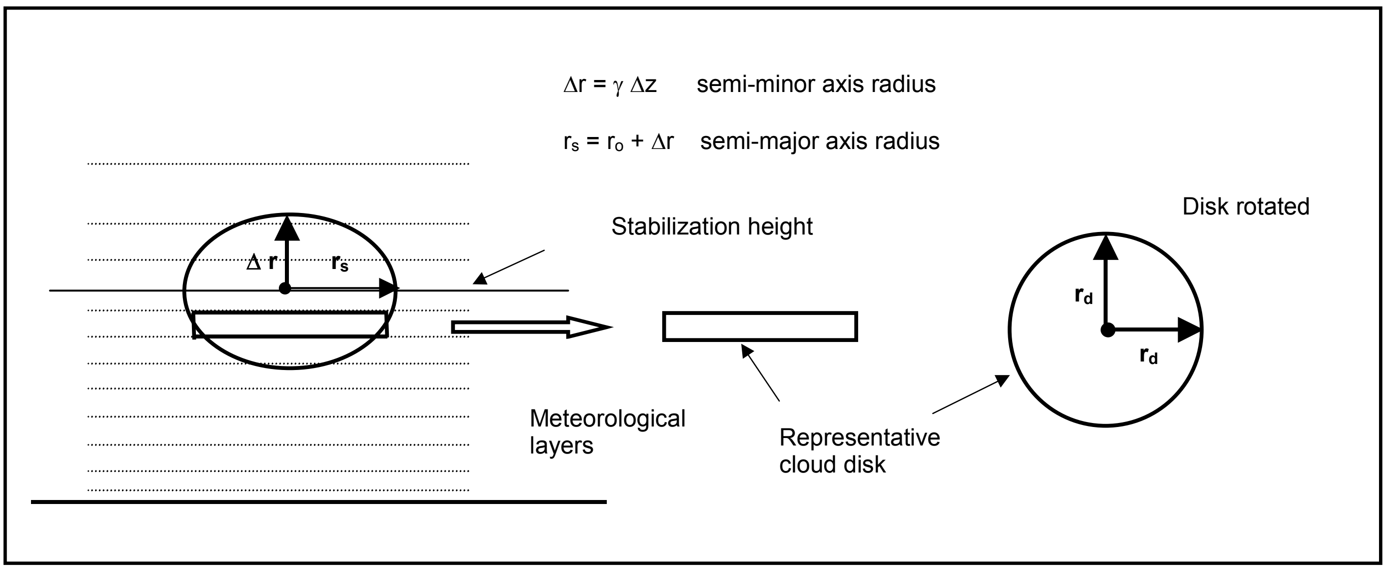

Figure 2-2. Illustration of REEDM Partitioning a Stabilized Cloud into Disks.

Once the cloud disks positions are initialized, future downwind transport applies the same average atmospheric boundary layer transport wind speed and direction to each cloud disk as illustrated in Figure 2-3.

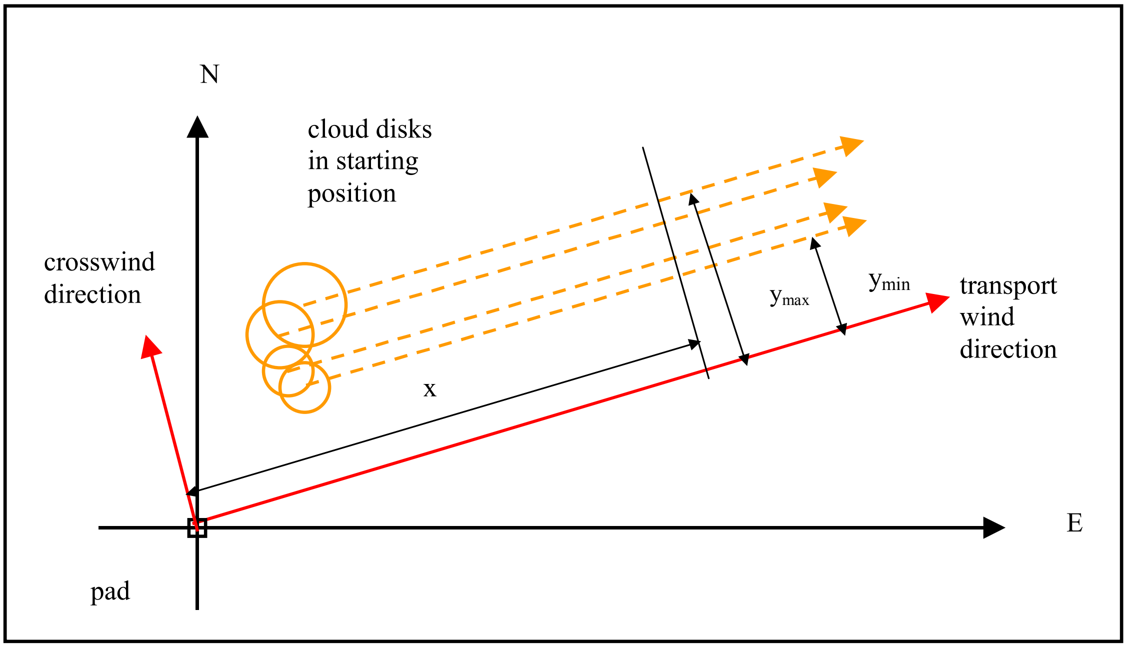

Figure 2-3. Illustration of Straight Line Transport of Stabilized Exhaust Cloud Disks Using Average Mixing Layer Wind Speed and Direction.

The assumption of straight-line transport used in REEDM during the cloud transport and dispersion phase ignores the possibility of complex wind fields that might arise in mountainous terrain or that could evolve during passage of a seabreeze front or synoptic scale weather front. It is recommended that the assumption of uniform winds be limited to plume transport distances of less that 20 kilometers. As will be shown in the analysis results section, REEDM predicted typical ranges of 5 to 10 kilometers from the launch pad to the location of the maximum far field ground level CO concentration point, thus the assumption of straight line transport should not be a problem.

In both Taurus II scenarios the exhaust emissions from the rocket combustion are at several thousand degrees Kelvin and are highly buoyant. The high temperature of these exhaust emissions causes the plume to be less dense than the surrounding atmosphere and buoyancy forces acting on the cloud cause it to lift off the ground and accelerate vertically. As the buoyant cloud rises, it entrains ambient air and grows in size while also cooling. In this initial cloud rise phase, the growth of the cloud volume is due primarily to internal velocity gradients and mixing induced by large temperature gradients within the cloud itself. Even though the cloud is entraining air and cooling by virtue of mixing hot combustion gases with cooler ambient air, the net thermal buoyancy in the cloud is conserved and the cloud will continue to rise until it either reaches a stable layer in the atmosphere or the cloud vertical velocity becomes slow enough to be damped by viscous forces. REEDM applies the following solution of Newton's second law of motion to a buoyant cloud in the atmosphere to iteratively predict cloud stabilization height:

$$z(t) = \left[\frac{3F_m}{u\gamma^2\sqrt{s}} \sin\left(t\sqrt{s}\right) + \frac{3F_c}{u\gamma^2 s}\left(1 - \cos\left(t\sqrt{s}\right)\right) + \left(\frac{r_o}{\gamma}\right)^3 \right]^{1/3} - \frac{r_o}{\gamma}$$

where:

s = atmospheric stability parameter = $\dfrac{g}{\theta_a} \dfrac{\Delta\theta_a}{\Delta Z}$ [sec^{-2}]

g = gravitational acceleration constant = 9.81 [m/sec^2]

θ_a = potential temperature of ambient air [K]

F_m = $r_o^2 w_o u$ = initial vertical momentum [m^4/sec^2]

u = mean ambient wind speed [m/sec]

w_o = initial vertical velocity [m/sec] (typically = 0.0)

r_o = initial plume cross-sectional radius [m]

F_c = initial buoyancy = $\dfrac{g\,\dot{q}}{\pi\,\rho_c\,C_p\,T_a}$ [m^4/s^3]

C_p = specific heat of exhaust cloud gases [cal/kg K]

γ = air entrainment coefficient (dimensionless)

z = plume height at time t [m]

$\dot{q}$ = initial plume heat flux [cal/sec]

T_a = ambient air temperature [K]

ρ_c = density of exhaust cloud gases [kg/m^3]

A critical parameter in the cloud rise equation is the rate of ambient air entrainment that is defined by the dimensionless air entrainment coefficient, γ. Cloud growth as a function of altitude is assumed to be linearly proportional and the air entrainment coefficient defines the constant of proportionality. REEDM's cloud rise equations have been compared with observations and measurements of Titan rocket ground clouds and a best-fit empirical cloud rise air entrainment coefficient has been derived from the test data, a sample of which is illustrated in Figure 2-4.

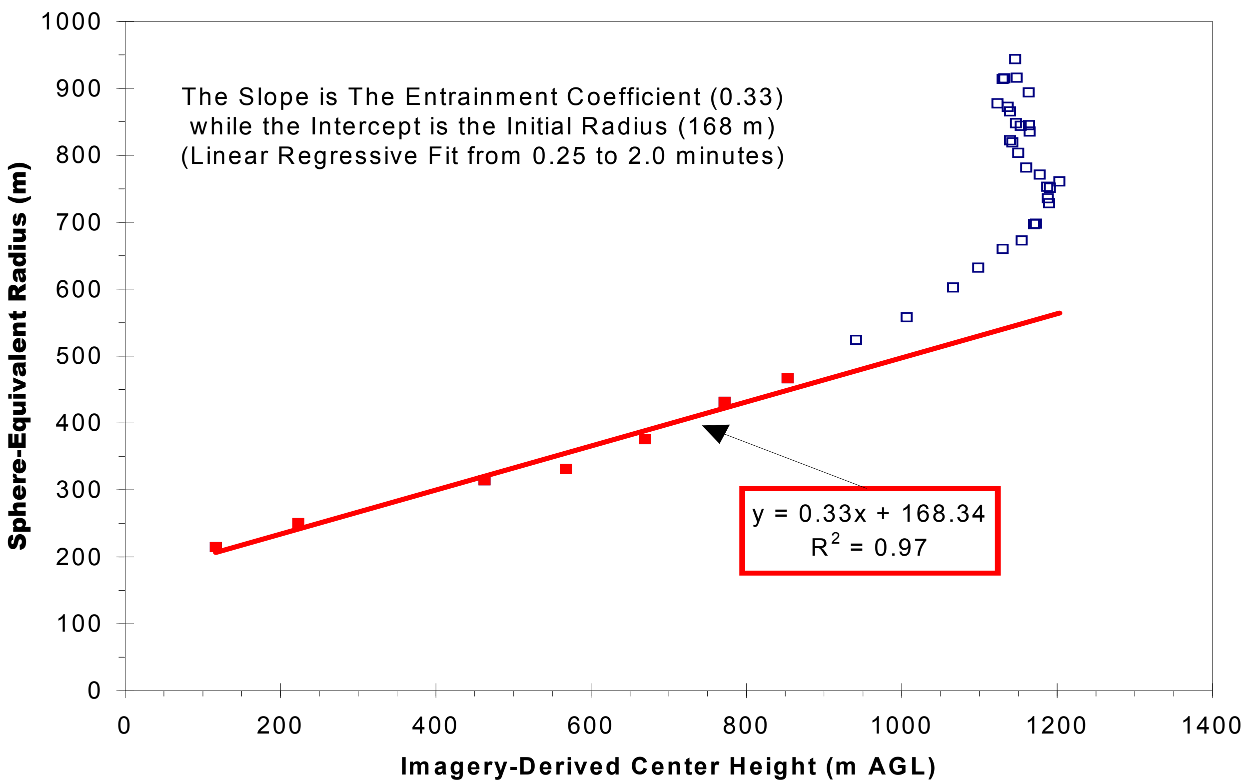

Figure 2-4. Observed Cloud Growth Versus Height for Titan IV A-17 Mission.

The Taurus II buoyant source clouds are predicted to rise from 500 to 1300 meters above the ground depending on atmospheric lapse rate conditions.

3. TAURUS II DATA DEVELOPMENT

Proper specification of vehicle characterization input data is critical to the overall toxic dispersion analysis problem. While many vehicle input parameters are straightforward and readily verifiable (e.g. types and amounts of propellants loaded on the vehicle), other parameters inherently involve greater uncertainty and are not readily verifiable (e.g. amount of ambient air entrained into the rocket plume at the flame duct inlet). In this report section the vehicle input data values used in the REEDM Taurus II normal launch and static test firing scenario analyses are itemized and explained. Input parameters that entail significant uncertainty were treated in a conservative fashion in the sense that choices were made to favor overestimating rather than underestimating the toxic chemical concentrations being evaluated for the Environmental Assessment study. Information pertaining to the vehicle propellant loads, burn rates and expected nominal launch flight trajectory were provided by WFF NASA or Orbital Sciences personnel and converted by ACTA into REEDM database format.

3.1 Normal Launch Vehicle Data

The following data items represent the vehicle data needed to characterize the normal launch scenario and are presented in the REEDM database format.

```
#05.00                       VEHICLE DATA SECTION
   VEHICLE TYPE = 4, NAME =     TAURUS-II,
   TIME HEIGHT COEFFICIENTS A,B,C =     0.967700,     0.471980,       2.2000,
#05.01 NORMAL LAUNCH ENGINE DATA FOR STAGES IGNITED AT LIFT-OFF:
   NUMBER OF IGNITED SRB'S           =   0,
   SOLID FUEL MASS             (LBM) =   0.0000000,
   SOLID FUEL BURN RATE      (LBM/S) =   0.0000000,
   LIQUID FUEL MASS            (LBM) =  142735.000,
   LIQUID FUEL BURN RATE     (LBM/S) =   645.90000,
   LIQUID OXIDIZER MASS        (LBM) =  390779.000,
   LIQUID OXIDIZER BURN RATE (LBM/S) =   1768.2000,
   AIR ENTRAINMENT RATE IN GROUND CLOUD       (LBM/S) =   0.0000000,
   TOTAL DELUGE WATER ENTRAINED IN GROUND CLOUD (LBM) =   0.0000000,
   AIR ENTRAINMENT RATE IN ROCKET CONTRAIL    (LBM/S) =   0.0000000,
   VEHICLE HEIGHT TO WHICH PLUME CONTRIBUTES TO GROUND CLOUD (FT) = 525,
   GROUND CLOUD INITIAL AVERAGE TEMPERATURE         (F) =  3487,
   GROUND CLOUD INITIAL HEAT CONTENT          (BTU/LBM) =  3475,
   INITIAL VERTICAL VELOCITY OF GROUND CLOUD     (FT/S) =   0.0,
   INITIAL RADIUS OF GROUND CLOUD                  (FT) = 160.0,
   INITIAL HEIGHT OF GROUND CLOUD                  (FT) =   0.0,
   INITIAL X DISPLACEMENT OF GROUND CLOUD FROM PAD (FT) =   0.0,
   INITIAL Y DISPLACEMENT OF GROUND CLOUD FROM PAD (FT) =   0.0,
   PLUME CONTRAIL INITIAL AVERAGE TEMPERATURE       (F) =  3487,
   PLUME CONTRAIL INITIAL HEAT CONTENT        (BTU/LBM) =  3475,
#05.02 NORMAL LAUNCH EXHAUST PRODUCT DATA:
 CHEMICAL NAME     MOL. WT.   MASS FRAC. GAS   MASS FRAC. COND  HAZARDOUS
 GROUND CLOUD:
   CO2              44.011        0.44824          0.00000           Y
   CO               28.011        0.25637          0.00000           Y
   H2O              18.015        0.28893          0.00000           N
```

```
  H2               2.016        0.00557         0.00000          N
  OH              17.007        0.00077         0.00000          N
  H                1.008        0.00006         0.00000          N
  O2              31.999        0.00005         0.00000          N
  O               15.999        0.00001         0.00000          N
  END
CONTRAIL:
  CO2             44.011        0.44824         0.00000          Y
  CO              28.011        0.25637         0.00000          Y
  H2O             18.015        0.28893         0.00000          N
  H2               2.016        0.00557         0.00000          N
  OH              17.007        0.00077         0.00000          N
  H                1.008        0.00006         0.00000          N
  O2              31.999        0.00005         0.00000          N
  O               15.999        0.00001         0.00000          N
  END
```

REEDM does not utilize the launch vehicle trajectory directly; instead a power law fit to the height of the vehicle above ground as a function of time is derived from the trajectory data. The fit achieved with the derived power law time-height coefficients is demonstrated in Figure 3-1

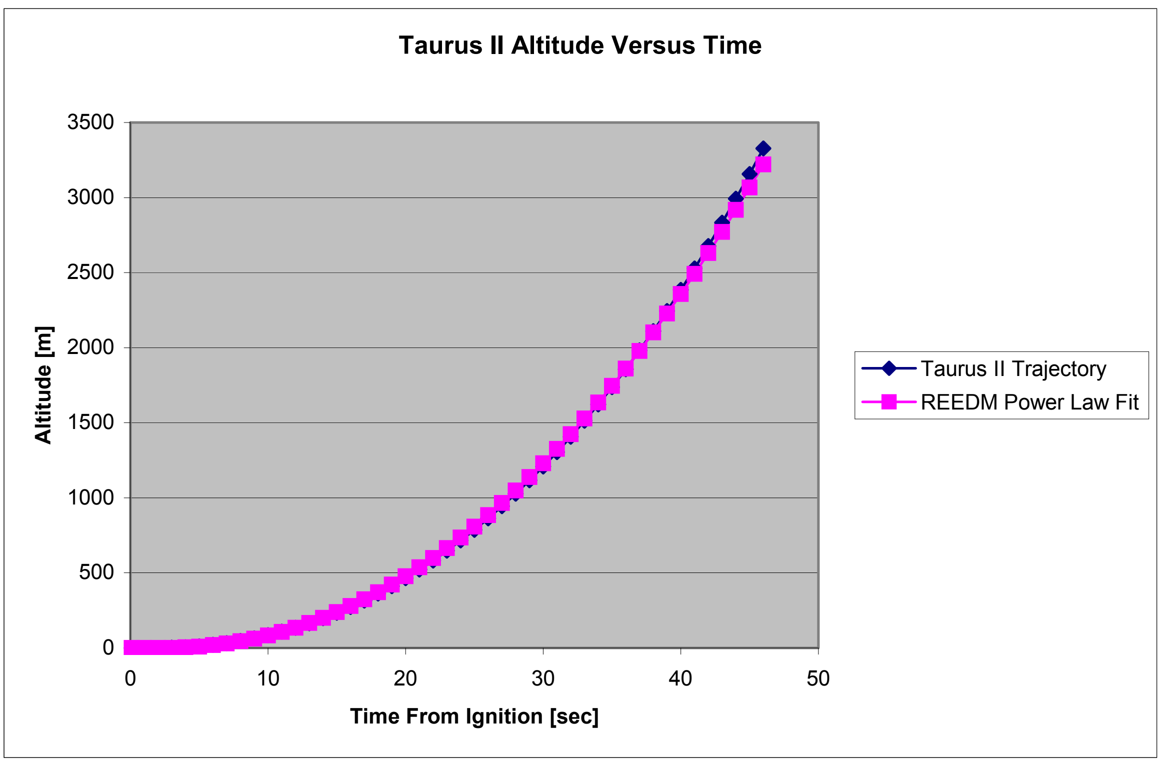

Figure 3-1. Plot of Vendor Taurus II Nominal Trajectory Compared with ACTA Derived Power Law Fit Used in REEDM.

REEDM allows for several chemical additions that may be included in the propellant exhaust of the normal launch ground cloud and the normal launch contrail cloud. In addition to specifying the nominal burn rates of the RP-1 fuel and the LOX oxidizer, the user may optionally consider adding deluge or sound suppression water and entrained ambient air. For these two items the REEDM database serves only as a source of documentation for the assumptions applied in deriving the chemical compositions of the exhaust specified in section #05.02 of the database. It is noted here that "air entrainment" as specified in this section represents the user assumption about the amount of air, if any, added as a ***reactant*** in the propellant combustion calculations. This "air entrainment" definition is not to be confused with the "air entrainment" process that takes place during the cloud rise calculations. REEDM assumes that all chemical combustion reactions are completed before the cloud rise process takes place and REEDM therefore does not attempt to recompute chemical composition and additional heat release during the cloud rise computations.

The REEDM database provides the chemical composition of the normal ground and contrail clouds. A mass fraction is assigned to each constituent and the total exhaust mass in the source cloud is multiplied by this fraction to determine the total mass of each chemical in the exhaust cloud. The molecular weight of each species is used to convert the concentration from mass per unit volume [e.g.mg/m^3] to parts per million. For this study ACTA computed the chemical composition of the Taurus II stage 1 RP-1/LOX exhaust using the NASA Lewis chemical equilibrium combustion model. The ACTA version of the NASA combustion model was modified slightly to output thermodynamic properties of the exhaust mixture that were needed to initialize the REEDM cloud rise equations. ACTA's combustion results for the Taurus II first stage agreed within 2% for the major constituents (CO, CO_2, H_2O) compared with similar data provided by Orbital Sciences 0 as shown in Table 3-1. ACTA ran the NASA combustion model in "rocket" analysis mode using an oxidizer to fuel ratio of 2.7 and a combustion chamber pressure of 2194 PSIA. The Orbital analysis appears to have been conducted with a newer version of the NASA equilibrium combustion model and was executed with a slightly different nozzle to throat area ratio than the ACTA model. The supporting thermodynamic databases between the two versions of the combustion models may also differ slightly. ACTA considers the small chemical composition differences to have insignificant effect on the analysis results and conclusions of this study.

Table 3-1. Comparison of ACTA and Orbital Taurus II Stage-1 Combustion Model Nozzle Exit Results.

Chemical	ACTA Mole Fraction	Orbital Mole Fraction	Ratio ACTA/Orbital
CO_2	0.26632	0.27071	0.984
CO	0.23932	0.23532	1.017
H_2O	0.41938	0.41627	1.007
H_2	0.07231	0.07650	0.945
OH	0.00118	0.00048	2.458
H	0.00144	0.00072	2.000
O_2	0.00004	0.00001	4.000
O	0.00002	0.00000	--

Both ACTA and Orbital ran combustion for only RP-1 and LOX and the chemical compositions listed in Table 3-1 do not consider the shift in chemical equilibrium that takes place if ambient air or water are added to the nozzle exit exhaust mixture.

3.2 Static Test Firing Vehicle Data

The REEDM database also includes a data section used to define the parameters that characterize a static test firing scenario. The data developed for the Taurus II stage-1 static test firing is listed as follows:

```
#05.20 TEST FIRING ENGINE DATA:
   SOLID FUEL MASS                           (LBM) = 123552.,
   SOLID FUEL BURN RATE                    (LBM/S) =   2376.,
   AIR ENTRAINMENT RATE IN CLOUD           (LBM/S) =       0,
   TOTAL DELUGE WATER ENTRAINED IN CLOUD     (LBM) =       0,
   CLOUD INITIAL AVERAGE TEMPERATURE           (F) =    3487,
   CLOUD INITIAL HEAT CONTENT            (BTU/LBM) =    3475,
   INITIAL VERTICAL VELOCITY OF CLOUD       (FT/S) =     0.0,
   INITIAL RADIUS OF CLOUD                    (FT) =   151.1,
   INITIAL HEIGHT OF CLOUD                    (FT) =     0.0,
   INITIAL X DISPLACEMENT OF CLOUD FROM STAND (FT) =     0.0,
   INITIAL Y DISPLACEMENT OF CLOUD FROM STAND (FT) =     0.0,
#05.21 TEST FIRING PLUME CHEMISTRY  DATA:
 CHEMICAL NAME      MOL. WT.   MASS FRAC. GAS   MASS FRAC. COND  HAZARDOUS
   CO2               44.011       0.44824          0.00000           Y
   CO                28.011       0.25637          0.00000           Y
   H2O               18.015       0.28893          0.00000           N
   H2                 2.016       0.00557          0.00000           N
   OH                17.007       0.00077          0.00000           N
   H                  1.008       0.00006          0.00000           N
   O2                31.999       0.00005          0.00000           N
   O                 15.999       0.00001          0.00000           N
   END
```

The REEDM static test firing scenario was originally developed for burns of solid propellant motors and the nomenclature used in the database is outdated and somewhat misleading. In the case of the Taurus II first stage test firing the line items identified as "solid fuel mass" and "solid fuel burn rate" are set to represent the total quantity of RP-1 + LOX and the average burn rate of the RP-1 + LOX mixture consumed during a 52 second static burn. The chemical composition of the static test firing exhaust is set the same as the normal launch ground cloud. As with the normal launch scenario, the effects of plume afterburning and deluge water injection are ignored.

3.3 Conservative Assumptions Applied In Data Development

The REEDM atmospheric dispersion model has been used operationally by the Air Force to make range safety launch decisions since 1989. During that time vehicle databases have been developed for many vehicles (e.g. Space Shuttle, Titan II, Titan III, Titan IV, Delta II, Delta III, Delta IV, Atlas II, Atlas III, Atlas V, Taurus, TaurusXL, Taurus Lite, Minotaur, Peacekeeper, Minuteman II, Minuteman III, Athena, Lance, Scud, ATK-ALV-1). As noted at the beginning of this section, some vehicle data is easily obtained and verified, such as the stage propellant types, quantities and burn rates. Other model input parameters required by REEDM are based on derived values obtained from mathematical and physical models, empirical measurement data or engineering judgment from the vehicle designer or range safety experts.

An example of a derived value is the selection of how much pad deluge water to include with the rocket engine exhaust when defining the normal launch cloud heat content, mass and chemical composition. A typical pad deluge system is comprised of a series of pressure fed sprayers and sprinkers that wet the launch pad, the launch service tower and the flame duct. The deluge system is typically turned on several seconds before the rocket motors are ignited and continues until the rocket has ascended above the launch tower and the plume no longer impinges on the ground. As the vehicle ascends, the rocket plume interaction with the pad structures is time varying, such that the gas flow velocity ranges from supersonic to subsonic and involves multiple shock fronts, reflected shocks, deflected flow from the pad surface, partial flow ducting through the flame trench and plume temperatures that range from 300 to 3000 K. A simple energy balance between the amount of heat available in the plume and the amount of water released in the deluge system may suggest that there is ample energy to vaporize all of the deluge water, but actual observation of launches indicates that residual deluge water is often collected in a concrete containment basin designed to collect residual deluge water. Likewise the initial ignition impulse often blows standing water out of the flame trench or away from the pad and depositing it as droplets before they can be fully mixed with the combustion gases and vaporized. Some parts of the launch plume during vehicle liftoff may become saturated with water vapor and other portions may remain relatively “dry”. Thus the task of selecting a specific deluge water inclusion amount for the REEDM database and setting the associated chemical and thermodynamic data for the exhaust products is challenging and typically not estimated by the launch agency or vehicle developer. This type of flow problem is extremely complex and would require advanced computational fluid dynamics analysis that is extremely costly and also constrained by modeling assumptions. Consequently, these types of detailed analyses are rarely performed or conducted only for limited specific design purposes.

Other examples of highly uncertain processes are the mixing of propellants from ruptured tanks in a vehicle explosion, and the fragmentation of a solid rocket motor propellant grain in the event of a case rupture. These latter events are related to vehicle failures that are not considered in this study, however, they illustrate the problem routinely faced by the launch community when attempting to set up REEDM database entries to model these scenarios. Historically the range safety community has taken a conservative approach in setting these uncertain database entries. The vast majority of vehicles characterized in the REEDM database ignore deluge water contributions (a notable exception being Shuttle). One reason for ignoring the deluge water effect is that it is known that water vapor and water droplets scrub hydrogen chloride (a common solid propellant toxic exhaust product) from the launch plume but the degree of the effect is difficult to quantify and verify, therefore ignoring this removal mechanism favors maximizing the downwind ground level concentrations of HCl at receptor sites of concern that must be protected.

The same philosophy of erring in favor of overestimating rather than underestimating potential emission hazards has been applied in this study of the Taurus II carbon monoxide emissions. There are two main factors to which conservative assumptions have been applied in this study; 1) ambient air entrainment and its effect on plume afterburning chemistry, and 2), deluge water injection into the plume. Both of these factors are discussed in further detail in the following paragraphs with an explanation for why it is believed that the REEDM modeling assumptions applied in this study are in fact conservative.

It is recognized that the Taurus II, like most rocket engines, is designed to run somewhat fuel rich for efficiency reasons and that the exhaust products will contain compounds (mainly CO and OH) that are not fully oxidized. Entrainment of ambient air into the superheated gases exiting from the rocket nozzle will allow for further oxidation in the plume, a process referred to as plume afterburning. The rate of air entrainment into the plume and the amount of additional oxidation that occurs in the plume downstream from the nozzle exit plane requires sophisticated computation fluid dynamic (CFD) solutions of the plume flow as it decelerates through multiple shock front to subsonic velocity that are beyond the design capabilities and run time requirements of REEDM. In this study ACTA has ignored the effect of air entrainment on the combustion products and heat content of the normal launch ground cloud and contrail cloud emissions. Ignoring air entrainment and after burning is assumed to be conservative for this study in that the ground level CO concentration predictions will err on the side of overestimating rather than underestimating the concentration for the following two reasons:

1. Ignoring ambient air entrainment in the combustion calculations will favor production of CO rather than CO_2 and CO is the more toxic species.

2. Ignoring ambient air afterburning reduces the total amount of heat released by the combustion process, which in turn leads to a lower stabilized cloud height prediction. Ground level concentrations of cloud chemicals vary approximately with the inverse cube of the stabilization height (e.g. doubling the cloud stabilization height reduces the ground concentrations by about a factor of 8, other factors being constant). Lower stabilization height therefore favors higher ground level CO predictions.

A deluge water system is planned for the Taurus II launch pad and serves to cool pad structures exposed to rocket engine exhaust as well as to suppress acoustic vibrations during motor ignition. An objective of the deluge water system design is to inject water into the plume just downstream of the nozzle exit plane at a rate of 2 lbm of water for every lbm of rocket propellant exhaust. Water is expected to chemically react with the high temperature rocket engine exhaust gases, which are fuel rich. In this situation water acts as an oxidizer and gives up oxygen to convert CO to CO_2 in the plume while simultaneously releasing hydrogen gas. The reaction between high temperature CO and H_2O is referred to as the "water-gas shift" reaction. ACTA evaluated the effect of 2:1 water to rocket exhaust mixing on the plume chemistry immediately downstream of the nozzle exit plane by running the NASA Lewis chemical equilibrium combustion model 0, 0 using the RP-1/LOX nozzle exit products as high temperature reactants at 2193 K mixed with liquid water at 298 K. The input reactant information entered into the combustion model is listed below:

NASA Lewis Combustion Model Input Reactants for RP-1/LOX Exhaust Products and Deluge Water Mixture.

```
THERMO
TRAN
REACTANTS
C 1.     O 2.0                         63.111  -69368.  G 2193.  F
C 1.     O 1.0                         36.096  -11178.  G 2193.  F
H 2.                                    0.784   14240.  G 2193.  F
H 1.                                    0.008   61472.  G 2193.  F
H 2.     O 1.0                         87.345  -68267.  L  298.  O
H 2.     O 1.0                         12.619  -37989.  G 2193.  O
O 2.                                    0.002   15877.  G 2193.  O
O 1.     H 1.0                          9.631   23759.  G 2193.  O
```

```
NAMELISTS
 &inpt2 kase=1,hp=t,p=1.000,of=t,mix=3.2239,siunit=t &end
```

The predicted combustion products and thermodynamic state properties for the exhaust plume + water mixture are listed below. Post combustion products are highlighted. Note that the plume is cooled from 2193 K to 856 K, but remains unsaturated. The predicted amount of CO in the exhaust has dropped from 25.6% to 0.3%, a reduction factor of approximately 100. CO_2 concentration is predicted to decrease from 44.8% to 27.9%. The total amount of CO_2 produced has actually increased but the percentage relative to the total exhaust mixture mass has decreased.

NASA Lewis Combustion Model Output Products for RP-1/LOX Exhaust and Deluge Water Mixture.

```
0                  O/F=   3.2239     PERCENT FUEL=   23.6748     EQUIVALENCE RATIO= 1.0383     PHI=
2.0181
0THERMODYNAMIC PROPERTIES

 P, MPA            0.10132
 T, DEG K           856.32
 RHO, KG/CU M    2.9654-1
 H, KJ/KG         -11095.9
 U, KJ/KG         -11437.6
 G, KJ/KG         -20674.8
 S, KJ/(KG)(K)     11.1861

 M, MOL WT          20.837
 (DLV/DLP)T       -1.00000
 (DLV/DLT)P         1.0000
 CP, KJ/(KG)(K)     1.9758
 GAMMA  (S)         1.2531
 SON VEL,M/SEC       654.3
   trace =    0.000000000000000E+000
   npt   =             1
 total product molecular wt. (including condensed sp) = 20.837

0MOLE FRACTIONS

   oxidizer mass fraction =    0.7632520
   fuel mass fraction     =    0.2367480
  C O           -69368.0    44.010  F    0.6311
  C O           -11178.0    28.010  F    0.3610
  H              14240.0     2.016  F    0.0078
  H              61472.0     1.008  F    0.0001
  H O           -68267.0    18.015  O    0.7970
  H O           -37989.0    18.015  O    0.1151
  O              15877.0    31.999  O    0.0000
  O H            23759.0    17.007  O    0.0879

   oxfl =     3.22390007972717
   temperature =     856.317902340247
   Total reactant enthalpy [cal/g] =    -2651.987

   INJECTOR CONDITIONS
chemical     mole      mole wt    wt       wt      hval       hf298        heat   heat@stag    hstag
             frac                 kg      frac   cal/gmole  cal/gmole      cal       cal    cal/gmole

 H2O         0.82599  18.015 14.88037 0.71412  -52929.2   -57754.7     3985.8     3985.8   -52929.2
 CO2         0.13216  44.010  5.81651 0.27914  -87837.4   -93983.8      812.3      812.3   -87837.4
 H2          0.03969   2.016  0.08002 0.00384    3910.7        0.6      155.2      155.2     3910.7
 CO          0.00215  28.010  0.06027 0.00289  -22342.6   -26398.0        8.7        8.7   -22342.6

  total kg products (per kgmole) =     20.83716
```

```
total heat of form. of prod. [cal/gmole] =   -60182.82
enthalpy of prod. at plume T [cal/gmole]=   -55220.72
heat content of prod. @ plume T & V [cal/gmole] =    4962.093
heat content of prod. @ plume T & V [cal/g] =    238.1358
total weight fractions of products =   0.9999962
total mole fractions of products =   0.9999994
gas velocity [m/sec] =   0.0000000E+00
stagnation enthalpy of prod. [cal/gmole]=   -55220.72
heat content of prod. @ stag T & V = 0 [cal/gmole] =    4962.093
heat content of prod. @ stag T & V = 0  [cal/g] =    238.1358
total heat of form. of reac. [cal/g] =   -2651.987
heat of combustion [cal/g] =    236.2465
```

The addition of deluge water has another effect in that it may reduce the net heat content of the cloud in proportion to the amount of liquid deluge water that is converted to gaseous phase and does not chemically react with other plume constituents. The amount of liquid water that is vaporized and then does not re-condense during the cloud rise phase reduces the cloud buoyancy. The effects of deluge water on the plume chemistry and plume rise where ignored in this study, in part because the normal launch plume has a time varying interaction with the deluge system and transitions from a high water injection condition to an essentially dry plume. Ignoring deluge or sound suppression water injection into the plume is expected to be conservative in that it should lead to model predictions that overestimate the downwind ground level CO concentrations. The reduction of in-cloud CO is expected to far outweigh the reduction in cloud stabilization height due to loss of thermal buoyancy.

4. ANALYSIS OF EMISSION SCENARIOS

The REEDM Taurus II database was used in conjunction with a large set of archived WFF weather balloon soundings to predict downwind concentrations of carbon monoxide and to achieve some statistical perspective of the potential toxic hazard corridors associated with normal launch and static test firing scenarios.

4.1 Meteorological Data Preparation

Gaseous dispersion of rocket exhaust clouds is extremely dependent upon the meteorological conditions at the time the source cloud is generated. The presence or absence of temperature inversions, the temperature lapse rate, wind speed and direction, wind shears and atmospheric turbulence are important factors that influence the cloud rise and rate of dispersion of the source cloud. Meteorological conditions that are adverse from a toxic chemical dispersion perspective are light winds with little wind speed or wind direction variation over the first several thousand feet of the atmosphere coupled with a capping temperature inversion just above the top of the stabilized source cloud. An additional adverse factor is suppression of atmospheric turbulence, as occurs at night or under cloudy or marine stratus and fog conditions.

ACTA acquired and ran REEDM analyses for 6432 meteorological cases based on actual weather balloon measurements made at Wallops Flight Facility between 2000 and 2008. The raw weather balloon data was not in a format usable by REEDM and needed to be preprocessed to reduce the number of measurement levels from several thousand to approximately one hundred, to quality control check the raw data, and to output the data in REEDM compatible format. A computer program written by ACTA and delivered to WFF for operational use in 2007 was used to perform the raw data file conversions. A critical part of the conversion process is to test for, and capture, inflection points where temperature, wind speed, wind direction or relative humidity reach minimum or maximum values and change slope as a function of altitude. An example of the weather profile testing algorithm capabilities is illustrated in Figure 4-1, which is contrived test data with positive, negative and infinite slopes and multiple inflection points. The resulting converted files were sorted into daytime and nighttime sets for each month of the year. Data was classified as “daytime” if the balloon release time was between 0600 and 1900 Eastern Standard Time.

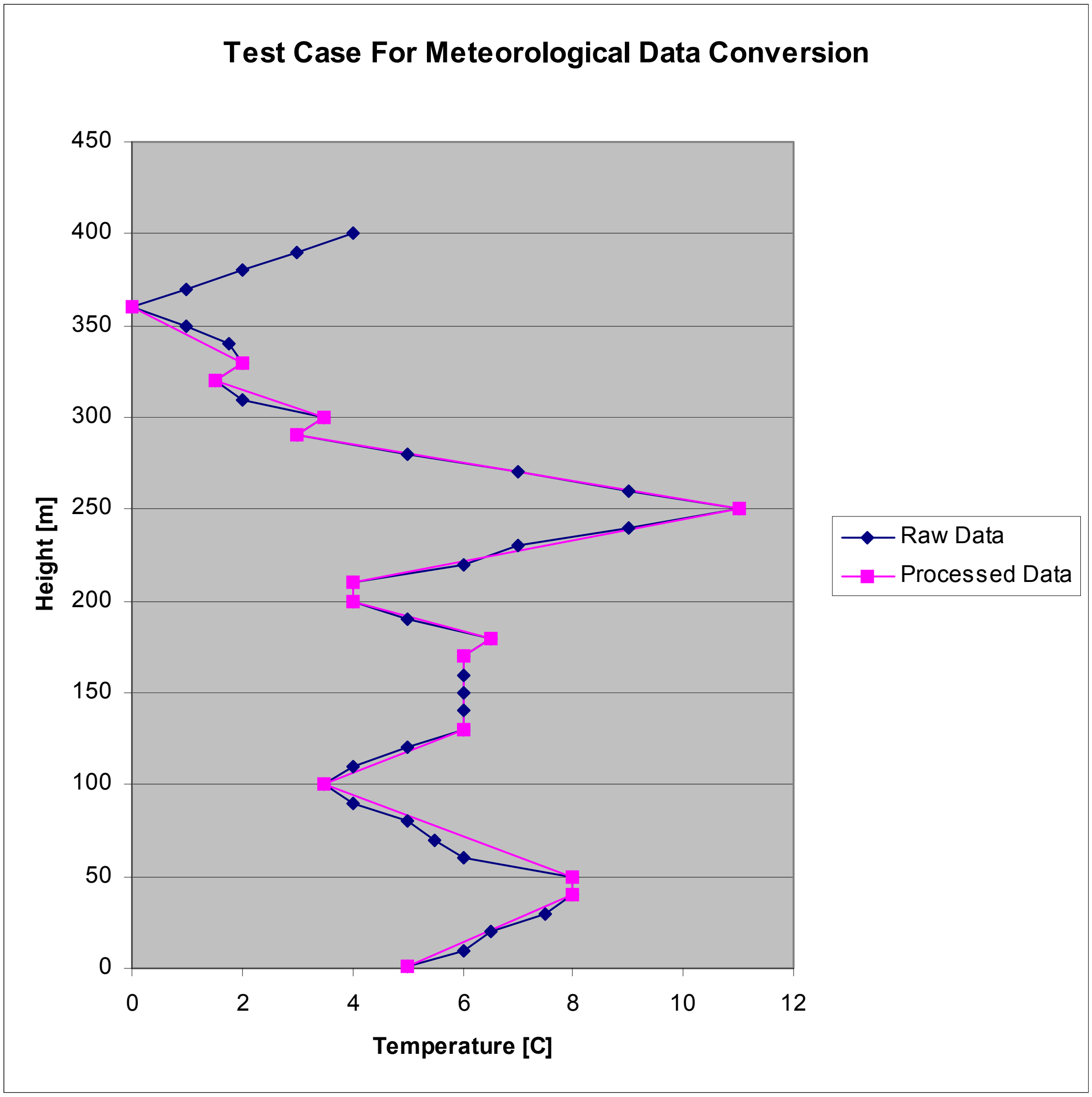

Figure 4-1. Illustration of Testing a Raw Data Profile to Capture Slope Inflection Points that Define Minimum and Maximum Values and Measure Inversions and Shear Effects.

4.2 REEDM Far Field Results For Taurus II Normal Launch Scenario

ACTA executed REEDM in batch processing mode to cycle through all archived meteorological cases and to extract key information to a summary table. Typically REEDM generates an output file for a single weather case that consists of 10 to 20 pages of information on the run setup, intermediate calculated value and tables of concentration versus downwind distance. When processing thousands of cases, saving the standard REEDM output file for each run results in an overwhelming amount of output data. ACTA developed a special batch version of REEDM for the Air Force that has been used over the years to execute thousands of scenarios and condense the REEDM output for all runs into a summary table containing the following critical analysis parameters:

1. Chemical being tracked in REEDM analysis.
2. Concentration threshold used to calculate concentration isopleth beginning and end distances.
3. Meteorological input file name.
4. Zulu time of balloon release.
5. REEDM computed mixing boundary depth.
6. REEDM predicted cloud stabilization height.
7. REEDM predicted average wind speed used to transport exhaust cloud.
8. REEDM predicted average wind direction used to transport exhaust cloud.
9. REEDM predicted maximum ground level concentration.
10. REEDM predicted distance from exhaust cloud source to location of maximum concentration.
11. REEDM predicted bearing from exhaust cloud source to location of maximum concentration.
12. REEDM predicted nearest distance from exhaust cloud source to the location where the ground concentration centerline first exceeds the user defined concentration threshold.
13. REEDM predicted farthest distance from exhaust cloud source to the location where the ground concentration centerline last exceeds the user defined concentration threshold.
14. REEDM predicted bearing from exhaust cloud source to location where the ground concentration centerline last exceeds the user defined concentration threshold.
15. REEDM derived average wind speed shear in the lower planetary boundary layer.
16. REEDM derived average wind direction shear in the lower planetary boundary layer.

17. REEDM derived average horizontal (azimuthal) turbulence intensity in the lower planetary boundary layer.

18. REEDM derived average vertical (elevation) turbulence intensity in the lower planetary boundary layer.

19. REEDM derived average wind speed shear in the region above the planetary boundary layer.

20. REEDM derived average wind direction shear in the region above the planetary boundary layer.

21. REEDM derived average horizontal (azimuthal) turbulence intensity in the region above the planetary boundary layer.

22. REEDM derived average vertical (elevation) turbulence intensity in the region above the planetary boundary layer.

The above list of parameters is provided for REEDM predictions of both peak instantaneous concentration and time weighted average (TWA) concentration. In the runs performed for this study a 1-hour averaging time was used to compute time weighted average concentrations. A fairly short averaging time is appropriate for rocket exhaust cloud exposures because the source cloud typically passes over a receptor with a time scale of tens of minutes rather than hours. The REEDM summary tables from the monthly batch runs were further condensed to identify the meteorological case that produced the highest peak concentration and record the range and bearing from the source location (WFF Taurus II launch Pad-0A). Table 4-1 presents the maximum far field CO peak instantaneous concentration predicted by REEDM for the hypothetical daytime launches of a Taurus II with subsequent dispersion of the normal launch ground and contrail clouds. The far field exposure is REEDM's prediction for concentrations at ground level downwind of the stabilized exhaust cloud. Far field peak CO concentrations ranged from 3 to 8 ppm with the maximum concentration predicted to occur from 5000 to 16000 meters downwind from the launch site. These values represent the maximum concentrations predicted over a sample set of 4704 WFF balloon soundings. Table 4-2 lists the maximum predicted far field 1-hour TWA concentrations of CO for daytime normal launch scenarios. The maximum TWA concentrations are all predicted to be less than 1 ppm. Table 4-3 and Table 4-4 show the REEDM predicted maximum peak and maximum TWA CO far field concentrations for 1728 nighttime cases for Taurus II normal launch scenarios. As with the daytime cases, the peak instantaneous CO concentrations are less than 10 ppm and the peak TWA CO concentrations are less than 1 ppm.

Table 4-1: Taurus II Normal Launch CO Concentration Summary – Daytime Meteorology.

Month	Number of Weather Cases	Peak CO Concentration [ppm]	Distance to Peak CO Concentration [m]	Bearing to Peak CO Concentration [deg]
January	344	4.7	8000	73
February	364	4.9	8000	158
March	397	5.1	7000	285
April	383	6.1	8000	249
May	398	7.9	7000	245
June	392	4.3	6000	258
July	416	5.4	5000	285
August	408	6.0	8000	226
September	413	4.7	9000	22
October	435	2.9	16000	240
November	382	4.0	11000	205
December	372	6.4	6000	83

Table 4-2. Taurus II Normal Launch CO TWA Concentration Summary – Daytime Meteorology.

Month	Number of Weather Cases	Peak CO Concentration [ppm]	Distance to Peak CO Concentration [m]	Bearing to Peak CO Concentration [deg]
January	344	0.22	7000	259
February	364	0.17	3000	23
March	397	0.19	11000	315
April	383	0.23	7000	228
May	398	0.34	11000	300
June	392	0.32	4000	51
July	416	0.32	7000	274
August	408	0.21	6000	133
September	413	0.18	7000	305
October	435	0.24	13000	108
November	382	0.20	28000	120
December	372	0.17	15000	127

Table 4-3: Taurus II Normal Launch CO Concentration Summary – Nighttime Meteorology.

Month	Number of Weather Cases	Peak CO Concentration [ppm]	Distance to Peak CO Concentration [m]	Bearing to Peak CO Concentration [deg]
January	93	5.5	8000	74
February	157	4.0	10000	74
March	162	3.7	10000	176
April	156	6.3	9000	226
May	158	6.2	11000	242
June	152	4.4	7000	114
July	153	4.4	8000	113
August	162	3.4	10000	82
September	163	2.7	9000	356
October	119	2.7	18000	259
November	125	3.8	9000	91
December	128	6.0	7000	149

Table 4-4. Taurus II Normal Launch CO TWA Concentration Summary – Nighttime Meteorology.

Month	Number of Weather Cases	Peak CO Concentration [ppm]	Distance to Peak CO Concentration [m]	Bearing to Peak CO Concentration [deg]
January	93	0.08	9000	74
February	157	.09	24000	77
March	162	0.10	13000	230
April	156	0.60	7000	46
May	158	0.17	16000	120
June	152	0.24	7000	210
July	153	0.15	14000	34
August	162	0.20	12000	223
September	163	0.16	12000	226
October	119	0.08	28000	59
November	125	0.20	7000	202
December	128	0.17	21000	146

The REEDM predicted CO concentrations for all daytime meteorological cases processed in the 8-year sample set was aggregated into bins to evaluate the peak far field concentration probability. This information is provided in Table 4-5 and it is noted that approximately 81% of all daytime meteorological cases resulted in REEDM maximum peak instantaneous ground level CO concentrations of less than 1 ppm.

Table 4-5. REEDM Predicted Maximum Far Field Ground Level Carbon Monoxide Concentrations For Daytime Taurus II Normal Launch Scenarios.

Concentration Bin	Count	Probability
0 - 1	3805	0.809
1 - 2	644	0.137
2 - 3	174	0.037
3 - 4	54	0.011
4 - 5	14	0.003
5 - 6	9	0.002
6 - 7	3	0.001
7 - 8	1	0.0002
8 - 9	0	0.0000
9 - 10	0	0.0000

The REEDM predicted CO 1-hour time weighted average concentrations for all daytime meteorological cases processed in the 8-year sample set was aggregated into bins to evaluate the peak far field TWA concentration probability. This information is provided in Table 4-6 and it is noted that approximately 88% of all daytime meteorological cases resulted in REEDM maximum 1-hour TWA ground level CO concentrations of less than 0.04 ppm. The fact that the TWA concentration is much less than the peak instantaneous concentration is consistent with the short cloud passage time.

The REEDM predicted cloud transport directions were also aggregated into bins representing 45-degree arc corridors around the compass (i.e. N, NE, E, SE, S, SW, W, NW). Table 4-7 indicates the predicted Taurus II normal launch plume direction probability of occurrence observed across the 4704 daytime balloon soundings. It is noted that for the daytime launch scenarios transport of the exhaust plume to the East is favored. The transport direction reflects the average airflow over a depth of approximately 1000 meters, hence the windrose observed for elevated rocket exhaust clouds may differ significantly from a windrose derived from a surface wind tower.

Table 4-6. REEDM Predicted Maximum Far Field Ground Level Carbon Monoxide TWA Concentrations For Daytime Taurus II Normal Launch Scenarios.

1-Hour TWA Concentration Bin	Count	Probability
0.00 – 0.02	1933	0.411
0.02 – 0.04	1464	0.311
0.04 - 0.06	735	0.156
0.06 - 0.08	285	0.061
0.08 - 0.10	126	0.027
0.10 - 0.12	66	0.014
0.12 - 0.14	35	0.007
0.14 - 0.16	18	0.004
0.16 - 0.18	17	0.004
0.18 – 0.20	10	0.002
0.20 – 0.22	3	0.001
0.22 – 0.24	3	0.001
0.24 – 0.26	2	0.0004
0.26 – 0.28	2	0.0004
0.28 – 0.30	2	0.0004
0.30 – 0.32	0	0.0000
0.32 – 0.34	2	0.0004
0.34 – 0.36	1	0.0002
0.36 – 0.38	0	0.0000
0.38 -0.40	0	0.0000

Table 4-7. REEDM Predicted Exhaust Cloud Transport Directions For Daytime Taurus II Normal Launch Scenarios.

Plume Transport Direction Bin	Count	Probability
337.5 – 22.5 (N)	363	0.077
22.5 – 67.5 (NE)	830	0.176
67.5 – 112.5 (E)	801	0.170
112.5 – 157.5 (SE)	976	0.207
157.5 – 202.5 (S)	515	0.109
202.5 – 247.5 (SW)	453	0.096
247.5 – 292.5 (W)	326	0.069
292.5 – 337.5 (NW)	440	0.094

Similar summary tables for the 1728 nighttime Taurus II normal launch simulations were compiled. Table 4-8 shows that the peak CO instantaneous concentration predictions for nighttime conditions continues with a high probability that the maximum far field concentration will be less than 1 ppm.

Table 4-8. REEDM Predicted Maximum Far Field Ground Level Carbon Monoxide Concentrations For Nighttime Taurus II Normal Launch Scenarios.

Concentration Bin	Count	Probability
0 - 1	1390	0.804
1 - 2	237	0.137
2 - 3	67	0.039
3 - 4	23	0.013
4 - 5	7	0.004
5 - 6	2	0.0012
6 - 7	2	0.0012
7 - 8	0	0.0000
8 - 9	0	0.0000
9 - 10	0	0.0000

The REEDM predicted CO 1-hour time weighted average concentrations for all nighttime meteorological cases is provided in Table 4-9 and it is noted that approximately 73% of all nighttime meteorological cases resulted in REEDM maximum 1-hour TWA ground level CO concentrations of less than 0.04 ppm.

Table 4-10 indicates the predicted Taurus II normal launch plume direction probability of occurrence observed across the 1728 nighttime balloon soundings. It is noted that for nighttime launch scenarios transport of the exhaust plume to the East is still favored as it was during the daytime.

Table 4-9. REEDM Predicted Maximum Far Field Ground Level Carbon Monoxide TWA Concentrations For Nighttime Taurus II Normal Launch Scenarios.

1-Hour TWA Concentration Bin	Count	Probability
0.00 – 0.02	817	0.473
0.02 – 0.04	449	0.260
0.04 - 0.06	264	0.153
0.06 - 0.08	114	0.066
0.08 - 0.10	52	0.030
0.10 - 0.12	12	0.007
0.12 - 0.14	6	0.0035
0.14 - 0.16	4	0.0023
0.16 - 0.18	5	0.0029
0.18 – 0.20	0	0.0000
0.20 – 0.22	3	0.0017
0.22 – 0.24	0	0.0000
0.24 – 0.26	0	0.0000
0.26 – 0.28	0	0.0000
0.28 – 0.30	0	0.0000
0.30 – 0.32	0	0.0000
0.32 – 0.34	0	0.0000
0.34 – 0.36	0	0.0000
0.36 – 0.38	0	0.0000
0.38 -0.40	0	0.0000

Table 4-10. REEDM Predicted Exhaust Cloud Transport Directions For Nighttime Taurus II Normal Launch Scenarios.

Plume Transport Direction Bin	Count	Probability
337.5 – 22.5 (N)	61	0.035
22.5 – 67.5 (NE)	315	0.182
67.5 – 112.5 (E)	296	0.171
112.5 – 157.5 (SE)	369	0.214
157.5 – 202.5 (S)	231	0.134
202.5 – 247.5 (SW)	215	0.124
247.5 – 292.5 (W)	106	0.061
292.5 – 337.5 (NW)	135	0.078

4.3 REEDM Far Field Results For The Taurus II Static Test Firing Scenario

REEDM was executed in batch mode using the same archived WFF meteorological soundings to evaluate the formation, transport and ground level concentration of CO from Taurus II static test firings on the launch stand. Table 4-11 presents the maximum peak instantaneous CO concentration predicted for the static test firing. It is noted that in general the static test firing is predicted to produce higher ground level CO concentrations than the normal launch scenario.

Table 4-11: Taurus II Static Test Firing CO Concentration Summary – Daytime Meteorology.

Month	Number of Weather Cases	Peak CO Concentration [ppm]	Distance to Peak CO Concentration [m]	Bearing to Peak CO Concentration [deg]
January	344	10.8	6000	53
February	364	15.5	6000	31
March	397	18.9	6000	34
April	383	13.5	6000	33
May	398	11.6	7000	16
June	392	6.1	8000	21
July	416	5.2	7000	75
August	408	5.2	11000	25
September	413	9.2	8000	249
October	435	5.9	6000	58
November	382	11.8	6000	92
December	372	13.6	8000	37

Table 4-12 lists the predicted daytime CO TWA concentrations for the Taurus II static test firing scenarios. The TWA concentrations are somewhat higher than the corresponding values predicted for the normal launch scenario, but the overall expectation is that the 1-hour TWA CO concentrations will be less than 1 ppm. Table 4-13 and Table 4-14 show the maximum predicted CO instantaneous and 1-hour TWA concentrations for the nighttime static test firing conditions.

Table 4-12. Taurus II Static Test Firing CO TWA Concentration Summary – Daytime Meteorology.

Month	Number of Weather Cases	Peak CO Concentration [ppm]	Distance to Peak CO Concentration [m]	Bearing to Peak CO Concentration [deg]
January	344	0.20	7000	53
February	364	0.27	8000	70
March	397	0.26	5000	46
April	383	0.23	9000	20
May	398	0.25	11000	251
June	392	0.16	5000	61
July	416	0.18	4000	181
August	408	0.14	14000	136
September	413	0.15	7000	241
October	435	0.17	14000	221
November	382	0.23	6000	92
December	372	0.25	9000	37

Table 4-13: Taurus II Static Test Firing CO Ceiling Concentration Summary – Nighttime Meteorology.

Month	Number of Weather Cases	Peak CO Concentration [ppm]	Distance to Peak CO Concentration [m]	Bearing to Peak CO Concentration [deg]
January	93	12.3	6000	100
February	157	8.7	7000	8
March	162	11.4	6000	40
April	156	13.7	5000	58
May	158	7.2	6000	80
June	152	5.9	6000	113
July	153	4.2	8000	83
August	162	4.7	9000	82
September	163	4.6	13000	72
October	119	6.1	8000	59
November	125	6.9	8000	92
December	128	13.6	8000	37

Table 4-14. Taurus II Static Test Firing CO TWA Concentration Summary – Nighttime Meteorology.

Month	Number of Weather Cases	Peak CO Concentration [ppm]	Distance to Peak CO Concentration [m]	Bearing to Peak CO Concentration [deg]
January	93	0.22	7000	100
February	157	0.24	16000	42
March	162	0.21	11000	29
April	156	0.28	7000	58
May	158	0.23	13000	100
June	152	0.15	7000	113
July	153	0.11	18000	83
August	162	0.12	10000	79
September	163	0.30	12000	226
October	119	0.13	12000	152
November	125	0.18	11000	66
December	128	0.25	9000	37

Histograms of REEDM predicted CO concentrations for Taurus II static test firings for all daytime meteorological cases were generated in a similar fashion to the normal launch scenario. Table 4-15 presents the maximum predicted CO concentrations and it is noted that approximately 76% of all daytime meteorological cases resulted in REEDM maximum peak instantaneous ground level CO concentrations of less than 1 ppm. The static test firing scenarios exhibited a trend toward somewhat higher concentrations than predicted for the normal launch.

Table 4-15. REEDM Predicted Maximum Far Field Ground Level Carbon Monoxide Concentrations For Daytime Taurus II Static Test Firing Scenarios.

Concentration Bin	Count	Probability
0 - 1	3568	0.759
1 - 2	632	0.134
2 - 3	195	0.041
3 - 4	125	0.027
4 - 5	51	0.011
5 - 6	48	0.010
6 - 7	21	0.004
7 - 8	18	0.004
8 - 9	14	0.003
9 +	12	0.003

Table 4-16 presents the REEDM predicted CO 1-hour time weighted average concentrations for all daytime meteorological cases processed for the Taurus II static test firing scenario. It is noted that approximately 60% of all daytime meteorological cases resulted in REEDM maximum 1-hour TWA ground level CO concentrations of less than 0.04 ppm.

The REEDM predicted cloud transport directions were also aggregated into bins for the static test firing scenario. Table 4-17 indicates the predicted Taurus II static test firing plume direction probability of occurrence observed across the 4704 daytime balloon soundings. It is noted that for the daytime launch scenarios transport of the exhaust plume to the East is favored.

Table 4-16. REEDM Predicted Maximum Far Field Ground Level Carbon Monoxide TWA Concentrations For Daytime Taurus II Static Test Firing Scenarios.

1-Hour TWA Concentration Bin	Count	Probability
0.00 – 0.02	1468	0.312
0.02 – 0.04	1372	0.292
0.04 - 0.06	863	0.183
0.06 - 0.08	446	0.095
0.08 - 0.10	230	0.049
0.10 - 0.12	138	0.029
0.12 - 0.14	74	0.016
0.14 - 0.16	40	0.009
0.16 - 0.18	29	0.006
0.18 – 0.20	17	0.004
0.20 – 0.22	15	0.003
0.22 – 0.24	6	0.0012
0.24 – 0.26	3	0.0006
0.26 – 0.28	2	0.0004
0.28 – 0.30	0	0.0000
0.30 – 0.32	0	0.0000
0.32 – 0.34	0	0.0000
0.34 – 0.36	0	0.0000
0.36 – 0.38	0	0.0000
0.38 -0.40	0	0.0000

Table 4-17. REEDM Predicted Exhaust Cloud Transport Directions For Daytime Taurus II Static Test Firing Scenarios.

Plume Transport Direction Bin	Count	Probability
337.5 – 22.5 (N)	397	0.084
22.5 – 67.5 (NE)	832	0.177
67.5 – 112.5 (E)	838	0.178
112.5 – 157.5 (SE)	955	0.203
157.5 – 202.5 (S)	489	0.104
202.5 – 247.5 (SW)	440	0.094
247.5 – 292.5 (W)	316	0.067
292.5 – 337.5 (NW)	437	0.093

Similar summary tables for the 1728 nighttime Taurus II static test firing simulations were compiled. Table 4-18 shows that the peak CO instantaneous concentration predictions for nighttime conditions continues with a high probability that the maximum far field concentration will be less than 1 ppm.

Table 4-18. REEDM Predicted Maximum Far Field Ground Level Carbon Monoxide Concentrations For Nighttime Taurus II Static Test Firing Scenarios.

Concentration Bin	Count	Probability
0 - 1	1231	0.712
1 - 2	279	0.161
2 - 3	99	0.057
3 - 4	42	0.024
4 - 5	33	0.019
5 - 6	15	0.009
6 - 7	9	0.005
7 - 8	9	0.005
8 - 9	3	0.002
9 +	3	0.002

The REEDM static test firing predicted CO 1-hour time weighted average concentrations for all nighttime meteorological cases is provided in Table 4-19 and it is noted that approximately 59% of all nighttime meteorological cases resulted in REEDM maximum 1-hour TWA ground level

CO concentrations of less than 0.04 ppm. Static test firing TWA CO concentrations trend higher than those observed in the normal launch simulations.

Table 4-20 indicates the predicted Taurus II static test firing plume direction probability of occurrence observed across the 1728 nighttime balloon soundings. It is noted that for nighttime launch scenarios transport of the exhaust plume to the East is still favored as it was during the daytime.

Table 4-19. REEDM Predicted Maximum Far Field Ground Level Carbon Monoxide TWA Concentrations For Nighttime Taurus II Static Test Firing Scenarios.

1-Hour TWA Concentration Bin	Count	Probability
0.00 – 0.02	605	0.350
0.02 – 0.04	407	0.236
0.04 - 0.06	293	0.170
0.06 - 0.08	197	0.114
0.08 - 0.10	84	0.049
0.10 - 0.12	58	0.034
0.12 - 0.14	31	0.018
0.14 - 0.16	9	0.005
0.16 - 0.18	19	0.011
0.18 – 0.20	11	0.006
0.20 – 0.22	7	0.004
0.22 – 0.24	3	0.002
0.24 – 0.26	2	0.001
0.26 – 0.28	0	0.000
0.28 – 0.30	1	0.001
0.30 – 0.32	1	0.001
0.32 – 0.34	0	0.0000
0.34 – 0.36	0	0.0000
0.36 – 0.38	0	0.0000
0.38 -0.40	0	0.0000

Table 4-20. REEDM Predicted Exhaust Cloud Transport Directions For Nighttime Taurus II Static Test Firing Scenarios.

Plume Transport Direction Bin	Count	Probability
337.5 – 22.5 (N)	72	0.042
22.5 – 67.5 (NE)	321	0.186
67.5 – 112.5 (E)	306	0.177
112.5 – 157.5 (SE)	378	0.219
157.5 – 202.5 (S)	221	0.128
202.5 – 247.5 (SW)	207	0.120
247.5 – 292.5 (W)	92	0.053
292.5 – 337.5 (NW)	131	0.076

4.4 REEDM Near Field Results For Taurus II Normal Launch Scenario

In REEDM terminology the "near field" is defined as the geographical region near the launch pad where the rocket exhaust cloud source is formed and undergoes vertical cloud rise due to buoyancy effects. REEDM is not specifically designed to predict cloud concentrations in this region because the area is typically evacuated during launches due to high risk from debris, blast, fire and toxics hazards. Emissions in this region are of interest for environmental considerations however; therefore ACTA modified the output of REEDM to report intermediate calculations of the exhaust cloud size, position and temperature during the cloud rise phase. Using information about the size and location of the exhaust cloud coupled with the known quantity of exhaust products emitted and the mass fractions of the exhaust chemical constituents allows an estimate to be made of chemical concentrations inside the cloud in the near field. When performing far field calculations, REEDM assumes that the mass distribution of exhaust products in the expanded and diluted exhaust cloud is Gaussian. In the near field, as the source cloud is initially formed, the exhaust products may be more uniformly distributed. ACTA computed in-cloud concentrations in the near field assuming both uniform and Gaussian mass distributions. For the Gaussian distribution the maximum concentration occurs at the cloud centroid and the edge of the cloud is defined as the point where the concentration is 10% of the centroid maximum values. This assumption defines the cloud radius as 2.14 standard deviations.

The size and shape of the near field ground level carbon monoxide concentration pattern depends upon several factors:

1. The dynamics of the exhaust flow emitted from the Taurus II Pad-0A flame duct.

2. The effects of thermal buoyancy that lifts the plume off the ground and imparts vertical acceleration to the hot plume gases.

3. The effect of local wind speed and direction after the jet momentum has dissipated and the plume is beginning to lift off the ground.

The jet dynamics of the high speed exhaust plume venting from the flame duct are largely independent of the weather conditions and are determined by the design of the flame duct and concrete ramp structure at the exit of the duct. These design features were still in development and evaluation at the time of this study. The vertical rise rate of the buoyant cloud after the jet dynamics have dampened are computed by REEDM and were used to estimate the vertical and horizontal cloud displacement from a point where the exhaust plume is assumed to become buoyancy dominated. For normal launches, only a portion of the main engine exhaust vents through the flame duct and some of the ground cloud forms around the launch pad. A detailed computational fluid dynamics flow analysis of the plume interaction with the flame duct and the launch pad surface is not available, however, based on photographs and video of other launch vehicle normal launch ground clouds, it is estimated that the center of the Taurus II normal launch ground cloud will be displaced about 100 meters from the vehicle liftoff position in the direction of the flame duct exit.

REEDM calculations for the near field normal launch cloud rise were processed for 6427 meteorological cases and summarized by month as shown in Table 4-21. REEDM approximates the Taurus II normal launch ground cloud as a sphere the radius of which grows linearly during the buoyant cloud rise phase according to the following relationship:

$$r(z) = r_0 + \gamma \Delta z$$

where:

$r(z)$	=	cloud radius at height z [m]
r_o	=	initial cloud radius [m] = 48.8 [m] (160 ft)
γ	=	air entrainment coefficient = 0.36
Δz	=	height of cloud centroid above the ground [m]

Based on the forgoing relationship, the spherical cloud will just touch the ground surface when the cloud centroid lifts to approximately 76 meters above the ground. This is also referred to in this report as the “cloud liftoff” point. Beyond this point the downwind ground CO concentration is assumed to be zero until the ground concentrations once again start to occur in the far field due to downward mixing from the stabilized normal launch cloud. The maximum distance from the point where the flame duct horizontal flow dynamics are dampened (REEDM initialization point) to the point where the wind driven normal launch plume lifts off the ground is estimated to be 144 meters. Average distance from the REEDM initialization point to the point of cloud liftoff is estimated to be about 25 meters. These distances are influenced by the initial amount of cloud “exhaust” materials as well as the air entrainment rate assumption. If deluge water injection and combustion air are added to the initial exhaust mass, then the initial cloud radius will be larger and the downwind distance to the liftoff point will be somewhat longer. Given uncertainties in the plume mass entrainment and other modeling assumptions, the maximum travel distance to Taurus II normal launch ground cloud liftoff is estimated at about 200 meters. Thus a circle with a radius of 200 meters centered 100 meters downstream from the flame duct exit would approximately define the region within which a toxic exposure to CO might occur under high surface wind conditions. The average potential toxic exposure zone is expected to be much smaller and is associated with moderate to light surface winds. Maximum ground level CO concentrations inside the near field toxic hazard zone could exceed 7000 ppm.

Table 4-21. Taurus II Normal Launch Near Field CO Concentration Summary.

Month	Number of Weather Cases	Ground CO Concentration at Cloud Liftoff Uniform Distribution [ppm]	Ground CO Concentration at Cloud Liftoff Gaussian Distribution [ppm]	Maximum Distance to Cloud Liftoff [m]	Average Distance to Cloud Liftoff [m]
January	435	7530	1980	78	22
February	521	7420	1950	86	23
March	559	7190	1890	99	25
April	538	8440	2220	93	25
May	556	7250	1910	86	23
June	544	7140	1880	55	21
July	569	6650	1750	62	20
August	570	7790	2050	61	18
September	576	7190	1890	144	21
October	554	7330	1930	98	19
November	507	7870	2070	101	20
December	498	8280	2180	76	22

An example of near field concentration calculations for a normal launch plume with a May meteorological case that produced a low cloud rise is listed below. As the ground cloud rises REEDM assumes it intersects and combines with the contrail cloud above it and the total amount of exhaust mass in the rising cloud continues to increase until the ground cloud stops rising at the stabilization altitude. As previously defined, when the predicted ground cloud radius just equals the height of the ground cloud centroid above the ground, the exhaust cloud is just at the point of lifting off the ground. In Table 4-22 this occurs as the cloud rises through the 8th meteorological layer where the top of the layer is 89.9 meters above the ground and the cloud radius is predicted to be 80.8 meters. At this point the cloud is predicted to have moved 20.6 meters in the downwind direction, has an average temperature of 329.5 Kelvin (133 F) and has an uniform CO concentration of 7615 ppm. As the cloud continues to move downwind it rises further above the ground and only flying birds or tall trees would be exposed to the concentrated cloud exhaust chemicals. This sample normal launch cloud is predicted to stabilize at 440 meters above the ground approximately 200 meters downwind from the initial source formation point and has a predicted radius of 206.9 meters. The bottom of the exhaust cloud would be approximately 233 meters above the ground. The centroid concentration, assuming the mass distribution has transitioned to Gaussian, is predicted to be 3881 ppm with the concentration at the edge of the cloud equal to 388 ppm (10% of the peak centroid concentration).

Table 4-22. Sample Near Field Taurus II Normal Launch Exhaust Cloud Concentration Estimates For a May WFF Meteorological Case.

```
     initial cloud radius          [m] =    48.76800
     initial cloud height          [m] =   0.0000000E+00
     initial cloud rise velocity [m/s] =   0.0000000E+00
```

met layer	cloud height [m]	cloud radius [m]	cloud volume [m**3]	exhaust mass [g]	downwind dist [m]	rise time [sec]	cloud temp [K]	uniform conc [ppm]	Gaussian conc [ppm]
1	11.0	52.4	.60123E+06	.17505E+08	2.3	1.295	590.5	6516.	17152.
2	20.6	55.8	.72845E+06	.23196E+08	5.8	0.632	498.6	7127.	18760.
3	30.2	59.3	.87234E+06	.30021E+08	8.0	0.580	443.6	7703.	20275.
4	39.8	62.7	.10341E+07	.37721E+08	10.1	0.573	407.6	8164.	21489.
5	49.4	66.2	.12148E+07	.46158E+08	12.2	0.584	382.5	8504.	22384.
6	59.3	69.8	.14221E+07	.55242E+08	14.4	0.622	363.7	8694.	22884.
7	69.2	73.3	.16517E+07	.64928E+08	16.7	0.647	349.6	8798.	23158.
8	89.9	80.8	.22091E+07	.75165E+08	20.6	1.451	329.5	7615.	20044.
9	108.5	87.5	.28051E+07	.86432E+08	26.0	1.423	317.9	6896.	18152.

10	126.5	94.0	.34754E+07	.98520E+08	31.5	1.490	310.0	6345.	16701.
11	144.5	100.4	.42446E+07	.11134E+09	37.3	1.605	304.2	5871.	15453.
12	176.0	111.8	.58536E+07	.12482E+09	46.4	3.091	297.9	4773.	12563.
13	207.6	123.2	.78254E+07	.13940E+09	59.1	3.425	294.1	3987.	10494.
14	222.5	128.5	.88963E+07	.15495E+09	69.4	1.734	292.7	3898.	10261.
15	240.2	134.9	.10285E+08	.17095E+09	77.2	2.141	291.2	3720.	9792.
16	295.4	154.8	.15530E+08	.18744E+09	96.9	7.536	288.8	2701.	7111.
17	339.9	170.8	.20869E+08	.20538E+09	127.3	7.224	287.6	2203.	5798.
18	386.5	187.6	.27649E+08	.22438E+09	158.3	9.055	286.9	1816.	4781.
19	440.1	206.9	.37099E+08	.24441E+09	198.2	14.517	286.9	1475.	3881.

4.5 REEDM Near Field Results For Taurus II Static Test Firing Scenario

REEDM calculations for the near field static test firing cloud rise were processed for 6427 meteorological cases and summarized by month as shown in Table 4-23. REEDM approximates the Taurus II static test firing cloud as a sphere the radius of which grows linearly during the buoyant cloud rise phase according to the following relationship:

$$r(z) = r_0 + \gamma \Delta z$$

where: $r(z)$ = cloud radius at height z [m]

r_o = initial cloud radius [m] = 46.05 [m] (151 ft)

γ = air entrainment coefficient = 0.5

Δz = height of cloud centroid above the ground [m]

Based on the forgoing relationship, the spherical cloud will just touch the ground surface when the cloud centroid lifts to approximately 91 meters above the ground. The initial cloud radius is calculated using the ideal gas law and the principle of mass conservation applied to the engine RP-1 and LOX propellant consumed in the test firing. Inclusion of deluge water and combustion air injected beyond the nozzle exit plane would increase the cloud exhaust mass and therefore would also increase the estimated initial cloud radius.

Table 4-23. Taurus II Static Test Firing Near Field CO Concentration Summary.

Month	Number of Weather Cases	Ground CO Concentration at Cloud Liftoff Uniform Distribution [ppm]	Ground CO Concentration at Cloud Liftoff Gaussian Distribution [ppm]	Maximum Distance to Cloud Liftoff [m]	Cloud Transport Bearing Associated With Max Cloud Liftoff [deg]	Average Distance to Cloud Liftoff [m]
January	435	3990	1050	212	181	36
February	521	3980	1050	249	298	40
March	559	4010	1055	299	269	43
April	538	3960	1040	271	316	43
May	556	4050	1065	259	302	38
June	544	3980	1050	126	328	33
July	569	4020	1060	161	101	31
August	570	4020	1060	143	333	27
September	576	3970	1040	557*	298	36
October	554	3960	1040	296	309	30
November	507	4050	1065	307	310	33
December	498	4020	1060	211	283	36

* September case with 557-meter downwind distance was under storm conditions with 60 knot surface winds, an unlikely weather condition for conducting a test firing.

Given uncertainties in the static test firing plume mass entrainment and other modeling assumptions, the maximum travel distance to Taurus II static test firing cloud liftoff is estimated at about 350 meters. Thus a circle with a radius of 350 meters centered 200 meters downstream from the flame duct exit would approximately define the region within which a toxic exposure to CO might occur under high surface wind conditions. The average potential toxic exposure zone is expected to be much smaller and is associated with moderate to light surface winds. Maximum ground level CO concentrations inside the near field static test firing toxic hazard zone could exceed 4000 ppm.

5. CONCLUSIONS

A conservative analysis approach has been applied to estimate carbon monoxide concentrations associated with Taurus II normal launch and static test firing scenarios. The analysis is deemed to be conservative in the sense that certain modeling assumptions, such as discounting the effect of uncertain processes such as the plume chemical alterations due to deluge water injection and plume afterburning with ambient air, favor predicting higher carbon monoxide concentrations than are expected to actually occur. The study also evaluated maximum chemical concentrations predicted using a set of over 6000 historical Wallops Flight Facility weather balloon soundings. Thus reasonable worst-case weather conditions should have inherently been captured in the study. The Taurus II first stage propellants are the hydrocarbon based fuel RP-1 and liquid oxygen (LOX). Under design combustion conditions the oxidizer to fuel burn ratio is approximately 2.7, which represents a somewhat fuel rich mixture. The main combustion byproduct of concern is carbon monoxide, which is estimated to comprise approximately 25.6 percent of the exhaust mixture by mass at the rocket nozzle exit. The other main combustion byproducts are carbon dioxide and water vapor. Rocket emissions from both the a normal vehicle launch and a static test firing on the launch pad are extremely hot and therefore less dense than surrounding ambient air and are accelerated vertically due to buoyancy forces that act on the exhaust cloud gases. The effect of buoyancy is to loft the exhaust clouds above the ground to a point of neutral stability in the atmosphere at altitudes ranging from 400 to 1300 meters above the ground. From the stabilization altitude, exhaust cloud materials eventually mix back down to the ground due to atmospheric turbulence, unless the entire cloud is predicted to rise above a capping thermal inversion. The geographic region near the launch pad where the source cloud forms and begins its thermal rise process is referred to as the "near field". Ground level CO concentrations in the near field region are estimate to be in the 4000 to 20000 ppm range, however the downwind transport distance before the cloud lifts off the ground is predicted to be relatively short—on the order of several hundred meters or less. The geographic region where the stabilized and neutrally buoyant cloud material mixes back to the ground is referred to as the "far field". REEDM predicts that the peak instantaneous CO concentrations in the far field region are typically less than 1 ppm but have the potential to reach as high as 20 ppm. One-hour time weighted average CO concentrations are estimated to be very low, typically less than 0.04 ppm, and these low TWA values are due to the short cloud passage time over a receptor location (e.g. minutes rather than hours). The far field CO concentration levels are well below published emergency exposure guidelines for humans and are considered to be benign to people, flora and fauna. Near field CO concentrations may reach hazardous levels that exceed the AEGL-3 10-minute exposure threshold or the IDLH exposure threshold. Given the proximity of the near field exposed region to the plume point of origin, other hazards, such as radiant heat transfer or direct exposure to the high temperature exhaust gas mixture, may be more severe than the hazard from CO chemical concentration exposure.

6. REFERENCES

Gordon, Sanford and Bonnie J. McBride, "Computer Program for Calculation of Complex Chemical Equilibrium Compositions, Rocket Performance, Incident and Reflected Shocks, and Chapman-Jouguet Detonations", Interim Revision NASA SP-273, Lewis Research Center, Cleveland OH, March 1976.

Gordon, Sanford and Bonnie J. McBride, "Computer Program for Calculation of Complex Chemical Equilibrium Compositions and Applications, I. Analysis", NASA Reference Publication 1311, Lewis Research Center, Cleveland OH, October 1994.

Dimal Patel, "Taurus2 Quick Look Launch Duct Plume Flow Field", Orbital memorandum to B. Light, November 25, 2008.

Report No. 12-834/1-01

Evaluation of Toxic Emissions for a Large Solid Propellant Launch Vehicle at Wallops Flight Facility

Purchase Order Subcontract No. 9600-27619

Prepared by

Randolph L. Nyman
Ken Conley

ACTA
2790 Skypark Dr Ste 310
Torrance, CA 90505

Prepared for:

CardnoTec, Inc.
2496 Old Ivy Road
Suite 300
Charlottesville, VA 22903

August 9, 2012

TABLE OF CONTENTS

LIST OF FIGURES

LIST OF TABLES

1. EXECUTIVE SUMMARY

This study investigated potential toxic hazards associated with normal launch and catastrophic vehicle failure scenarios for a large space launch booster that utilizes four successively smaller solid propellant stages. The vehicle design was based on a concept vehicle proposed by Alliant Techsystems Inc. (ATK) that is comprised of Castor solid rocket motors designed and built by ATK. These motors are closely related to the motor segments used on the Space Shuttle solid rocket boosters. The first stage of this vehicle is designated as the Castor 1200 and contains just over 1.1 million pounds of solid propellant that is a mixture of ammonium perchlorate (AP), aluminum powder and a rubbery polybutadiene acrylic acid acrylonitrile (PBAN) binder. When burned, this propellant generates exhaust that is about 20% by mass toxic hydrogen chloride gas. The aluminum powder, which is part of the fuel component in the propellant, is oxidized during combustion to aluminum oxide and generates small particulates of solid Al_2O_3 in the rocket engine plume after the plume expands and cools. For the purposes of this study a set of default particle size and mass distribution assumptions contained in the Rocket Exhaust Effluent Diffusion Model (REEDM) were applied to the Castor 1200 motor. These default assumptions have been applied by Air Force range safety analysts in the past to evaluate emissions from the large solid rocket boosters on the Space shuttle and Titan vehicles. The entire mass distribution of Al_2O_3 in assigned to size bins that are all under 10 microns in size and fall within pollution and health standards that pertain to the "PM_{10}" classification. Approximately 70% of the Al_2O_3 particulate mass falls in a smaller "PM_5" category that is also defined as "respirable dust" with average sizes of 5 microns or less. In addition to chemical releases associated with the solid propellant, this study considered potential releases of hypergolic nitrogen tetroxide (N_2O_4) oxidizer and monomethyl hydrazine fuel (MMH) ($CH_3(NH)NH_2$) from a representative generic spacecraft that would be a payload on the candidate launch vehicle. When released to the atmosphere N_2O_4 readily dissociates to NO_2, therefore concentrations for the oxidizer are evaluated as NO_2. Both NO_2 and MMH are highly toxic and have human health effect thresholds in the 2 to 20 part per million range.

New launch vehicles have a high probability of failure due to the complexity of the launch system and the inability to fully test vehicle integration and flight performance at the manufacturing facility. Catastrophic loss of the entire launch vehicle is the most common result of a launch system failure. The Federal Aviation Administration (FAA) office of commercial space transport has established guidelines that assign probable launch vehicle failure rates to new launch vehicles that are based on historical performance of similar vehicles. New launch vehicles under the FAA binomial failure probability allocation have mission failure probabilities on the 3rd flight ranging from 0.276 to 0.724 with a median of 0.5. In other words, there is historical supporting evidence that the statistical probability of a launch failure is as high as 72.4% for a new launch vehicle on a third flight attempt with prior failures. For this reason, it is prudent to consider the environmental effect of launch vehicle failures as well as normal launch successes. The chemical emissions that result from a catastrophic launch vehicle failure are invariably more severe than the emissions from the normal launch, in part because 100% of the launch vehicle propellants are released simultaneously in a vehicle breakup and in part because rupture of liquid propellant tanks leads to inefficient mixing and only partial combustion of the hypergolic propellants.

To assess formation of the launch vehicle emissions and the subsequent cloud rise and atmosphere transport and dispersion, two recognized range safety computer programs were employed for this study. The Rocket Exhaust Effluent Diffusion Model (REEDM) was used to simulate HCl and AL_2O_3 releases associated with the normal launch scenarios. REEDM supports calculations that account for gravitational settling of Al_2O_3 particulates. The Launch Area Toxic Risk Analysis 3-Dimensional (LATRA3D) program was used to simulate releases from launch vehicle catastrophic failures and liquid propellant spills. Explosion of the pressurized Castor 1200 during first stage flight from 0 to 20 seconds into flight was evaluated to assess the formation of toxic plumes from the explosion and the burning propellant fragments that result as the motor breaks up. This is referred to as the "conflagration" scenario. It was assumed that the payload containing 1000 pound of MMH and 1640 pound of nitrogen tetroxide would be ejected from a Castor 1200 explosion and fall back to the ground intact resulting in either a liquid propellant explosion and fire (called the "deflagration" scenario) or rupture the propellant tanks and spill the liquid propellants without initiating a fire or explosion (called the "evaporating pool" scenario).

Each of these release scenarios were evaluated by running REEDM or LATRA3D for 6430 archived meteorological weather balloon soundings obtained from the Wallops Flight Facility. Approximately 102,000 computer simulations were generated for the combination of release scenarios and weather cases. Toxic dispersion predictions from these runs were post processed to summarize general characteristics, trends and to identify bounding worst case hazard conditions expressed in terms of maximum expected ground level concentrations and maximum downwind distances to the endpoint of a concentration threshold or to the maximum predicted concentration location. Except for the evaporating pool scenarios, the sources are initially buoyant and rise hundreds to thousands of feet into the atmosphere and then gradually mix back down to the ground level. Elevated sources typically exhibit a "clear" zone near the source where the buoyant cloud passes overhead and there is no detectable concentration at the ground. As the cloud material mixes back to the ground, the ground level concentration starts to increase, reaches a maximum and then decreases due to continued dilution as the expanding cloud moves further downwind. We summarize here the general observations and findings from the large set of simulations.

Normal Launch Scenario:

The normal launch scenario releases HCl and Al_2O_3 and is deemed by the author to constitute relatively benign toxic hazards (at ground level) with following characteristics:

Peak HCl concentrations:	2 to 5 ppm
Maximum downwind distance to peak concentration:	11000 to 19000 meters
Concentration probabilities:	63% of cases < 1 ppm
Duration of exposure:	< 60 minutes

Peak Al_2O_3 PM_5 concentrations:	2 to 6 mg/m^3
Maximum downwind distance to peak concentration:	10000 to 33000 meters
Concentration probabilities:	67% of cases < 1 mg/m^3
Duration of exposure:	< 90 minutes

Conflagration Scenario for Failures over the First 20 Seconds of Flight:

The conflagration scenario releases HCl and Al_2O_3 and results in significantly higher ground level concentrations than the normal launch scenario. The magnitude of ground level HCl concentrations vary depending on the launch vehicle failure time. The worst case for the candidate launch vehicle appears to be for a failure at about 4 seconds into flight. The following general characteristics are noted:

For HCl:

T-0 failure peak HCl concentrations:	18 to 65 ppm
Maximum downwind distance to peak concentration:	1000 to 6000 meters
Concentration probabilities:	79% of cases < 10 ppm
Duration of exposure:	< 60 minutes

T+4 failure peak HCl concentrations:	31 to 315 ppm
Maximum downwind distance to peak concentration:	40 to 2300 meters
Concentration probabilities:	72% of cases < 10 ppm
Duration of exposure:	< 60 minutes

T+8 failure peak HCl concentrations:	30 to 120 ppm
Maximum downwind distance to peak concentration:	90 to 5400 meters
Concentration probabilities:	76% of cases < 10 ppm

Duration of exposure:	< 60 minutes
T+12 failure peak HCl concentrations:	18 to 118 ppm
Maximum downwind distance to peak concentration:	90 to 3500 meters
Concentration probabilities:	79% of cases < 10 ppm
Duration of exposure:	< 60 minutes
T+16 failure peak HCl concentrations:	19 to 153 ppm
Maximum downwind distance to peak concentration:	330 to 2700 meters
Concentration probabilities:	82% of cases < 10 ppm
Duration of exposure:	< 60 minutes
T+20 failure peak HCl concentrations:	14 to 153 ppm
Maximum downwind distance to peak concentration:	980 to 3000 meters
Concentration probabilities:	87% of cases < 10 ppm
Duration of exposure:	< 60 minutes

For Al_2O_3:

T-0 failure peak Al_2O_3 concentrations:	5 to 18 mg/m^3 PM_{10}
Maximum downwind distance to peak concentration:	7000 to 18000 meters
Concentration probabilities:	2.8% of cases >5 mg/m^3 PM_5
Duration of exposure:	< 60 minutes
T+4 failure peak Al_2O_3 concentrations:	7 to 30 mg/m^3 PM_{10}
Maximum downwind distance to peak concentration:	5000 to 18000 meters
Concentration probabilities:	6.7% of cases >5 mg/m^3 PM_5
Duration of exposure:	< 60 minutes
T+8 failure peak Al_2O_3 concentrations:	15 to 423 mg/m^3 PM_{10}
Maximum downwind distance to peak concentration:	1000 to 8000 meters
Concentration probabilities:	21.4% of cases >5 mg/m^3 PM_5
Duration of exposure:	< 60 minutes
T+12 failure peak Al_2O_3 concentrations:	33 to 1000 mg/m^3 PM_{10}
Maximum downwind distance to peak concentration:	1000 to 5000 meters
Concentration probabilities:	40.2% of cases >5 mg/m^3 PM_5

Duration of exposure:	< 60 minutes

T+16 failure peak Al_2O_3 concentrations:	55 to 765 mg/m^3 PM_{10}
Maximum downwind distance to peak concentration:	1000 to 3000 meters
Concentration probabilities:	52.5% of cases >5 mg/m^3 PM_5
Duration of exposure:	< 60 minutes

T+20 failure peak Al_2O_3 concentrations:	79 to 550 mg/m^3 PM_{10}
Maximum downwind distance to peak concentration:	1000 to 7000 meters
Concentration probabilities:	60.2% of cases >5 mg/m^3 PM_5
Duration of exposure:	< 60 minutes

Payload Hypergol Deflagration Scenario:

The payload deflagration scenario releases NO_2 and MMH as constituents in an instantaneous fireball. These are present because of incomplete mixing and incomplete combustion of fuel and oxidizer. The following general characteristics are noted:

Peak NO_2 concentrations:	7 to 42 ppm
Maximum downwind distance to peak concentration:	500 to 2100 meters
Maximum 0.5 ppm hazard distance:	9000 meters
Concentration probabilities:	5.4% of cases >10 ppm
Duration of exposure:	< 30 minutes

Peak MMH concentrations:	0.8 to 4.6 ppm
Maximum downwind distance to peak concentration:	500 to 2100 meters
Maximum 0.5 ppm hazard distance:	5000 meters
Concentration probabilities:	0.7% of cases >2 ppm
Duration of exposure:	< 30 minutes

Payload Hypergol Pool Evaporation Scenario:

The payload pool evaporation scenario releases NO_2 and MMH as single constituents in separate evaporating pools that are assumed to have no chemical interaction. Extremely high concentrations occur right at the evaporating pool. Exposure to these concentrations for even a short duration could be lethal to humans and animals.

The 5 ppm hazard zone distances reported here contain within their borders much higher concentrations nearer to the source. The 5 ppm hazard zone could be considered a containment area or distance within which moderate health effects (or worse) in people are expected. The following general characteristics are noted:

Peak NO_2 concentrations:	10000 to 50000 ppm
Maximum downwind distance to peak concentration:	-- not meaningful (at pool) --
Maximum 5.0 ppm hazard distance:	800 to 2500 meters
Concentration probabilities:	100% of cases >10 ppm
Duration of exposure:	< 20 minutes
Peak MMH concentrations:	200 to 5000 ppm
Maximum downwind distance to peak concentration:	-- not meaningful (at pool) --
Maximum 5.0 ppm hazard distance:	100 to 280 meters
Concentration probabilities:	100% of cases >10 ppm
Duration of exposure:	< 120 minutes

How best to interpret and use these toxic hazard assessment is left to the judgment of range planner and NASA policy directives. The Air Force ranges employ detailed risk mitigation procedures for launch vehicles and missions that have potential for exposing workers or the general public to planned or accidental releases. Mitigations include holding a launch until meteorological conditions are favorable, moving people out of potential toxic hazard corridors and sheltering in place in approved shelters. While these types of policies can be applied to people, they cannot all be applied to sensitive flora and fauna that may be present at the launch facility.

2. INTRODUCTION AND BACKGROUND

In recent years Wallops Flight Facility (WFF) has expanded launch vehicle operations to include increasingly larger launch vehicles such as the Minotaur 1. Planned future missions anticipate launches of the Orbital Sciences Corporation Antares vehicle and the Minotaur 4 and 5. This report evaluates atmospheric dispersion of chemical emissions resulting from the launch of a hypothetical large solid rocket booster that might be launched from Wallops Flight Facility at some point in the future. These findings are intended to supplement a broader range programmatic Environmental Impact Study (EIS) being conducted by CardnoTec Inc. to assess impacts at WFF related to infrastructure development for, and launch of, a large solid rocket booster. Traditionally the Air Force and NASA have supported mission planning and day of launch hazard assessments for the launch of large vehicles from Cape Canaveral and Vandenberg Air Force Base. Recognized launch hazards can be categorized into the following classes that affect the larger launch area:

1. Inert Debris Impact Hazards
2. Explosive Debris Impact and Air Blast Overpressure Hazards
3. Distant Focused Overpressure Hazards
4. Toxic Emission Hazards

In general these hazards are associated with catastrophic failure of the launch vehicle or range safety command destruct of a vehicle exhibiting errant flight behavior. Debris hazards can affect a long flight corridor extending thousands of miles downrange. In the case of an orbital launch from WFF, the debris hazard region can include Europe or Africa. Depending on the type of first stage propellants used, toxic emission hazards may also be associated with normal (successful) launch of the vehicle.

Additional hazards that affect a more limited area near the launch pad are:

1. Acoustic Energy and Ignition Over Pressure (IOP) Hazards
2. Thermal Energy Hazards

The scope of this study is restricted to evaluation of toxic hazard emissions from both normal launch and early flight failures (e.g. the first 20 seconds of flight) that can deposit large quantities of chemicals in the convective boundary layer of the atmosphere. The convective boundary layer is generally that region of the atmosphere that is affected by surface heating and terrain topography. The boundary layer thickness varies with a diurnal cycle and is also affected by synoptic scale weather patterns (e.g. frontal systems). In this study the wind, temperature, humidity and pressure profiles in the lower 10,000 feet of the atmosphere are used to define the region of interest for chemical release and subsequent downwind transport and dispersion. Chemical concentrations of vaporized propellants or propellant combustion products at ground level are predicted as a measure of hazard potential.

Although dozens of rocket propellant types have been developed and tested over the years, the current inventory of large rockets manufactured in the United States employ a relatively few combinations of propellant types, which are:

1. Liquid stages using RP-1 fuel + liquid oxygen
2. Liquid stages using liquid hydrogen fuel + liquid oxygen
3. Liquid stages using hydrazine based fuel + nitrogen tetroxide oxidizer
4. Solid propellant stages using aluminum metal and organic binder fuel + ammonium perchlorate oxidizer.

A previous WFF Environmental Assessment (EA) study [1] was performed to evaluate chemical emissions from static test firing and normal launch of the Taurus II (Antares) launch vehicle. The Antares vehicle is representative of the first class of vehicles that use RP-1 (refined rocket propellant grade kerosene) and liquid oxygen (LOX). Although these propellants are burned in a fuel rich mixture the exhaust products can be considered environmentally friendly compared to solid propellant exhaust. The use of RP-1/LOX also avoids handling and spill toxic hazards associated with liquid hypergolic propellants. Consequently, the primary chemical exhaust constituent of concern for RP-1/LOX combustion from a toxicity standpoint is carbon monoxide (CO). The vehicle configuration evaluated in this study was assumed to be a four stage vehicle with each stage using solid propellant. A payload (e.g. satellite) was assumed to contain relatively small quantities of commonly used liquid hypergolic monomethylhdrazine (MMH) ($CH_3(NH)NH_2$) fuel and liquid hypergolic nitrogen tetroxide (N_2O_4) oxidizer. The last U.S. launch vehicle to use large quantities of hypergols in the main propulsion stages was the Titan IV, which is no longer in production. Many Russian and Chinese launch vehicles still use hypergolic propellants, but these are unlikely to be used at WFF. All of the commonly used hypergolic fuel and oxidizer chemicals are highly toxic. Since the candidate vehicle did not employ RP-1 + LOX or the cryogenic combination of liquid hydrogen + LOX, no further consideration is given to these common propellant combinations.

3. REPRESENTATIVE LAUNCH VEHICLE CHARACTERISTICS

The launch vehicle selected for this analysis is based on a design concept proposed by ATK [2]. The proposed launch vehicle has not yet been built but the stages are based on motors or motor segments used on other existing launch vehicles. ATK provide sufficiently detailed motor ballistics and propellant data for ACTA to develop database parameters needed by the toxic dispersion models used in this analysis. The first stage of the proposed launch vehicle is designated by ATK as a Castor 1200, which is a 4-segment motor built from slightly modified motor segments used on the now retired Space Shuttle Reusable Solid Rocket Motor (RSRM) design. The solid propellant formulation is designated as TP H1148 Type VIII (RSRMV) by ATK. This formulation is very similar to that used in the Shuttle RSRM segments differing primarily in the amount of iron oxide, a minor constituent that is used to control the burn rate of the propellant. The major constituents of TP-1148 on a percent by weight basis are:

Ammonium Perchlorate (AP)	69.7%
Aluminum	16.0%
PBAN binder and curatives	14.3%

PBAN (polybutadiene acrylonitrile) copolymer is a viscous organic binder used to mix the aluminum powder, AP crystals and curing agents together into a propellant slurry that is poured into castings and cured to form a rubbery solid propellant grain inside the motor. Motor propellant castings are typically cylindrical in shape with a center bore where the casting mandrel is removed. The propellant castings have a star pattern to increase the burning surface area during the early stage of the propellant burn. The burn rate of solid propellant is pressure dependent, a factor that will be significant to this analysis because in the catastrophic failure scenario analyses the solid propellant motor is assumed to break up into many pieces with the propellant burning at atmospheric pressure (14.7 PSIA). Normal motor burn has an internal pressure around 900 PSIA with a substantially higher burn rate. This study used the following atmospheric burn rate provided by Thiokol for Shuttle SRB TP-1148 propellant that is also used by the Air Force to predict toxic dispersion from catastrophic failures of Shuttle SRBs:

Burn rate at 14.7 PSIA = 0.065 in/sec

At normal Castor 1200 operating pressure, ATK indicated that the average burn rate of the solid propellant is about 0.347 in/sec. Figure 3-1 illustrates the general design and dimensions of the Castor 1200 motor.

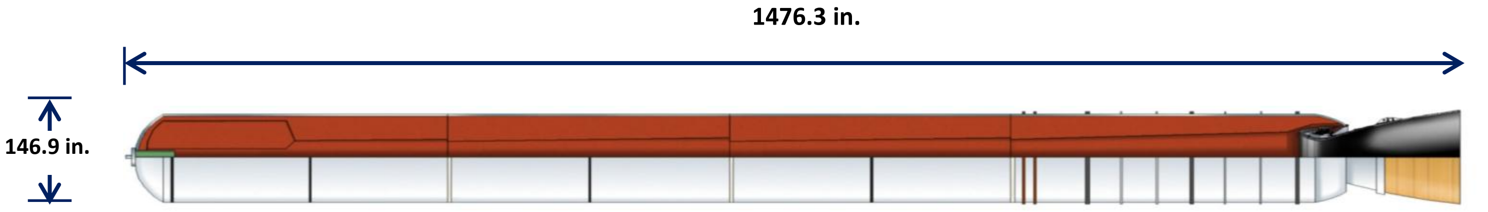

Figure 3-1. Motor Dimensions of the Castor 1200 First Stage.

The Castor 1200 motor contains 1,114,155 pounds of solid propellant and has a burn time of approximately 132.8 seconds.

During a nominal launch event the first stage motor is ignited with a starter cartridge and a flame front develops on the interior surface of the propellant grain. Hot combustion gases build up pressure within a few tenths of a second to approximately 870 pounds per square inch (PSIA). The combustion temperature inside the motor chamber is approximately 3400 Kelvin. The hot gases flow out of the combustion chamber through the rocket nozzle and exit the nozzle at supersonic flow at about Mach 3 giving the motor the thrust that lifts the vehicle from the pad and accelerates the vehicle as it ascends. The mass flux exiting the nozzle is somewhat time dependent and is a function of the burn rate and pressure inside the solid rocket motor.

Large launch vehicles are designed to carry a payload into orbit around the Earth. The first stage typically contains the largest percentage of the total vehicle propellant load and gets the vehicle to a position high above the dense part of the atmosphere and well downrange from the launch pad. The Ares-1X test vehicle launched from Cape Canaveral in October 2009 used a first stage very similar in design to the Castor 1200 motor. At burn out of the Ares-1x first stage the vehicle was approximately at 24.5 miles altitude, 41 miles down range and traveling at almost 5000 feet per second. At first stage separation, even if the second stage failed to ignite, the upper stage and payload would have sufficient velocity to carry the upper stage assembly 142 miles downrange. In the event that the vehicle guidance system had a gross azimuth failure, a large launch vehicle like the Castor 1200 or the Ares-1X launched from WFF could thrust an upper stage assembly (with explosive rocket motors) in an unintended direction with an impact in the Washington DC or Baltimore area. To prevent this type of consequence from errant flight failure conditions, the range tracks the launch vehicle with ground radars and monitors telemetry signals sent to the ground tracking station from the vehicle. If the vehicle deviates from the intended downrange "safe" flight corridor, the Range Safety Office (RSO) sends command destruct signals to the launch vehicle. The launch vehicle stages contain linear shaped explosive charges that destroy the launch vehicle and terminate thrust such that the debris still falls within a “safe” area. In the event of a command destruct action during early first stage flight, the Castor 1200 motor is shattered into hundreds of burning propellant fragments that fall to the ground in the launch area. Sudden release of the high pressure combustion gases inside the first stage solid rocket motor imparts additional “explosion induced” velocities to the propellant fragments. The net velocity of each fragment is the sum of the vehicle velocity at the explosion time plus a randomly oriented explosion induced component. In general the propellant fragments will impact in approximately a circular debris field surrounding the launch pad as the vehicle first begins its vertical ascent. As the vehicle climbs above the launch tower the guidance system initiates a pitch program that starts moving the vehicle downrange and gradually the resulting ground debris impact patterns also shift downrange and grow larger in diameter. In the event of a first stage explosive failure, the upper stage will experience a lesser degree of breakup and because the upper stage motors are unpressurized and are massive, they will only receive a small explosion induced velocity from the energetic gas expansion of the first stage.

The vehicle design evaluated for catastrophic aborts in this study was assigned the stage characteristics presented in Table 3-1. Castor information was provided courtesy of ATK. The payload designation was selected by ACTA based on typical propellant quantities and an oxidizer to fuel ratio of 1.64 used on payloads previously launched on Delta and Atlas launch vehicles.

Table 3-1: Castor 1200 Vehicle Stage Characteristics.

Stage	Stage Name	Propellant Type	Propellant Mass [lbm]	Motor Length [in]	Motor Diameter [in]
Stage 1	Castor 1200	TP-1148	1,114,115	1476	146.9
Stage 2	Castor 120	TP-1148	107,466	354.5	93.1
Stage 3	Castor 30B	TP-1148	28,278	164.5	92.1
Stage 4	Castor 20	TP-1148	17,790	146.7	92.1
Payload	---	MMH + N_2O_4	1,000 MMH 1,640 N_2O_4	---	---

Given the early stage of the Castor 1200 vehicle design development, ATK did not yet have a representative nominal trajectory (position and velocity of the vehicle as a function of time). Based on technical discussions between ACTA and ATK, it was agreed that use of the Ares-1X nominal trajectory would be an adequate representation of the early stage 1 flight profile of a Castor 1200 launch vehicle. A plot of the first 40 seconds of the Ares-1X flight profile is illustrated in Figure 3-2. As will be presented later, abort analyses considered only the first 20 seconds of flight and normal launch considered approximately the first 28 seconds of flight to a vehicle altitude of 10,000 feet. Normal launch chemical emissions consider only the portion of propellant burned from stage 1 during ascent to 10,000 feet. Catastrophic abort of the launch vehicle applies a conservative assumption that all 4 stages of the launch vehicle will have their solid propellant contents burned to depletion in the lower atmosphere. The upper stages are assumed to be non-burning during free fall from the breakup altitude but are ignited at ground impact by the impact energy.

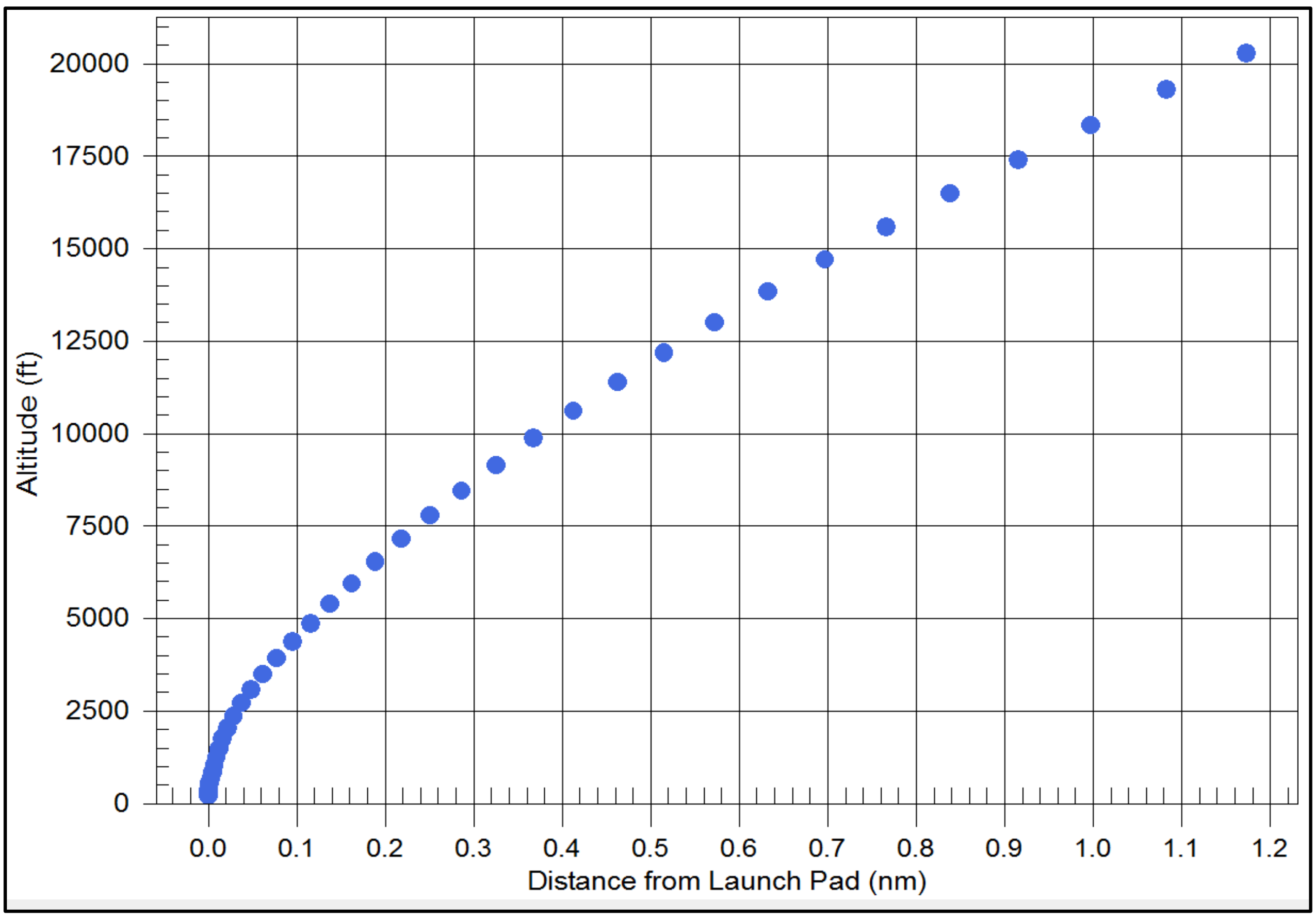

Figure 3-2. The Ares-1X Nominal Trajectory Flight Profile that was Applied to the Castor 1200 Vehicle Configuration.

4. TOXICITY THRESHOLDS FOR HAZARDOUS CHEMICALS

Regarding human toxicity, the chemicals of concern in the combustion products produced by burning TP-1148 propellant are hydrogen chloride gas (HCl) and aluminum oxide (Al_2O_3) particulates. HCl is a highly reactive gas that readily forms hydrochloric acid when it contacts water (this includes human lung, eye and skin tissues). Human response to high concentrations of HCl gas is prompt irritation with symptoms of coughing, choking, watering eyes, burning sensation and mucus membrane response. This prompt response characteristic correlates with toxic thresholds that are defined in terms of peak ceiling concentration values rather than accumulated dosage. (Lead poisoning would be an example of a toxic chemical exposure with delayed health response that is based on total dosage rather than time varying peak concentrations). The aluminum metal used in most solid propellant formulations is first melted and then oxidized to molten Al_2O_3 in the combustion chamber of the motor. The molten Al_2O_3 is entrained in the gas stream exiting through the throat of the nozzle and the mixture of liquid droplets and gas is accelerated to supersonic flow exiting the nozzle. As the jet exiting the nozzle expands and cools, the aluminum oxide solidifies into particulates of varying sizes. The exhaust flow is a complex two-phase flow with a slip velocity between the particles and the gas. Particles of differing sizes can agglomerate in the plume jet. Microscopic examination of Al_2O_3 particles that settled out from the Space Shuttle solid rocket motors indicated that many of the particles were actually hollow spheres. Particulate matter is a potential health hazard to humans and the following definitions give an idea of how the hazard varies with the size of the particles.

Total inhalable dust = The fraction of airborne particles that enters the nose and mouth during normal breathing. Generally considered as particles 100 microns and smaller.

Thoracic dust = The fraction of dust approximately 10 microns and less and will pass the nose and throat region and enter the lungs.

Respirable dust = The fraction of dust particles approximately 5 microns or less that can enter the gas exchange regions of the lungs. This region of the lungs is beyond the cilia and mucous clearance regions and these particles are more likely to be retained in the lung tissue.

Real particulates are not necessarily spheres with a definable diameter; consequently particulate material size is defined in terms of "aerodynamic diameter" where:

Aerodynamic Diameter = The diameter of a unit-density sphere having the same terminal settling velocity as the particle in question.

Toxicologists define two general categories of particulates that are of interest in lung disease:

Coarse particles (PM10) = Particles ranging in size from 2.5 to 10 microns in diameter.

Fine particles (PM2.5) = Particles under 2.5 microns in size.

- Ultra-fine particles (PM0.1) are a subset of fine particles and are drawing some attention as a unique category.

The particulate sizes emitted by solid rocket motors are at least partially dependent on the throat and nozzle size and is not well characterized by mathematical calculations. Measurements of particle sizes drawn from plume gas flow samples is often required to estimate the range of particle sizes and the distribution of the total Al_2O_3 mass among the size "bins". Such data is not available for the Castor 1200 motor. Consequently this study used the default particle size categories and mass distribution set in the Air Force Rocket Exhaust Effluent Diffusion Model (REEDM) that has been applied to other large solid rocket motors on the Titan launch vehicle and the Space Shuttle. The REEDM Al_2O_3 characteristics are presented in Table 4-1.

Table 4-1. REEDM Default Al_2O_3 Particulate Data.

Category	Diameter [microns]	Settling Velocity [m/sec]	Mass Fraction
1	0.95	0.0001	0.04
2	1.95	0.0003	0.14
3	2.95	0.0006	0.19
4	3.95	0.0010	0.18
5	4.95	0.0014	0.15
6	5.95	0.0019	0.11
7	6.95	0.0025	0.08
8	7.95	0.0032	0.05
9	8.95	0.0040	0.03
10	9.95	0.0049	0.02

It is noteworthy that the settling velocities for these small particle sizes are small, which means that the suspended particulate matter essential travels with the gas cloud and can result in simultaneous exposure of receptors to both HCl gas and small Al_2O_3 respirable particles. The 9.95 micron particle size has a settling velocity of 0.0049 meters per second. During the first 30 minutes of downwind transport, these largest particles will settle only about 9 meters relative to a neutral density gas. The propellant exhaust cloud itself rises under the influence of thermal buoyancy to a stabilization height that is dependent on the prevailing temperature profile in the atmosphere but is typically in the range of several hundred meters to a thousand meters. At stabilization, the exhaust cloud has dimensions of hundreds of meters and continues to grow in size during downwind transport due to wind shears and atmospheric turbulence. Thus a 9 meter settling distance represents only a small percentage of the overall cloud size and the particulate concentration will disperse approximately at the same rate as the gaseous material.

The hazard associated with exposure to HCl can be associated with several industry standard exposure criteria. Since emissions from rocket launches are relatively short duration events that only occur a few times a year over the course of the program, short duration or emergency exposure standards are more appropriate than long duration exposure standards designed for work place environments. One such emergency exposure standard is the National Institute for Occupational Safety and Health (NIOSH) definition of the Immediately Dangerous to Life or Health (IDLH) exposure threshold for an airborne chemical. The IDLH is intended to be used in conjunction with workers wearing respirators in contaminated areas, such that if the respirator fails the person could escape the contaminated area without being incapacitated given a maximum exposure of 30 minutes. Perhaps a more appropriate set of exposure guidelines are the Acute Exposure Guideline Levels (AEGLs) that are supported by the EPA. The development of AEGLs is a collaborative effort of the public and private sectors worldwide. AEGLs are intended to describe the risk to humans resulting from once-in-a-lifetime, or rare, exposure to airborne chemicals. The National Advisory Committee for the Development of Acute Exposure Guideline Levels for Hazardous Substances (AEGL Committee) is involved in developing these guidelines to help both national and local authorities, as well as private companies, deal with emergencies involving spills, or other catastrophic exposures. The recommended final AEGLs for HCl are listed in Table 4-2.

Table 4-2: Final Acute Exposure Guideline Levels (AEGLs) for Hydrogen Chloride.

AEGL Level	10 min Exposure [ppm]	30 min Exposure [ppm]	60 min Exposure [ppm]	4 hr. Exposure [ppm]
AEGL 1	1.8	1.8	1.8	1.8
AEGL 2	100	43	22	11
AEGL 3	620	210	100	26

Definitions of the AEGL levels are as follows:

AEGL-1 is the airborne concentration, expressed as parts per million or milligrams per cubic meter (ppm or mg/m3) of a substance above which it is predicted that the general population, including susceptible individuals, could experience notable discomfort, irritation, or certain asymptomatic nonsensory effects. However, the effects are not disabling and are transient and reversible upon cessation of exposure.

AEGL-2 is the airborne concentration (expressed as ppm or mg/m3) of a substance above which it is predicted that the general population, including susceptible individuals, could experience irreversible or other serious, long-lasting adverse health effects or an impaired ability to escape.

AEGL-3 is the airborne concentration (expressed as ppm or mg/m3) of a substance above which it is predicted that the general population, including susceptible individuals, could experience life-threatening health effects or death.

The time duration that a receptor is exposed to a rocket exhaust plume emission depends upon the cloud transport wind speed and the size of the cloud. The cloud or plume grows in size as it transports downwind. Typical exposure durations are estimated to be in the 10 to 30 minute range but may approach one hour under very light wind conditions.

The payload hypergolic propellants are quite toxic and pose an airborne hazard when released to the atmosphere as the consequence of a vehicle failure. In this study the payload propellants considered were MMH and N_2O_4. Hydrazine is sometimes used on payloads as a monopropellant where the liquid propellant is reacted in an exothermic catalytic process to produce a hot gas that provides thrust to maneuver the payload. The recommended final AEGLs for MMH are listed in Table 4-3.

Table 4-3: Final Acute Exposure Guideline Levels (AEGLs) for Methyl Hydrazine (MMH).

AEGL Level	10 min Exposure [ppm]	30 min Exposure [ppm]	60 min Exposure [ppm]	4 hr. Exposure [ppm]
AEGL 1	NR	NR	NR	NR
AEGL 2	5.3	1.8	0.9	0.23
AEGL 3	16	5.5	2.7	0.68

Numeric values for AEGL-1 are not recommended, because (1) studies suggest that notable toxic effects may occur at or below the odor threshold or other modes of sensory detection, (2) an inadequate margin of safety exists between the derived AEGL-1 and the AEGL-2, or (3) the derived AEGL-1 is greater than the AEGL-2. The absence of an AEGL-1 does not imply that exposure below the AEGL-2 is without any adverse effects.
Abbreviations: NR, not recommended; ppm, parts per million

The recommended final AEGLs for Hydrazine are listed in Table 4-4.

Table 4-4: Final Acute Exposure Guideline Levels (AEGLs) for Hydrazine (N_2H_4).

AEGL Level	10 min Exposure [ppm]	30 min Exposure [ppm]	60 min Exposure [ppm]	4 hr. Exposure [ppm]
AEGL 1	0.1	0.1	0.1	0.1
AEGL 2	23	16	13	3.1
AEGL 3	64	45	35	8.9

The hypergolic oxidizer nitrogen tetroxide (N_2O_4) boils at 70.1 F and when released to the atmosphere the molecule readily dissociates into two molecules of nitrogen dioxide (NO_2), which effectively doubles the ppm concentration of NO_2 relative to N_2O_4. The recommended final AEGLs for nitrogen dioxide are listed in Table 4-5. The AEGLs for nitrogen tetroxide are exactly ½ of the values listed in Table 4-5.

Table 4-5: Final Acute Exposure Guideline Levels (AEGLs) for Nitrogen Dioxide (NO_2).

AEGL Level	10 min Exposure [ppm]	30 min Exposure [ppm]	60 min Exposure [ppm]	4 hr. Exposure [ppm]
AEGL 1	0.5	0.5	0.5	0.5
AEGL 2	20	15	12	8.2
AEGL 3	34	25	20	14

AEGL thresholds have not been established for Al_2O_3. The Environmental Protection Agency (EPA) has defined National Ambient Air Quality Standards (NAAQS) for 24-hour ("short term") and annual PM_{10} and $PM_{2.5}$ exposures in the 2006 71 FR 61144. The 24-hour NAAQS 2006 standards are:

2006 (PM2.5) 35 $\mu g/m^3$ 98th percentile averaged over 3 years

2006 (PM10) 150 $\mu g/m^3$ not more than once per year over a 3 year period

The NAAQS are intended primarily to address pollution sources that tend to be area wide and which can be exacerbated under adverse meteorological conditions ("pollution episodes"). It is unclear how meaningful the 24-hour exposure standards are to rocket emissions which are from a mobile transient source with exposure durations generally less than 1 hour and perhaps as short as 10 to 20 minutes. The Occupational Safety and Health Administration (OSHA) have also published standards for certain particulates that are codified in CFR Part 29 1910.1000 subpart Z "Toxic and Hazardous Substances". OSHA standards are geared toward protecting workers from excessive exposure during an 8-hour work day and 40-hour work week environment. The nearest applicable OSHA standards for Al_2O_3 are for "emery" (CAS 12415-34-8) and "Particulates Not Otherwise Regulated" (PNOR). PNOR values apply to "Inert or Nuisance Dust" and the recommended threshold OSHA standards for both are:

– 15 mg/m^3 total dust (8-hour time weighted average concentration)

– 5 mg/m^3 respirable dust (8-hour time weighted average concentration)

It is unclear how applicable the OSHA standards are to emissions from rocket launches that may only occur several times a year and that produce transient short term exposures in toxic corridors that vary with prevailing wind speed and wind direction.

The American Industrial Hygiene Association has published recommended Emergency Response Planning Guidelines (ERPGs), which have very similar definitions to AEGLs. ERPGs cover a wide range of chemicals but no ERPG standards are defined for Al_2O_3 or emery.

The National Institute for Occupational Safety and Health (NIOSH) derives authority from Occupational Health and Safety Act (OSHA 1970) and Federal Mine Safety and Health Act (MSHA 1977). OSHA and MSHA have responsibility to promulgate and enforce legal standards. NIOSH develops and periodically revises recommended exposure limits (RELs) for hazardous substances or conditions in the workplace. NIOSH publishes the "Pocket Guide to Chemical Hazards" ref. http://www.cdc.gov/NIOSH/NPG/. Several NIOSH standards are:

- IDLH = Immediately Dangerous to Life and Health
- REL = 10-hour TWA for 40-hour workweek
- STEL = 15 minute TWA not to be exceeded anytime during workday.

The 2007 NIOSH Pocket Guide has the following guideline standards and comments pertaining to Al_2O_3 (α-Alumina) particulates:

- IDLH – not defined
- Respirator requirements - Not Available
- OSHA PEL = 8-hour TWA 15 mg/m^3 total dust, 5 mg/m^3 respirable dust
- NIOSH REL = No recommendation, however, NIOSH review of OSHA PEL supporting literature was criticized as being insufficient to justify selection of PEL thresholds.

The American Conference of Governmental Industrial Hygienists (ACGIH) provides guidance in the form of Threshold Limit Values (TLVs). ACGIH Threshold Limit Values are defined as follows:

- Threshold Limit Values (TLVs®) and Biological Exposure Indices (BEIs®) are determinations made by a voluntary body of independent knowledgeable individuals. They represent the opinion of the scientific community that has reviewed the data described in the *Documentation*, that exposure at or below the level of the TLV® or BEI® does not create an unreasonable risk of disease or injury.

- TLVs® and BEIs® are not standards. They are guidelines designed for use by industrial hygienists in making decisions regarding safe levels of exposure to various chemical substances and physical agents found in the workplace. In using these guidelines, industrial hygienists are cautioned that the TLVs® and BEIs® are only one of multiple factors to be considered in evaluating specific workplace situations and conditions.

  Source: http://www.acgih.org/TLV/

The ACGIH recommended exposure threshold for Al_2O_3 is: 10 mg/m^3 8-hour TWA

- Ref. 2001 New Jersey Dept. of Health and Senior Services, Hazardous Substance Fact Sheet

The bio-environmental organization at the NASA Kennedy Space Center launch complex prefers to use ACGIH recommendations when AEGLs are not available.

The Subcommittee on Consequence Assessment and Protective Actions (SCAPA) supports the Department of Energy/National Nuclear Security Administration. SCAPA developed standards called Temporary Emergency Exposure Limits (TEELs) through their Chemical Exposures Working Group. TEELs are recommended by SCAPA when ERPGs or AEGLs are not defined. The TEEL threshold descriptions are virtually identical to the ERPGs. The formal TEEL definitions are:

- **TEEL-3** = The maximum concentration in air below which it is believed nearly all individuals could be exposed without experiencing or developing life-threatening health effects.

- **TEEL-2** = The maximum concentration in air below which it is believed nearly all individuals could be exposed without experiencing or developing irreversible or other serious health effects or symptoms that could impair their abilities to take protective action.

- **TEEL-1** = The maximum concentration in air below which it is believed nearly all individuals could be exposed without experiencing other than mild transient adverse health effects or perceiving a clearly defined, objectionable odor.

- **TEEL-0** = The threshold concentration below which most people will experience no appreciable risk of health effects.

The National Oceanic and Atmospheric Administration (NOAA) provide the following explanation of TEELs:

- TEELs estimate the concentrations at which most people will begin to experience health effects if they are exposed to a toxic chemical for a given duration.

- Sensitive members of the public--such as old, sick, or very young people--are not covered by these guidelines and they may experience adverse effects at concentrations below the TEEL values.

- TEELs are used in similar situations as the 60-minute AEGLs and ERPGs. However, in situations where the concentration varies over time, the TEEL developers recommend using a conservative 15-minute time-weighted average concentration. A chemical may have up to four TEEL values, each of which corresponds to a specific tier of health effects.

- Source: http://response.restoration.noaa.gov/

SCAPA uses the various guidelines and thresholds to define “Protective Action Criteria” (PACs), which are equivalent to the TEEL threshold definitions.

- Used by DOE facilities for emergency planning purposes.

- Intended to approximate ERPGs.

- AEGLs and ERPGs evaluated more rigorously but limited to several hundred chemicals.

- SCAPA PACs available for over 3000 chemicals.

PAC thresholds for Al_2O_3 are:

- TEEL-0 1.5 mg/m^3

- PAC-1 1.5 mg/m^3

- PAC-2 15 mg/m^3

- PAC-3 25 mg/m^3

Although no AEGLs have been published for Al_2O_3 particulates, the review of multiple guidelines published by various agencies suggests that a reasonable exposure standard for Al_2O_3 falls somewhere in the 1 to 25 mg/m^3 concentration range. This report provides information on concentration versus distance predictions for Al_2O_3 that allow for evaluation of toxic hazard corridor size and probability of occurrence over a range of possible threshold values that may be deemed by various parties to be applicable to an EIS assessment. Co-authors of this EIS have suggested that 5 mg/m^3 of respirable particulates (those particles 5 microns or less in size) is a suitable threshold for EIS evaluation.

The report authors do not have toxicological expertise regarding hazardous HCl, Al_2O_3, NO_2 or MMH thresholds for flora and fauna that may be of environmental concern. The selection of the most appropriate exposure level to apply to exposed flora and fauna is left to the judgment of others. We note that human toxicity and adverse health response data are often based on studies of laboratory mice, rats, and rhesus monkeys and that this type of data may be quite applicable to mammalian species. We also note that HCl and NO_2 are both reactive chemicals that form strong acids with water. They pose a short term acute hazard but do not persist long in the environment. We also know of one anecdotal event that occurred in Colorado at a rocket manufacturer processing facility. An accidental spill of N_2O_4 left a visible trail of vegetation damage along the plume path for several weeks after the release event. The following spring the same plume path was visible as a corridor with lusher green vegetation. The judgment of the propulsion chemists at that facility was that the NO_2 and HNO_3 resulting from the release entered the nitrification cycle and acted as a fertilizer the following spring.

5. COMPUTER MODELS AND EMISSION SCENARIOS

This study considered four hazardous chemical species (HCl, Al_2O_3, MMH and NO_2) and four launch vehicle emission scenarios. The emission scenarios are:

1. Normal launch
2. Catastrophic failure resulting in scattered burning propellant fragments (Conflagration)
3. Catastrophic failure leading to intact payload impact and hypergols fireball (Deflagration)
4. Catastrophic failure leading to intact payload impact with spill of liquid hypergols (Cold Spill)

ACTA elected to use two different Range Safety toxic dispersion models to simulate this combination of release scenarios and chemical types. The Rocket Exhaust Effluent Diffusion Model was used to simulate the normal launch scenario for both HCl and Al_2O_3. REEDM was also used to model Al_2O_3 dispersion for the conflagration scenario. The Launch Area Toxic Risk Analysis 3-Dimensional (LATRA3D) computer program was used to simulate HCl dispersion from the conflagration scenario and the hypergol releases for both the deflagration and cold spill scenarios. Both models are used by the Air Force, NASA, the Army and the FAA to perform toxic dispersion assessments for launch vehicles launched from Federal and commercial ranges.

5.1 Castor 1200 Normal Launch Emission Scenario

In this scenario a fully configured launch vehicle with payload is ignited on the launch pad at time T-0. The vehicle may be secured to the launch pad by hold down bolts as the first stage motor builds thrust after which the hold-downs are released allowing the vehicle to begin ascent to orbit. During ascent the vehicle velocity steadily increases resulting in a time and altitude varying exhaust product emission rate. Initially the rocket engine exhaust is largely directed into and through a flame duct. As the vehicle lifts off from the pad and clears the launch tower, a portion of the exhaust plume impinges on the pad structure and is directed radially around the launch pad stand. The portion of the rocket plume that interacts with the launch pad and flame trench is referred to as the “ground cloud”. As the vehicle climbs to several hundred feet above the pad, the rocket plume reaches a point where the gases no longer interact with the ground surface and the exhaust plume is referred to as the “contrail cloud”.

The concepts of the ground and contrail clouds are illustrated in Figure 5-1 using the Ares-1X launch from Cape Canaveral as an example. The Ares-1X first stage is very similar to the Castor

1200 first stage. For atmospheric dispersion analyses of rocket emissions that could affect receptors on the ground, it has been standard practice at the Federal Ranges (Cape Canaveral and Vandenberg Air Force Base) to simulate the emissions from the ascending launch vehicle from the ground to a vehicle altitude of approximately 3000 meters. The operational toxic dispersion analysis tool used by the Federal Ranges for launch support and public risk assessment has been Version 7.13 of the Rocket Exhaust Effluent Diffusion Model (REEDM). Most of the Ranges are now transitioning from REEDM to LATRA3D as the operational support tool. ACTA used REEDM Version 7.13 to simulate the normal launch emission scenario because REEDM includes a sub model to handle gravitational deposition of Al_2O_3 particulates that LATRA3D does not have. In order to maintain a consistent set of modeling assumptions and source cloud formation algorithms, REEDM was also used to predict HCl dispersion and downwind concentrations for the normal launch scenario. The features of REEDM pertinent to this study are discussed in the next section.

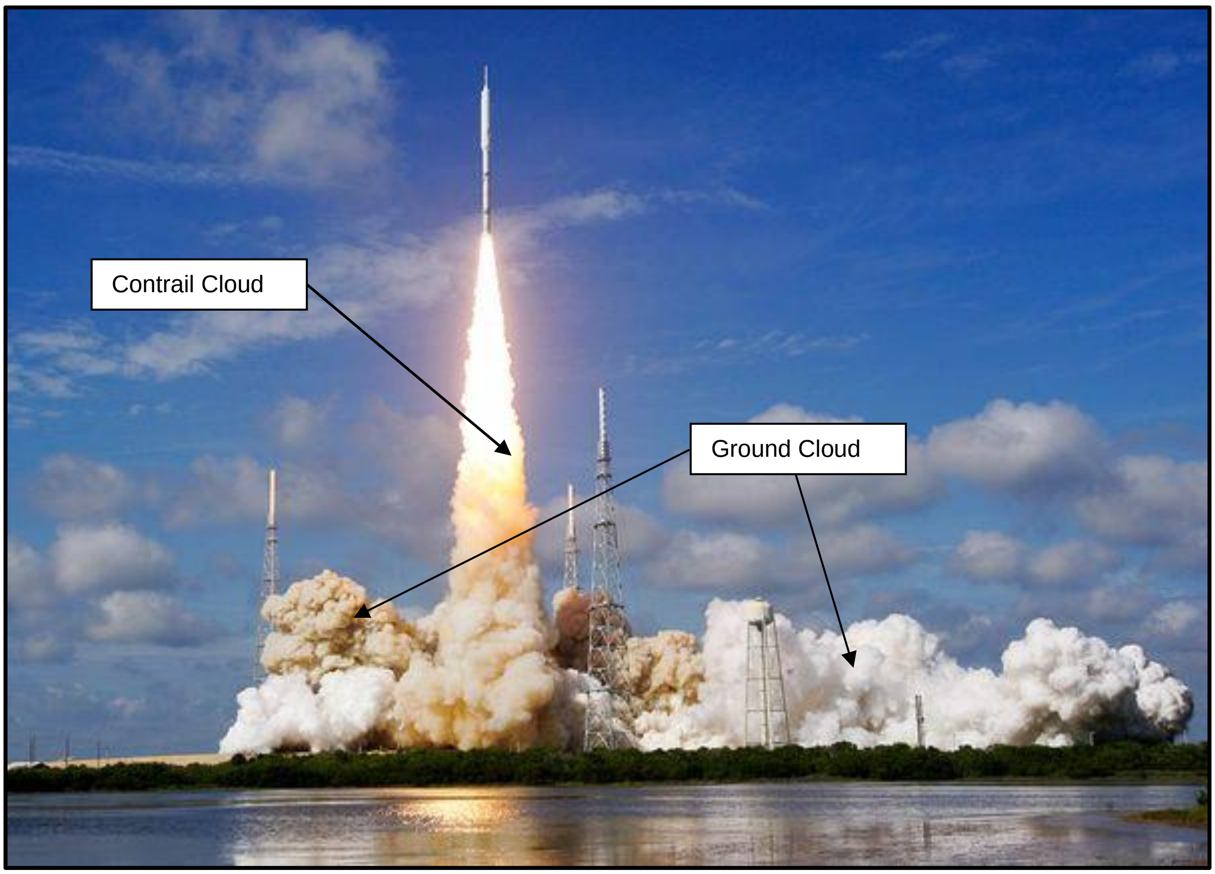

Figure 5-1. Illustration of the Ground Cloud and Contrail Cloud Portions of the Ares-1X Rocket Emission Plume Associated With Normal Vehicle Launch.

5.2 The Rocket Exhaust Effluent Dispersion Model (REEDM)

REEDM is a toxic dispersion model specifically tailored to address the large buoyant source clouds produced by rocket launches, test firings and catastrophic launch vehicle explosions. Under ongoing Air Force support, REEDM evolved from the NASA Multi-Layer Diffusion Model, which was written initially to evaluate environmental effects associated with the Space Shuttle, and has been generalized to handle a wide variety of launch vehicle types and propellant combinations. REEDM falls in the category of "Gaussian puff" atmospheric dispersion models in that the initial mass distribution of toxic materials within the cloud at the time the cloud reaches thermal stabilization height in the atmosphere is assumed to be normally distributed. By making the Gaussian mass distribution assumption, the differential equation defining mass diffusion can be solved in closed form using exponential functions and may be readily implemented in a fast running computer program. Gaussian puff models are still widely used by the EPA for environmental and permitting studies, by Homeland Security and the Defense Threat Reduction Agency for assessment of chemical, biological and radiological materials, and by the petrochemical industry for accidental releases of industrial chemicals.

REEDM processing of an emission event can be partitioned into the following basic steps:

1. Acquire and process vehicle related data from an input vehicle database file.

2. Acquire and process meteorological data, which in this study is a combination of archived weather balloon soundings used in conjunction with an internal REEDM climatological turbulence algorithm.

3. Acquire the chemical composition and thermodynamic properties of the rocket exhaust emissions and define the initial size, shape, location and heat content of the exhaust cloud (herein referred to as the "source term" or "source cloud"). REEDM has an internal propellant equilibrium combustion model that is used to compute these terms for vehicle catastrophic failure modes but for normal launch and static test firing scenarios this data is calculated external to REEDM and placed in the vehicle database file read by REEDM.

4. Iteratively calculate the buoyant cloud rise rate and cloud growth rate to achieve a converged estimate of the cloud stabilization height above ground, size and downwind position. The cloud rise equations evaluate both cloud thermodynamic state as well as the local atmospheric stability, which is defined by the potential temperature lapse rate.

5. Partition the stabilized cloud into disks and mark whether or not part of the stabilized cloud is above a capping atmospheric temperature inversion. Inversions (or other sufficiently stable air masses) act as a barrier to gaseous mixing and are treated in REEDM as reflective boundaries. Aluminum oxide particulates however are assumed to settle through a stable meteorological layer and are not reflected at the gaseous reflection boundary.

6. Transport the cloud disks downwind and grow the disk size using climatologic model estimates of atmospheric turbulence intensity. Turbulence intensity is a function of wind speed and solar radiation intensity. Turbulence varies with time of day and cloud cover conditions because these influence the solar radiation intensity. Particulate matter and gases are assumed to disperse at the same rate albeit the particulate matter is allowed to settle toward the ground.

7. Calculate concentrations at ground receptor points and determine the plume or cloud track “centerline” that defines the peak concentration as a function of downwind distance. Concentration at any given receptor point is computed as the sum of exposure contributions from each cloud disk. Concentration is solved using the closed form Gaussian dispersion equation and accounts for the effect of ground and capping inversion reflections.

8. Report concentration centerline values in table format as a function of distance from the source origin (e.g. launch pad)

There are other features and sub models of REEDM that are more fully described in the REEDM technical description manual [3] and will not be reviewed in this report.

There are several important assumptions made in REEDM that have a bearing on this Environmental Impact Study. REEDM was designed to primarily predict hazard conditions downwind from the stabilized exhaust cloud. REEDM does not directly calculate or report cloud concentrations during the buoyant cloud rise phase, however, advanced model users can extract sufficient pertinent cloud data from internal calculations to derive concentration estimates during the cloud rise phase manually. One assumption that REEDM makes about the nature and behavior of a rocket exhaust cloud is that it can be initially defined as a single cloud entity that grows and moves but remains as a single cloud during the formation and cloud rise phases. A consequence of this assumption is that once the cloud lifts off the ground during the buoyant cloud rise phase, there will be no predicted cloud chemical concentration on the ground immediately below the cloud. Ground level concentrations will be predicted to remain at zero ppm until the some of the elevated cloud material is eventually brought back down to ground level by mixing due to atmospheric turbulence. This concept is illustrated in Figure 5-2 and it is noted that REEDM is designed to report concentrations downwind from the stabilized cloud position. The region downwind from the stabilized exhaust cloud is referred to as the "far field". It is also noted here that the most concentrated part of these rocket exhaust clouds remains at an altitude well above the ground level. REEDM is not able to model stochastic uncertainty in the source cloud and atmospheric flow such that if a gust of wind, small turbulence eddy or nuance of the launch pad flame duct structure causes a small portion of the main exhaust cloud to detach from the main cloud, the model will not correctly predict the transport, dispersion or concentration contribution from the detached cloud material. Likewise if there are strong atmospheric updrafts or down drafts, such as associated with development of thunderstorm cells or towering cumulus clouds, REEDM will not correctly model strong vertical displacements of the entire exhaust cloud or strong shearing forces that may completely breakup the cloud under such conditions (these are not favorable conditions for launch either and a planned launch would never be conducted with strong thunderstorm and cloud development activity in the launch area).

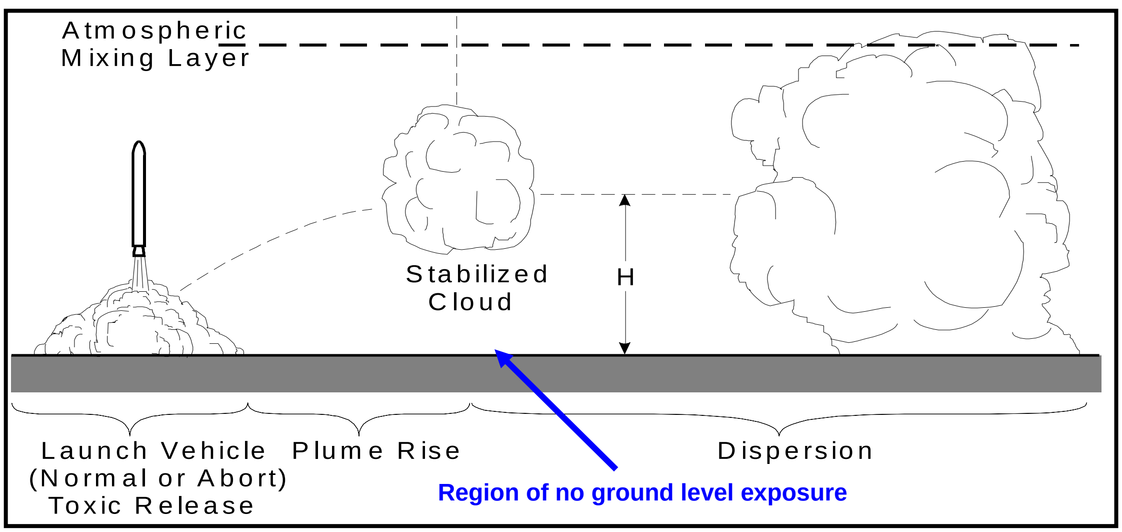

Figure 5-2. Conceptual Illustration of Rocket Exhaust Source Cloud Formation, Cloud Rise and Cloud Atmospheric Dispersion.

REEDM is also somewhat constrained by the Gaussian assumptions inherent in the model that require a single average transport wind speed and direction. The portion of the atmosphere selected for averaging the transport winds has been improved over the years of operational use at the Air Force ranges. Old versions of REEDM averaged the winds over the entire boundary layer, which in the absence of a capping inversion, was treated as being 3000 meters deep. The modern version of REEDM now selects the appropriate atmospheric layer based on the stabilization height of the cloud, the top of the cloud and the location of the reflective boundary layers. Comparison of REEDM predicted rocket exhaust cloud transport direction and speed with Doppler weather radar tracks of rocket exhaust clouds has indicated that the modern version of REEDM performs very satisfactorily in predicting the correct average cloud transport direction and speed. The “multi-layer” aspect of REEDM is still retained from its early development and refers to the partitioning of the stabilized rocket exhaust cloud into “disks” of cloud material assigned to meteorological levels at different altitudes. The altitude bands are typically 20 to 50 meters in depth. REEDM models the initial formation of a rocket exhaust cloud as either an ellipsoid or a sphere and predicts the buoyant could rise of the source as a single cloud entity. Once the cloud is predicted to have achieved a condition of thermal stability in the atmosphere, the cloud is partitioned into disks. The placement of each disk relative to the source origin (e.g. the launch pad) is determined based on the rise time of the cloud through a sequence of meteorological layers that are defined using the measurement levels obtained from a mandatory weather balloon input data file. Each meteorological layer may have a unique wind speed and direction that displaces the cloud disk in the down wind direction. The initial placement of cloud disks that are associated with the lower portion of the overall source cloud are not influenced by winds above their stabilized altitude level whereas disks near the top of the stabilized cloud will be displaced by the winds all the way from the ground level to the disk stabilization altitude. Thus the vertical stack of cloud disks can be displaced relative to each other due to the influence of wind speed and direction shears. The concept of the stabilized cloud partition into disks is illustrated in Figure 5-3.

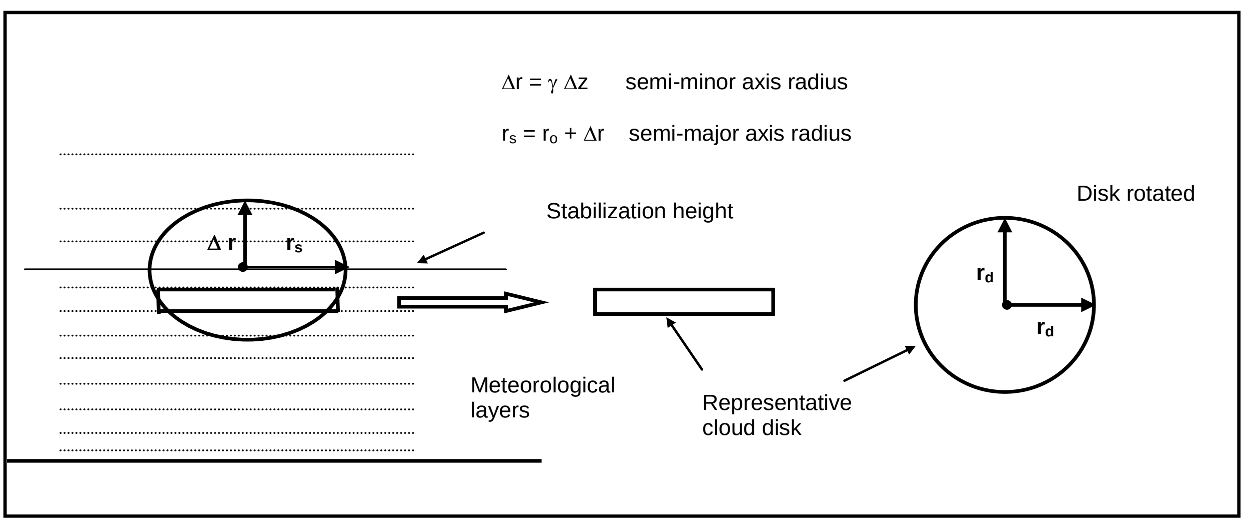

Figure 5-3. Illustration of REEDM Partitioning a Stabilized Cloud into Disks.

Once the cloud disks positions are initialized, future downwind transport applies the same average atmospheric boundary layer transport wind speed and direction to each cloud disk as illustrated in Figure 5-4.

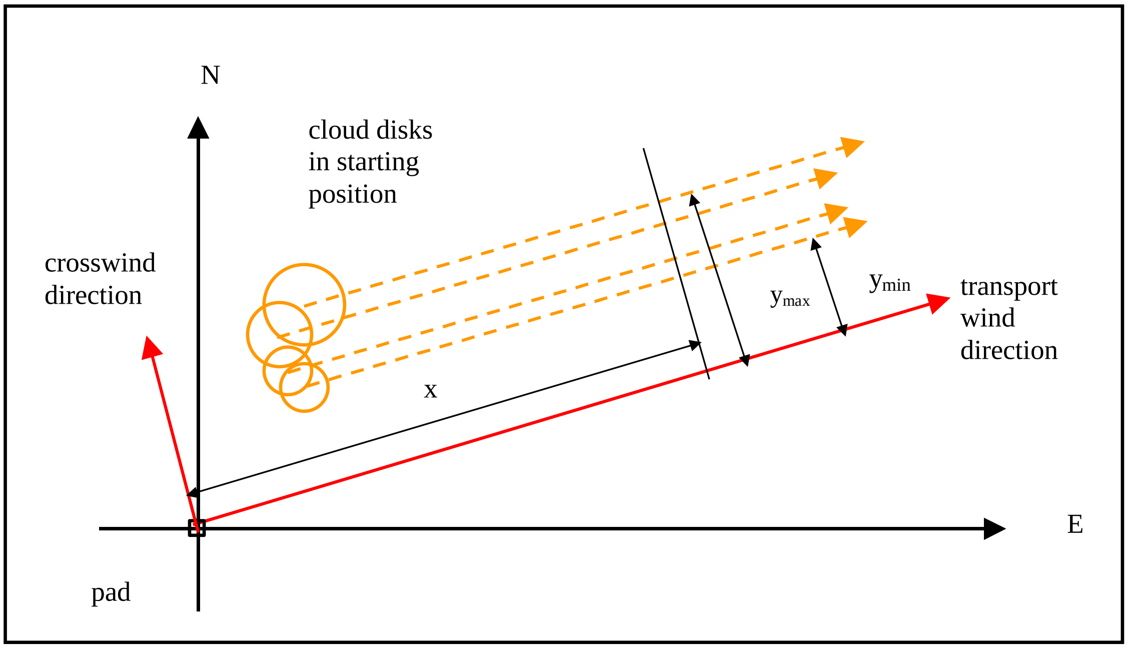

Figure 5-4. Illustration of Straight Line Transport of Stabilized Exhaust Cloud Disks Using Average Mixing Layer Wind Speed and Direction.

The assumption of straight-line transport used in REEDM during the cloud transport and dispersion phase ignores the possibility of complex wind fields that might arise in mountainous terrain or that could evolve during passage of a seabreeze front or synoptic scale weather front. It is recommended that the assumption of uniform winds be limited to plume transport distances of less than 20 kilometers. As will be shown in the analysis results section, REEDM predicted typical ranges of 10 to 20 kilometers from the launch pad to the location of the maximum far field ground level HCl concentration point, thus the assumption of straight line transport should not be a problem.

In the Castor 1200 normal launch scenario the exhaust emissions from the rocket combustion are at several thousand degrees Kelvin and are highly buoyant. The high temperature of these exhaust emissions causes the plume to be less dense than the surrounding atmosphere and buoyancy forces acting on the cloud cause it to lift off the ground and accelerate vertically. As the buoyant cloud rises, it entrains ambient air and grows in size while also cooling. In this initial cloud rise phase, the growth of the cloud volume is due primarily to internal velocity gradients and mixing induced by large temperature gradients within the cloud itself. Even though the cloud is entraining air and cooling by virtue of mixing hot combustion gases with cooler ambient air, the net thermal buoyancy in the cloud is conserved and the cloud will continue to rise until it either reaches a stable layer in the atmosphere or the cloud vertical velocity becomes slow enough to be damped by viscous forces. REEDM applies the following solution of Newton’s second law of motion to a buoyant cloud in the atmosphere to iteratively predict cloud stabilization height:

$$z(t)=\left[\frac{3F_m}{u\gamma^2\sqrt{s}}\sin\left(t\sqrt{s}\right)+\frac{3F_c}{u\gamma^2 s}\left(1-\cos\left(t\sqrt{s}\right)\right)+\left(\frac{r_o}{\gamma}\right)^3\right]^{1/3}-\frac{r_o}{\gamma}$$

where:

s = atmospheric stability parameter = $\dfrac{g}{\theta_a}\dfrac{\Delta\theta_a}{\Delta Z}$ [sec^{-2}]

g = gravitational acceleration constant = 9.81 [m/sec^2]

θ_a = potential temperature of ambient air [K]

F_m = $r_o^2 w_o u$ = initial vertical momentum [m^4/sec^2]

u = mean ambient wind speed [m/sec]

w_o = initial vertical velocity [m/sec] (typically = 0.0)

r_o = initial plume cross-sectional radius [m]

F_c = initial buoyancy = $\dfrac{g\,\dot{q}}{\pi\,\rho_c\,C_p\,T_a}$ [m^4/s^3]

C_p = specific heat of exhaust cloud gases [cal/kg K]

= air entrainment coefficient (dimensionless)

z = plume height at time t [m]

$\dot{q}$ = initial plume heat flux [cal/sec]

T_a = ambient air temperature [K]

ρ_c = density of exhaust cloud gases [kg/m^3]

A critical parameter in the cloud rise equation is the rate of ambient air entrainment that is defined by the dimensionless air entrainment coefficient, γ. Cloud growth as a function of altitude is assumed to be linearly proportional and the air entrainment coefficient defines the constant of proportionality. REEDM's cloud rise equations have been compared with observations and measurements of Titan rocket ground clouds and a best-fit empirical cloud rise air entrainment coefficient has been derived from the test data, a sample of which is illustrated in Figure 5-5.

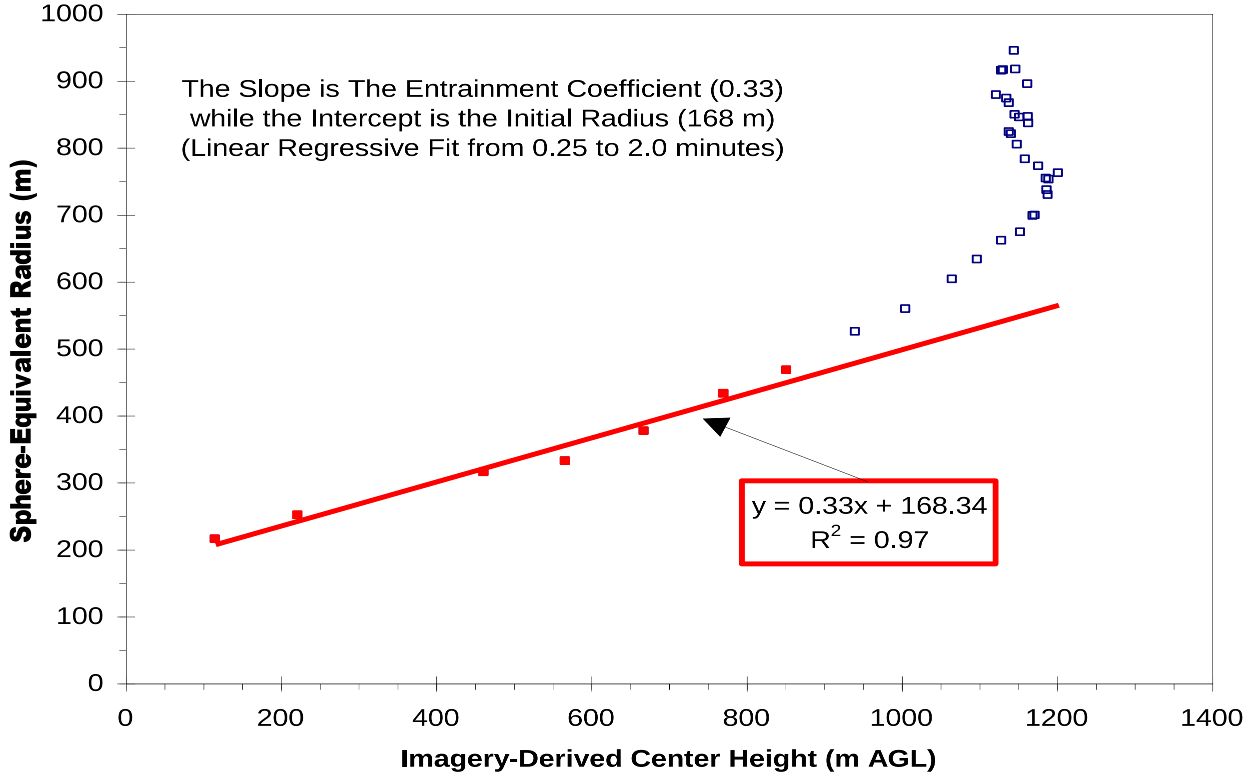

Figure 5-5. Observed Cloud Growth Versus Height for Titan IV A-17 Mission.

The Castor 1200 buoyant source clouds are predicted to rise from 500 to 1300 meters above the ground depending on atmospheric lapse rate conditions.

5.3 Castor 1200 Normal Launch Data Development

Proper specification of vehicle characterization input data is critical to the overall toxic dispersion analysis problem. While many vehicle input parameters are straightforward and readily verifiable (e.g. types and amounts of propellants loaded on the vehicle), other parameters inherently involve greater uncertainty and are not readily verifiable (e.g. amount of ambient air entrained into the rocket plume at the flame duct inlet). In this report section the vehicle input data values used in the REEDM Castor 1200 normal launch scenario analyses are itemized and explained. Input parameters that entail significant uncertainty were treated in a conservative fashion in the sense that choices were made to favor overestimating rather than underestimating the toxic chemical concentrations being evaluated for the Environmental Impact Study. Information pertaining to the vehicle propellant loads and burn rates were provided by ATK personnel whereas the expected nominal launch flight trajectory was based on the Ares-1X nominal trajectory provided by NASA to the 45th Space Wing and converted by ACTA into REEDM database format.

5.4 Castor 1200 Normal Launch REEDM Vehicle Data

The following data items represent the vehicle data needed to characterize the normal launch scenario and are presented in the REEDM database format.

```
#05.00                         VEHICLE DATA SECTION
   VEHICLE TYPE = 4, NAME =  CASTOR1200  ,
   TIME HEIGHT COEFFICIENTS A,B,C =     0.74678 ,     0.45406 ,       0.0000,
#05.01 NORMAL LAUNCH ENGINE DATA FOR STAGES IGNITED AT LIFT-OFF:
   NUMBER OF IGNITED SRB'S           =   1,
   SOLID FUEL MASS             (LBM) =   1.11416E6,
   SOLID FUEL BURN RATE      (LBM/S) =   1.0940E4 ,          avg over first 20 sec
   LIQUID FUEL MASS            (LBM) =   0.0000000,
   LIQUID FUEL BURN RATE     (LBM/S) =   0.0000000,
   LIQUID OXIDIZER MASS        (LBM) =   0.0000000,
   LIQUID OXIDIZER BURN RATE (LBM/S) =   0.0000000,
   AIR ENTRAINMENT RATE IN GROUND CLOUD    (LBM/S) =   8752.0000,80% of propellant burn
rate
   TOTAL DELUGE WATER ENTRAINED IN GROUND CLOUD (LBM) =   0.0000000,
   AIR ENTRAINMENT RATE IN ROCKET CONTRAIL    (LBM/S) =   8752.0000,
   VEHICLE HEIGHT TO WHICH PLUME CONTRIBUTES TO GROUND CLOUD (FT) = 525,   ares1x values
   GROUND CLOUD INITIAL AVERAGE TEMPERATURE         (F) =  3100,
   GROUND CLOUD INITIAL HEAT CONTENT            (BTU/LBM) =  2169,
   INITIAL VERTICAL VELOCITY OF GROUND CLOUD      (FT/S) =   0.0,
   INITIAL RADIUS OF GROUND CLOUD                   (FT) = 150.0,
   INITIAL HEIGHT OF GROUND CLOUD                   (FT) =   0.0,
   INITIAL X DISPLACEMENT OF GROUND CLOUD FROM PAD (FT) =   0.0,
   INITIAL Y DISPLACEMENT OF GROUND CLOUD FROM PAD (FT) =   0.0,
   PLUME CONTRAIL INITIAL AVERAGE TEMPERATURE       (F) =  3100,
   PLUME CONTRAIL INITIAL HEAT CONTENT          (BTU/LBM) =  2169,
#05.02 NORMAL LAUNCH EXHAUST PRODUCT DATA:
 CHEMICAL NAME       MOL. WT.    MASS FRAC. GAS    MASS FRAC. COND   HAZARDOUS    ares1x
values
 GROUND CLOUD:
   HCL              36.460        0.11865          0.00000          Y
```

```
  CO2             44.010        0.11299          0.00000          Y
  CO              28.010        0.07519          0.00000          Y
  AL2O3          101.960        0.16797          0.00000          Y
  END
CONTRAIL:
  HCL             36.460        0.11865          0.00000          Y
  CO2             44.010        0.11299          0.00000          Y
  CO              28.010        0.07519          0.00000          Y
  AL2O3          101.960        0.16797          0.00000          Y
  END
```

REEDM does not utilize the launch vehicle trajectory directly; instead a power law fit to the height of the vehicle above ground as a function of time is derived from the trajectory data. The fit achieved with the derived power law time-height coefficients is demonstrated in Figure 5-6

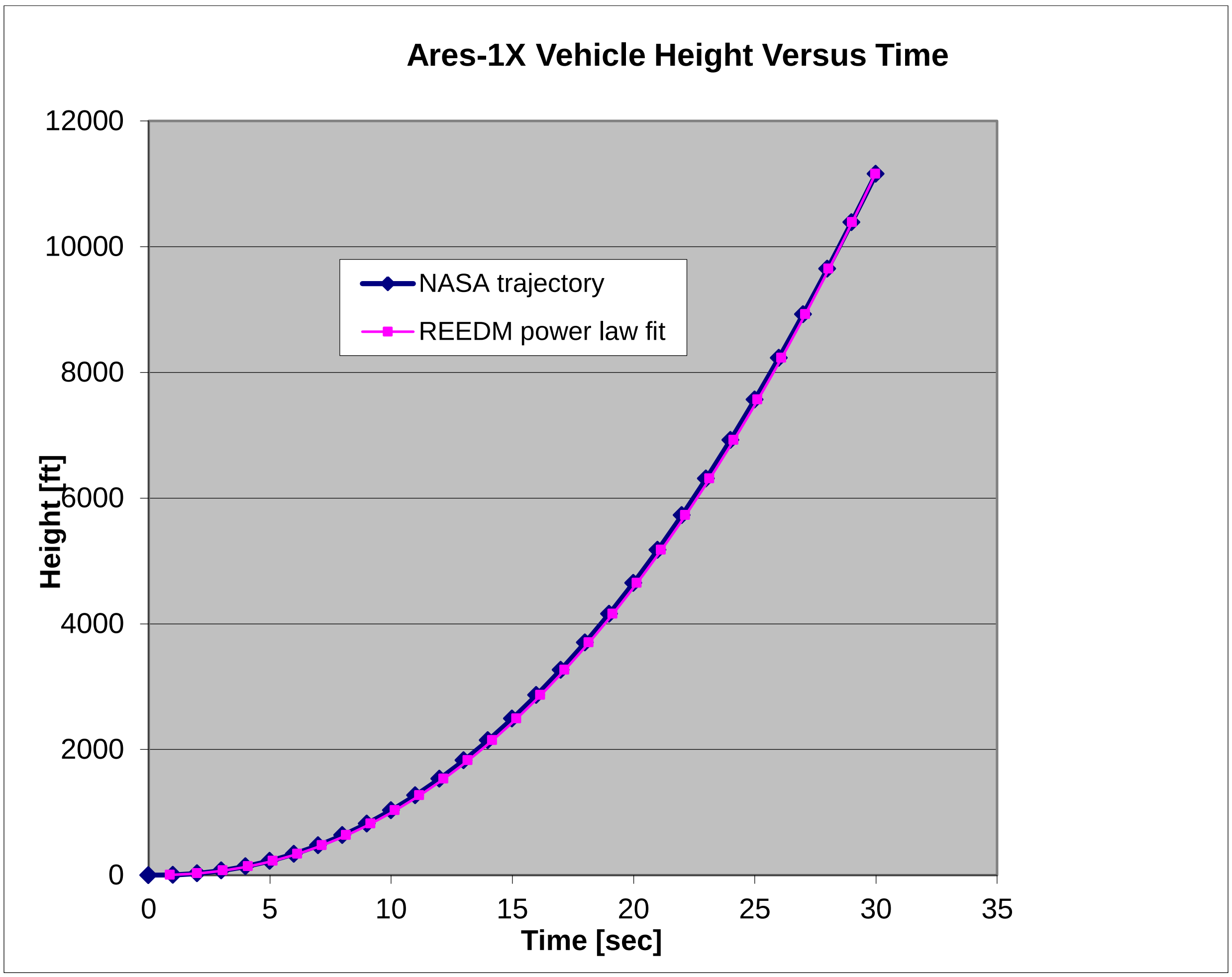

Figure 5-6. Plot of NASA Ares-1X Nominal Trajectory Compared with ACTA Derived Power Law Fit Used in REEDM.

REEDM allows for several chemical additions that may be included in the propellant exhaust of the normal launch ground cloud and the normal launch contrail cloud. In addition to specifying the nominal burn rates of the TP-1148 propellant, the user may optionally consider adding deluge or sound suppression water and entrained ambient air. For these two items the REEDM database serves only as a source of documentation for the assumptions applied in deriving the chemical compositions of the exhaust specified in section #05.02 of the database. It is noted here that "air entrainment" as specified in this section represents the user assumption about the amount of air, if any, added as a ***reactant*** in the propellant combustion calculations. This "air entrainment" definition is not to be confused with the "air entrainment" process that takes place during the cloud rise calculations. REEDM assumes that all chemical combustion reactions are completed before the cloud rise process takes place and REEDM therefore does not attempt to recompute chemical composition and additional heat release during the cloud rise computations.

The REEDM database provides the chemical composition of the normal ground and contrail clouds. A mass fraction is assigned to each constituent and the total exhaust mass in the source cloud is multiplied by this fraction to determine the total mass of each chemical in the exhaust cloud. The molecular weight of each species is used to convert the concentration from mass per unit volume [e.g.mg/m^3] to parts per million. For this study ACTA computed the chemical composition of the TP-1148 solid propellant exhaust using the NASA Lewis chemical equilibrium combustion model. The ACTA version of the NASA combustion model was modified slightly to output thermodynamic properties of the exhaust mixture that were needed to initialize the REEDM cloud rise equations. ACTA's combustion results for TP-1148 combustion with 80% added air to account for plume afterburning are shown in Table 5-1 ACTA ran the NASA combustion model in "rocket" analysis mode using an oxidizer (AP + Air) to fuel (aluminum + PBAN) ratio of 4.9406 and a combustion chamber pressure of 909 PSIA. ATK was provided the combustion product data developed by ACTA for the Ares-1X TP-1148 and ATK offered no comment or alternative data. The TP-1148 combustion data used by ACTA for the Shuttle RSRM (and later for the Ares-1X) was reviewed by Thiokol in the 1999 time frame and minor adjustments to the propellant formulation were made at that time giving ACTA combustion product results nearly identical to the Thiokol values. ACTA and ATK concurred that the ACTA TP-1148 propellant formulation used in this study was sufficiently close to the revised TP-1148 formulation to be used in the Castor 1200 as to not require modification of the REEDM database.

Table 5-1. Listing of ACTA Castor 1200 TP-1148 Propellant Combustion Products in the Normal Launch Exhaust Cloud Including Afterburning with Ambient Air.

Chemical	ACTA Weight Fraction
Ar	0.00570
Al_2O_3	0.16797
CO	0.07519
CO_2	0.11299
Cl	0.00052
HCl	0.11813
H	0.00001
OH	0.00007
H_2	0.00333
H_2O	0.12725
NO	0.00001
N_2	0.38621
$FeCl_2$	0.00261

5.5 Conservative Assumptions Applied In Data Development

The REEDM atmospheric dispersion model has been used operationally by the Air Force to make range safety launch decisions since 1989. During that time vehicle databases have been developed for many vehicles (e.g. Space Shuttle, Titan II, Titan III, Titan IV, Delta II, Delta III, Delta IV, Atlas II, Atlas III, Atlas V, Taurus, TaurusXL, Taurus Lite, Minotaur, Peacekeeper, Minuteman II, Minuteman III, Athena, Lance, Scud, ATK-ALV-1). As noted at the beginning of this section, some vehicle data is easily obtained and verified, such as the stage propellant types, quantities and burn rates. Other model input parameters required by REEDM are based on derived values obtained from mathematical and physical models, empirical measurement data or engineering judgment from the vehicle designer or range safety experts.

An example of a derived value is the selection of how much pad deluge water to include with the rocket engine exhaust when defining the normal launch cloud heat content, mass and chemical composition. A typical pad deluge system is comprised of a series of pressure fed sprayers and sprinklers that wet the launch pad, the launch service tower and the flame duct. The deluge system is typically turned on several seconds before the rocket motors are ignited and continues until the rocket has ascended above the launch tower and the plume no longer impinges on the ground. As the vehicle ascends, the rocket plume interaction with the pad structures is time varying, such that the gas flow velocity ranges from supersonic to subsonic and involves multiple shock fronts, reflected shocks, deflected flow from the pad surface, partial flow ducting through the flame trench and plume temperatures that range from 300 to 3000 K. A simple energy balance between the amount of heat available in the plume and the amount of water released in the deluge system may suggest that there is ample energy to vaporize all of the deluge water, but actual observation of launches indicates that residual deluge water is often collected in a concrete containment basin designed to collect residual deluge water. Likewise the initial ignition impulse often blows standing water out of the flame trench or away from the pad and depositing it as droplets before they can be fully mixed with the combustion gases and vaporized. Some parts of the launch plume during vehicle liftoff may become saturated with water vapor and other portions may remain relatively "dry". Thus the task of selecting a specific deluge water inclusion amount for the REEDM database and setting the associated chemical and thermodynamic data for the exhaust products is challenging and typically not estimated by the launch agency or vehicle developer. This type of flow problem is extremely complex and would require advanced computational fluid dynamics analysis that is extremely costly and also constrained by modeling assumptions. Consequently, these types of detailed analyses are rarely performed or conducted only for limited specific design purposes.

For the purposes of this study, it was agreed with CardnoTec to ignore the effect of any deluge water on normal launch ground cloud chemistry since an actual launch system and pad design remains unknown at present.

5.6 Castor 1200 Conflagration Al_2O_3 Emission Scenario

In REEDM terminology a conflagration event is defined as the explosion of a pressurized solid rocket motor that shatters the solid propellant casting (the "grain") and ejects burning solid propellant fragments away from the center of explosion due to the sudden release of the pressurized combustion gases. This event may be initiated by a failure within the motor that leads to over pressurization of the motor case, or, it may be deliberately initiated by activation of shaped explosive charges placed on the exterior of the motor as part of a range safety system. In the event that the launch vehicle exhibits an errant flight trajectory or erratic flight behavior, the Range Safety Officer sends a command destruct signal to destroy the vehicle before it can leave the approved "safe launch" corridor. Unlike the normal launch scenario, analysis of the conflagration event requires a series of abort simulations at time intervals along the nominal flight path. In this study failure times at 0, 4, 8, 2, 16 and 20 seconds were simulated. Given the complex interaction of fragment trajectories, scatter of impacting propellant fragments, buoyant cloud rise from scattered fragments and differing meteorological conditions, it is difficult to predetermine what failure time creates the worst case downwind toxic hazard corridor. Consequently a series of failure times are analyzed. The analysis procedure requires the following general steps:

1. Define the fragmentation of the pressurized solid rocket motor at the failure time.
2. Apply randomly sampled explosion induced velocities to the fragments and vector sum these with the vehicle velocity at the time of failure.
3. For each fragment perform a drag corrected ballistic trajectory computation.
4. Account for depletion of propellant mass and formation of combustion exhaust as each burning fragment falls to the ground (smaller fragments may burn up before impacting the ground).
5. Map the impact point, residual mass and dimensions of the propellant fragments that survive to ground impact. Determine the size of the impact region, which is typically referred to as a “debris footprint” and takes on the form of an ellipse that depends on fragment ballistic coefficients.
6. Account for exhaust plumes that emanate from ground burning propellant fragments until these fragments burn to depletion.

Figure 5-7 and Figure 5-8 illustrate a Delta II 7925 launch vehicle failure that would be modeled as a conflagration event. The first photo is take a fraction of a second after the initiating explosion and illustrates the large number of high velocity solid propellant fragments ejected for the center of the explosion. In this case the fragments came from 6 pressurized strap-on graphite epoxy motors rather than a single large solid rocket motor. The second photo is taken about 30 seconds after the explosion and shows the large exhaust cloud formed by the trails of exhaust created by the falling fragments. The second photo also shows the early stage of plumes forming from propellant burning on the ground. Figure 5-9 illustrated both a conflagration source and a deflagration source associated with explosion of a large Titan 34D-9 launch vehicle.

Figure 5-7. High Velocity Burning Propellant Fragments from a Delta II 7925 Solid Rocket Motor Explosion 13 Seconds into Flight.

Figure 5-8. Trails of Toxic Exhaust From Burning Delta II 7925 Propellant Fragments that Fell to The Ground and Continue Burning.

Figure 5-9. Solid Propellant Conflagration Cloud (White) and Liquid Hypergol Deflagration Cloud (Red) Formed When the Titan 34D-9 Vehicle Exploded at Vandenberg AFB.

REEDM is not designed to model burning propellant fragment trajectories directly and requires the conflagration source cloud to be defined in simplified terms based on calculations made external to the program. ACTA develops conflagration data for REEDM using the following procedure:

1. Define the pressurized motor dimensions including the length, weight and outer radius of the propellant grain.
2. Define the internal combustion chamber average radius as a function of time. The interior radius increases and the propellant web thickness decreases as propellant burns away.

3. Define the motor chamber pressure as a function of time.
4. Define the motor case material, thickness and density.
5. Define the vehicle altitude as a function of time.
6. Define the smallest expected solid propellant fragment size (typically a 2 inch cube).
7. Define the largest expected solid propellant fragment size (typically 6% of the total propellant weight at the time of failure).
8. Enter items 1 through 7 into the Air Force FRAG model to predict fragmentation of the entire motor as a function of time. FRAG assumes a log normal distribution of fragment sizes based on the upper and lower bound pieces the user assigns and applies a hydrodynamic algorithm to estimate fragment velocities induced by the rapidly expanding chamber gases. FRAG outputs fragment debris tables with 10 to 20 fragment size groups. Each group is allocated a shape factor, number of fragments, weight, average ballistic coefficient, maximum explosion induced velocity and dimensions.
9. Manually add upper stage unpressurized solid propellant motors to the fragment list.

A representative set of FRAG output data is presented in Table 5-2.

Table 5-2. FRAG Generated Propellant Fragmentation Data for the Castor 1200 Motor Given a Failure at 12 Seconds into Flight.

TIME = 12.0

(Burning) Index	Type	Number	Area (in^2)	Weight (lbs)	Beta (psf)	High Vel (ft/sec)	Burn Flag	Length (in)	Arcseg (rad)	Rout (in)	Rin (in)
1	CAS	1	13835.48	50620.97	1573	107	1	228.655	1.885	72.350	39.300
2	CAS	1	10903.91	38914.10	1535	107	1	175.775	1.885	72.350	39.300
3	CAS	1	9195.48	32091.67	1501	107	1	144.958	1.885	72.350	39.300
4	CAS	1	8048.66	27511.98	1470	107	1	124.272	1.885	72.350	39.300
5	CAS	1	7219.13	24199.36	1441	107	1	109.308	1.885	72.350	39.300
6	CAS	2	6327.46	20638.57	1402	107	1	93.224	1.885	72.350	39.300
7	CAS	3	5341.32	16700.58	1344	107	1	75.436	1.885	72.350	39.300
8	CAS	4	4477.74	13252.70	1273	107	1	66.592	1.694	72.350	39.300
9	CAS	7	3623.14	10041.96	1192	107	1	57.967	1.475	72.350	39.300
10	CAS	10	2857.81	7347.44	1105	107	1	49.584	1.262	72.350	39.300
11	CAS	14	2236.22	5296.82	1018	107	1	42.100	1.071	72.350	39.300
12	CAS	22	1716.58	3694.88	926	107	1	35.162	0.895	72.350	39.300
13	CAS	35	1274.29	2434.10	821	110	1	28.539	0.726	72.350	39.300
14	Cube	56	1231.96	1498.33	523	120	1	28.658	0.000	72.350	39.300
15	Cube	90	842.37	847.16	432	132	1	23.698	0.000	72.350	39.300
16	Cube	150	528.36	420.83	342	150	1	18.768	0.000	72.350	39.300
17	Cube	244	287.79	169.17	253	177	1	13.851	0.000	72.350	39.300
18	Cube	341	123.53	47.57	166	226	1	9.075	0.000	72.350	39.300
19	Cube	219	36.48	7.64	90	384	1	4.932	0.000	72.350	39.300
20	Stg	1	30025.00	107466.00	1244	10	3	322.500	6.282	44.940	10.000
21	Stg	1	10921.00	28278.00	897	15	3	75.130	6.282	44.170	8.300
22	Stg	1	8333.00	17790.00	773	20		58.500	6.282	43.160	14.800

10. Define a nominal trajectory file and launch azimuth for the vehicle.
11. Define an Earth gravitational model and site file for the launch mission.

12. Define a set of "standard" ballistic coefficients, explosion induced velocities, and failure times.
13. Define a standard atmosphere density profile.
14. Enter items 10 through 13 into the Air Force DVDISP (Delta Velocity Dispersions) computer program and generate a set of "standard" debris impact ellipses as a function of failure time, ballistic coefficient and fragment velocity.
15. Define the burn rate of the propellant fragments at 1 atmosphere of pressure.
16. Enter item 15 and output files from the FRAG and DVDISP analyses into the Air Force PIMP (Propellant Impact) computer program and generate estimated average propellant impact footprint 2-sigma standard deviation ellipse size, mass of propellant surviving to ground impact, mass averaged burn time of fragments impacting the ground and distance of impact distribution centroid from the launch pad.
17. Set up the REEDM conflagration database entries using the PIMP output.

ACTA performed this sequence of steps to generate REEDM input data needed to simulate Castor 1200 conflagration events over the first 20 seconds of flight for a launch from Pad-OA at Wallops Flight Facility.

5.7 Castor 1200 Conflagration Abort REEDM Vehicle Data

The resulting REEDM conflagration Castor 1200 vehicle data entries are as follows:

```
#05.10 ON-PAD CONFLAGRATION PROPELLANT DATA:
   REACTANT#1 NAME AND MASS [LBM] =PBAN2 ,1.238e6,
   REACTANT#2 NAME AND MASS [LBM] =AIR   ,3.715e6,
   REACTANT#3 NAME AND MASS [LBM] =      ,0.0    ,
   REACTANT#4 NAME AND MASS [LBM] =      ,0.0    ,
   REACTANT#5 NAME AND MASS [LBM] =      ,0.0    ,
   REACTANT#6 NAME AND MASS [LBM] =      ,0.0    ,
   AVERAGE REACTANT BURN TIME (S)                =   287.4,
   INITIAL VERTICAL VELOCITY OF CLOUD (FT/S)     =     0.0,
   INITIAL RADIUS OF CLOUD (FT)                  =   285.0,
   INITIAL HEIGHT OF CLOUD (FT)                  =     0.0,
   INITIAL X DISPLACEMENT OF CLOUD FROM PAD (FT) =     0.0,
   INITIAL Y DISPLACEMENT OF CLOUD FROM PAD (FT) =     0.0,
   COMBUSTION PRESS FOR CONFLAGRATION BURN [ATM] =     1.0,
   COMBUSTION TEMP. FOR CONFLAGRATION BURN   [K] =     0.0,
#05.11 ELEVATED ABORT CONFLAGRATION PROPELLANT DATA:
   REACTANT#1 NAME AND MASS FRAC  =PBAN2 ,0.25000,
   REACTANT#2 NAME AND MASS FRAC  =AIR   ,0.75000,
   REACTANT#3 NAME AND MASS FRAC  =      ,0.00000,
   REACTANT#4 NAME AND MASS FRAC  =      ,0.00000,
   REACTANT#5 NAME AND MASS FRAC  =      ,0.00000,
```

```
   REACTANT#6 NAME AND MASS FRAC  =      ,0.00000,
   LAUNCH AZIMUTH (DEGREES)       = 115.0,
#05.12 ELEVATED ABORT CONFLAGRATION FAILURE AND IMPACT DATA:
   FAILURE TIMES (S)                 =   4.0,   8.0,  12.0,  16.0,  20.0,
   AVERAGE REACTANT BURN TIMES (S)   = 283.3, 275.0, 264.0, 257.3, 251.4,
   INITIAL RADIUS OF CLOUD (FT)      = 456.0, 868.0, 1305., 1653., 1902.,
   INITIAL HEIGHT OF CLOUD (FT)      =   0.0,   0.0,   0.0,   0.0,   0.0,
   INITIAL VERT. VEL. OF CLOUD (FT/S)=   0.0,   0.0,   0.0,   0.0,   0.0,
   TOTAL REACTANT MASS IN CLOUD (LBM)=4684644,4172240,3698396,3267396,2868540,
   DOWNRANGE  DISTANCE      (FT)     =    20.,   182.,   664.,  2214.,  4544.,
   DEVIATION FROM LAUNCH AZ (DEG)    =     0.,    -3.,    -2.,    -1.,     0.,
```

The REEDM conflagration database was set up specifically to run abort simulations at 4 second failure time intervals and predict downwind ground level Al_2O_3 concentrations and hazard corridor distances.

5.8 The Launch Area Toxic Risk Analysis 3-Dimensional (LATRA3D) Model

LATRA3D was developed by ACTA under Air Force sponsorship over the 2000 to 2008 time frame. During the late 1990's a peer review team evaluated REEDM and found that while the model physics and concepts were sound, the program was becoming outdated and was constrained in certain assumptions by software design that was developed for memory and processor speeds of 1980's computer hardware. LATRA3D was developed to address known deficiencies in REEDM, most notably the following items:

1. The use of excessive averaging of wind speed and direction in the mixing layer to drive stabilized exhaust cloud "disks" (see section 5.2).
2. Application of uniform propellant burn rate per unit area within a large propellant fragment impact ellipse footprint area leading to low heat flux and low stabilized cloud rise predictions.

For the purposes of this report, only a summary of several pertinent LATRA3D features will be summarized here. An extensive description of LATRA3D is documented in the Technical Description Manual [4]. In 2010 LATRA3D Version 2.4 was also submitted to a highly qualified scientific review team for Independent Verification and Validation (IV&V). The IV&V team drew the following conclusions:

1. ***“We conclude that the LATRA3D model meets the user’s requirements. There are, however, a few improvements that could be made and some additional evaluations with field observations that could be carried out, as described in the remainder of this Executive Summary, and as explained in more detail in the body of the report.”***

2. ***“We conclude from our scientific review that LATRA3D has no major technical flaws and its science is adequate for operational use at the launch sites.”***

ACTA incorporated a number of the IV&V team recommended improvements in 2011 and LATRA3D analyses that were performed for this study used Version 3.0 with the IV&V enhancements.

LATRA3D differs from REEDM in that is defines a fully 3-dimensional wind field. If suitable meteorological measurements are provided, or mesoscale prognostic weather model output data is provided, LATRA3D will read and process the data to assign wind speed, wind direction and temperature at every grid node within a 3-D grid. The wind field grid set up for Wallops Flight Facility has horizontal grid spacing at one kilometer intervals and vertical spacing over the lower 3000 meters of the atmosphere set at measurement levels taken from mandatory weather balloon input data. There are typically about 80 vertical levels in a WFF archived weather balloon data file spanning this 3,000 meter region. LATRA3D requires as a minimum a single weather balloon input to run. When given a single balloon the horizontal domain is set with the same vertical profile at each node and the wind field becomes essentially 2-dimensional. This was the case for this study where approximately 6,430 archived weather balloons were used as inputs one at a time to run LATRA3D. Even with a single balloon sounding input, LATRA3D provides better resolution of the effects of wind speed and direction shears within the vertical profile than REEDM. LATRA3D accomplishes this by subdividing the normal launch and conflagration initial sources into many smaller Gaussian puffs and allows the local wind at the puff centroid altitude to transport the puff. As individual puffs grow due to atmospheric turbulence, LATRA3D invokes puff splitting criteria that are based on either maximum puff size or maximum amount of wind shear distortion. Puffs that are split to higher and lower altitudes are then driven by the unique measured wind conditions at the new puff centroid altitudes. REEDM averages the vertical winds over a vertical region between the top of the stabilized cloud and the ground surface and applies a single wind speed and single wind direction to all dispersing cloud disks.

The other major feature incorporated into LATRA3D is internal processing of solid propellant fragment trajectories and mapping of propellant combustion products generated by the fragments as they are ejected from the point of explosion to the point of ground impact. LATRA3D still requires a FRAG type analysis external to the code to define input data for propellant fragments versus time, but the external processes reflected in DVDISP and PIMP calculations are performed internally. Within LATRA3D the conflagration exhaust cloud is resolved into as many as 1000 volume "bins" encompassing the fragment trajectories and as many as 100 ground cells covering the ground impact region. In REEDM the ground impact region is defined as a single area with uniform burn rate of propellant and a single, extremely wide, "chimney" of propellant exhaust. Since LATRA3D maps the fragment impact points within the impact grid, it can model "hot spots" and "low density" regions of burning propellant. This results in more realistic simulation of the actual event depicted in Figure 5-8.

Figure 5-10 through Figure 5-13 illustrate how LATRA3D simulates various rocket emission sources with initial source Gaussian puffs that are allowed to move with local winds and split as puff growth occurs during downwind transport and dispersion.

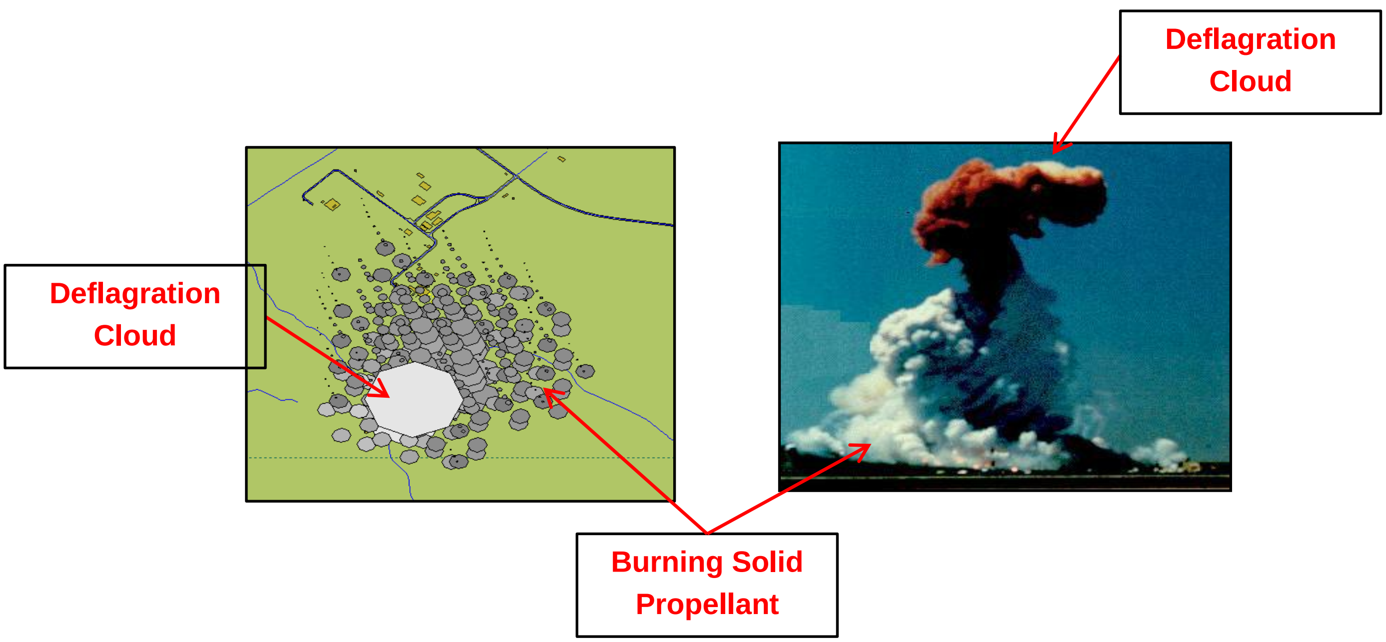

Figure 5-10. LATRA3D Puffs Generated For an Atlas V 411 Vehicle Abort Simulation Compared with Titan 34D-9 Abort Photo – Both at 8-Second Failure Time.

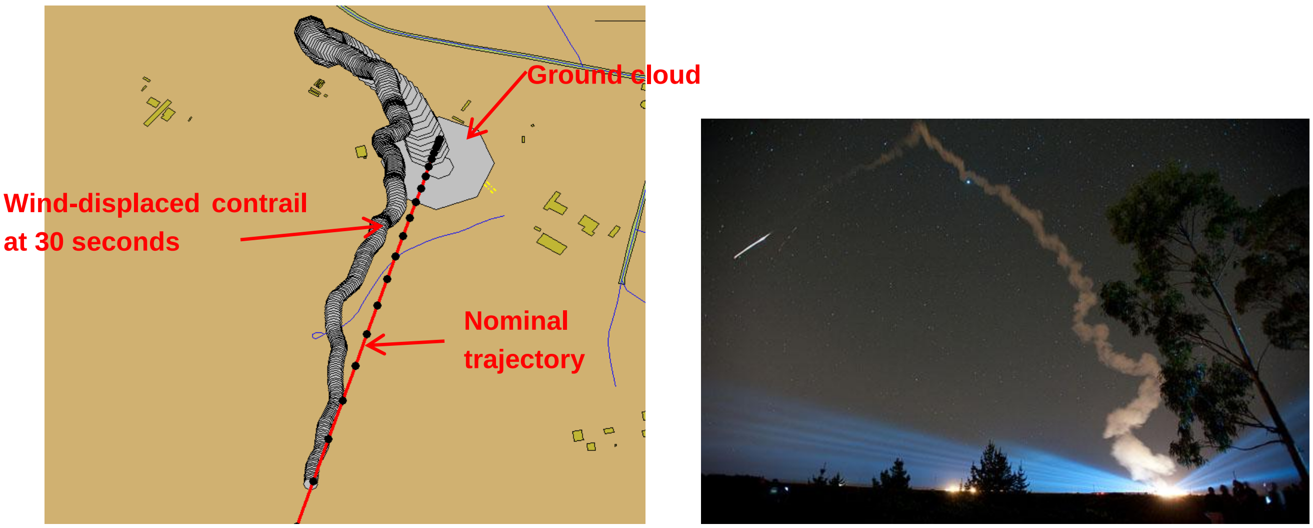

Figure 5-11. Comparison of LATRA3D Normal Launch Plume Puffs for a Delta II Vehicle Versus Photo of a Delta II Normal Launch Plume.

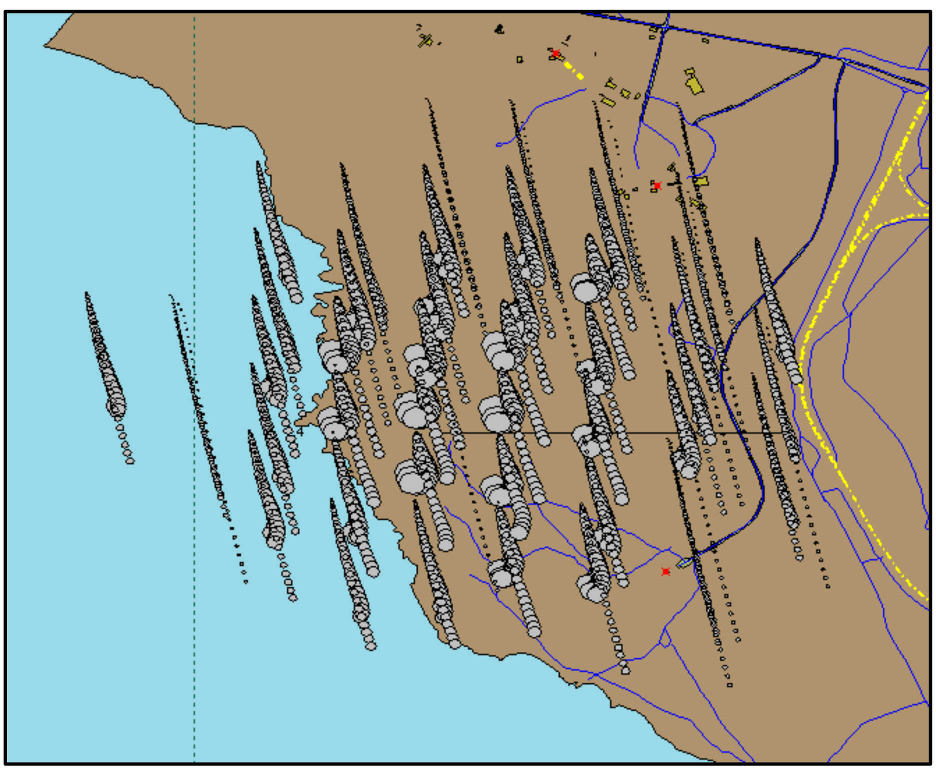

Figure 5-12. Depiction of LATRA3D Solid Propellant Impacts and Source Puffs for a Late Flight Failure.

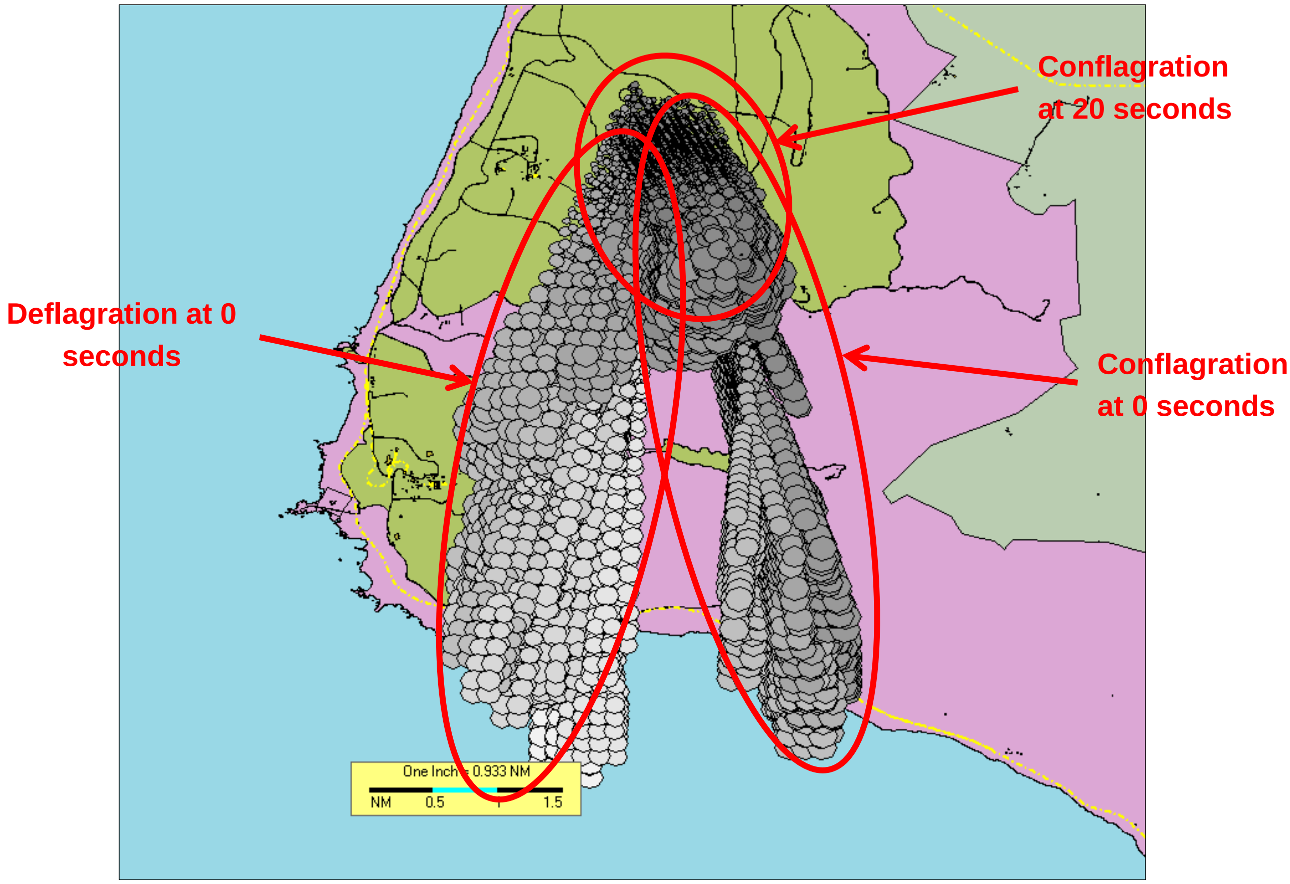

Figure 5-13. Depiction of LATRA3D Ensemble of Source Puff Transport Directions for a Single Vehicle Launch with Simulations at Different Assumed Failure Times.

5.9 Payload Deflagration MMH and NO_2 Emission Scenario

Actual early flight launch failures have demonstrated that the payload has a reasonable probability of surviving explosive breakup of the first stage during an early flight failure. In this scenario simulation it is assumed that the payload containing separate tanks of hypergolic fuel (MMH) and oxidizer (N_2O_4) impact the ground rupturing the propellant tanks and confining the propellants sufficiently to generate a mixing and partial combustion resulting in a small liquid propellant fireball (i.e. a deflagration source). This type of scenario has been routinely modeled at the Air Force ranges and ACTA applied the same deflagration propellant mixing assumptions in this study that are used for Air Force launch simulations. By definition, hypergols react upon contact of fuel and oxidizer without the need for an ignition source. For this reason, hypergol mixing tends to be somewhat self-limiting. As soon as a contact interface occurs the propellants react with each other generating hot expansion gases that tend to drive the unmixed portions of the propellants away from each other. Propulsion chemists studying launch vehicle abort conditions at Martin Marietta estimated that only about 20 to 25% of the hypergol mass reacts and the remainder is subject to thermal decomposition or vaporization reactions. It is the vaporized (unreacted) portion of the material that presents the toxic hazard because complete hypergol combustion produces benign combustion products.

In this study the following mixing conditions and reaction pathways were assigned to the payload LATRA3D deflagration scenario. LATRA3D permits three mixing scenarios to be defined for deflagration events. For this study, where a falling payload is assumed to impact the ground, the "column B: Confined by Ground Surface" mixing assumptions were applied as being more conservative that column C, which includes afterburning and further depletes MMH fuel.

```
DEFLAGRATION DATA:
   INITIAL VERTICAL VELOCITY OF CLOUD (FT/S)     =   0.0,
   INITIAL X DISPLACEMENT OF CLOUD FROM PAD (FT) =   0.0,
   INITIAL Y DISPLACEMENT OF CLOUD FROM PAD (FT) =   0.0,
   INITIAL Z DISPLACEMENT OF CLOUD FROM PAD (FT) =   0.0,
   COMBUSTION PRESS. FOR DEFLAGRATION BURN [ATM] =   1.0,
   COMBUSTION TEMP. FOR DEFLAGRATION BURN    [K] =   0.0,

DEFLAGRATION REACTANTS:
   NAME                TOTAL MASS [LBM]    IGNITION TIME [S]   BURN RATE [LBM/S]
   MMH                 1000                278.9               5.87
   N2O4                1640                278.9               22.14
   END


DEFLAGRATION EVENT MODES:
   column A scenario description: COMMAND DESTRUCT
   column B scenario description: CONFINED BY GROUND SURFACE
   column C scenario description: LOW VELOCITY IMPACT WITH AFTERBURNING
```

```
DEFLAGRATION, EXPLOSIVE REACTIONS (MAX 10):
    FUEL   OXIDIZER   FRACTION OF TOTAL FUEL      FRACTION OF TOTAL OXIDIZER
    NAME     NAME      A         B         C         A         B         C
   MMH       N2O4   0.0146    0.0013    0.0063    0.0222148 0.0019780 0.0095858
   END

DEFLAGRATION, SECONDARY FIREBALL BURNING MIXTURE (MAX 10):
  REACTANT              FRACTION OF TOTAL
   NAME                A         B         C
   MMH              0.2174    0.2277    0.2367
   N2O4             0.2174    0.2277    0.2367
   END

DEFLAGRATION, CLOUD CONTRIBUTIONS FROM SOLID PROPELLANT EXHAUST (MAX 5):
PROPELLANT              FRACTION OF TOTAL              AIR/PROP RATIO
   NAME                A         B         C         A         B         C
   END

DEFLAGRATION, PROPELLANT AFTERBURNING REACTIONS (MAX 10):
   FUEL                 FRACTION OF TOTAL              AIR/PROP RATIO
   NAME                A         B         C         A         B         C
   MMH              0.0000    0.0000    0.3785    0.0000    0.0000    7.531039
   END


DEFLAGRATION, PROPELLANT THERMAL DECOMPOSITION REACTIONS (MAX 10):
 CHEMICAL               FRACTION OF TOTAL
   NAME                A         B         C
   MMH              0.62976   0.63222   0.31037
   N2O4             0.7603852 0.770322  0.7537142
   END

DEFLAGRATION, PROPELLANT VAPORIZATION REACTIONS (MAX 10):
  LIQUID                FRACTION OF TOTAL
   NAME                A         B         C
   MMH              0.13824   0.13878   0.06813
   END

DEFLAGRATION, FIREBALL REACTIONS INVOLVING PRODUCT SPECIES:
   FRACTION OF AVAILABLE N2O4 DECOMPOSED TO NO2           1.0000    1.0000    1.0000
   FRACTION OF AVAILABLE NO2 DECOMPOSED TO N2 AND O2      0.0000    0.0000    0.0000
   FRACTION OF AVAILABLE NO2 CONVERTED TO HNO3 GAS        0.0000    0.0000    0.0000
```

5.10 Payload Liquid Spill of MMH and NO_2 Emission Scenario

In this scenario simulation it is assumed that the payload containing separate tanks of hypergolic fuel (MMH) and oxidizer (N_2O_4) impact the ground rupturing the propellant tanks but the propellants are not sufficiently confined and no combustion of fuel and oxidizer takes place. Instead it is assumed that the propellant tanks rupture or feed and pressurization lines are severed and the liquid propellant spills out on to the ground resulting in an evaporating pool. LATRA3D has incorporated the pool evaporation algorithms of the Air Force Toxics (AFTOX) code and these algorithms are used for this scenario simulation. AFTOX is used operationally at Vandenberg AFB to simulate spills of hypergols associated with propellant transfers of other ground processing applications. AFTOX has also been used at Vandenberg to estimate toxic hazard corridors for potential impacts of large intact payloads flown on Titan launch vehicles. Like AFTOS, LATRA3D invokes the Vossler pool evaporation model for MMH and N_2O_4 spills. The Vossler evaporation model is the most sophisticated of three internal evaporation models and it has been tailored to evaluation of hypergols spills. This evaporation model performs a full energy transfer and mass balance calculation on the evaporating pool and uses ground heating, solar heating and wind convection to estimate the evaporation rate. It automatically recognizes N_2O_4 as a unique case and converts the evaporated gas to NO_2 rather than N_2O_4 vapor. Physical and chemical properties for the spilled commodities are acquired by LATRA3D from the AFTOX and Vossler chemical databases, which have been vetted by a 30th Space Wing IV&V team in the past.

6. METEOROLOGICAL DATA PREPARATION

Gaseous dispersion of rocket exhaust clouds is extremely dependent upon the meteorological conditions at the time the source cloud is generated. The presence or absence of temperature inversions, the temperature lapse rate, wind speed and direction, wind shears and atmospheric turbulence are important factors that influence the cloud rise and rate of dispersion of the source cloud. Meteorological conditions that are adverse from a toxic chemical dispersion perspective are light winds with little wind speed or wind direction variation over the first several thousand feet of the atmosphere coupled with a capping temperature inversion just above the top of the stabilized source cloud. An additional adverse factor is suppression of atmospheric turbulence, as occurs at night or under cloudy or marine stratus and fog conditions.

ACTA ran LATRA3D and REEDM analyses for this study using 6432 meteorological data sets based on actual weather balloon measurements made at Wallops Flight Facility between 2000 and 2008. This data was previously processed by ACTA to support the Taurus II Environmental Assessment and was converted to REEDM format at that time. The original raw weather balloon data was not in a format usable by REEDM and needed to be preprocessed to reduce the number of measurement levels from several thousand to approximately one hundred, to quality control check the raw data, and to output the data in REEDM compatible format. A computer program written by ACTA and delivered to WFF for operational use in 2007 was used to perform the raw data file conversions. A critical part of the conversion process was to test for, and capture, inflection points where temperature, wind speed, wind direction or relative humidity reach minimum or maximum values and change slope as a function of altitude. An example of the weather profile testing algorithm capabilities is illustrated in Figure 6-1, which is contrived test data with positive, negative and infinite slopes and multiple inflection points. The resulting converted files were sorted into daytime and nighttime sets for each month of the year. Data was classified as "daytime" if the balloon release time was between 0600 and 1900 Eastern Standard Time. The archived converted files generated in 2009 were recovered for this study and tested in LATRA3D to verify compatibility with LATRA3D processing. Two "bad" weather data sets were found and discarded leaving an archive of 6430 cases.

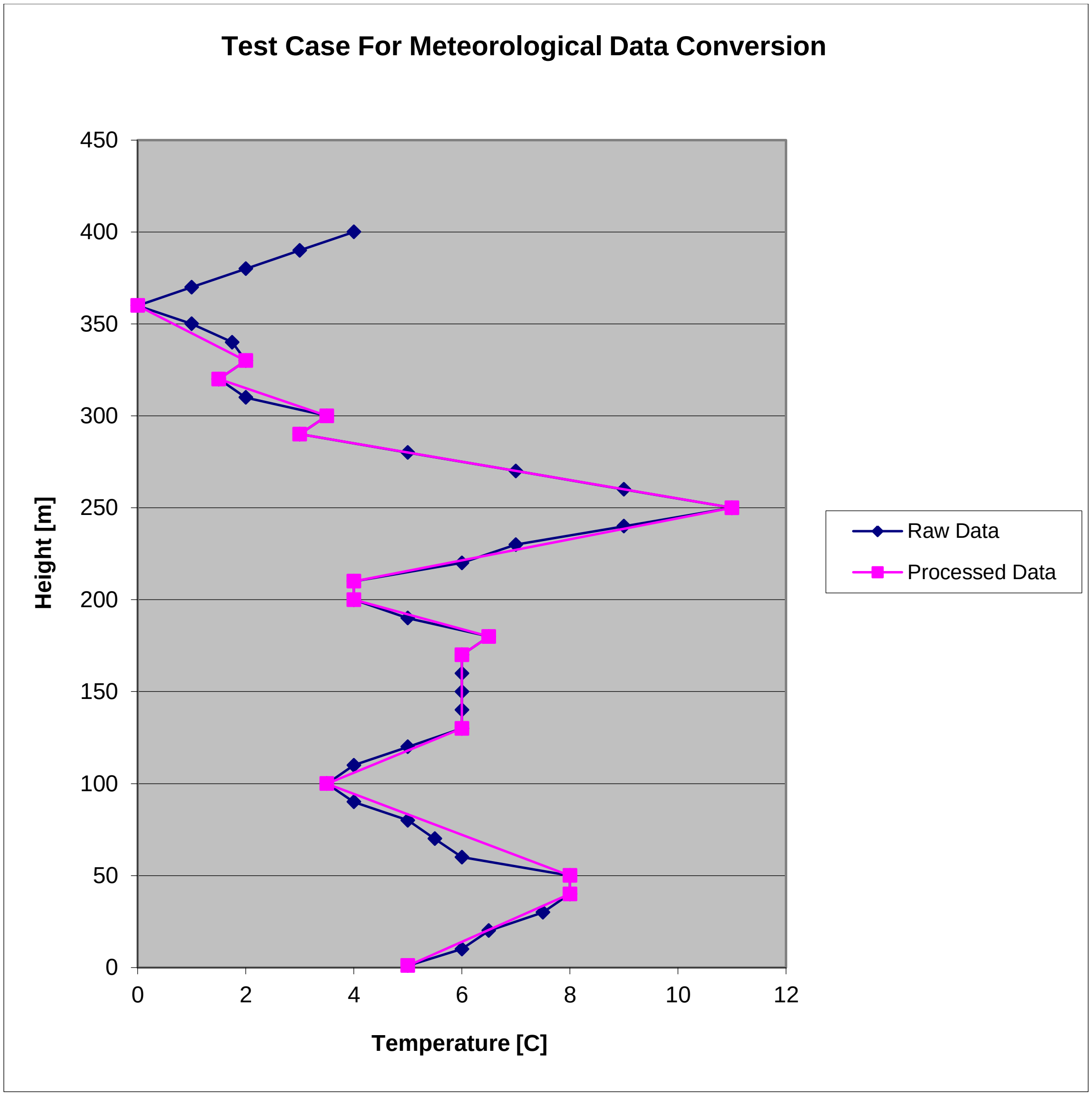

Figure 6-1. Illustration of Testing a Raw Data Profile to Capture Slope Inflection Points that Define Minimum and Maximum Values and Measure Inversions and Shear Effects.

6.1 REEDM Castor 1200 Normal Launch Scenario Setup

ACTA executed REEDM in batch processing mode to cycle through all archived meteorological cases and to extract key information to a summary table. Typically REEDM generates an output file for a single weather case that consists of 10 to 20 pages of information on the run setup, intermediate calculated values and tables of concentration versus downwind distance. Saving the standard REEDM output file for each run over thousands of simulations results in an overwhelming amount of output data. ACTA developed a special batch version of REEDM for the Air Force that has been used over the years to execute thousands of scenarios and condense the REEDM output for all runs into a summary table containing the following critical analysis parameters:

1. Chemical being tracked in REEDM analysis.
2. Concentration threshold used to calculate concentration isopleth beginning and end distances.
3. Meteorological input file name.
4. Zulu time of balloon release.
5. REEDM computed mixing boundary depth.
6. REEDM predicted cloud stabilization height.
7. REEDM predicted average wind speed used to transport exhaust cloud.
8. REEDM predicted average wind direction used to transport exhaust cloud.
9. REEDM predicted maximum ground level concentration.
10. REEDM predicted distance from exhaust cloud source to location of maximum concentration.
11. REEDM predicted bearing from exhaust cloud source to location of maximum concentration.
12. REEDM predicted nearest distance from exhaust cloud source to the location where the ground concentration centerline first exceeds the user defined concentration threshold.

13. REEDM predicted farthest distance from exhaust cloud source to the location where the ground concentration centerline last exceeds the user defined concentration threshold.

14. REEDM predicted bearing from exhaust cloud source to location where the ground concentration centerline last exceeds the user defined concentration threshold.

15. REEDM derived average wind speed shear in the lower planetary boundary layer.

16. REEDM derived average wind direction shear in the lower planetary boundary layer.

17. REEDM derived average horizontal (azimuthal) turbulence intensity in the lower planetary boundary layer.

18. REEDM derived average vertical (elevation) turbulence intensity in the lower planetary boundary layer.

19. REEDM derived average wind speed shear in the region above the planetary boundary layer.

20. REEDM derived average wind direction shear in the region above the planetary boundary layer.

21. REEDM derived average horizontal (azimuthal) turbulence intensity in the region above the planetary boundary layer.

22. REEDM derived average vertical (elevation) turbulence intensity in the region above the planetary boundary layer.

The above list of parameters is provided for REEDM predictions of both peak instantaneous concentration and time weighted average (TWA) concentration. In the runs performed for this study the time weighted average concentrations for HCl were not needed because the health response time is acute and toxicity thresholds call for comparison with model peak concentration predictions. In any event, if TWA concentration estimates are needed, a fairly short averaging time is appropriate for rocket exhaust cloud exposures because the source cloud typically passes over a receptor with a time scale of tens of minutes rather than hours. The REEDM summary tables from the monthly batch runs were further condensed to identify the meteorological case that produced the highest peak concentration and record the range and bearing from the source location (WFF Castor 1200 launch Pad-0A).

6.2 REEDM Far Field HCl Results for the Castor 1200 Normal Launch Scenario

Table 6-1 presents the maximum far field HCl peak instantaneous concentration predicted by REEDM for the hypothetical daytime launches of a Castor 1200 vehicle with subsequent dispersion of the normal launch ground and contrail clouds. The far field exposure is REEDM's prediction for concentrations at ground level downwind of the stabilized exhaust cloud. Far field peak HCl concentrations ranged from 2 to 5 ppm with the maximum concentration predicted to occur from 11000 to 19000 meters downwind from the launch site. These values represent the maximum concentrations predicted over a sample set of 4679 WFF balloon soundings. Table 6-2 shows the REEDM predicted maximum peak HCl far field concentrations for 1751 nighttime cases for Castor 1200 vehicle normal launch scenarios. As with the daytime cases, the peak instantaneous HCl concentrations are less than 10 ppm.

Table 6-1: Castor 1200 Normal Launch HCl Peak Concentration Summary – Daytime Meteorology.

Month	Number of Weather Cases	Peak HCl Concentration [ppm]	Distance to Peak HCl Concentration [m]	Bearing to Peak HCl Concentration [deg]
January	341	2.1	15000	80
February	363	2.4	12000	141
March	393	3.3	17000	241
April	382	2.3	19000	227
May	398	2.5	13000	231
June	391	2.7	16000	47
July	417	3.0	11000	87
August	410	2.0	14000	212
September	412	5.0	16000	257
October	429	2.0	15000	183
November	376	2.3	17000	201
December	367	3.3	13000	227

Table 6-2: Castor 1200 Normal Launch HCl Peak Concentration Summary – Nighttime Meteorology.

Month	Number of Weather Cases	Peak HCl Concentration [ppm]	Distance to Peak HCl Concentration [m]	Bearing to Peak HCl Concentration [deg]
January	95	2.9	12000	134
February	158	2.4	14000	227
March	165	2.5	16000	227
April	158	5.1	10000	207
May	159	2.2	27000	231
June	153	1.8	14000	308
July	153	2.3	13000	104
August	162	1.7	12000	74
September	163	2.9	11000	204
October	125	1.3	19000	168
November	129	2.1	14000	177
December	131	1.8	15000	135

The REEDM predicted HCl concentration data for all daytime meteorological cases processed in the 8-year sample set was aggregated into bins to evaluate the peak far field concentration probability. This information is provided in Table 6-3.

Table 6-3. REEDM Predicted Maximum Far Field Ground Level HCl Concentrations for Daytime Castor 1200 Normal Launch Scenarios.

Concentration Bin	Count	Probability
0 - 1	2938	0.6279
1 - 2	280	0.0598
2 - 3	23	0.0049
3 - 4	3	0.0006
4 - 5	0	0.000
5 - 6	1	0.0002
6 - 7	0	0.0000
7 - 8	0	0.0000
8 - 9	0	0.0000
9 - 10	0	0.0000

It is noted that approximately 63% of all daytime meteorological cases resulted in REEDM maximum peak instantaneous ground level HCl concentrations of less than 1 ppm. Approximately

31% (1434) of the daytime meteorological cases resulted in zero ground level HCl concentration predictions because the normal launch cloud was predicted to rise entirely above a capping inversion that defined the top of the mixed boundary layer. Thus a total of 93.4% of the daytime meteorological cases had very benign predictions of zero or less than 1 ppm ground level HCl concentration for the normal launch scenario.

The REEDM predicted cloud transport directions for the normal launch HCl dispersion were also aggregated into bins representing 45-degree arc corridors around the compass (i.e. N, NE, E, SE, S, SW, W, NW). Table 6-4 indicates the predicted Castor 1200 normal launch plume direction probability of occurrence observed across the 3245 daytime balloon sounding cases that produced non-zero predicted ground level HCl concentrations. It is noted that for the daytime launch scenarios transport of the exhaust plume to the East and Southeast are favored. This would tend to carry the toxic cloud in an offshore direction for the launch pads located on the WFF barrier island on the Atlantic coastline of Virginia. The transport direction reflects the average airflow over a depth of approximately 1000 meters, hence the windrose observed for elevated rocket exhaust clouds may differ significantly from a windrose derived from a surface wind tower.

Table 6-4. REEDM Predicted Exhaust Cloud Transport Directions for Daytime Castor 1200 Normal Launch HCl Scenarios.

Plume Transport Direction Bin	Count	Probability
337.5 – 22.5 (N)	178	0.055
22.5 – 67.5 (NE)	497	0.153
67.5 – 112.5 (E)	766	0.236
112.5 – 157.5 (SE)	879	0.271
157.5 – 202.5 (S)	361	0.111
202.5 – 247.5 (SW)	264	0.081
247.5 – 292.5 (W)	175	0.054
292.5 – 337.5 (NW)	125	0.039

Similar summary tables for the 1751 nighttime Castor 1200 normal launch simulations were compiled. Table 6-5 shows that the peak HCl instantaneous concentration predictions for nighttime conditions continues with a high probability that the maximum far field concentration will be less than 1 ppm. Approximately 43% (748) of the nighttime meteorological cases resulted in zero ground level HCl concentration predictions because the normal launch cloud was predicted to rise entirely above a capping inversion that defined the top of the mixed boundary layer. Thus a total of 94.2% of the nighttime meteorological cases had very benign predictions of zero or less than 1 ppm ground level HCl concentration for the normal launch scenario.

Table 6-5. REEDM Predicted Maximum Far Field Ground Level HCl Concentrations for Nighttime Castor 1200 Normal Launch Scenarios.

Concentration Bin	Count	Probability
0 - 1	902	0.5151
1 - 2	90	0.0514
2 - 3	9	0.0051
3 - 4	0	0.0000
4 - 5	1	0.0006
5 - 6	1	0.0006
6 - 7	0	0.0000
7 - 8	0	0.0000
8 - 9	0	0.0000
9 - 10	0	0.0000

Table 6-6 indicates the predicted Castor 1200 vehicle normal launch plume direction probability of occurrence observed across the 1003 nighttime balloon sounding cases that produced non-zero predicted ground level HCl concentrations. It is noted that for nighttime launch scenarios transport of the exhaust plume to the East and Southeast are still favored as they were during the daytime.

Table 6-6. REEDM Predicted Exhaust Cloud Transport Directions for Nighttime Castor 1200 Normal Launch Scenarios.

Plume Transport Direction Bin	Count	Probability
337.5 – 22.5 (N)	54	0.035
22.5 – 67.5 (NE)	128	0.182
67.5 – 112.5 (E)	214	0.171
112.5 – 157.5 (SE)	287	0.214
157.5 – 202.5 (S)	115	0.134
202.5 – 247.5 (SW)	101	0.124
247.5 – 292.5 (W)	55	0.061
292.5 – 337.5 (NW)	49	0.078

6.3 REEDM Far Field Al_2O_3 Results for the Castor 1200 Normal Launch Scenario

Table 6-7 presents the maximum far field Al_2O_3 peak instantaneous concentration predicted by REEDM for the hypothetical daytime launches of a Castor 1200 vehicle with subsequent dispersion of the aluminum oxide particulates in the normal launch ground and contrail clouds. The far field exposure is REEDM's prediction for concentrations at ground level downwind of the stabilized exhaust cloud. Far field peak Al_2O_3 PM_{10} concentrations ranged from 2 to 9 mg/m^3 with the maximum concentration predicted to occur from 10000 to 33000 meters downwind from the launch site. Respirable dust is primarily under 5 microns in size. The default mass distribution among particle size categories used in the REEDM analysis places about 70% of the dispersed Al_2O_3 mass in the particle size bins 5 microns and less. The table values represent the maximum concentrations predicted over a sample set of 4679 WFF balloon soundings. Table 6-8 shows the REEDM predicted maximum peak Al_2O_3 far field concentrations for 1751 nighttime cases for Castor 1200 vehicle normal launch scenarios. As with the daytime cases, the peak instantaneous Al_2O_3 concentrations are less than 10 mg/m^3.

Table 6-7: Castor 1200 Normal Launch Al_2O_3 Peak Concentration Summary – Daytime Meteorology.

Month	Number of Weather Cases	Peak Al_2O_3 PM_{10} Concentration [mg/m^3]	Peak Al_2O_3 PM_5 Respirable Dust Concentration [mg/m^3]	Distance to Peak Al_2O_3 Concentration [m]	Bearing to Peak Al_2O_3 Concentration [deg]
January	341	3.6	2.5	31000	40
February	363	3.7	2.6	33000	205
March	393	3.8	2.7	17000	241
April	382	9.1	6.4	10000	136
May	398	3.1	2.2	24000	238
June	391	2.6	1.8	21000	113
July	417	2.8	2.0	11000	83
August	410	2.1	1.5	13000	213
September	412	5.1	3.6	16000	255
October	429	3.4	2.4	22000	256
November	376	4.0	2.8	18000	197
December	367	3.1	2.2	13000	106

Table 6-8: Castor 1200 Normal Launch Al_2O_3 Peak Concentration Summary – Nighttime Meteorology.

Month	Number of Weather Cases	Peak Al_2O_3 PM_{10} Concentration [mg/m^3]	Peak Al_2O_3 PM_5 Respirable Dust Concentration [mg/m^3]	Distance to Peak Al_2O_3 Concentration [m]	Bearing to Peak Al_2O_3 Concentration [deg]
January	95	5.1	3.6	20000	183
February	158	3.4	2.4	20000	172
March	165	4.7	3.3	18000	227
April	158	5.0	3.5	11000	225
May	159	3.1	2.2	24000	77
June	153	2.5	1.8	27000	77
July	153	2.3	1.6	12000	111
August	162	1.7	1.2	11000	75
September	163	3.1	2.2	10000	202
October	125	2.8	2.0	26000	168
November	129	2.5	1.8	42000	165
December	131	3.9	2.7	29000	67

The REEDM predicted Al_2O_3 concentrations for all daytime meteorological cases processed in the 8-year sample set was aggregated into bins to evaluate the peak far field concentration probability. This information is provided in Table 6-9.

Table 6-9. REEDM Predicted Maximum Far Field Ground Level Al_2O_3 Concentrations for Daytime Castor 1200 Normal Launch Scenarios.

Concentration Bin	Count	Probability
0 - 1	4069	0.8696
1 - 2	485	0.1037
2 - 3	82	0.0175
3 - 4	20	0.0043
4 - 5	0	0.0000
5 - 6	1	0.0002
6 - 7	0	0.0000
7 - 8	0	0.0000
8 - 9	0	0.0000
9 - 10	1	0.0002

It is noted that approximately 67% of all daytime meteorological cases resulted in REEDM maximum peak instantaneous ground level Al_2O_3 PM_{10} concentrations of less than 1 mg/m^3.

The REEDM predicted cloud transport directions for the normal launch Al_2O_3 dispersion were also aggregated into bins representing 45-degree arc corridors around the compass (i.e. N, NE, E, SE, S, SW, W, NW). Table 6-10 indicates the predicted Castor 1200 normal launch plume direction probability of occurrence observed across the 4679 daytime balloon sounding cases that produced non-zero predicted ground level Al_2O_3 concentrations. It is noted that for the daytime launch scenarios transport of the exhaust plume to the Northeast, East and Southeast are favored. This would tend to carry the toxic cloud in an offshore direction for the launch pads located on the WFF barrier island on the Atlantic coastline of Virginia. The transport direction reflects the average airflow over a depth of approximately 3000 meters, hence the windrose observed for these elevated rocket exhaust clouds may differ significantly from a windrose derived from a surface wind tower.

Table 6-10. REEDM Predicted Exhaust Cloud Transport Directions for Daytime Castor 1200 Normal Launch Al_2O_3 Scenarios.

Plume Transport Direction Bin	Count	Probability
337.5 – 22.5 (N)	385	0.083
22.5 – 67.5 (NE)	971	0.208
67.5 – 112.5 (E)	957	0.205
112.5 – 157.5 (SE)	1058	0.227
157.5 – 202.5 (S)	489	0.105
202.5 – 247.5 (SW)	386	0.083
247.5 – 292.5 (W)	221	0.047
292.5 – 337.5 (NW)	191	0.041

Similar summary tables for the 1751 nighttime Castor 1200 normal launch simulations were compiled. Table 6-11 shows that the peak Al_2O_3 PM_{10} instantaneous concentration predictions for nighttime conditions continues with a high probability that the maximum far field concentration will be less than 1 mg/m^3.

Table 6-11. REEDM Predicted Maximum Far Field Ground Level Al_2O_3 Concentrations for Nighttime Castor 1200 Normal Launch Scenarios.

Concentration Bin	Count	Probability
0 - 1	1511	0.8629
1 - 2	186	0.1062
2 - 3	39	0.0223
3 - 4	7	0.0040
4 - 5	2	0.0011
5 - 6	2	0.0011
6 - 7	0	0.0000
7 - 8	0	0.0000
8 - 9	0	0.0000
9 - 10	0	0.0000

Table 6-12 indicates the predicted Castor 1200 vehicle normal launch plume direction probability of occurrence observed across the 1751 nighttime balloon sounding cases that produced non-zero predicted ground level Al_2O_3 concentrations. It is noted that for nighttime launch scenarios transport of the exhaust plume to the Northeast, East and Southeast are favored as they were during the daytime.

Table 6-12. REEDM Predicted Exhaust Cloud Transport Directions for Nighttime Castor 1200 Normal Launch Scenarios.

Plume Transport Direction Bin	Count	Probability
337.5 – 22.5 (N)	110	0.0630
22.5 – 67.5 (NE)	328	0.1877
67.5 – 112.5 (E)	382	0.2187
112.5 – 157.5 (SE)	420	0.2404
157.5 – 202.5 (S)	209	0.1196
202.5 – 247.5 (SW)	136	0.0779
247.5 – 292.5 (W)	85	0.0487
292.5 – 337.5 (NW)	77	0.0441

6.4 LATRA3D Far Field HCl Results for the Castor 1200 Conflagration Scenarios

Conflagration results are difficult to characterize with just a few parameters because the toxic hazard corridor varies with both the meteorological case and the assumed failure time. ACTA run LATRA3D HCl dispersion simulations for all 6430 archived weather balloon soundings for failure times set at 0, 4, 8, 12, 16 and 20 seconds (38,580 simulations). Results are present by day versus night, month and launch vehicle failure time.

6.4.1 T-0 Conflagration HCl Results

Table 6-13 presents the maximum far field HCl peak instantaneous concentration predicted by LATRA3D for a simulated T-0 conflagration failure of a Castor 1200 vehicle with subsequent dispersion of the exhaust from burning fragments falling to the ground and from burning propellant fragments on the ground. The far field exposure is LATRA3D's prediction for concentrations at ground level downwind of the stabilized exhaust cloud. Far field peak HCl concentrations ranged from 30 to 65 ppm with the maximum concentration predicted to occur from 1000 to 3400 meters downwind from the conflagration debris field source location. These values represent the maximum concentrations predicted over a sample set of 4655 WFF balloon soundings. Table 6-14 provides information about the general size (length) and direction of a low threshold 1-ppm hazard zone for the daytime T-0 conflagration scenarios. Hazard zones for higher concentration thresholds will always be shorter than the reported 1-ppm hazard zone length but due to non-linearity factors in the dispersion equations the hazard zone lengths for other threshold ppm values cannot be directly scaled from the 1-ppm hazard zone length.

Table 6-15 shows the LATRA3D predicted maximum peak HCl far field concentrations for 1749 nighttime cases for Castor 1200 vehicle T-0 conflagration scenario. Nighttime far field peak HCl concentrations ranged from 18 to 58 ppm with the maximum concentration predicted to occur from 1000 to 6000 meters downwind from the conflagration debris field source location. Table 6-16 provides information about the general size (length) and direction of a low threshold 1-ppm hazard zone for the nighttime T-0 conflagration scenarios.

Table 6-13: Castor 1200 T-0 Conflagration HCl Concentration Summary – Daytime Meteorology.

Month	Number of Weather Cases	Peak HCl Concentration [ppm]	Distance to Peak HCl Concentration [m]	Bearing to Peak HCl Concentration [deg]
January	341	5.33E+01	2007	215
February	362	5.29E+01	2679	15
March	391	6.09E+01	1615	343
April	378	6.49E+01	1955	314
May	395	4.75E+01	2059	12
June	389	3.58E+01	1363	48
July	410	4.78E+01	2250	350
August	409	3.46E+01	1064	347
September	408	3.17E+01	3412	6
October	429	2.94E+01	2320	40
November	376	3.38E+01	2249	42
December	367	3.42E+01	3088	85

Table 6-14: Castor 1200 T-0 Conflagration 1-ppm HCl Concentration Hazard Zone Summary – Daytime Meteorology.

Month	Number of Weather Cases	HCl Hazard Zone Concentration [ppm]	Distance to End of Hazard Zone [m]	Bearing to End of Hazard Zone [deg]
January	280	1.00E+00	8606	78
February	284	1.00E+00	8332	350
March	279	1.00E+00	8156	11
April	252	1.00E+00	8011	19
May	267	1.00E+00	7854	298
June	272	1.00E+00	6397	218
July	266	1.00E+00	6004	31
August	295	1.00E+00	7613	242
September	295	1.00E+00	8898	339
October	369	1.00E+00	8127	241
November	338	1.00E+00	8479	27
December	322	1.00E+00	8391	81

Table 6-15: Castor 1200 T-0 Conflagration HCl Concentration Summary – Nighttime Meteorology.

Month	Number of Weather Cases	Peak HCl Concentration [ppm]	Distance to Peak HCl Concentration [m]	Bearing to Peak HCl Concentration [deg]
January	95	3.57E+01	2980	96
February	158	5.48E+01	2118	37
March	165	2.95E+01	2642	46
April	157	5.18E+01	2072	6
May	158	1.77E+01	2615	47
June	153	2.92E+01	1683	19
July	153	3.23E+01	1271	359
August	162	2.46E+01	1545	157
September	163	3.45E+01	5724	231
October	125	3.35E+01	3165	104
November	129	5.76E+01	2580	239
December	131	4.16E+01	2893	164

Table 6-16: Castor 1200 T-0 Conflagration 1-ppm HCl Concentration Hazard Zone Summary – Nighttime Meteorology.

Month	Number of Weather Cases	HCl Hazard Zone Concentration [ppm]	Distance to End of Hazard Zone [m]	Bearing to End of Hazard Zone [deg]
January	280	1.00E+00	8606	78
February	284	1.00E+00	8332	350
March	279	1.00E+00	8156	11
April	252	1.00E+00	8011	19
May	267	1.00E+00	7854	298
June	272	1.00E+00	6397	218
July	266	1.00E+00	6004	31
August	295	1.00E+00	7613	242
September	295	1.00E+00	8898	339
October	369	1.00E+00	8127	241
November	338	1.00E+00	8479	27
December	322	1.00E+00	8391	81

The LATRA3D T-0 conflagration predicted HCl concentrations for all daytime meteorological cases processed in the 8-year sample set were aggregated into bins to evaluate the peak far field concentration probability. This information is provided in Table 6-17.

Table 6-17. LATRA3D Predicted Maximum Far Field Ground Level HCl Concentrations for Daytime Castor 1200 T-0 Conflagration Scenarios.

Concentration Bin	Count	Probability
0 - 2	1755	0.37701
2- 4	714	0.15338
4 - 6	533	0.11450
6 - 8	380	0.08163
8 - 10	293	0.06294
10 - 20	705	0.15145
20 - 30	188	0.04039
30 - 40	68	0.01461
40 - 50	14	0.00301
50 - 60	3	0.00064
60 – 70	2	0.00043
70 – 80	0	0.00000
80 – 90	0	0.00000
90 - 100	0	0.00000
> 100	0	0.00000

It is noted that approximately 79% of all daytime meteorological cases resulted in LATRA3D maximum peak instantaneous ground level HCl concentrations of less than 10 ppm. Approximately 15% of the daytime meteorological cases resulted in in LATRA3D maximum peak instantaneous ground level HCl concentrations in the 10 to 20 ppm range.

The LATRA3D predicted cloud transport directions for the T-0 conflagration HCl dispersion were aggregated into bins representing 45-degree arc corridors around the compass (i.e. N, NE, E, SE, S, SW, W, NW). The transport direction for conflagration modes is defined relative to the center of the propellant impact debris field. Table 6-18 indicates the predicted Castor 1200 T-0 conflagration plume direction probability of occurrence for the direction to the maximum concentration point. The table is based on 4655 daytime balloon sounding cases that produced non-zero predicted ground level HCl concentrations. Estimation of plume direction using LATRA3D peak concentration for conflagration scenarios should be considered as a rough approximation only. Recall that LATRA3D simulates a conflagration event with up to 1000 volume elements encompassing the fragment trajectory space and up to 100 grid cells on the ground for burning fragment plumes. A small plume on the edge of the grid that has a low cloud rise stabilization height can result in a LATRA3D predicted maximum concentration at a ground location relatively close to the small plume location (e.g. within several thousand meters). The "plume transport" direction reported in Table 6-18 is estimated as the bearing from the center of the debris field (i.e. not the offending small plume location) to the point of the maximum concentration location. When the maximum predicted concentration point is near the debris field and the debris field has a large radius, the computed "plume transport direction" can be off by many degrees. Geometrically these points form a triangle whereas a more accurate transport direction calculation would have the three points co-linear. In general, the transport direction to the peak concentration point is driven by the puffs with the lowest stabilization heights and the region of the atmosphere under consideration is probably the first 200 to 300 meters, rather than the deeper layer that drives the normal launch ground cloud transport direction. The plume transport directions derived from the computed direction to the endpoint of the 1-ppm hazard zone listed in Table 6-19 provide a better estimate of expected plume transport directions over the ensemble of weather cases. It is noted that for the daytime launch scenarios transport of the conflagration exhaust plume to the Northeast is favored. There is a lower probability for transport of the conflagration plumes to the West.

Table 6-18. LATRA3D Predicted Exhaust Cloud Transport Directions for Daytime Castor 1200 T-0 Conflagration HCl Scenarios.

Plume Transport Direction Bin	Count	Probability
337.5 – 22.5 (N)	759	0.16305
22.5 – 67.5 (NE)	901	0.19356
67.5 – 112.5 (E)	492	0.10569
112.5 – 157.5 (SE)	691	0.14844
157.5 – 202.5 (S)	507	0.10892
202.5 – 247.5 (SW)	572	0.12288
247.5 – 292.5 (W)	397	0.08528
292.5 – 337.5 (NW)	336	0.07218

Table 6-19. LATRA3D Predicted Exhaust Cloud Transport Directions for Daytime Castor 1200 T-0 Conflagration HCl Scenarios Using the 1-ppm Hazard Zone Endpoint.

Plume Transport Direction Bin	Count	Probability
337.5 – 22.5 (N)	559	0.15885
22.5 – 67.5 (NE)	841	0.23899
67.5 – 112.5 (E)	479	0.13612
112.5 – 157.5 (SE)	517	0.14692
157.5 – 202.5 (S)	379	0.10770
202.5 – 247.5 (SW)	293	0.08326
247.5 – 292.5 (W)	240	0.06820
292.5 – 337.5 (NW)	211	0.05996

Similar summary tables for the 1751 nighttime Castor 1200 T-0 conflagration simulations were compiled. Table 6-20 shows the peak HCl instantaneous concentration predictions for nighttime conditions. It is noted that approximately 82% of all nighttime meteorological cases resulted in LATRA3D maximum peak instantaneous ground level HCl concentrations of less than 10 ppm. Approximately 15% of the nighttime meteorological cases resulted in in LATRA3D maximum peak instantaneous ground level HCl concentrations in the 10 to 20 ppm range.

Table 6-20. LATRA3D Predicted Maximum Far Field Ground Level HCl Concentrations for Nighttime Castor 1200 T-0 Conflagration Scenarios.

Concentration Bin	Count	Probability
0 - 2	555	0.31732
2- 4	308	0.17610
4 - 6	268	0.15323
6 - 8	197	0.11264
8 - 10	102	0.05832
10 - 20	262	0.14980
20 - 30	41	0.02344
30 - 40	12	0.00686
40 - 50	1	0.00057
50 - 60	3	0.00172
60 – 70	0	0.00000
70 – 80	0	0.00000
80 – 90	0	0.00000
90 - 100	0	0.00000
> 100	0	0.00000

Table 6-21 indicates the predicted Castor 1200 vehicle T-0 conflagration plume direction probability of occurrence observed across the 1749 nighttime balloon sounding cases based on the direct to the maximum concentration point. The plume transport directions derived from the computed direction to the endpoint of the 1-ppm hazard zone listed in Table 6-22 provide a better estimate of expected plume transport directions over the ensemble of weather cases. It is noted that for nighttime launch scenarios transport of the exhaust plume is least favored for transport to the West, Northwest and North, which is similar but not identical to the estimated daytime transport directions.

Table 6-21. REEDM Predicted Exhaust Cloud Transport Directions for Nighttime Castor 1200 T-0 Conflagration Scenarios.

Plume Transport Direction Bin	Count	Probability
337.5 – 22.5 (N)	151	0.08634
22.5 – 67.5 (NE)	339	0.19383
67.5 – 112.5 (E)	214	0.12236
112.5 – 157.5 (SE)	305	0.17439
157.5 – 202.5 (S)	252	0.14408
202.5 – 247.5 (SW)	271	0.15495
247.5 – 292.5 (W)	124	0.07090
292.5 – 337.5 (NW)	93	0.05317

Table 6-22. LATRA3D Predicted Exhaust Cloud Transport Directions for Nighttime Castor 1200 T-0 Conflagration HCl Scenarios Using the 1-ppm Hazard Zone Endpoint.

Plume Transport Direction Bin	Count	Probability
337.5 – 22.5 (N)	109	0.07649
22.5 – 67.5 (NE)	279	0.19579
67.5 – 112.5 (E)	244	0.17123
112.5 – 157.5 (SE)	220	0.15439
157.5 – 202.5 (S)	227	0.15930
202.5 – 247.5 (SW)	194	0.13614
247.5 – 292.5 (W)	87	0.06105
292.5 – 337.5 (NW)	65	0.04561

6.4.2 T+4 Conflagration HCl Results

Maximum predicted ground level HCl concentrations are higher and closer to the source for the T+4 second failure than for the "on-pad" T-0 conflagration failure time. This is due to greater scatter of the burning propellant fragments as the launch vehicle begins its ascent. The large scatter region reduces the net heat flux of burning propellant mass per unit area in the debris field. This leads to lower stabilization heights of the source puffs, which in turn equates to higher ground level concentrations. Ground level concentration is very sensitive to the stabilization heights of the puffs and varies approximately in proportion to the invers cube of the stabilization height (i.e. reducing the stabilization height by ½ increases the ground concentration by about a factor of 8).

Table 6-23 presents the maximum far field HCl peak instantaneous concentration predicted by LATRA3D for a simulated T+4 conflagration failure of a Castor 1200 vehicle with subsequent dispersion of the exhaust from burning fragments falling to the ground and from burning propellant fragments on the ground. The far field exposure is LATRA3D's prediction for concentrations at ground level downwind of the stabilized exhaust cloud. Far field peak HCl concentrations ranged from 46 to 315 ppm with the maximum concentration predicted to occur from 70 to 2300 meters downwind from the conflagration debris field source location. Concentrations above 100 ppm are generally associated with low puff stabilization heights for portions of the ground burning plumes that are in the debris impact regions. These high concentration points are either within the impact region or very close to it. The table values represent the maximum concentrations predicted over a sample set of 4662 WFF balloon soundings. Table 6-24 provides information about the general size (length) and direction of a low threshold 1-ppm hazard zone for the daytime T+4 conflagration scenarios. Hazard zones for higher concentration thresholds will always be shorter than the reported 1-ppm hazard zone length but due to non-linearity factors in the dispersion equations the hazard zone lengths for other threshold ppm values cannot be directly scaled from the 1-ppm hazard zone length.

Table 6-25 shows the LATRA3D predicted maximum peak HCl far field concentrations for 1751 nighttime cases for Castor 1200 vehicle T+4 conflagration scenario. Nighttime far field peak HCl concentrations ranged from 31 to 213 ppm with the maximum concentration predicted to occur from 40 to 2400 meters downwind from the conflagration debris field source location. Table 6-26 provides information about the general size (length) and direction of a low threshold 1-ppm hazard zone for the nighttime T+4 conflagration scenarios.

Table 6-23: Castor 1200 T+4 Conflagration HCl Concentration Summary – Daytime Meteorology.

Month	Number of Weather Cases	Peak HCl Concentration [ppm]	Distance to Peak HCl Concentration [m]	Bearing to Peak HCl Concentration [deg]
January	341	3.15E+02	104	352
February	362	1.79E+02	73	47
March	389	1.49E+02	535	32
April	378	1.67E+02	176	89
May	396	1.65E+02	254	31
June	389	8.87E+01	133	358
July	414	4.62E+01	2308	350
August	410	4.59E+01	236	223
September	411	6.67E+01	202	240
October	429	1.27E+02	772	23
November	376	1.15E+02	260	136
December	367	1.07E+02	71	93

Table 6-24: Castor 1200 T+4 Conflagration 1-ppm HCl Concentration Hazard Zone Summary – Daytime Meteorology.

Month	Number of Weather Cases	HCl Hazard Zone Concentration [ppm]	Distance to End of Hazard Zone [m]	Bearing to End of Hazard Zone [deg]
January	280	1.00E+00	9567	24
February	292	1.00E+00	9673	306
March	297	1.00E+00	9431	346
April	282	1.00E+00	8307	330
May	319	1.00E+00	7976	297
June	308	1.00E+00	6036	218
July	306	1.00E+00	6144	31
August	319	1.00E+00	7698	242
September	302	1.00E+00	9141	339
October	385	1.00E+00	8261	240
November	342	1.00E+00	8907	55
December	329	1.00E+00	9476	95

Table 6-25: Castor 1200 T+4 Conflagration HCl Concentration Summary – Nighttime Meteorology.

Month	Number of Weather Cases	Peak HCl Concentration [ppm]	Distance to Peak HCl Concentration [m]	Bearing to Peak HCl Concentration [deg]
January	95	1.18E+02	229	57
February	158	2.13E+02	101	173
March	165	1.89E+02	283	56
April	158	1.30E+02	84	100
May	159	1.32E+02	40	129
June	153	5.56E+01	314	189
July	153	3.82E+01	2386	173
August	162	3.12E+01	1122	149
September	163	6.41E+01	280	159
October	125	1.54E+02	48	150
November	129	1.02E+02	149	196
December	131	7.76E+01	332	53

Table 6-26: Castor 1200 T+4 Conflagration 1-ppm HCl Concentration Hazard Zone Summary – Nighttime Meteorology.

Month	Number of Weather Cases	HCl Hazard Zone Concentration [ppm]	Distance to End of Hazard Zone [m]	Bearing to End of Hazard Zone [deg]
January	70	1.00E+00	9273	59
February	134	1.00E+00	9761	126
March	140	1.00E+00	9645	318
April	135	1.00E+00	7639	332
May	140	1.00E+00	6486	29
June	141	1.00E+00	7626	44
July	143	1.00E+00	6273	359
August	155	1.00E+00	6466	52
September	149	1.00E+00	7375	229
October	123	1.00E+00	10366	127
November	118	1.00E+00	10585	182
December	113	1.00E+00	8617	42

The LATRA3D T+4 conflagration predicted HCl concentrations for all daytime meteorological cases processed in the 8-year sample set were aggregated into bins to evaluate the peak far field concentration probability. This information is provided in Table 6-27.

Table 6-27. LATRA3D Predicted Maximum Far Field Ground Level HCl Concentrations for Daytime Castor 1200 T+4 Conflagration Scenarios.

Concentration Bin	Count	Probability
0 - 2	1508	0.32347
2- 4	684	0.14672
4 - 6	490	0.10511
6 - 8	366	0.07851
8 - 10	283	0.06070
10 - 20	730	0.15659
20 - 30	269	0.05770
30 - 40	139	0.02982
40 - 50	69	0.01480
50 - 60	32	0.00686
60 – 70	15	0.00322
70 – 80	21	0.00450
80 – 90	15	0.00322
90 - 100	10	0.00215
> 100	31	0.00665

It is noted that approximately 71.5% of all daytime meteorological cases resulted in LATRA3D maximum peak instantaneous ground level HCl concentrations of less than 10 ppm. Approximately 15.6% of the daytime meteorological cases resulted in in LATRA3D maximum peak instantaneous ground level HCl concentrations in the 10 to 20 ppm range. Approximately 2.7% of the cases produced HCl ground concentration predictions above 50 ppm.

The LATRA3D predicted cloud transport directions for the T+4 conflagration HCl dispersion were aggregated into bins representing 45-degree arc corridors around the compass (i.e. N, NE, E, SE, S, SW, W, NW). The transport direction for conflagration modes is defined relative to the center of the propellant impact debris field. Table 6-28 indicates the predicted Castor 1200 T+4 conflagration plume direction probability of occurrence for the direction to the maximum concentration point. The table is based on 4662 daytime balloon sounding cases that produced non-zero predicted ground level HCl concentrations. Estimation of plume direction using LATRA3D peak concentration for conflagration scenarios should be considered as a rough

approximation only. The plume transport directions derived from the computed direction to the endpoint of the 1-ppm hazard zone listed in Table 6-29 provide a better estimate of expected plume transport directions over the ensemble of weather cases. It is noted that for the daytime launch scenarios transport of the conflagration exhaust plume to the Northeast is favored. There is a lower probability for transport of the conflagration plumes to the West.

Table 6-28. LATRA3D Predicted Exhaust Cloud Transport Directions for Daytime Castor 1200 T+4 Conflagration HCl Scenarios.

Plume Transport Direction Bin	Count	Probability
337.5 – 22.5 (N)	791	0.16967
22.5 – 67.5 (NE)	888	0.19048
67.5 – 112.5 (E)	561	0.12033
112.5 – 157.5 (SE)	612	0.13127
157.5 – 202.5 (S)	524	0.11240
202.5 – 247.5 (SW)	541	0.11604
247.5 – 292.5 (W)	388	0.08323
292.5 – 337.5 (NW)	357	0.07658

Table 6-29. LATRA3D Predicted Exhaust Cloud Transport Directions for Daytime Castor 1200 T+4 Conflagration HCl Scenarios Using the 1-ppm Hazard Zone Endpoint.

Plume Transport Direction Bin	Count	Probability
337.5 – 22.5 (N)	615	0.16352
22.5 – 67.5 (NE)	863	0.22946
67.5 – 112.5 (E)	498	0.13241
112.5 – 157.5 (SE)	503	0.13374
157.5 – 202.5 (S)	397	0.10556
202.5 – 247.5 (SW)	367	0.09758
247.5 – 292.5 (W)	277	0.07365
292.5 – 337.5 (NW)	241	0.06408

Similar summary tables for the 1751 nighttime Castor 1200 T+4 conflagration simulations were compiled. Table 6-30 shows the peak HCl instantaneous concentration predictions for nighttime conditions. It is noted that approximately 66% of all nighttime meteorological cases resulted in LATRA3D maximum peak instantaneous ground level HCl concentrations of less than 10 ppm. Approximately 18.6% of the nighttime meteorological cases resulted in in LATRA3D maximum peak instantaneous ground level HCl concentrations in the 10 to 20 ppm range. Approximately 4.2% of the cases produced HCl ground concentration predictions above 50 ppm.

Table 6-30. LATRA3D Predicted Maximum Far Field Ground Level HCl Concentrations for Nighttime Castor 1200 T+4 Conflagration Scenarios.

Concentration Bin	Count	Probability
0 - 2	372	0.21245
2- 4	243	0.13878
4 - 6	243	0.13878
6 - 8	179	0.10223
8 - 10	120	0.06853
10 - 20	326	0.18618
20 - 30	108	0.06168
30 - 40	54	0.03084
40 - 50	33	0.01885
50 - 60	26	0.01485
60 – 70	11	0.00628
70 – 80	8	0.00457
80 – 90	9	0.00514
90 - 100	5	0.00286
> 100	14	0.00800

Table 6-31 indicates the predicted Castor 1200 vehicle T+4 conflagration plume direction probability of occurrence observed across the 1751 nighttime balloon sounding cases based on the direct to the maximum concentration point. The plume transport directions derived from the computed direction to the endpoint of the 1-ppm hazard zone listed in Table 6-32 provide a better estimate of expected plume transport directions over the ensemble of weather cases. It is noted that for the nighttime launch scenarios transport of the conflagration exhaust plume to the Northeast is favored. There is a lower probability for transport of the conflagration plumes to the West.

Table 6-31. REEDM Predicted Exhaust Cloud Transport Directions for Nighttime Castor 1200 T+4 Conflagration Scenarios.

Plume Transport Direction Bin	Count	Probability
337.5 – 22.5 (N)	145	0.08281
22.5 – 67.5 (NE)	327	0.18675
67.5 – 112.5 (E)	274	0.15648
112.5 – 157.5 (SE)	278	0.15877
157.5 – 202.5 (S)	267	0.15248
202.5 – 247.5 (SW)	249	0.14220
247.5 – 292.5 (W)	122	0.06967
292.5 – 337.5 (NW)	89	0.05083

Table 6-32. LATRA3D Predicted Exhaust Cloud Transport Directions for Daytime Castor 1200 T+4 Conflagration HCl Scenarios Using the 1-ppm Hazard Zone Endpoint.

Plume Transport Direction Bin	Count	Probability
337.5 – 22.5 (N)	124	0.07944
22.5 – 67.5 (NE)	308	0.19731
67.5 – 112.5 (E)	266	0.17040
112.5 – 157.5 (SE)	243	0.15567
157.5 – 202.5 (S)	222	0.14222
202.5 – 247.5 (SW)	207	0.13261
247.5 – 292.5 (W)	108	0.06919
292.5 – 337.5 (NW)	83	0.05317

6.4.3 T+8 Conflagration HCl Results

Maximum predicted ground level HCl concentrations are higher and closer to the source for the T+8 second failure are approximately comparable to the T+4 second conflagration failure time.

Table 6-33 presents the maximum far field HCl peak instantaneous concentration predicted by LATRA3D for a simulated T+8 conflagration failure of a Castor 1200 vehicle with subsequent dispersion of the exhaust from burning fragments falling to the ground and from burning propellant fragments on the ground. The far field exposure is LATRA3D's prediction for concentrations at ground level downwind of the stabilized exhaust cloud. Far field peak HCl concentrations ranged from 30 to 120 ppm with the maximum concentration predicted to occur from 200 to 3200 meters downwind from the conflagration debris field source location. Concentrations above 100 ppm are generally associated with low puff stabilization heights for portions of the ground burning plumes that are in the debris impact regions. These high concentration points are either within the impact region or very close to it. The table values represent the maximum concentrations predicted over a sample set of 4660 WFF balloon soundings. Table 6-34 provides information about the general size (length) and direction of a low threshold 1-ppm hazard zone for the daytime T+8 conflagration scenarios. Hazard zones for higher concentration thresholds will always be shorter than the reported 1-ppm hazard zone length but due to non-linearity factors in the dispersion equations the hazard zone lengths for other threshold ppm values cannot be directly scaled from the 1-ppm hazard zone length.

Table 6-35 shows the LATRA3D predicted maximum peak HCl far field concentrations for 1750 nighttime cases for Castor 1200 vehicle T+8 conflagration scenario. Nighttime far field peak HCl concentrations ranged from 22 to 114 ppm with the maximum concentration predicted to occur from 90 to 5400 meters downwind from the conflagration debris field source location. Table 6-36 provides information about the general size (length) and direction of a low threshold 1-ppm hazard zone for the nighttime T+8 conflagration scenarios.

Table 6-33: Castor 1200 T+8 Conflagration HCl Concentration Summary – Daytime Meteorology.

Month	Number of Weather Cases	Peak HCl Concentration [ppm]	Distance to Peak HCl Concentration [m]	Bearing to Peak HCl Concentration [deg]
January	341	1.20E+02	218	14
February	361	1.07E+02	249	287
March	390	1.60E+02	586	27
April	378	8.90E+01	211	347
May	396	6.09E+01	2109	12
June	389	3.70E+01	1399	50
July	415	4.34E+01	2353	351
August	409	4.01E+01	2382	6
September	410	3.01E+01	3247	6
October	429	9.40E+01	647	25
November	376	5.24E+01	742	146
December	366	4.61E+01	1070	4

Table 6-34: Castor 1200 T+8 Conflagration 1-ppm HCl Concentration Hazard Zone Summary – Daytime Meteorology.

Month	Number of Weather Cases	HCl Hazard Zone Concentration [ppm]	Distance to End of Hazard Zone [m]	Bearing to End of Hazard Zone [deg]
January	276	1.00E+00	9283	24
February	286	1.00E+00	9586	60
March	291	1.00E+00	8514	346
April	287	1.00E+00	7912	19
May	315	1.00E+00	7779	297
June	308	1.00E+00	6046	17
July	298	1.00E+00	5698	30
August	310	1.00E+00	7534	341
September	297	1.00E+00	8981	338
October	383	1.00E+00	7882	242
November	344	1.00E+00	8147	54
December	324	1.00E+00	8641	70

Table 6-35: Castor 1200 T+8 Conflagration HCl Concentration Summary – Nighttime Meteorology.

Month	Number of Weather Cases	Peak HCl Concentration [ppm]	Distance to Peak HCl Concentration [m]	Bearing to Peak HCl Concentration [deg]
January	95	4.29E+01	2838	95
February	158	8.73E+01	279	33
March	164	1.14E+02	160	35
April	158	7.68E+01	2607	334
May	159	4.73E+01	92	40
June	153	2.99E+01	1654	20
July	153	3.11E+01	2321	172
August	162	2.79E+01	1631	157
September	163	2.16E+01	5382	232
October	125	4.73E+01	2584	34
November	129	5.59E+01	2622	238
December	131	5.27E+01	2915	165

Table 6-36: Castor 1200 T+8 Conflagration 1-ppm HCl Concentration Hazard Zone Summary – Nighttime Meteorology.

Month	Number of Weather Cases	HCl Hazard Zone Concentration [ppm]	Distance to End of Hazard Zone [m]	Bearing to End of Hazard Zone [deg]
January	73	1.00E+00	8355	72
February	134	1.00E+00	10171	37
March	138	1.00E+00	9177	34
April	138	1.00E+00	7519	333
May	144	1.00E+00	6333	48
June	142	1.00E+00	7477	44
July	143	1.00E+00	6200	359
August	154	1.00E+00	6457	197
September	151	1.00E+00	7339	345
October	122	1.00E+00	7917	99
November	117	1.00E+00	7867	2
December	111	1.00E+00	8385	136

The LATRA3D T+8 conflagration predicted HCl concentrations for all daytime meteorological cases processed in the 8-year sample set were aggregated into bins to evaluate the peak far field concentration probability. This information is provided in Table 6-37.

Table 6-37. LATRA3D Predicted Maximum Far Field Ground Level HCl Concentrations for Daytime Castor 1200 T+8 Conflagration Scenarios.

Concentration Bin	Count	Probability
0 - 2	1668	0.35794
2- 4	800	0.17167
4 - 6	487	0.10451
6 - 8	349	0.07489
8 - 10	257	0.05515
10 - 20	662	0.14206
20 - 30	253	0.05429
30 - 40	98	0.02103
40 - 50	44	0.00944
50 - 60	21	0.00451
60 – 70	8	0.00172
70 – 80	6	0.00129
80 – 90	3	0.00064
90 - 100	1	0.00021
> 100	3	0.00064

It is noted that approximately 76.4% of all daytime meteorological cases resulted in LATRA3D maximum peak instantaneous ground level HCl concentrations of less than 10 ppm. Approximately 14.2% of the daytime meteorological cases resulted in in LATRA3D maximum peak instantaneous ground level HCl concentrations in the 10 to 20 ppm range. Approximately 0.9% of the cases produced HCl ground concentration predictions above 50 ppm.

The LATRA3D predicted cloud transport directions for the T+8 conflagration HCl dispersion were aggregated into bins representing 45-degree arc corridors around the compass (i.e. N, NE, E, SE, S, SW, W, NW). The transport direction for conflagration modes is defined relative to the center of the propellant impact debris field. Table 6-38 indicates the predicted Castor 1200 T+8 conflagration plume direction probability of occurrence for the direction to the maximum concentration point. The table is based on 4660 daytime balloon sounding cases that produced non-zero predicted ground level HCl concentrations. Estimation of plume direction using LATRA3D peak concentration for conflagration scenarios should be considered as a rough

approximation only. The plume transport directions derived from the computed direction to the endpoint of the 1-ppm hazard zone listed in Table 6-39 provide a better estimate of expected plume transport directions over the ensemble of weather cases. It is noted that for the daytime launch scenarios transport of the conflagration exhaust plume to the Northeast is favored. There is a lower probability for transport of the conflagration plumes to the West.

Table 6-38. LATRA3D Predicted Exhaust Cloud Transport Directions for Daytime Castor 1200 T+8 Conflagration HCl Scenarios.

Plume Transport Direction Bin	Count	Probability
337.5 – 22.5 (N)	889	0.19077
22.5 – 67.5 (NE)	817	0.17532
67.5 – 112.5 (E)	455	0.09764
112.5 – 157.5 (SE)	559	0.11996
157.5 – 202.5 (S)	493	0.10579
202.5 – 247.5 (SW)	586	0.12575
247.5 – 292.5 (W)	472	0.10129
292.5 – 337.5 (NW)	389	0.08348

Table 6-39. LATRA3D Predicted Exhaust Cloud Transport Directions for Daytime Castor 1200 T+8 Conflagration HCl Scenarios Using the 1-ppm Hazard Zone Endpoint.

Plume Transport Direction Bin	Count	Probability
337.5 – 22.5 (N)	635	0.17074
22.5 – 67.5 (NE)	829	0.22291
67.5 – 112.5 (E)	500	0.13444
112.5 – 157.5 (SE)	463	0.12450
157.5 – 202.5 (S)	407	0.10944
202.5 – 247.5 (SW)	356	0.09572
247.5 – 292.5 (W)	290	0.07798
292.5 – 337.5 (NW)	239	0.06426

Similar summary tables for the 1750 nighttime Castor 1200 T+8 conflagration simulations were compiled. Table 6-40 shows the peak HCl instantaneous concentration predictions for nighttime conditions. It is noted that approximately 76.2% of all nighttime meteorological cases resulted in LATRA3D maximum peak instantaneous ground level HCl concentrations of less than 10 ppm. Approximately 15.8% of the nighttime meteorological cases resulted in in LATRA3D maximum peak instantaneous ground level HCl concentrations in the 10 to 20 ppm range. Approximately 0.8% of the cases produced HCl ground concentration predictions above 50 ppm.

Table 6-40. LATRA3D Predicted Maximum Far Field Ground Level HCl Concentrations for Nighttime Castor 1200 T+8 Conflagration Scenarios.

Concentration Bin	Count	Probability
0 - 2	410	0.23429
2- 4	358	0.20457
4 - 6	261	0.14914
6 - 8	197	0.11257
8 - 10	107	0.06114
10 - 20	277	0.15829
20 - 30	78	0.04457
30 - 40	33	0.01886
40 - 50	15	0.00857
50 - 60	4	0.00229
60 – 70	2	0.00114
70 – 80	5	0.00286
80 – 90	1	0.00057
90 - 100	1	0.00057
> 100	1	0.00057

Table 6-41 indicates the predicted Castor 1200 vehicle T+8 conflagration plume direction probability of occurrence observed across the 1750 nighttime balloon sounding cases based on the direct to the maximum concentration point. The plume transport directions derived from the computed direction to the endpoint of the 1-ppm hazard zone listed in Table 6-42 provide a better estimate of expected plume transport directions over the ensemble of weather cases. It is noted that for the nighttime launch scenarios transport of the conflagration exhaust plume to the Northeast is favored. There is a lower probability for transport of the conflagration plumes to the West.

Table 6-41. REEDM Predicted Exhaust Cloud Transport Directions for Nighttime Castor 1200 T+8 Conflagration Scenarios.

Plume Transport Direction Bin	Count	Probability
337.5 – 22.5 (N)	180	0.10286
22.5 – 67.5 (NE)	319	0.18229
67.5 – 112.5 (E)	234	0.13371
112.5 – 157.5 (SE)	247	0.14114
157.5 – 202.5 (S)	245	0.14000
202.5 – 247.5 (SW)	251	0.14343
247.5 – 292.5 (W)	158	0.09029
292.5 – 337.5 (NW)	116	0.06629

Table 6-42. LATRA3D Predicted Exhaust Cloud Transport Directions for Daytime Castor 1200 T+8 Conflagration HCl Scenarios Using the 1-ppm Hazard Zone Endpoint.

Plume Transport Direction Bin	Count	Probability
337.5 – 22.5 (N)	125	0.07977
22.5 – 67.5 (NE)	314	0.20038
67.5 – 112.5 (E)	264	0.16847
112.5 – 157.5 (SE)	218	0.13912
157.5 – 202.5 (S)	231	0.14742
202.5 – 247.5 (SW)	215	0.13720
247.5 – 292.5 (W)	121	0.07722
292.5 – 337.5 (NW)	79	0.05041

6.4.4 T+12 Conflagration HCl Results

Maximum predicted ground level HCl concentrations for the T+12 second failure are approximately comparable to the T+8 second conflagration failure time.

Table 6-43 presents the maximum far field HCl peak instantaneous concentration predicted by LATRA3D for a simulated T+12 conflagration failure of a Castor 1200 vehicle with subsequent dispersion of the exhaust from burning fragments falling to the ground and from burning propellant fragments on the ground. The far field exposure is LATRA3D's prediction for concentrations at ground level downwind of the stabilized exhaust cloud. Far field peak HCl concentrations ranged from 26 to 118 ppm with the maximum concentration predicted to occur from 380 to 3500 meters downwind from the conflagration debris field source location. Concentrations above 100 ppm are generally associated with low puff stabilization heights for portions of the ground burning plumes that are in the debris impact regions. These high concentration points are either within the impact region or very close to it. The table values represent the maximum concentrations predicted over a sample set of 4663 WFF balloon soundings. Table 6-44 provides information about the general size (length) and direction of a low threshold 1-ppm hazard zone for the daytime T+12 conflagration scenarios. Hazard zones for higher concentration thresholds will always be shorter than the reported 1-ppm hazard zone length but due to non-linearity factors in the dispersion equations the hazard zone lengths for other threshold ppm values cannot be directly scaled from the 1-ppm hazard zone length.

Table 6-45 shows the LATRA3D predicted maximum peak HCl far field concentrations for 1751 nighttime cases for Castor 1200 vehicle T+12 conflagration scenario. Nighttime far field peak HCl concentrations ranged from 18 to 112 ppm with the maximum concentration predicted to occur from 90 to 2800 meters downwind from the conflagration debris field source location. Table 6-46 provides information about the general size (length) and direction of a low threshold 1-ppm hazard zone for the nighttime T+12 conflagration scenarios.

Table 6-43: Castor 1200 T+12 Conflagration HCl Concentration Summary – Daytime Meteorology.

Month	Number of Weather Cases	Peak HCl Concentration [ppm]	Distance to Peak HCl Concentration [m]	Bearing to Peak HCl Concentration [deg]
January	341	1.18E+02	385	354
February	361	1.08E+02	587	292
March	392	1.44E+02	638	10
April	376	8.81E+01	528	351
May	395	5.76E+01	560	16
June	390	3.33E+01	1435	112
July	415	3.58E+01	2201	351
August	410	3.11E+01	2386	5
September	411	2.55E+01	3457	5
October	429	9.21E+01	662	8
November	376	5.24E+01	379	159
December	367	4.53E+01	886	80

Table 6-44: Castor 1200 T+12 Conflagration 1-ppm HCl Concentration Hazard Zone Summary – Daytime Meteorology.

Month	Number of Weather Cases	HCl Hazard Zone Concentration [ppm]	Distance to End of Hazard Zone [m]	Bearing to End of Hazard Zone [deg]
January	281	1.00E+00	9303	23
February	293	1.00E+00	9487	59
March	293	1.00E+00	8593	345
April	288	1.00E+00	7379	18
May	322	1.00E+00	7414	297
June	318	1.00E+00	5853	18
July	318	1.00E+00	5509	348
August	311	1.00E+00	7476	341
September	303	1.00E+00	8709	338
October	385	1.00E+00	7697	40
November	348	1.00E+00	8225	233
December	323	1.00E+00	8521	69

Table 6-45: Castor 1200 T+12 Conflagration HCl Concentration Summary – Nighttime Meteorology.

Month	Number of Weather Cases	Peak HCl Concentration [ppm]	Distance to Peak HCl Concentration [m]	Bearing to Peak HCl Concentration [deg]
January	95	4.33E+01	260	26
February	158	8.95E+01	312	353
March	165	1.12E+02	232	335
April	158	7.64E+01	113	318
May	159	4.57E+01	92	348
June	153	2.43E+01	1657	17
July	153	2.77E+01	2354	173
August	162	2.34E+01	2819	39
September	163	1.84E+01	1873	64
October	125	3.90E+01	2567	35
November	129	4.69E+01	2613	239
December	131	4.63E+01	952	51

Table 6-46: Castor 1200 T+12 Conflagration 1-ppm HCl Concentration Hazard Zone Summary – Nighttime Meteorology.

Month	Number of Weather Cases	HCl Hazard Zone Concentration [ppm]	Distance to End of Hazard Zone [m]	Bearing to End of Hazard Zone [deg]
January	72	1.00E+00	8212	71
February	131	1.00E+00	10131	36
March	135	1.00E+00	9173	33
April	141	1.00E+00	7024	54
May	144	1.00E+00	6035	29
June	148	1.00E+00	7287	43
July	149	1.00E+00	6247	359
August	157	1.00E+00	6545	197
September	155	1.00E+00	7446	344
October	123	1.00E+00	7652	99
November	119	1.00E+00	7786	1
December	116	1.00E+00	8135	137

The LATRA3D T+12 conflagration predicted HCl concentrations for all daytime meteorological cases processed in the 8-year sample set were aggregated into bins to evaluate the peak far field concentration probability. This information is provided in Table 6-47.

Table 6-47. LATRA3D Predicted Maximum Far Field Ground Level HCl Concentrations for Daytime Castor 1200 T+12 Conflagration Scenarios.

Concentration Bin	Count	Probability
0 - 2	1628	0.34913
2- 4	911	0.19537
4 - 6	522	0.11195
6 - 8	371	0.07956
8 - 10	258	0.05533
10 - 20	611	0.13103
20 - 30	226	0.04847
30 - 40	69	0.01480
40 - 50	33	0.00708
50 - 60	16	0.00343
60 – 70	6	0.00129
70 – 80	5	0.00107
80 – 90	3	0.00064
90 - 100	1	0.00021
> 100	3	0.00064

It is noted that approximately 79.1% of all daytime meteorological cases resulted in LATRA3D maximum peak instantaneous ground level HCl concentrations of less than 10 ppm. Approximately 13.1% of the daytime meteorological cases resulted in in LATRA3D maximum peak instantaneous ground level HCl concentrations in the 10 to 20 ppm range. Approximately 0.7% of the cases produced HCl ground concentration predictions above 50 ppm.

The LATRA3D predicted cloud transport directions for the T+12 conflagration HCl dispersion were aggregated into bins representing 45-degree arc corridors around the compass (i.e. N, NE, E, SE, S, SW, W, NW). The transport direction for conflagration modes is defined relative to the center of the propellant impact debris field. Table 6-48 indicates the predicted Castor 1200 T+12 conflagration plume direction probability of occurrence for the direction to the maximum concentration point. The table is based on 4663 daytime balloon sounding cases that produced non-zero predicted ground level HCl concentrations. Estimation of plume direction using LATRA3D peak concentration for conflagration scenarios should be considered as a rough

approximation only. The plume transport directions derived from the computed direction to the endpoint of the 1-ppm hazard zone listed in Table 6-49 provide a better estimate of expected plume transport directions over the ensemble of weather cases. It is noted that for the daytime launch scenarios transport of the conflagration exhaust plume to the Northeast is favored. There is a lower probability for transport of the conflagration plumes to the West and Northwest.

Table 6-48. LATRA3D Predicted Exhaust Cloud Transport Directions for Daytime Castor 1200 T+12 Conflagration HCl Scenarios.

Plume Transport Direction Bin	Count	Probability
337.5 – 22.5 (N)	961	0.20609
22.5 – 67.5 (NE)	752	0.16127
67.5 – 112.5 (E)	550	0.11795
112.5 – 157.5 (SE)	427	0.09157
157.5 – 202.5 (S)	462	0.09908
202.5 – 247.5 (SW)	555	0.11902
247.5 – 292.5 (W)	523	0.11216
292.5 – 337.5 (NW)	433	0.09286

Table 6-49. LATRA3D Predicted Exhaust Cloud Transport Directions for Daytime Castor 1200 T+12 Conflagration HCl Scenarios Using the 1-ppm Hazard Zone Endpoint.

Plume Transport Direction Bin	Count	Probability
337.5 – 22.5 (N)	671	0.17737
22.5 – 67.5 (NE)	806	0.21306
67.5 – 112.5 (E)	542	0.14327
112.5 – 157.5 (SE)	427	0.11287
157.5 – 202.5 (S)	402	0.10626
202.5 – 247.5 (SW)	348	0.09199
247.5 – 292.5 (W)	328	0.08670
292.5 – 337.5 (NW)	259	0.06846

Similar summary tables for the 1751 nighttime Castor 1200 T+12 conflagration simulations were compiled. Table 6-50Table 6-40 shows the peak HCl instantaneous concentration predictions for nighttime conditions. It is noted that approximately 79% of all nighttime meteorological cases resulted in LATRA3D maximum peak instantaneous ground level HCl concentrations of less than 10 ppm. Approximately 14% of the nighttime meteorological cases resulted in in LATRA3D

maximum peak instantaneous ground level HCl concentrations in the 10 to 20 ppm range. Approximately 0.7% of the cases produced HCl ground concentration predictions above 50 ppm.

Table 6-50. LATRA3D Predicted Maximum Far Field Ground Level HCl Concentrations for Nighttime Castor 1200 T+12 Conflagration Scenarios.

Concentration Bin	Count	Probability
0 - 2	375	0.21416
2- 4	426	0.24329
4 - 6	273	0.15591
6 - 8	198	0.11308
8 - 10	111	0.06339
10 - 20	246	0.14049
20 - 30	73	0.04169
30 - 40	26	0.01485
40 - 50	11	0.00628
50 - 60	4	0.00228
60 – 70	1	0.00057
70 – 80	4	0.00228
80 – 90	2	0.00114
90 - 100	0	0.00000
> 100	1	0.00057

Table 6-51 indicates the predicted Castor 1200 vehicle T+12 conflagration plume direction probability of occurrence observed across the 1751 nighttime balloon sounding cases based on the direct to the maximum concentration point. The plume transport directions derived from the computed direction to the endpoint of the 1-ppm hazard zone listed in Table 6-52 provide a better estimate of expected plume transport directions over the ensemble of weather cases. It is noted that for the nighttime launch scenarios transport of the conflagration exhaust plume to the Northeast is favored. There is a lower probability for transport of the conflagration plumes to the West.

Table 6-51. REEDM Predicted Exhaust Cloud Transport Directions for Nighttime Castor 1200 T+12 Conflagration Scenarios.

Plume Transport Direction Bin	Count	Probability
337.5 – 22.5 (N)	209	0.11936
22.5 – 67.5 (NE)	309	0.17647
67.5 – 112.5 (E)	248	0.14163
112.5 – 157.5 (SE)	198	0.11308
157.5 – 202.5 (S)	205	0.11708
202.5 – 247.5 (SW)	273	0.15591
247.5 – 292.5 (W)	190	0.10851
292.5 – 337.5 (NW)	119	0.06796

Table 6-52. LATRA3D Predicted Exhaust Cloud Transport Directions for Daytime Castor 1200 T+12 Conflagration HCl Scenarios Using the 1-ppm Hazard Zone Endpoint.

Plume Transport Direction Bin	Count	Probability
337.5 – 22.5 (N)	127	0.07987
22.5 – 67.5 (NE)	316	0.19874
67.5 – 112.5 (E)	271	0.17044
112.5 – 157.5 (SE)	217	0.13648
157.5 – 202.5 (S)	227	0.14277
202.5 – 247.5 (SW)	214	0.13459
247.5 – 292.5 (W)	137	0.08616
292.5 – 337.5 (NW)	81	0.05094

6.4.5 T+16 Conflagration HCl Results

Maximum predicted ground level HCl concentrations for the T+16 second failure are approximately comparable to the T+12 second conflagration failure time.

Table 6-53 presents the maximum far field HCl peak instantaneous concentration predicted by LATRA3D for a simulated T+16 conflagration failure of a Castor 1200 vehicle with subsequent dispersion of the exhaust from burning fragments falling to the ground and from burning propellant fragments on the ground. The far field exposure is LATRA3D's prediction for concentrations at ground level downwind of the stabilized exhaust cloud. Far field peak HCl concentrations ranged from 20 to 153 ppm with the maximum concentration predicted to occur from 330 to 2200 meters downwind from the conflagration debris field source location. Concentrations above 100 ppm are generally associated with low puff stabilization heights for portions of the ground burning plumes that are in the debris impact regions. These high concentration points are either within the impact region or very close to it. The table values represent the maximum concentrations predicted over a sample set of 4669 WFF balloon soundings. Table 6-54 provides information about the general size (length) and direction of a low threshold 1-ppm hazard zone for the daytime T+16 conflagration scenarios. Hazard zones for higher concentration thresholds will always be shorter than the reported 1-ppm hazard zone length but due to non-linearity factors in the dispersion equations the hazard zone lengths for other threshold ppm values cannot be directly scaled from the 1-ppm hazard zone length.

Table 6-55 shows the LATRA3D predicted maximum peak HCl far field concentrations for 1751 nighttime cases for Castor 1200 vehicle T+16 conflagration scenario. Nighttime far field peak HCl concentrations ranged from 19 to 115 ppm with the maximum concentration predicted to occur from 580 to 2700 meters downwind from the conflagration debris field source location. Table 6-56 provides information about the general size (length) and direction of a low threshold 1-ppm hazard zone for the nighttime T+16 conflagration scenarios.

Table 6-53: Castor 1200 T+16 Conflagration HCl Concentration Summary – Daytime Meteorology.

Month	Number of Weather Cases	Peak HCl Concentration [ppm]	Distance to Peak HCl Concentration [m]	Bearing to Peak HCl Concentration [deg]
January	341	1.20E+02	736	315
February	362	1.10E+02	944	293
March	391	1.53E+02	887	338
April	379	8.79E+01	831	306
May	396	5.49E+01	777	339
June	390	2.90E+01	2032	298
July	416	2.92E+01	2150	349
August	410	2.48E+01	1304	130
September	412	1.99E+01	2213	67
October	429	9.35E+01	940	340
November	376	4.82E+01	330	251
December	367	4.70E+01	578	46

Table 6-54: Castor 1200 T+16 Conflagration 1-ppm HCl Concentration Hazard Zone Summary – Daytime Meteorology.

Month	Number of Weather Cases	HCl Hazard Zone Concentration [ppm]	Distance to End of Hazard Zone [m]	Bearing to End of Hazard Zone [deg]
January	275	1.00E+00	9315	21
February	281	1.00E+00	9444	282
March	290	1.00E+00	8963	342
April	286	1.00E+00	7504	332
May	320	1.00E+00	7274	298
June	307	1.00E+00	5739	18
July	297	1.00E+00	5407	23
August	307	1.00E+00	7380	341
September	301	1.00E+00	8872	251
October	382	1.00E+00	7580	41
November	341	1.00E+00	8457	236
December	315	1.00E+00	8587	18

Table 6-55: Castor 1200 T+16 Conflagration HCl Concentration Summary – Nighttime Meteorology.

Month	Number of Weather Cases	Peak HCl Concentration [ppm]	Distance to Peak HCl Concentration [m]	Bearing to Peak HCl Concentration [deg]
January	95	4.32E+01	594	321
February	158	8.32E+01	686	317
March	165	1.15E+02	656	304
April	158	7.57E+01	582	302
May	159	4.71E+01	611	300
June	153	2.01E+01	2736	45
July	153	2.17E+01	2683	173
August	162	1.98E+01	1693	151
September	163	1.91E+01	881	225
October	125	3.31E+01	2549	36
November	129	3.84E+01	2604	239
December	131	4.40E+01	702	9

Table 6-56: Castor 1200 T+16 Conflagration 1-ppm HCl Concentration Hazard Zone Summary – Nighttime Meteorology.

Month	Number of Weather Cases	HCl Hazard Zone Concentration [ppm]	Distance to End of Hazard Zone [m]	Bearing to End of Hazard Zone [deg]
January	71	1.00E+00	8100	39
February	134	1.00E+00	10040	34
March	139	1.00E+00	9159	28
April	135	1.00E+00	6952	78
May	142	1.00E+00	6302	251
June	145	1.00E+00	7068	308
July	147	1.00E+00	6341	360
August	155	1.00E+00	6386	196
September	155	1.00E+00	7803	341
October	121	1.00E+00	7540	100
November	121	1.00E+00	7633	1
December	113	1.00E+00	7889	137

The LATRA3D T+16 conflagration predicted HCl concentrations for all daytime meteorological cases processed in the 8-year sample set were aggregated into bins to evaluate the peak far field concentration probability. This information is provided in Table 6-57.

Table 6-57. LATRA3D Predicted Maximum Far Field Ground Level HCl Concentrations for Daytime Castor 1200 T+16 Conflagration Scenarios.

Concentration Bin	Count	Probability
0 - 2	1773	0.37974
2- 4	923	0.19769
4 - 6	525	0.11244
6 - 8	377	0.08075
8 - 10	245	0.05247
10 - 20	585	0.12529
20 - 30	147	0.03148
30 - 40	45	0.00964
40 - 50	18	0.00386
50 - 60	11	0.00236
60 – 70	8	0.00171
70 – 80	5	0.00107
80 – 90	3	0.00064
90 - 100	1	0.00021
> 100	3	0.00064

It is noted that approximately 82.3% of all daytime meteorological cases resulted in LATRA3D maximum peak instantaneous ground level HCl concentrations of less than 10 ppm. Approximately 12.5% of the daytime meteorological cases resulted in in LATRA3D maximum peak instantaneous ground level HCl concentrations in the 10 to 20 ppm range. Approximately 0.7% of the cases produced HCl ground concentration predictions above 50 ppm.

The LATRA3D predicted cloud transport directions for the T+16 conflagration HCl dispersion were aggregated into bins representing 45-degree arc corridors around the compass (i.e. N, NE, E, SE, S, SW, W, NW). The transport direction for conflagration modes is defined relative to the center of the propellant impact debris field. Table 6-58 indicates the predicted Castor 1200 T+16 conflagration plume direction probability of occurrence for the direction to the maximum concentration point. The table is based on 4669 daytime balloon sounding cases that produced non-zero predicted ground level HCl concentrations. Estimation of plume direction using LATRA3D peak concentration for conflagration scenarios should be considered as a rough

approximation only. The plume transport directions derived from the computed direction to the endpoint of the 1-ppm hazard zone listed in Table 6-59 provide a better estimate of expected plume transport directions over the ensemble of weather cases. It is noted that for the daytime launch scenarios transport of the conflagration exhaust plume to the North and Northeast is favored. Transport in other directions is approximately uniformly distributed.

Table 6-58. LATRA3D Predicted Exhaust Cloud Transport Directions for Daytime Castor 1200 T+16 Conflagration HCl Scenarios.

Plume Transport Direction Bin	Count	Probability
337.5 – 22.5 (N)	896	0.19190
22.5 – 67.5 (NE)	647	0.13857
67.5 – 112.5 (E)	285	0.06104
112.5 – 157.5 (SE)	360	0.07710
157.5 – 202.5 (S)	558	0.11951
202.5 – 247.5 (SW)	657	0.14072
247.5 – 292.5 (W)	617	0.13215
292.5 – 337.5 (NW)	649	0.13900

Table 6-59. LATRA3D Predicted Exhaust Cloud Transport Directions for Daytime Castor 1200 T+16 Conflagration HCl Scenarios Using the 1-ppm Hazard Zone Endpoint.

Plume Transport Direction Bin	Count	Probability
337.5 – 22.5 (N)	668	0.18044
22.5 – 67.5 (NE)	751	0.20286
67.5 – 112.5 (E)	354	0.09562
112.5 – 157.5 (SE)	374	0.10103
157.5 – 202.5 (S)	481	0.12993
202.5 – 247.5 (SW)	334	0.09022
247.5 – 292.5 (W)	338	0.09130
292.5 – 337.5 (NW)	402	0.10859

Similar summary tables for the 1751 nighttime Castor 1200 T+16 conflagration simulations were compiled. Table 6-60Table 6-40 shows the peak HCl instantaneous concentration predictions for nighttime conditions. It is noted that approximately 81.2% of all nighttime meteorological cases resulted in LATRA3D maximum peak instantaneous ground level HCl concentrations of less than 10 ppm. Approximately 13.5% of the nighttime meteorological cases resulted in in LATRA3D

maximum peak instantaneous ground level HCl concentrations in the 10 to 20 ppm range. Approximately 0.5% of the cases produced HCl ground concentration predictions above 50 ppm.

Table 6-60. LATRA3D Predicted Maximum Far Field Ground Level HCl Concentrations for Nighttime Castor 1200 T+16 Conflagration Scenarios.

Concentration Bin	Count	Probability
0 - 2	463	0.26442
2- 4	429	0.24500
4 - 6	251	0.14335
6 - 8	172	0.09823
8 - 10	107	0.06111
10 - 20	236	0.13478
20 - 30	51	0.02913
30 - 40	24	0.01371
40 - 50	9	0.00514
50 - 60	1	0.00057
60 – 70	1	0.00057
70 – 80	4	0.00228
80 – 90	1	0.00057
90 - 100	1	0.00057
> 100	1	0.00057

Table 6-61 indicates the predicted Castor 1200 vehicle T+16 conflagration plume direction probability of occurrence observed across the 1751 nighttime balloon sounding cases based on the direct to the maximum concentration point. The plume transport directions derived from the computed direction to the endpoint of the 1-ppm hazard zone listed in Table 6-62 provide a better estimate of expected plume transport directions over the ensemble of weather cases. It is noted that for the nighttime launch scenarios transport of the conflagration exhaust plume to the Northeast is favored. There is a lower probability for transport of the conflagration plumes to the Northwest.

Table 6-61. REEDM Predicted Exhaust Cloud Transport Directions for Nighttime Castor 1200 T+16 Conflagration Scenarios.

Plume Transport Direction Bin	Count	Probability
337.5 – 22.5 (N)	209	0.11936
22.5 – 67.5 (NE)	263	0.15020
67.5 – 112.5 (E)	146	0.08338
112.5 – 157.5 (SE)	167	0.09537
157.5 – 202.5 (S)	230	0.13135
202.5 – 247.5 (SW)	282	0.16105
247.5 – 292.5 (W)	221	0.12621
292.5 – 337.5 (NW)	233	0.13307

Table 6-62. LATRA3D Predicted Exhaust Cloud Transport Directions for Daytime Castor 1200 T+16 Conflagration HCl Scenarios Using the 1-ppm Hazard Zone Endpoint.

Plume Transport Direction Bin	Count	Probability
337.5 – 22.5 (N)	144	0.09125
22.5 – 67.5 (NE)	300	0.19011
67.5 – 112.5 (E)	221	0.14005
112.5 – 157.5 (SE)	206	0.13054
157.5 – 202.5 (S)	249	0.15779
202.5 – 247.5 (SW)	205	0.12991
247.5 – 292.5 (W)	142	0.08999
292.5 – 337.5 (NW)	111	0.07034

6.4.6 T+20 Conflagration HCl Results

Maximum predicted ground level HCl concentrations for the T+20 second failure are approximately comparable to the T+16 second conflagration failure time.

Table 6-63 presents the maximum far field HCl peak instantaneous concentration predicted by LATRA3D for a simulated T+20 conflagration failure of a Castor 1200 vehicle with subsequent dispersion of the exhaust from burning fragments falling to the ground and from burning propellant fragments on the ground. The far field exposure is LATRA3D's prediction for concentrations at ground level downwind of the stabilized exhaust cloud. Far field peak HCl concentrations ranged from 15 to 153 ppm with the maximum concentration predicted to occur from 980 to 2300 meters downwind from the conflagration debris field source location. Concentrations above 100 ppm are generally associated with low puff stabilization heights for portions of the ground burning plumes that are in the debris impact regions. These high concentration points are either within the impact region or very close to it. The table values represent the maximum concentrations predicted over a sample set of 4668 WFF balloon soundings. Table 6-64 provides information about the general size (length) and direction of a low threshold 1-ppm hazard zone for the daytime T+20 conflagration scenarios. Hazard zones for higher concentration thresholds will always be shorter than the reported 1-ppm hazard zone length but due to non-linearity factors in the dispersion equations the hazard zone lengths for other threshold ppm values cannot be directly scaled from the 1-ppm hazard zone length.

Table 6-65 shows the LATRA3D predicted maximum peak HCl far field concentrations for 1749 nighttime cases for Castor 1200 vehicle T+20 conflagration scenario. Nighttime far field peak HCl concentrations ranged from 14 to 115 ppm with the maximum concentration predicted to occur from 1000 to 3000 meters downwind from the conflagration debris field source location. Table 6-66 provides information about the general size (length) and direction of a low threshold 1-ppm hazard zone for the nighttime T+20 conflagration scenarios.

Table 6-63: Castor 1200 T+20 Conflagration HCl Concentration Summary – Daytime Meteorology.

Month	Number of Weather Cases	Peak HCl Concentration [ppm]	Distance to Peak HCl Concentration [m]	Bearing to Peak HCl Concentration [deg]
January	341	1.16E+02	1429	303
February	363	1.07E+02	1680	294
March	392	1.53E+02	1447	319
April	379	8.67E+01	1508	302
May	395	5.82E+01	1399	320
June	390	2.63E+01	1250	299
July	414	1.83E+01	2258	347
August	410	1.84E+01	1609	282
September	412	1.50E+01	2271	66
October	429	9.07E+01	1482	321
November	376	4.79E+01	984	280
December	367	4.52E+01	1964	324

Table 6-64: Castor 1200 T+20 Conflagration 1-ppm HCl Concentration Hazard Zone Summary – Daytime Meteorology.

Month	Number of Weather Cases	HCl Hazard Zone Concentration [ppm]	Distance to End of Hazard Zone [m]	Bearing to End of Hazard Zone [deg]
January	268	1.00E+00	9379	16
February	278	1.00E+00	10142	282
March	283	1.00E+00	9428	339
April	274	1.00E+00	7394	335
May	310	1.00E+00	7225	298
June	292	1.00E+00	5928	348
July	279	1.00E+00	5576	359
August	296	1.00E+00	7194	340
September	282	1.00E+00	9363	254
October	371	1.00E+00	7661	263
November	336	1.00E+00	8848	240
December	311	1.00E+00	8674	13

Table 6-65: Castor 1200 T+20 Conflagration HCl Concentration Summary – Nighttime Meteorology.

Month	Number of Weather Cases	Peak HCl Concentration [ppm]	Distance to Peak HCl Concentration [m]	Bearing to Peak HCl Concentration [deg]
January	95	4.34E+01	1158	310
February	158	9.05E+01	1396	308
March	164	1.15E+02	1373	299
April	157	7.13E+01	1276	299
May	159	4.73E+01	1346	297
June	153	1.94E+01	1489	286
July	153	1.57E+01	2978	170
August	162	1.60E+01	1167	310
September	163	1.39E+01	1108	225
October	125	2.82E+01	1021	312
November	129	2.47E+01	1258	298
December	131	4.26E+01	1138	332

Table 6-66: Castor 1200 T+20 Conflagration 1-ppm HCl Concentration Hazard Zone Summary – Nighttime Meteorology.

Month	Number of Weather Cases	HCl Hazard Zone Concentration [ppm]	Distance to End of Hazard Zone [m]	Bearing to End of Hazard Zone [deg]
January	71	1.00E+00	7920	34
February	132	1.00E+00	9940	30
March	133	1.00E+00	9082	25
April	133	1.00E+00	7440	325
May	139	1.00E+00	6841	256
June	137	1.00E+00	7069	307
July	139	1.00E+00	5238	171
August	150	1.00E+00	6255	195
September	142	1.00E+00	7068	338
October	119	1.00E+00	7544	99
November	116	1.00E+00	7631	97
December	111	1.00E+00	7935	136

The LATRA3D T+20 conflagration predicted HCl concentrations for all daytime meteorological cases processed in the 8-year sample set were aggregated into bins to evaluate the peak far field concentration probability. This information is provided in Table 6-67.

Table 6-67. LATRA3D Predicted Maximum Far Field Ground Level HCl Concentrations for Daytime Castor 1200 T+20 Conflagration Scenarios.

Concentration Bin	Count	Probability
0 - 2	1973	0.42266
2- 4	963	0.20630
4 - 6	511	0.10947
6 - 8	351	0.07519
8 - 10	244	0.05227
10 - 20	464	0.09940
20 - 30	75	0.01607
30 - 40	39	0.00835
40 - 50	17	0.00364
50 - 60	12	0.00257
60 – 70	7	0.00150
70 – 80	5	0.00107
80 – 90	3	0.00064
90 - 100	1	0.00021
> 100	3	0.00064

It is noted that approximately 86.6% of all daytime meteorological cases resulted in LATRA3D maximum peak instantaneous ground level HCl concentrations of less than 10 ppm. Approximately 10.0% of the daytime meteorological cases resulted in in LATRA3D maximum peak instantaneous ground level HCl concentrations in the 10 to 20 ppm range. Approximately 0.7% of the cases produced HCl ground concentration predictions above 50 ppm.

The LATRA3D predicted cloud transport directions for the T+20 conflagration HCl dispersion were aggregated into bins representing 45-degree arc corridors around the compass (i.e. N, NE, E, SE, S, SW, W, NW). The transport direction for conflagration modes is defined relative to the center of the propellant impact debris field. Table 6-68 indicates the predicted Castor 1200 T+20 conflagration plume direction probability of occurrence for the direction to the maximum concentration point. The table is based on 4668 daytime balloon sounding cases that produced non-zero predicted ground level HCl concentrations. Estimation of plume direction using LATRA3D peak concentration for conflagration scenarios should be considered as a rough

approximation only. The plume transport directions derived from the computed direction to the endpoint of the 1-ppm hazard zone listed in Table 6-69 provide a better estimate of expected plume transport directions over the ensemble of weather cases. It is noted that for the daytime launch scenarios transport of the conflagration exhaust plume to the North and Northeast is favored. Transport to the East and Southeast are least favored.

Table 6-68. LATRA3D Predicted Exhaust Cloud Transport Directions for Daytime Castor 1200 T+20 Conflagration HCl Scenarios.

Plume Transport Direction Bin	Count	Probability
337.5 – 22.5 (N)	745	0.15960
22.5 – 67.5 (NE)	484	0.10368
67.5 – 112.5 (E)	256	0.05484
112.5 – 157.5 (SE)	303	0.06491
157.5 – 202.5 (S)	290	0.06213
202.5 – 247.5 (SW)	654	0.14010
247.5 – 292.5 (W)	642	0.13753
292.5 – 337.5 (NW)	1294	0.27721

Table 6-69. LATRA3D Predicted Exhaust Cloud Transport Directions for Daytime Castor 1200 T+20 Conflagration HCl Scenarios Using the 1-ppm Hazard Zone Endpoint.

Plume Transport Direction Bin	Count	Probability
337.5 – 22.5 (N)	691	0.19302
22.5 – 67.5 (NE)	678	0.18939
67.5 – 112.5 (E)	304	0.08492
112.5 – 157.5 (SE)	292	0.08156
157.5 – 202.5 (S)	283	0.07905
202.5 – 247.5 (SW)	315	0.08799
247.5 – 292.5 (W)	455	0.12709
292.5 – 337.5 (NW)	562	0.15698

Similar summary tables for the 1749 nighttime Castor 1200 T+20 conflagration simulations were compiled. Table 6-70Table 6-40 shows the peak HCl instantaneous concentration predictions for nighttime conditions. It is noted that approximately 86% of all nighttime meteorological cases resulted in LATRA3D maximum peak instantaneous ground level HCl concentrations of less than 10 ppm. Approximately 9.7% of the nighttime meteorological cases resulted in in LATRA3D

maximum peak instantaneous ground level HCl concentrations in the 10 to 20 ppm range. Approximately 0.5% of the cases produced HCl ground concentration predictions above 50 ppm.

Table 6-70. LATRA3D Predicted Maximum Far Field Ground Level HCl Concentrations for Nighttime Castor 1200 T+20 Conflagration Scenarios.

Concentration Bin	Count	Probability
0 - 2	585	0.33448
2- 4	413	0.23613
4 - 6	235	0.13436
6 - 8	169	0.09663
8 - 10	103	0.05889
10 - 20	169	0.09663
20 - 30	38	0.02173
30 - 40	20	0.01144
40 - 50	9	0.00515
50 - 60	0	0.00000
60 – 70	1	0.00057
70 – 80	4	0.00229
80 – 90	0	0.00000
90 - 100	2	0.00114
> 100	1	0.00057

Table 6-71 indicates the predicted Castor 1200 vehicle T+20 conflagration plume direction probability of occurrence observed across the 1749 nighttime balloon sounding cases based on the direct to the maximum concentration point. The plume transport directions derived from the computed direction to the endpoint of the 1-ppm hazard zone listed in Table 6-72 provide a better estimate of expected plume transport directions over the ensemble of weather cases. It is noted that for the nighttime launch scenarios transport of the conflagration exhaust plume to the Northeast is favored. There is approximately equal probability for transport of the conflagration plumes in the other directions.

Table 6-71. REEDM Predicted Exhaust Cloud Transport Directions for Nighttime Castor 1200 T+20 Conflagration Scenarios.

Plume Transport Direction Bin	Count	Probability
337.5 – 22.5 (N)	190	0.10863
22.5 – 67.5 (NE)	191	0.10921
67.5 – 112.5 (E)	91	0.05203
112.5 – 157.5 (SE)	153	0.08748
157.5 – 202.5 (S)	124	0.07090
202.5 – 247.5 (SW)	306	0.17496
247.5 – 292.5 (W)	243	0.13894
292.5 – 337.5 (NW)	451	0.25786

Table 6-72. LATRA3D Predicted Exhaust Cloud Transport Directions for Daytime Castor 1200 T+20 Conflagration HCl Scenarios Using the 1-ppm Hazard Zone Endpoint.

Plume Transport Direction Bin	Count	Probability
337.5 – 22.5 (N)	172	0.11301
22.5 – 67.5 (NE)	274	0.18003
67.5 – 112.5 (E)	182	0.11958
112.5 – 157.5 (SE)	189	0.12418
157.5 – 202.5 (S)	164	0.10775
202.5 – 247.5 (SW)	191	0.12549
247.5 – 292.5 (W)	179	0.11761
292.5 – 337.5 (NW)	171	0.11235

6.4.7 T+0 Conflagration Al_2O_3 Results

REEDM was used to estimate the aluminum oxide dispersion because it includes settling velocity deposition algorithms for airborne transport of particulates that LATRA3D does not contain.

Table 6-73 presents the maximum far field Al_2O_3 peak instantaneous concentration predicted by REEDM for the hypothetical daytime launches of a Castor 1200 vehicle with subsequent dispersion of the aluminum oxide particulates in the T-0 conflagration cloud. The far field exposure is REEDM's prediction for concentrations at ground level downwind from the stabilized exhaust cloud. Far field peak Al_2O_3 PM_{10} concentrations for daytime weather cases ranged from 5 to 16 mg/m^3 with the maximum concentration predicted to occur from 7000 to 15000 meters downwind from the launch site. Respirable dust is primarily under 5 microns in size. The default mass distribution among particle size categories used in the REEDM analysis places about 70% of the dispersed Al_2O_3 mass in the particle size bins 5 microns and less. The table values represent the maximum concentrations predicted over a sample set of 4679 WFF balloon soundings.

Table 6-74 shows the REEDM predicted maximum peak Al_2O_3 far field concentrations for 1751 nighttime cases for Castor 1200 vehicle T-0 conflagration scenarios Far field peak Al_2O_3 PM_{10} concentrations for nighttime weather cases ranged from 5 to 18 mg/m^3 with the maximum concentration predicted to occur from 7000 to 18000 meters downwind from the launch site.

Table 6-73: Castor 1200 T-0 Conflagration Al_2O_3 Peak Concentration Summary – Daytime Meteorology.

Month	Number of Weather Cases	Peak Al_2O_3 PM_{10} Concentration [mg/m^3]	Peak Al_2O_3 PM_5 Respirable Dust Concentration [mg/m^3]	Distance to Peak Al_2O_3 Concentration [m]	Bearing to Peak Al_2O_3 Concentration [deg]
January	341	1.26E+01	8.8	12000	10
February	363	1.51E+01	10.6	8000	30
March	393	1.64E+01	11.5	7000	32
April	382	1.36E+01	9.5	13000	9
May	398	1.10E+01	7.7	9000	15
June	391	6.64E+00	4.6	15000	83
July	417	6.70E+00	4.7	10000	76
August	410	4.84E+00	3.4	15000	25
September	412	7.20E+00	5.0	9000	241
October	429	6.29E+00	4.4	14000	196
November	376	1.23E+01	8.6	8000	92
December	367	1.34E+01	9.4	9000	107

Table 6-74: Castor 1200 T-0 Conflagration Al_2O_3 Peak Concentration Summary – Nighttime Meteorology.

Month	Number of Weather Cases	Peak Al_2O_3 PM_{10} Concentration [mg/m^3]	Peak Al_2O_3 PM_5 Respirable Dust Concentration [mg/m^3]	Distance to Peak Al_2O_3 Concentration [m]	Bearing to Peak Al_2O_3 Concentration [deg]
January	95	1.36E+01	9.5	8000	73
February	158	1.38E+01	9.7	15000	51
March	165	1.38E+01	9.7	12000	28
April	158	1.77E+01	12.4	7000	52
May	159	9.68E+00	6.8	13000	32
June	153	5.74E+00	4.0	8000	108
July	153	5.86E+00	4.1	17000	48
August	162	5.44E+00	3.8	11000	79
September	163	6.23E+00	4.4	17000	71
October	125	7.97E+00	5.6	17000	119
November	129	1.00E+01	7.0	18000	55
December	131	1.67E+01	11.7	10000	36

The REEDM predicted Al_2O_3 concentrations for all daytime meteorological cases processed in the 8-year sample set was aggregated into bins to evaluate the peak far field concentration probability. This information is provided in Table 6-75.

Table 6-75. REEDM Predicted Maximum Far Field Ground Level Al_2O_3 PM_{10} Concentrations for Daytime Castor 1200 T-0 Conflagration Scenarios.

Concentration Bin	Count	Probability
0 - 1	2467	0.52725
1 - 2	1099	0.23488
2 - 3	499	0.10665
3 - 4	225	0.04809
4 - 5	148	0.03163
5 - 6	73	0.01560
6 - 7	54	0.01154
7 - 8	35	0.00748
8 - 9	31	0.00663
9 - 10	12	0.00256
> 10	36	0.00769

It is noted that approximately 52.7% of all daytime meteorological cases resulted in REEDM maximum peak instantaneous ground level Al_2O_3 PM_{10} concentrations of less than 1 mg/m^3. Approximately 2.4% of all daytime meteorological cases resulted in REEDM maximum peak instantaneous ground level Al_2O_3 PM_5 (respirable dust) concentrations of 5 mg/m^3 or higher.

The REEDM predicted cloud transport directions for the T-0 conflagration Al_2O_3 dispersion were also aggregated into bins representing 45-degree arc corridors around the compass (i.e. N, NE, E, SE, S, SW, W, NW). Table 6-76 indicates the predicted Castor 1200 T-0 conflagration plume direction probability of occurrence observed across the 4679 daytime balloon sounding cases that produced non-zero predicted ground level Al_2O_3 concentrations. It is noted that for the daytime T-0 conflagration scenarios transport of the exhaust plume to the Northeast, East and Southeast are favored. This would tend to carry the particulate cloud in an offshore direction for the launch pads located on the WFF barrier island on the Atlantic coastline of Virginia.

Table 6-76. REEDM Predicted Exhaust Cloud Transport Directions for Daytime Castor 1200 T-0 Conflagration Al_2O_3 Scenarios.

Plume Transport Direction Bin	Count	Probability
337.5 – 22.5 (N)	535	0.11434
22.5 – 67.5 (NE)	890	0.19021
67.5 – 112.5 (E)	812	0.17354
112.5 – 157.5 (SE)	948	0.20261
157.5 – 202.5 (S)	517	0.11049
202.5 – 247.5 (SW)	436	0.09318
247.5 – 292.5 (W)	309	0.06604
292.5 – 337.5 (NW)	232	0.04958

Similar summary tables for the 1751 nighttime Castor 1200 T-0 conflagration simulations were compiled. Table 6-77 shows the Al_2O_3 PM_{10} concentration histogram results. Approximately 43.7% of all nighttime meteorological cases resulted in REEDM maximum peak instantaneous ground level Al_2O_3 PM_{10} concentrations of less than 1 mg/m^3. Approximately 3.9% of all nighttime meteorological cases resulted in REEDM maximum peak instantaneous ground level Al_2O_3 PM_5 (respirable dust) concentrations of 5 mg/m^3 or higher.

Table 6-77. REEDM Predicted Maximum Far Field Ground Level Al_2O_3 PM_{10} Concentrations for Nighttime Castor 1200 T-0 Conflagration Scenarios.

Concentration Bin	Count	Probability
0 - 1	765	0.43689
1 - 2	397	0.22673
2 - 3	253	0.14449
3 - 4	132	0.07539
4 - 5	63	0.03598
5 - 6	53	0.03027
6 - 7	20	0.01142
7 - 8	27	0.01542
8 - 9	16	0.00914
9 - 10	8	0.00457
> 10	17	0.00971

Table 6-78 indicates the predicted Castor 1200 vehicle T-0 conflagration plume direction probability of occurrence observed across the 1751 nighttime balloon sounding cases that produced non-zero predicted ground level Al_2O_3 concentrations. It is noted that for nighttime T-0 conflagration scenarios transport of the exhaust plume to the Northeast, East and Southeast are favored as they were during the daytime.

Table 6-78. REEDM Predicted Exhaust Cloud Transport Directions for Nighttime Castor 1200 T-0 Conflagration Scenarios.

Plume Transport Direction Bin	Count	Probability
337.5 – 22.5 (N)	123	0.07025
22.5 – 67.5 (NE)	309	0.17647
67.5 – 112.5 (E)	333	0.19018
112.5 – 157.5 (SE)	370	0.21131
157.5 – 202.5 (S)	238	0.13592
202.5 – 247.5 (SW)	196	0.11194
247.5 – 292.5 (W)	96	0.05483
292.5 – 337.5 (NW)	86	0.04911

6.4.8 T+4 Conflagration Al_2O_3 Results

REEDM was used to estimate the aluminum oxide dispersion because it includes settling velocity deposition algorithms for airborne transport of particulates that LATRA3D does not contain.

Table 6-79 presents the maximum far field Al_2O_3 peak instantaneous concentration predicted by REEDM for the hypothetical daytime launches of a Castor 1200 vehicle with subsequent dispersion of the aluminum oxide particulates in the T+4 conflagration cloud. The far field exposure is REEDM's prediction for concentrations at ground level downwind from the stabilized exhaust cloud. Far field peak Al_2O_3 PM_{10} concentrations for daytime weather cases ranged from 7 to 30 mg/m^3 with the maximum concentration predicted to occur from 5000 to 13000 meters downwind from the launch site. Respirable dust is primarily under 5 microns in size. The default mass distribution among particle size categories used in the REEDM analysis places about 70% of the dispersed Al_2O_3 mass in the particle size bins 5 microns and less. The table values represent the maximum concentrations predicted over a sample set of 4679 WFF balloon soundings. Table 6-80 shows the REEDM predicted maximum peak Al_2O_3 far field concentrations for 1751 nighttime cases for Castor 1200 vehicle T+4 conflagration scenarios. Far field peak Al_2O_3 PM_{10} concentrations for nighttime weather cases ranged from 7 to 28 mg/m^3 with the maximum concentration predicted to occur from 5000 to 18000 meters downwind from the launch site.

Table 6-79: Castor 1200 T+4 Conflagration Al_2O_3 Peak Concentration Summary – Daytime Meteorology.

Month	Number of Weather Cases	Peak Al_2O_3 PM_{10} Concentration [mg/m^3]	Peak Al_2O_3 PM_5 Respirable Dust Concentration [mg/m^3]	Distance to Peak Al_2O_3 Concentration [m]	Bearing to Peak Al_2O_3 Concentration [deg]
January	341	2.16E+01	15.1	9000	10
February	363	2.75E+01	19.3	5000	29
March	393	2.99E+01	20.9	5000	30
April	382	2.28E+01	16.0	9000	8
May	398	1.82E+01	12.7	11000	29
June	391	1.01E+01	7.1	8000	19
July	417	9.73E+00	6.8	13000	40
August	410	6.75E+00	4.7	13000	25
September	412	1.09E+01	7.6	7000	241
October	429	1.10E+01	7.7	7000	59
November	376	2.13E+01	14.9	6000	93
December	367	2.09E+01	14.6	6000	17

Table 6-80: Castor 1200 T+4 Conflagration Al_2O_3 Peak Concentration Summary – Nighttime Meteorology.

Month	Number of Weather Cases	Peak Al_2O_3 PM_{10} Concentration [mg/m^3]	Peak Al_2O_3 PM_5 Respirable Dust Concentration [mg/m^3]	Distance to Peak Al_2O_3 Concentration [m]	Bearing to Peak Al_2O_3 Concentration [deg]
January	95	2.23E+01	15.6	6000	96
February	158	2.40E+01	16.8	9000	50
March	165	1.88E+01	13.2	6000	32
April	158	2.73E+01	19.1	5000	50
May	159	1.57E+01	11.0	9000	32
June	153	8.08E+00	5.7	11000	155
July	153	8.13E+00	5.7	13000	48
August	162	6.99E+00	4.9	10000	79
September	163	1.06E+01	7.4	9000	225
October	125	1.22E+01	8.5	18000	84
November	129	1.49E+01	10.4	13000	54
December	131	2.83E+01	19.8	8000	36

The REEDM predicted Al_2O_3 concentrations for all daytime meteorological cases processed in the 8-year sample set was aggregated into bins to evaluate the peak far field concentration probability. This information is provided in Table 6-81.

Table 6-81. REEDM Predicted Maximum Far Field Ground Level Al_2O_3 PM_{10} Concentrations for Daytime Castor 1200 T+4 Conflagration Scenarios.

Concentration Bin	Count	Probability
0 - 1	2157	0.46100
1 - 2	1053	0.22505
2 - 3	539	0.11520
3 - 4	279	0.05963
4 - 5	176	0.03761
5 - 6	105	0.02244
6 - 7	78	0.01667
7 - 8	49	0.01047
8 - 9	53	0.01133
9 - 10	44	0.00940
> 10	146	0.03120

It is noted that approximately 46.1% of all daytime meteorological cases resulted in REEDM maximum peak instantaneous ground level Al_2O_3 PM_{10} concentrations of less than 1 mg/m^3. Approximately 6.2% of all daytime meteorological cases resulted in REEDM maximum peak instantaneous ground level Al_2O_3 PM_5 (respirable dust) concentrations of 5 mg/m^3 or higher.

The REEDM predicted cloud transport directions for the T+4 conflagration Al_2O_3 dispersion were also aggregated into bins representing 45-degree arc corridors around the compass (i.e. N, NE, E, SE, S, SW, W, NW). Table 6-82 indicates the predicted Castor 1200 T+4 conflagration plume direction probability of occurrence observed across the 4679 daytime balloon sounding cases that produced non-zero predicted ground level Al_2O_3 concentrations. It is noted that for the daytime T+4 conflagration scenarios transport of the exhaust plume to the Northeast, East and Southeast are favored. This would tend to carry the particulate cloud in an offshore direction for the launch pads located on the WFF barrier island on the Atlantic coastline of Virginia.

Table 6-82. REEDM Predicted Exhaust Cloud Transport Directions for Daytime Castor 1200 T+4 Conflagration Al_2O_3 Scenarios.

Plume Transport Direction Bin	Count	Probability
337.5 – 22.5 (N)	543	0.11605
22.5 – 67.5 (NE)	873	0.18658
67.5 – 112.5 (E)	800	0.17098
112.5 – 157.5 (SE)	971	0.20752
157.5 – 202.5 (S)	519	0.11092
202.5 – 247.5 (SW)	434	0.09275
247.5 – 292.5 (W)	302	0.06454
292.5 – 337.5 (NW)	237	0.05065

Similar summary tables for the 1751 nighttime Castor 1200 T+4 conflagration simulations were compiled. Table 6-83 shows the Al_2O_3 PM_{10} concentration histogram results. Approximately 38% of all nighttime meteorological cases resulted in REEDM maximum peak instantaneous ground level Al_2O_3 PM_{10} concentrations of less than 1 mg/m^3. Approximately 8.2% of all nighttime meteorological cases resulted in REEDM maximum peak instantaneous ground level Al_2O_3 PM_5 (respirable dust) concentrations of 5 mg/m^3 or higher.

Table 6-83. REEDM Predicted Maximum Far Field Ground Level Al_2O_3 PM_{10} Concentrations for Nighttime Castor 1200 T+4 Conflagration Scenarios.

Concentration Bin	Count	Probability
0 - 1	666	0.38035
1 - 2	331	0.18903
2 - 3	252	0.14392
3 - 4	153	0.08738
4 - 5	98	0.05597
5 - 6	51	0.02913
6 - 7	56	0.03198
7 - 8	32	0.01828
8 - 9	19	0.01085
9 - 10	13	0.00742
> 10	80	0.04569

Table 6-84 indicates the predicted Castor 1200 vehicle T+4 conflagration plume direction probability of occurrence observed across the 1751 nighttime balloon sounding cases that produced non-zero predicted ground level Al_2O_3 concentrations. It is noted that for nighttime T+4 conflagration scenarios transport of the exhaust plume to the Northeast, East and Southeast are favored as they were during the daytime.

Table 6-84. REEDM Predicted Exhaust Cloud Transport Directions for Nighttime Castor 1200 T+4 Conflagration Scenarios.

Plume Transport Direction Bin	Count	Probability
337.5 – 22.5 (N)	118	0.06739
22.5 – 67.5 (NE)	317	0.18104
67.5 – 112.5 (E)	324	0.18504
112.5 – 157.5 (SE)	365	0.20845
157.5 – 202.5 (S)	248	0.14163
202.5 – 247.5 (SW)	200	0.11422
247.5 – 292.5 (W)	94	0.05368
292.5 – 337.5 (NW)	85	0.04854

6.4.9 T+8 Conflagration Al_2O_3 Results

REEDM was used to estimate the aluminum oxide dispersion because it includes settling velocity deposition algorithms for airborne transport of particulates that LATRA3D does not contain.

Table 6-85 presents the maximum far field Al_2O_3 peak instantaneous concentration predicted by REEDM for the hypothetical daytime launches of a Castor 1200 vehicle with subsequent dispersion of the aluminum oxide particulates in the T+8 conflagration cloud. The far field exposure is REEDM's prediction for concentrations at ground level downwind from the stabilized exhaust cloud. Far field peak Al_2O_3 PM_{10} concentrations for daytime weather cases ranged from 17 to 423 mg/m^3 with the maximum concentration predicted to occur from 1000 to 7000 meters downwind from the launch site. Respirable dust is primarily under 5 microns in size. The default mass distribution among particle size categories used in the REEDM analysis places about 70% of the dispersed Al_2O_3 mass in the particle size bins 5 microns and less. The table values represent the maximum concentrations predicted over a sample set of 4679 WFF balloon soundings. Table 6-86 shows the REEDM predicted maximum peak Al_2O_3 far field concentrations for 1751 nighttime cases for Castor 1200 vehicle T+8 conflagration scenarios. Far field peak Al_2O_3 PM_{10} concentrations for nighttime weather cases ranged from 15 to 84 mg/m^3 with the maximum concentration predicted to occur from 3000 to 8000 meters downwind from the launch site.

Table 6-85: Castor 1200 T+8 Conflagration Al_2O_3 Peak Concentration Summary – Daytime Meteorology.

Month	Number of Weather Cases	Peak Al_2O_3 PM_{10} Concentration [mg/m^3]	Peak Al_2O_3 PM_5 Respirable Dust Concentration [mg/m^3]	Distance to Peak Al_2O_3 Concentration [m]	Bearing to Peak Al_2O_3 Concentration [deg]
January	341	6.97E+01	48.8	4000	214
February	363	9.64E+01	67.5	3000	26
March	393	2.29E+02	160.3	2000	26
April	382	9.05E+01	63.4	3000	16
May	398	7.26E+01	50.8	3000	38
June	391	2.32E+01	16.2	5000	71
July	417	3.19E+01	22.3	7000	38
August	410	1.66E+01	11.6	5000	63
September	412	1.70E+02	119.0	2000	242
October	429	4.23E+02	296.1	1000	17
November	376	4.52E+01	31.6	4000	94
December	367	6.05E+01	42.4	3000	5

Table 6-86: Castor 1200 T+8 Conflagration Al_2O_3 Peak Concentration Summary – Nighttime Meteorology.

Month	Number of Weather Cases	Peak Al_2O_3 PM_{10} Concentration [mg/m^3]	Peak Al_2O_3 PM_5 Respirable Dust Concentration [mg/m^3]	Distance to Peak Al_2O_3 Concentration [m]	Bearing to Peak Al_2O_3 Concentration [deg]
January	95	5.84E+01	40.9	4000	9
February	158	8.35E+01	58.5	3000	24
March	165	6.91E+01	48.4	3000	41
April	158	4.83E+01	33.8	3000	47
May	159	4.34E+01	30.4	5000	31
June	153	2.20E+01	15.4	8000	83
July	153	2.06E+01	14.4	8000	46
August	162	1.45E+01	10.2	6000	206
September	163	2.84E+01	19.9	4000	205
October	125	4.16E+01	29.1	7000	83
November	129	3.52E+01	24.6	7000	31
December	131	6.84E+01	47.9	4000	30

The REEDM predicted Al_2O_3 concentrations for all daytime meteorological cases processed in the 8-year sample set was aggregated into bins to evaluate the peak far field concentration probability. This information is provided in Table 6-87.

Table 6-87. REEDM Predicted Maximum Far Field Ground Level Al_2O_3 PM_{10} Concentrations for Daytime Castor 1200 T+8 Conflagration Scenarios.

Concentration Bin	Count	Probability
0 - 1	1522	0.32528
1 - 2	834	0.17824
2 - 3	515	0.11007
3 - 4	342	0.07309
4 - 5	251	0.05364
5 - 6	192	0.04103
6 - 7	131	0.02800
7 - 8	98	0.02094
8 - 9	82	0.01753
9 - 10	69	0.01475
> 10	643	0.13742

It is noted that approximately 32.5% of all daytime meteorological cases resulted in REEDM maximum peak instantaneous ground level Al_2O_3 PM_{10} concentrations of less than 1 mg/m^3. Approximately 19.1% of all daytime meteorological cases resulted in REEDM maximum peak instantaneous ground level Al_2O_3 PM_5 (respirable dust) concentrations of 5 mg/m^3 or higher.

The REEDM predicted cloud transport directions for the T+8 conflagration Al_2O_3 dispersion were also aggregated into bins representing 45-degree arc corridors around the compass (i.e. N, NE, E, SE, S, SW, W, NW). Table 6-88 indicates the predicted Castor 1200 T+8 conflagration plume direction probability of occurrence observed across the 4679 daytime balloon sounding cases that produced non-zero predicted ground level Al_2O_3 concentrations. It is noted that for the daytime T+8 conflagration scenarios transport of the exhaust plume to the Northeast, East and Southeast are favored. This would tend to carry the particulate cloud in an offshore direction for the launch pads located on the WFF barrier island on the Atlantic coastline of Virginia.

Table 6-88. REEDM Predicted Exhaust Cloud Transport Directions for Daytime Castor 1200 T+8 Conflagration Al_2O_3 Scenarios.

Plume Transport Direction Bin	Count	Probability
337.5 – 22.5 (N)	555	0.11862
22.5 – 67.5 (NE)	871	0.18615
67.5 – 112.5 (E)	734	0.15687
112.5 – 157.5 (SE)	974	0.20816
157.5 – 202.5 (S)	524	0.11199
202.5 – 247.5 (SW)	473	0.10109
247.5 – 292.5 (W)	305	0.06518
292.5 – 337.5 (NW)	243	0.05193

Similar summary tables for the 1751 nighttime Castor 1200 T+8 conflagration simulations were compiled. Table 6-89 shows the Al_2O_3 PM_{10} concentration histogram results. Approximately 23.5% of all nighttime meteorological cases resulted in REEDM maximum peak instantaneous ground level Al_2O_3 PM_{10} concentrations of less than 1 mg/m^3. Approximately 27.7% of all nighttime meteorological cases resulted in REEDM maximum peak instantaneous ground level Al_2O_3 PM_5 (respirable dust) concentrations of 5 mg/m^3 or higher.

Table 6-89. REEDM Predicted Maximum Far Field Ground Level Al_2O_3 PM_{10} Concentrations for Nighttime Castor 1200 T+8 Conflagration Scenarios.

Concentration Bin	Count	Probability
0 - 1	412	0.23529
1 - 2	242	0.13821
2 - 3	191	0.10908
3 - 4	121	0.06910
4 - 5	144	0.08224
5 - 6	92	0.05254
6 - 7	63	0.03598
7 - 8	67	0.03826
8 - 9	43	0.02456
9 - 10	35	0.01999
> 10	341	0.19475

Table 6-90 indicates the predicted Castor 1200 vehicle T+8 conflagration plume direction probability of occurrence observed across the 1751 nighttime balloon sounding cases that produced non-zero predicted ground level Al_2O_3 concentrations. It is noted that for nighttime T+8 conflagration scenarios transport of the exhaust plume to the Northeast, East and Southeast are favored as they were during the daytime.

Table 6-90. REEDM Predicted Exhaust Cloud Transport Directions for Nighttime Castor 1200 T+8 Conflagration Scenarios.

Plume Transport Direction Bin	Count	Probability
337.5 – 22.5 (N)	129	0.07367
22.5 – 67.5 (NE)	317	0.18104
67.5 – 112.5 (E)	304	0.17362
112.5 – 157.5 (SE)	359	0.20503
157.5 – 202.5 (S)	231	0.13192
202.5 – 247.5 (SW)	225	0.12850
247.5 – 292.5 (W)	101	0.05768
292.5 – 337.5 (NW)	85	0.04854

6.4.10 T+12 Conflagration Al_2O_3 Results

REEDM was used to estimate the aluminum oxide dispersion because it includes settling velocity deposition algorithms for airborne transport of particulates that LATRA3D does not contain.

Table 6-91 presents the maximum far field Al_2O_3 peak instantaneous concentration predicted by REEDM for the hypothetical daytime launches of a Castor 1200 vehicle with subsequent dispersion of the aluminum oxide particulates in the T+12 conflagration cloud. The far field exposure is REEDM's prediction for concentrations at ground level downwind from the stabilized exhaust cloud. Far field peak Al_2O_3 PM_{10} concentrations for daytime weather cases ranged from 33 to 1000 mg/m^3 with the maximum concentration predicted to occur from 1000 to 4000 meters downwind from the launch site. Respirable dust is primarily under 5 microns in size. The default mass distribution among particle size categories used in the REEDM analysis places about 70% of the dispersed Al_2O_3 mass in the particle size bins 5 microns and less. The table values represent the maximum concentrations predicted over a sample set of 4679 WFF balloon soundings. Table 6-92 shows the REEDM predicted maximum peak Al_2O_3 far field concentrations for 1751 nighttime cases for Castor 1200 vehicle T+12 conflagration scenarios. Far field peak Al_2O_3 PM_{10} concentrations for nighttime weather cases ranged from 42 to 249 mg/m^3 with the maximum concentration predicted to occur from 2000 to 5000 meters downwind from the launch site.

Table 6-91: Castor 1200 T+12 Conflagration Al_2O_3 Peak Concentration Summary – Daytime Meteorology.

Month	Number of Weather Cases	Peak Al_2O_3 PM_{10} Concentration [mg/m^3]	Peak Al_2O_3 PM_5 Respirable Dust Concentration [mg/m^3]	Distance to Peak Al_2O_3 Concentration [m]	Bearing to Peak Al_2O_3 Concentration [deg]
January	341	3.04E+02	212.8	2000	17
February	363	1.61E+02	112.7	2000	32
March	393	2.78E+02	194.6	1000	24
April	382	2.14E+02	149.8	2000	35
May	398	1.88E+02	131.6	2000	43
June	391	8.68E+01	60.8	3000	13
July	417	6.56E+01	45.9	3000	23
August	410	3.26E+01	22.8	4000	34
September	412	1.82E+02	127.4	3000	242
October	429	1.01E+03	707.0	1000	15
November	376	1.37E+02	95.9	2000	132
December	367	1.58E+02	110.6	2000	27

Table 6-92: Castor 1200 T+12 Conflagration Al_2O_3 Peak Concentration Summary – Nighttime Meteorology.

Month	Number of Weather Cases	Peak Al_2O_3 PM_{10} Concentration [mg/m^3]	Peak Al_2O_3 PM_5 Respirable Dust Concentration [mg/m^3]	Distance to Peak Al_2O_3 Concentration [m]	Bearing to Peak Al_2O_3 Concentration [deg]
January	95	1.08E+02	75.6	5000	72
February	158	2.47E+02	172.9	2000	106
March	165	1.64E+02	114.8	2000	104
April	158	1.28E+02	89.6	3000	54
May	159	1.05E+02	73.5	2000	94
June	153	5.39E+01	37.7	3000	181
July	153	4.23E+01	29.6	4000	102
August	162	5.54E+01	38.8	3000	235
September	163	8.08E+01	56.6	2000	216
October	125	7.77E+01	54.4	3000	84
November	129	1.11E+02	77.7	3000	166
December	131	2.49E+02	174.3	3000	25

The REEDM predicted Al_2O_3 concentrations for all daytime meteorological cases processed in the 8-year sample set was aggregated into bins to evaluate the peak far field concentration probability. This information is provided in Table 6-93.

Table 6-93. REEDM Predicted Maximum Far Field Ground Level Al_2O_3 PM_{10} Concentrations for Daytime Castor 1200 T+12 Conflagration Scenarios.

Concentration Bin	Count	Probability
0 - 1	1038	0.22184
1 - 2	677	0.14469
2 - 3	426	0.09105
3 - 4	293	0.06262
4 - 5	214	0.04574
5 - 6	170	0.03633
6 - 7	164	0.03505
7 - 8	143	0.03056
8 - 9	119	0.02543
9 - 10	108	0.02308
> 10	1327	0.28361

It is noted that approximately 22.2% of all daytime meteorological cases resulted in REEDM maximum peak instantaneous ground level Al_2O_3 PM_{10} concentrations of less than 1 mg/m^3. Approximately 36.3% of all daytime meteorological cases resulted in REEDM maximum peak instantaneous ground level Al_2O_3 PM_5 (respirable dust) concentrations of 5 mg/m^3 or higher.

The REEDM predicted cloud transport directions for the T+12 conflagration Al_2O_3 dispersion were also aggregated into bins representing 45-degree arc corridors around the compass (i.e. N, NE, E, SE, S, SW, W, NW). Table 6-94 indicates the predicted Castor 1200 T+12 conflagration plume direction probability of occurrence observed across the 4679 daytime balloon sounding cases that produced non-zero predicted ground level Al_2O_3 concentrations. It is noted that for the daytime T+12 conflagration scenarios transport of the exhaust plume to the Northeast, East and Southeast are favored. This would tend to carry the particulate cloud in an offshore direction for the launch pads located on the WFF barrier island on the Atlantic coastline of Virginia.

Table 6-94. REEDM Predicted Exhaust Cloud Transport Directions for Daytime Castor 1200 T+12 Conflagration Al_2O_3 Scenarios.

Plume Transport Direction Bin	Count	Probability
337.5 – 22.5 (N)	620	0.13251
22.5 – 67.5 (NE)	857	0.18316
67.5 – 112.5 (E)	666	0.14234
112.5 – 157.5 (SE)	954	0.20389
157.5 – 202.5 (S)	527	0.11263
202.5 – 247.5 (SW)	492	0.10515
247.5 – 292.5 (W)	323	0.06903
292.5 – 337.5 (NW)	240	0.05129

Similar summary tables for the 1751 nighttime Castor 1200 T+12 conflagration simulations were compiled. Table 6-95 shows the Al_2O_3 PM_{10} concentration histogram results. Approximately 14.4% of all nighttime meteorological cases resulted in REEDM maximum peak instantaneous ground level Al_2O_3 PM_{10} concentrations of less than 1 mg/m^3. Approximately 50.8% of all nighttime meteorological cases resulted in REEDM maximum peak instantaneous ground level Al_2O_3 PM_5 (respirable dust) concentrations of 5 mg/m^3 or higher.

Table 6-95. REEDM Predicted Maximum Far Field Ground Level Al_2O_3 PM_{10} Concentrations for Nighttime Castor 1200 T+12 Conflagration Scenarios.

Concentration Bin	Count	Probability
0 - 1	252	0.14392
1 - 2	159	0.09081
2 - 3	126	0.07196
3 - 4	105	0.05997
4 - 5	84	0.04797
5 - 6	73	0.04169
6 - 7	62	0.03541
7 - 8	67	0.03826
8 - 9	51	0.02913
9 - 10	46	0.02627
> 10	726	0.41462

Table 6-96 indicates the predicted Castor 1200 vehicle T+12 conflagration plume direction probability of occurrence observed across the 1751 nighttime balloon sounding cases that produced non-zero predicted ground level Al_2O_3 concentrations. It is noted that for nighttime T+12 conflagration scenarios transport of the exhaust plume to the Northeast, East and Southeast are favored as they were during the daytime.

Table 6-96. REEDM Predicted Exhaust Cloud Transport Directions for Nighttime Castor 1200 T+12 Conflagration Scenarios.

Plume Transport Direction Bin	Count	Probability
337.5 – 22.5 (N)	129	0.07367
22.5 – 67.5 (NE)	341	0.19475
67.5 – 112.5 (E)	269	0.15363
112.5 – 157.5 (SE)	339	0.19360
157.5 – 202.5 (S)	242	0.13821
202.5 – 247.5 (SW)	244	0.13935
247.5 – 292.5 (W)	101	0.05768
292.5 – 337.5 (NW)	86	0.04911

6.4.11 T+16 Conflagration Al_2O_3 Results

REEDM was used to estimate the aluminum oxide dispersion because it includes settling velocity deposition algorithms for airborne transport of particulates that LATRA3D does not contain.

Table 6-97 presents the maximum far field Al_2O_3 peak instantaneous concentration predicted by REEDM for the hypothetical daytime launches of a Castor 1200 vehicle with subsequent dispersion of the aluminum oxide particulates in the T+16 conflagration cloud. The far field exposure is REEDM's prediction for concentrations at ground level downwind from the stabilized exhaust cloud. Far field peak Al_2O_3 PM_{10} concentrations for daytime weather cases ranged from 64 to 765 mg/m^3 with the maximum concentration predicted to occur from 1000 to 3000 meters downwind from the launch site. Respirable dust is primarily under 5 microns in size. The default mass distribution among particle size categories used in the REEDM analysis places about 70% of the dispersed Al_2O_3 mass in the particle size bins 5 microns and less. The table values represent the maximum concentrations predicted over a sample set of 4679 WFF balloon soundings. Table 6-98 shows the REEDM predicted maximum peak Al_2O_3 far field concentrations for 1751 nighttime cases for Castor 1200 vehicle T+16 conflagration scenarios. Far field peak Al_2O_3 PM_{10} concentrations for nighttime weather cases ranged from 55 to 380 mg/m^3 with the maximum concentration predicted to occur from 1000 to 3000 meters downwind from the launch site.

Table 6-97: Castor 1200 T+16 Conflagration Al_2O_3 Peak Concentration Summary – Daytime Meteorology.

Month	Number of Weather Cases	Peak Al_2O_3 PM_{10} Concentration [mg/m^3]	Peak Al_2O_3 PM_5 Respirable Dust Concentration [mg/m^3]	Distance to Peak Al_2O_3 Concentration [m]	Bearing to Peak Al_2O_3 Concentration [deg]
January	341	4.83E+02	338.1	1000	28
February	363	3.11E+02	217.7	1000	12
March	393	3.48E+02	243.6	1000	54
April	382	2.95E+02	206.5	1000	31
May	398	2.58E+02	180.6	1000	21
June	391	1.24E+02	86.8	3000	114
July	417	8.68E+01	60.8	2000	220
August	410	6.42E+01	44.9	2000	146
September	412	1.77E+02	123.9	3000	241
October	429	7.65E+02	535.5	1000	15
November	376	1.90E+02	133.0	1000	160
December	367	1.83E+02	128.1	2000	26

Table 6-98: Castor 1200 T+16 Conflagration Al_2O_3 Peak Concentration Summary – Nighttime Meteorology.

Month	Number of Weather Cases	Peak Al_2O_3 PM_{10} Concentration [mg/m^3]	Peak Al_2O_3 PM_5 Respirable Dust Concentration [mg/m^3]	Distance to Peak Al_2O_3 Concentration [m]	Bearing to Peak Al_2O_3 Concentration [deg]
January	95	2.99E+02	209.3	2000	356
February	158	3.81E+02	266.7	2000	105
March	165	3.51E+02	245.7	2000	30
April	158	2.24E+02	156.8	1000	48
May	159	1.67E+02	116.9	2000	93
June	153	8.32E+01	58.2	2000	55
July	153	5.49E+01	38.4	3000	100
August	162	9.27E+01	64.9	2000	228
September	163	1.75E+02	122.5	2000	224
October	125	2.22E+02	155.4	2000	176
November	129	3.49E+02	244.3	2000	161
December	131	2.99E+02	209.3	2000	56

The REEDM predicted Al_2O_3 concentrations for all daytime meteorological cases processed in the 8-year sample set was aggregated into bins to evaluate the peak far field concentration probability. This information is provided in Table 6-99.

Table 6-99. REEDM Predicted Maximum Far Field Ground Level Al_2O_3 PM_{10} Concentrations for Daytime Castor 1200 T+16 Conflagration Scenarios.

Concentration Bin	Count	Probability
0 - 1	735	0.15708
1 - 2	518	0.11071
2 - 3	375	0.08015
3 - 4	253	0.05407
4 - 5	231	0.04937
5 - 6	176	0.03761
6 - 7	142	0.03035
7 - 8	116	0.02479
8 - 9	131	0.02800
9 - 10	105	0.02244
> 10	1897	0.40543

It is noted that approximately 15.7% of all daytime meteorological cases resulted in REEDM maximum peak instantaneous ground level Al_2O_3 PM_{10} concentrations of less than 1 mg/m^3. Approximately 48.1% of all daytime meteorological cases resulted in REEDM maximum peak instantaneous ground level Al_2O_3 PM_5 (respirable dust) concentrations of 5 mg/m^3 or higher.

The REEDM predicted cloud transport directions for the T+16 conflagration Al_2O_3 dispersion were also aggregated into bins representing 45-degree arc corridors around the compass (i.e. N, NE, E, SE, S, SW, W, NW). Table 6-100 indicates the predicted Castor 1200 T+16 conflagration plume direction probability of occurrence observed across the 4679 daytime balloon sounding cases that produced non-zero predicted ground level Al_2O_3 concentrations. It is noted that for the daytime T+16 conflagration scenarios transport of the exhaust plume to the Northeast and Southeast are favored. This would tend to carry the particulate cloud in an offshore direction for the launch pads located on the WFF barrier island on the Atlantic coastline of Virginia.

Table 6-100. REEDM Predicted Exhaust Cloud Transport Directions for Daytime Castor 1200 T+16 Conflagration Al_2O_3 Scenarios.

Plume Transport Direction Bin	Count	Probability
337.5 – 22.5 (N)	667	0.14255
22.5 – 67.5 (NE)	864	0.18465
67.5 – 112.5 (E)	601	0.12845
112.5 – 157.5 (SE)	929	0.19855
157.5 – 202.5 (S)	531	0.11349
202.5 – 247.5 (SW)	515	0.11007
247.5 – 292.5 (W)	331	0.07074
292.5 – 337.5 (NW)	241	0.05151

Similar summary tables for the 1751 nighttime Castor 1200 T+16 conflagration simulations were compiled. Table 6-101 shows the Al_2O_3 PM_{10} concentration histogram results. Approximately 9% of all nighttime meteorological cases resulted in REEDM maximum peak instantaneous ground level Al_2O_3 PM_{10} concentrations of less than 1 mg/m^3. Approximately 64.1% of all nighttime meteorological cases resulted in REEDM maximum peak instantaneous ground level Al_2O_3 PM_5 (respirable dust) concentrations of 5 mg/m^3 or higher.

Table 6-101. REEDM Predicted Maximum Far Field Ground Level Al_2O_3 PM_{10} Concentrations for Nighttime Castor 1200 T+16 Conflagration Scenarios.

Concentration Bin	Count	Probability
0 - 1	157	0.08966
1 - 2	118	0.06739
2 - 3	94	0.05368
3 - 4	71	0.04055
4 - 5	76	0.04340
5 - 6	56	0.03198
6 - 7	56	0.03198
7 - 8	54	0.03084
8 - 9	57	0.03255
9 - 10	37	0.02113
> 10	975	0.55682

Table 6-102 indicates the predicted Castor 1200 vehicle T+16 conflagration plume direction probability of occurrence observed across the 1751 nighttime balloon sounding cases that produced non-zero predicted ground level Al_2O_3 concentrations. It is noted that for nighttime T+16 conflagration scenarios transport of the exhaust plume to the Northeast and Southeast are favored.

Table 6-102. REEDM Predicted Exhaust Cloud Transport Directions for Nighttime Castor 1200 T+16 Conflagration Scenarios.

Plume Transport Direction Bin	Count	Probability
337.5 – 22.5 (N)	131	0.07481
22.5 – 67.5 (NE)	348	0.19874
67.5 – 112.5 (E)	262	0.14963
112.5 – 157.5 (SE)	328	0.18732
157.5 – 202.5 (S)	249	0.14220
202.5 – 247.5 (SW)	241	0.13764
247.5 – 292.5 (W)	108	0.06168
292.5 – 337.5 (NW)	84	0.04797

6.4.12 T+20 Conflagration Al_2O_3 Results

REEDM was used to estimate the aluminum oxide dispersion because it includes settling velocity deposition algorithms for airborne transport of particulates that LATRA3D does not contain.

Table 6-103 presents the maximum far field Al_2O_3 peak instantaneous concentration predicted by REEDM for the hypothetical daytime launches of a Castor 1200 vehicle with subsequent dispersion of the aluminum oxide particulates in the T+20 conflagration cloud. The far field exposure is REEDM's prediction for concentrations at ground level downwind from the stabilized exhaust cloud. Far field peak Al_2O_3 PM_{10} concentrations for daytime weather cases ranged from 130 to 550 mg/m^3 with the maximum concentration predicted to occur from 1000 to 7000 meters downwind from the launch site. Respirable dust is primarily under 5 microns in size. The default mass distribution among particle size categories used in the REEDM analysis places about 70% of the dispersed Al_2O_3 mass in the particle size bins 5 microns and less. The table values represent the maximum concentrations predicted over a sample set of 4679 WFF balloon soundings. Table 6-104 shows the REEDM predicted maximum peak Al_2O_3 far field concentrations for 1751 nighttime cases for Castor 1200 vehicle T+20 conflagration scenarios. Far field peak Al_2O_3 PM_{10} concentrations for nighttime weather cases ranged from 79 to 520 mg/m^3 with the maximum concentration predicted to occur from 1000 to 2000 meters downwind from the launch site.

Table 6-103: Castor 1200 T+20 Conflagration Al_2O_3 Peak Concentration Summary – Daytime Meteorology.

Month	Number of Weather Cases	Peak Al_2O_3 PM_{10} Concentration [mg/m^3]	Peak Al_2O_3 PM_5 Respirable Dust Concentration [mg/m^3]	Distance to Peak Al_2O_3 Concentration [m]	Bearing to Peak Al_2O_3 Concentration [deg]
January	341	4.79E+02	335.3	1000	10
February	363	4.54E+02	317.8	1000	8
March	393	3.39E+02	237.3	1000	53
April	382	3.51E+02	245.7	1000	30
May	398	3.31E+02	231.7	1000	19
June	391	1.51E+02	105.7	3000	114
July	417	1.31E+02	91.7	1000	216
August	410	1.55E+02	108.5	1000	145
September	412	2.45E+02	171.5	7000	242
October	429	5.46E+02	382.2	1000	298
November	376	2.77E+02	193.9	2000	99
December	367	2.44E+02	170.8	2000	71

Table 6-104: Castor 1200 T+20 Conflagration Al_2O_3 Peak Concentration Summary – Nighttime Meteorology.

Month	Number of Weather Cases	Peak Al_2O_3 PM_{10} Concentration [mg/m^3]	Peak Al_2O_3 PM_5 Respirable Dust Concentration [mg/m^3]	Distance to Peak Al_2O_3 Concentration [m]	Bearing to Peak Al_2O_3 Concentration [deg]
January	95	2.97E+02	207.9	2000	356
February	158	3.29E+02	230.3	1000	105
March	165	5.17E+02	361.9	1000	22
April	158	4.57E+02	319.9	1000	29
May	159	1.91E+02	133.7	2000	94
June	153	9.14E+01	64.0	2000	53
July	153	7.89E+01	55.2	2000	68
August	162	1.01E+02	70.7	2000	224
September	163	2.79E+02	195.3	2000	145
October	125	3.86E+02	270.2	1000	81
November	129	2.83E+02	198.1	2000	160
December	131	3.21E+02	224.7	1000	228

The REEDM predicted Al_2O_3 concentrations for all daytime meteorological cases processed in the 8-year sample set was aggregated into bins to evaluate the peak far field concentration probability. This information is provided in Table 6-105.

Table 6-105. REEDM Predicted Maximum Far Field Ground Level Al_2O_3 PM_{10} Concentrations for Daytime Castor 1200 T+20 Conflagration Scenarios.

Concentration Bin	Count	Probability
0 - 1	580	0.12401
1 - 2	421	0.09001
2 - 3	327	0.06992
3 - 4	241	0.05153
4 - 5	196	0.04191
5 - 6	171	0.03656
6 - 7	133	0.02844
7 - 8	119	0.02544
8 - 9	109	0.02331
9 - 10	110	0.02352
> 10	2270	0.48535

It is noted that approximately 12.4% of all daytime meteorological cases resulted in REEDM maximum peak instantaneous ground level Al_2O_3 PM_{10} concentrations of less than 1 mg/m^3. Approximately 55.7% of all daytime meteorological cases resulted in REEDM maximum peak instantaneous ground level Al_2O_3 PM_5 (respirable dust) concentrations of 5 mg/m^3 or higher.

The REEDM predicted cloud transport directions for the T+20 conflagration Al_2O_3 dispersion were also aggregated into bins representing 45-degree arc corridors around the compass (i.e. N, NE, E, SE, S, SW, W, NW). Table 6-106 indicates the predicted Castor 1200 T+20 conflagration plume direction probability of occurrence observed across the 4679 daytime balloon sounding cases that produced non-zero predicted ground level Al_2O_3 concentrations. It is noted that for the daytime T+20 conflagration scenarios transport of the exhaust plume to the Northeast and Southeast are favored. This would tend to carry the particulate cloud in an offshore direction for the launch pads located on the WFF barrier island on the Atlantic coastline of Virginia.

Table 6-106. REEDM Predicted Exhaust Cloud Transport Directions for Daytime Castor 1200 T+20 Conflagration Al_2O_3 Scenarios.

Plume Transport Direction Bin	Count	Probability
337.5 – 22.5 (N)	704	0.15052
22.5 – 67.5 (NE)	851	0.18195
67.5 – 112.5 (E)	588	0.12572
112.5 – 157.5 (SE)	906	0.19371
157.5 – 202.5 (S)	524	0.11204
202.5 – 247.5 (SW)	520	0.11118
247.5 – 292.5 (W)	340	0.07270
292.5 – 337.5 (NW)	244	0.05217

Similar summary tables for the 1751 nighttime Castor 1200 T+20 conflagration simulations were compiled. Table 6-101 shows the Al_2O_3 PM_{10} concentration histogram results. Approximately 5.6% of all nighttime meteorological cases resulted in REEDM maximum peak instantaneous ground level Al_2O_3 PM_{10} concentrations of less than 1 mg/m^3. Approximately 72.2% of all nighttime meteorological cases resulted in REEDM maximum peak instantaneous ground level Al_2O_3 PM_5 (respirable dust) concentrations of 5 mg/m^3 or higher.

Table 6-107. REEDM Predicted Maximum Far Field Ground Level Al_2O_3 PM_{10} Concentrations for Nighttime Castor 1200 T+20 Conflagration Scenarios.

Concentration Bin	Count	Probability
0 - 1	99	0.05654
1 - 2	94	0.05368
2 - 3	76	0.04340
3 - 4	61	0.03484
4 - 5	49	0.02798
5 - 6	63	0.03598
6 - 7	44	0.02513
7 - 8	42	0.02399
8 - 9	44	0.02513
9 - 10	47	0.02684
> 10	1132	0.64649

Table 6-108 indicates the predicted Castor 1200 vehicle T+20 conflagration plume direction probability of occurrence observed across the 1751 nighttime balloon sounding cases that produced non-zero predicted ground level Al_2O_3 concentrations. It is noted that for nighttime T+20 conflagration scenarios transport of the exhaust plume to the Northeast and Southeast are favored.

Table 6-108. REEDM Predicted Exhaust Cloud Transport Directions for Nighttime Castor 1200 T+20 Conflagration Scenarios.

Plume Transport Direction Bin	Count	Probability
337.5 – 22.5 (N)	135	0.07710
22.5 – 67.5 (NE)	344	0.19646
67.5 – 112.5 (E)	262	0.14963
112.5 – 157.5 (SE)	321	0.18332
157.5 – 202.5 (S)	258	0.14734
202.5 – 247.5 (SW)	237	0.13535
247.5 – 292.5 (W)	111	0.06339
292.5 – 337.5 (NW)	83	0.04740

6.4.13 Payload Deflagration NO_2 Results

LATRA3D was used to estimate the chemical reactions, heat of combustion, buoyancy, cloud rise and dispersion of a liquid propellant fireball that could occur when a payload assembly impacts the ground after a launch vehicle failure. For the purposes of this study, two hypergolic propellants that are commonly used on satellites were assumed for a generic payload. The propellants are MMH fuel and nitrogen tetroxide oxidizer. Standard mixing and reaction pathway assumptions used by the Air Force range safety organizations were applied in this study such that approximately 23% of the N_2O_4 oxidizer reacts and 77% is vaporized. The vaporized portion produces the toxic airborne chemical NO_2. Total mass of oxidizer in the payload is assumed to be 1640 pounds (a small to medium sized satellite). Dispersion of approximately 1263 pounds of NO_2 within a buoyant release is evaluated in this scenario. Since the payload is not depleting propellant and is assumed to remain as a single fragment during stage 1 flight there is no time dependency associated with the payload deflagration scenario.

Table 6-109 presents the maximum far field NO_2 peak instantaneous concentration predicted by LATRA3D for the hypothetical daytime launches of a Castor 1200 vehicle with subsequent core vehicle breakup that leaves the payload assembly intact and ejected from the vehicle explosion center. Far field peak NO_2 concentrations for daytime weather cases ranged from 13 to 42 ppm with the maximum concentration predicted to occur from 500 to 1550 meters downwind from the launch site. The table values represent the maximum concentrations predicted over a sample set of 3732 WFF balloon soundings that resulted in non-zero surface concentrations. Table 6-110 shows the LATRA3D predicted maximum peak NO_2 far field concentrations for 1568 nighttime cases for payload deflagration scenarios the produced non-zero grid concentrations. Far field peak NO_2 concentrations for nighttime weather cases ranged from 7 to 26 ppm with the maximum concentration predicted to occur from 500 to 2100 meters downwind from the payload impact point near the launch site.

Table 6-109: Castor 1200 Payload Deflagration NO_2 Peak Concentration Summary – Daytime Meteorology.

Month	Number of Weather Cases	Peak NO_2 Concentration [ppm]	Distance to Peak NO_2 Concentration [m]	Bearing to Peak NO_2 Concentration [deg]
January	247	4.19E+01	504	27
February	255	2.05E+01	1547	305
March	305	3.75E+01	506	27
April	345	2.73E+01	847	20
May	367	1.82E+01	1029	45
June	352	1.47E+01	696	7
July	383	1.51E+01	868	22
August	350	1.32E+01	1246	23
September	333	1.25E+01	664	200
October	313	1.42E+01	1062	37
November	245	2.05E+01	658	136
December	237	2.29E+01	712	32

Table 6-110: Castor 1200 Payload Deflagration NO_2 Peak Concentration Summary – Nighttime Meteorology.

Month	Number of Weather Cases	Peak NO_2 Concentration [ppm]	Distance to Peak NO_2 Concentration [m]	Bearing to Peak NO_2 Concentration [deg]
January	81	1.19E+01	2077	48
February	121	2.60E+01	809	112
March	133	1.92E+01	749	117
April	156	1.45E+01	734	48
May	158	1.66E+01	593	13
June	152	1.25E+01	614	156
July	152	7.12E+00	681	272
August	155	1.33E+01	681	240
September	155	2.10E+01	498	217
October	100	2.13E+01	1031	189
November	100	1.93E+01	849	172
December	105	1.79E+01	1110	33

The LATRA3D predicted NO_2 concentrations for all daytime meteorological cases processed in the 8-year sample set was aggregated into bins to evaluate the peak far field concentration probability. This information is provided in Table 6-111

Table 6-111. LATRA3D Predicted Maximum Far Field Ground Level NO_2 Concentrations for Daytime Payload Deflagration Scenarios.

Concentration Bin	Count	Probability
0 - 2	1971	0.52814
2- 4	853	0.22856
4 - 6	374	0.10021
6 - 8	202	0.05413
8 - 10	130	0.03483
10 - 20	188	0.05038
20 - 30	12	0.00322
30 - 40	1	0.00027
40 - 50	1	0.00027
50 - 60	0	0.00000
60 – 70	0	0.00000
70 – 80	0	0.00000
80 – 90	0	0.00000
90 - 100	0	0.00000
> 100	0	0.00000

It is noted that approximately 52.8% of the daytime meteorological cases with non-zero concentration resulted in LATRA3D maximum peak instantaneous ground level NO_2 concentrations of less than 2 ppm. Approximately 5.4% of the cases resulted in LATRA3D maximum peak instantaneous ground level NO_2 concentrations of 10 ppm or higher.

Table 6-112 lists the maximum downwind distance from the source to the endpoint for a low NO_2 peak instantaneous concentration value of 0.5 ppm for the daytime weather cases. This could be thought of as a containment distance beyond which negligible effects to NO_2 exposure occur. Maximum distances range from 5800 to 11000 meters from the source. Table 6-113 lists the maximum downwind distance from the source to the endpoint for a low NO_2 peak instantaneous concentration value of 0.5 ppm for the nighttime weather cases. Maximum nighttime 0.5 ppm distances range from 6300 to 10000 meters from the source.

Table 6-112: Castor 1200 Payload Deflagration 0.5 ppm NO_2 Concentration Hazard Zone Summary – Daytime Meteorology.

Month	Number of Weather Cases	NO_2 Hazard Zone Concentration [ppm]	Distance to End of Hazard Zone [m]	Bearing to End of Hazard Zone [deg]
January	187	5.00E-01	9621	221
February	185	5.00E-01	10710	308
March	228	5.00E-01	8205	224
April	282	5.00E-01	9906	330
May	304	5.00E-01	7522	223
June	303	5.00E-01	5858	329
July	304	5.00E-01	6368	258
August	280	5.00E-01	7900	44
September	223	5.00E-01	8983	338
October	259	5.00E-01	9854	27
November	202	5.00E-01	10702	55
December	192	5.00E-01	10026	39

Table 6-113: Castor 1200 Payload Deflagration 0.5 ppm NO_2 Concentration Hazard Zone Summary – Nighttime Meteorology.

Month	Number of Weather Cases	NO_2 Hazard Zone Concentration [ppm]	Distance to End of Hazard Zone [m]	Bearing to End of Hazard Zone [deg]
January	60	5.00E-01	8905	79
February	99	5.00E-01	9191	38
March	106	5.00E-01	9819	307
April	139	5.00E-01	6262	232
May	140	5.00E-01	6619	53
June	145	5.00E-01	6354	306
July	139	5.00E-01	6935	34
August	133	5.00E-01	6581	245
September	141	5.00E-01	7098	339
October	90	5.00E-01	7590	272
November	85	5.00E-01	9404	223
December	88	5.00E-01	10013	207

The LATRA3D predicted cloud transport directions for the payload deflagration NO_2 dispersion were also aggregated into bins representing 45-degree arc corridors around the compass (i.e. N, NE, E, SE, S, SW, W, NW). Table 6-115 indicates the predicted Castor 1200 payload deflagration cloud direction probability of occurrence observed across the 2949 daytime balloon sounding cases that produced predicted ground level NO_2 concentrations above 0.5 ppm. It is noted that for the daytime payload deflagration scenarios transport of the exhaust plume to the North and Northeast are favored.

Table 6-114. LATRA3D Predicted Exhaust Cloud Transport Directions for Daytime Castor 1200 Payload Deflagration NO_2 Scenarios.

Plume Transport Direction Bin	Count	Probability
337.5 – 22.5 (N)	620	0.21024
22.5 – 67.5 (NE)	705	0.23906
67.5 – 112.5 (E)	306	0.10376
112.5 – 157.5 (SE)	301	0.10207
157.5 – 202.5 (S)	270	0.09156
202.5 – 247.5 (SW)	344	0.11665
247.5 – 292.5 (W)	231	0.07833
292.5 – 337.5 (NW)	172	0.05832

Similar summary tables for the 1568 nighttime Castor 1200 payload deflagration simulations that produced non-zero concentrations were compiled. Although a total of 1751 meteorological cases were run, 183 cases had the predicted stabilized deflagration cloud completely above a mixing boundary, which results in a prediction of zero ground level concentrations. Table 6-115 shows the NO_2 concentration histogram results for the nighttime payload deflagration cases. Approximately 47.8% of all nighttime meteorological cases resulted in LATRA3D maximum peak instantaneous ground level NO_2 concentrations of less than 2 ppm. Approximately 5.1% of the nighttime cases resulted in LATRA3D maximum peak instantaneous ground level NO_2 concentrations of 10 ppm or higher.

.

Table 6-115. LATRA3D Predicted Maximum Far Field Ground Level NO_2 Concentrations for Nighttime Payload Deflagration Scenarios.

Concentration Bin	Count	Probability
0 - 2	749	0.47768
2- 4	403	0.25702
4 - 6	178	0.11352
6 - 8	99	0.06314
8 - 10	59	0.03763
10 - 20	77	0.04911
20 - 30	3	0.00191
30 - 40	0	0.00000
40 - 50	0	0.00000
50 - 60	0	0.00000
60 – 70	0	0.00000
70 – 80	0	0.00000
80 – 90	0	0.00000
90 - 100	0	0.00000
> 100	0	0.00000

Table 6-116 indicates the predicted Castor 1200 vehicle payload deflagration plume direction probability of occurrence observed across the 1365 nighttime balloon sounding cases that produced predicted ground level NO_2 concentrations above 0.5 ppm. It is noted that for nighttime payload deflagration scenarios transport of the exhaust plume to the Northeast is slightly favored.

Table 6-116. LATRA3D Predicted Exhaust Cloud Transport Directions for Nighttime Castor 1200 Payload Deflagration Scenarios.

Plume Transport Direction Bin	Count	Probability
337.5 – 22.5 (N)	108	0.07912
22.5 – 67.5 (NE)	292	0.21392
67.5 – 112.5 (E)	223	0.16337
112.5 – 157.5 (SE)	199	0.14579
157.5 – 202.5 (S)	175	0.12821
202.5 – 247.5 (SW)	205	0.15018
247.5 – 292.5 (W)	97	0.07106
292.5 – 337.5 (NW)	66	0.04835

6.4.14 Payload Deflagration MMH Results

LATRA3D was used to estimate the chemical reactions, heat of combustion, buoyancy, cloud rise and dispersion of a liquid propellant fireball that could occur when a payload assembly impacts the ground after a launch vehicle failure. For the purposes of this study, two hypergolic propellants that are commonly used on satellites were assumed for a generic payload. The propellants are MMH fuel and nitrogen tetroxide oxidizer. Standard mixing and reaction pathway assumptions used by the Air Force range safety organizations were applied in this study such that approximately 23% of the MMH fuel reacts with oxidizer, 63.1% thermally decomposes and 13.9% is vaporized. The vaporized portion produces the toxic airborne chemical MMH. Total mass of fuel in the payload is assumed to be 1000 pounds (a small to medium sized satellite). Dispersion of approximately 139 pounds of MMH within a buoyant release is evaluated in this scenario. Since the payload is not depleting propellant and is assumed to remain as a single fragment during stage 1 flight there is no time dependency associated with the payload deflagration scenario.

Table 6-117 presents the maximum far field MMH peak instantaneous concentration predicted by LATRA3D for the hypothetical daytime launches of a Castor 1200 vehicle with subsequent core vehicle breakup that leaves the payload assembly intact and ejected from the vehicle explosion center. Far field peak MMH concentrations for daytime weather cases ranged from 1.4 to 4.6 ppm with the maximum concentration predicted to occur from 500 to 1550 meters downwind from the launch site. The table values represent the maximum concentrations predicted over a sample set of 3732 WFF balloon soundings that resulted in non-zero surface concentrations. Table 6-118 shows the LATRA3D predicted maximum peak MMH far field concentrations for 1568 nighttime cases for payload deflagration scenarios the produced non-zero grid concentrations. Far field peak MMH concentrations for nighttime weather cases ranged from 0.8 to 2.9 ppm with the maximum concentration predicted to occur from 500 to 2100 meters downwind from the payload impact point near the launch site.

Table 6-117: Castor 1200 Payload Deflagration MMH Peak Concentration Summary – Daytime Meteorology.

Month	Number of Weather Cases	Peak MMH Concentration [ppm]	Distance to Peak MMH Concentration [m]	Bearing to Peak MMH Concentration [deg]
January	247	4.60E+00	504	27
February	255	2.25E+00	1547	305
March	305	4.12E+00	506	27
April	345	3.00E+00	847	20
May	367	2.00E+00	1029	45
June	352	1.61E+00	696	7
July	383	1.66E+00	868	22
August	350	1.45E+00	1246	23
September	333	1.37E+00	664	200
October	313	1.56E+00	1062	37
November	245	2.25E+00	658	136
December	237	2.51E+00	712	32

Table 6-118: Castor 1200 Payload Deflagration MMH Peak Concentration Summary – Nighttime Meteorology.

Month	Number of Weather Cases	Peak MMH Concentration [ppm]	Distance to Peak MMH Concentration [m]	Bearing to Peak MMH Concentration [deg]
January	81	1.31E+00	2077	48
February	121	2.86E+00	809	112
March	133	2.10E+00	749	117
April	156	1.59E+00	734	48
May	158	1.83E+00	593	13
June	152	1.38E+00	614	156
July	152	7.83E-01	681	272
August	155	1.46E+00	681	240
September	155	2.30E+00	498	217
October	100	2.34E+00	1031	189
November	100	2.12E+00	849	172
December	105	1.96E+00	1110	33

The LATRA3D predicted MMH concentrations for all daytime meteorological cases processed in the 8-year sample set was aggregated into bins to evaluate the peak far field concentration probability. This information is provided in Table 6-119

Table 6-119. LATRA3D Predicted Maximum Far Field Ground Level MMH Concentrations for Daytime Payload Deflagration Scenarios.

Concentration Bin	Count	Probability
0 - 1	3479	0.93221
1 - 2	226	0.06056
2 - 3	23	0.00616
3 - 4	2	0.00054
4 - 5	2	0.00054
5 - 6	0	0.00000
6 - 7	0	0.00000
7 - 8	0	0.00000
8 - 9	0	0.00000
9 - 10	0	0.00000
10 - 11	0	0.00000
11 - 12	0	0.00000
12 - 13	0	0.00000
13 - 14	0	0.00000
14 - 15	0	0.00000

It is noted that approximately 93.2% of the daytime meteorological cases with non-zero concentration resulted in LATRA3D maximum peak instantaneous ground level MMH concentrations of less than 1 ppm. Approximately 0.7% of the cases resulted in LATRA3D maximum peak instantaneous ground level MMH concentrations of 2 ppm or higher (approximately the 30 minute AEGL 2 threshold).

Table 6-120 lists the maximum downwind distance from the source to the endpoint for a low MMH peak instantaneous concentration value of 0.5 ppm for the daytime weather cases. This could be thought of as a containment distance beyond which negligible effects to MMH exposure occur. Maximum distances range from 2000 to 5300 meters from the source for the daytime cases. Table 6-121 lists the maximum downwind distance from the source to the endpoint for a low MMH peak instantaneous concentration value of 0.5 ppm for the nighttime weather cases. Maximum nighttime 0.5 ppm distances range from 1900 to 4900 meters from the source.

Table 6-120: Castor 1200 Payload Deflagration 0.5 ppm MMH Concentration Hazard Zone Summary – Daytime Meteorology.

Month	Number of Weather Cases	MMH Hazard Zone Concentration [ppm]	Distance to End of Hazard Zone [m]	Bearing to End of Hazard Zone [deg]
January	67	5.00E-01	4454	61
February	61	5.00E-01	5285	307
March	87	5.00E-01	4135	115
April	104	5.00E-01	3114	48
May	86	5.00E-01	2401	29
June	70	5.00E-01	2130	18
July	49	5.00E-01	1980	38
August	52	5.00E-01	2499	20
September	26	5.00E-01	2390	4
October	39	5.00E-01	4021	88
November	79	5.00E-01	5330	55
December	53	5.00E-01	4836	39

Table 6-121: Castor 1200 Payload Deflagration 0.5 ppm MMH Concentration Hazard Zone Summary – Nighttime Meteorology.

Month	Number of Weather Cases	MMH Hazard Zone Concentration [ppm]	Distance to End of Hazard Zone [m]	Bearing to End of Hazard Zone [deg]
January	20	5.00E-01	4460	47
February	36	5.00E-01	4936	40
March	42	5.00E-01	4552	180
April	41	5.00E-01	2454	358
May	37	5.00E-01	2386	32
June	27	5.00E-01	1942	57
July	13	5.00E-01	1962	43
August	22	5.00E-01	1877	32
September	17	5.00E-01	2354	188
October	33	5.00E-01	2661	83
November	30	5.00E-01	4461	85
December	30	5.00E-01	4596	140

The LATRA3D predicted cloud transport directions for the payload deflagration MMH dispersion were also aggregated into bins representing 45-degree arc corridors around the compass (i.e. N, NE, E, SE, S, SW, W, NW). Table 6-122 indicates the predicted Castor 1200 payload deflagration cloud direction probability of occurrence observed across the 773 daytime balloon sounding cases that produced predicted ground level MMH concentrations above 0.5 ppm. It is noted that for the daytime payload deflagration scenarios transport of the exhaust plume to the North and Northeast are favored.

Table 6-122. LATRA3D Predicted Exhaust Cloud Transport Directions for Daytime Castor 1200 Payload Deflagration MMH Scenarios.

Plume Transport Direction Bin	Count	Probability
337.5 – 22.5 (N)	221	0.28590
22.5 – 67.5 (NE)	310	0.40103
67.5 – 112.5 (E)	61	0.07891
112.5 – 157.5 (SE)	30	0.03881
157.5 – 202.5 (S)	57	0.07374
202.5 – 247.5 (SW)	48	0.06210
247.5 – 292.5 (W)	24	0.03105
292.5 – 337.5 (NW)	22	0.02846

Similar summary tables for the 348 nighttime Castor 1200 payload deflagration simulations that produced non-zero concentrations were compiled. Although a total of 1751 meteorological cases were run, 183 cases had the predicted stabilized deflagration cloud completely above a mixing boundary, which results in a prediction of zero ground level concentrations. An additional 1220 cases had maximum ground concentrations below 0.5 ppm due to the small 139 pound mass quantity of the release. Table 6-123 shows the MMH concentration histogram results for the nighttime payload deflagration cases. Approximately 93.4% of all nighttime meteorological cases resulted in LATRA3D maximum peak instantaneous ground level MMH concentrations of less than 1 ppm. Approximately 0.4% of the cases resulted in LATRA3D maximum peak instantaneous ground level MMH concentrations of 2 ppm or higher (approximately the 30 minute AEGL 2 threshold).

.

Table 6-123. LATRA3D Predicted Maximum Far Field Ground Level MMH Concentrations for Nighttime Payload Deflagration Scenarios.

Concentration Bin	Count	Probability
0 - 1	1465	0.93431
1 - 2	96	0.06122
2 - 3	7	0.00446
3 - 4	0	0.00000
4 - 5	0	0.00000
5 - 6	0	0.00000
6 - 7	0	0.00000
7 - 8	0	0.00000
8 - 9	0	0.00000
9 - 10	0	0.00000
10 - 11	0	0.00000
11 - 12	0	0.00000
12 - 13	0	0.00000
13 - 14	0	0.00000
14 - 15	0	0.00000

Table 6-124 indicates the predicted Castor 1200 vehicle payload deflagration plume direction probability of occurrence observed across the 348 nighttime balloon sounding cases that produced predicted ground level MMH concentrations above 0.5 ppm. It is noted that for nighttime payload deflagration scenarios transport of the exhaust plume to the Northeast is favored.

Table 6-124. LATRA3D Predicted Exhaust Cloud Transport Directions for Nighttime Castor 1200 Payload Deflagration Scenarios.

Plume Transport Direction Bin	Count	Probability
337.5 – 22.5 (N)	33	0.09483
22.5 – 67.5 (NE)	126	0.36207
67.5 – 112.5 (E)	51	0.14655
112.5 – 157.5 (SE)	26	0.07471
157.5 – 202.5 (S)	40	0.11494
202.5 – 247.5 (SW)	55	0.15805
247.5 – 292.5 (W)	9	0.02586
292.5 – 337.5 (NW)	8	0.02299

6.4.15 Payload Spill and Pool Evaporation NO_2 Results

LATRA3D was used to estimate the evaporation rate from a spill of N_2O_4 oxidizer assuming that payload impact ruptures the propellant tanks but does not lead to a fire or explosion. The evaporated oxidizer produces the toxic airborne chemical NO_2. The boiling point of N_2O_4 is 71 F so it is volatile and evaporates quickly. The total mass of oxidizer in the payload is assumed to be 1640 pounds (a small to medium sized satellite). Neutral buoyancy dispersion of all 1640 pounds of NO_2 is evaluated in this scenario. Since this is a neutral buoyancy release there is no "cloud rise" as with the sources that release combustion heat. The neutral buoyancy source forms at ground level where the concentrations of interest are being estimated. The pool evaporation scenarios can have very high concentrations right at the pool location and concentration decreases monotonically moving away from the pool in the downwind direction. For this reason, reporting statistics on the "maximum peak ground level concentration" is not very informative about the size of the toxic hazard corridor. Concentrations of NO_2 near the evaporating pool are estimated to be in the 10,000 to 50,000 ppm range, which is extremely hazardous to health. To give a better assessment of the downwind extent of a potential toxic hazard corridor, a threshold of 5 ppm of NO_2 was selected as a reference value. The 5-ppm hazard zone for NO_2 could be thought of as a region within which adverse effect would be low (or worst) but not negligible. Solar heating and ground temperature effects generally result in higher predicted evaporation rates during the day than at night, consequently the daytime hazard corridors are somewhat longer than the nighttime hazard corridors.

Table 6-125 presents the estimated 5-ppm maximum hazard corridor distances predicted over a sample set of 4678 WFF daytime balloon soundings. The predicted daytime 5-ppm NO_2 maximum hazard zone distances ranged from 1000 to 2500 meters downwind from the spill site. Table 6-126 presents the estimated 5-ppm maximum hazard corridor distances predicted over a sample set of 1751 WFF nighttime balloon soundings. The predicted nighttime 5-ppm NO_2 maximum hazard zone distances ranged from 800 to 1500 meters downwind from the spill site.

Table 6-125: Castor 1200 Payload Pool Evaporation 5-ppm NO_2 Concentration Summary – Daytime Meteorology.

Month	Number of Weather Cases	Reference NO_2 Concentration [ppm]	Max Distance to Reference NO_2 Concentration [m]	Bearing to Reference NO_2 Concentration [deg]
January	341	5.00E+00	1585	55
February	363	5.00E+00	1038	328
March	393	5.00E+00	2330	80
April	381	5.00E+00	1685	90
May	398	5.00E+00	1806	174
June	391	5.00E+00	1444	49
July	417	5.00E+00	1696	95
August	410	5.00E+00	1963	70
September	412	5.00E+00	1952	270
October	429	5.00E+00	1469	230
November	376	5.00E+00	2524	261
December	367	5.00E+00	1024	50

Table 6-126: Castor 1200 Payload Pool Evaporation 5-ppm NO_2 Concentration Summary – Nighttime Meteorology.

Month	Number of Weather Cases	Reference NO_2 Concentration [ppm]	Max Distance to Reference NO_2 Concentration [m]	Bearing to Reference NO_2 Concentration [deg]
January	95	5.00E+00	900	111
February	158	5.00E+00	955	150
March	165	5.00E+00	1509	310
April	158	5.00E+00	827	54
May	159	5.00E+00	823	40
June	153	5.00E+00	823	184
July	153	5.00E+00	821	133
August	162	5.00E+00	885	35
September	163	5.00E+00	987	100
October	125	5.00E+00	977	90
November	129	5.00E+00	997	140
December	131	5.00E+00	963	70

The LATRA3D predicted cloud transport directions for the payload evaporating pool NO_2 dispersion were also aggregated into bins representing 45-degree arc corridors around the compass (i.e. N, NE, E, SE, S, SW, W, NW). Table 6-127 indicates the predicted Castor 1200 payload evaporating pool plume direction probability of occurrence observed across the 4678 daytime balloon sounding cases that produced predicted ground level NO_2 concentrations above 5 ppm. It is noted that for the daytime payload pool evaporation scenarios transport of the exhaust plume to the North is favored. This is a reflection of prevailing wind directions near the ground surface.

Table 6-127. LATRA3D Predicted Exhaust Cloud Transport Directions for Daytime Castor 1200 Payload Pool Evaporation NO_2 Scenarios.

Plume Transport Direction Bin	Count	Probability
337.5 – 22.5 (N)	1020	0.21804
22.5 – 67.5 (NE)	714	0.15263
67.5 – 112.5 (E)	569	0.12163
112.5 – 157.5 (SE)	686	0.14664
157.5 – 202.5 (S)	560	0.11971
202.5 – 247.5 (SW)	461	0.09855
247.5 – 292.5 (W)	413	0.08829
292.5 – 337.5 (NW)	255	0.05451

Table 6-128 indicates the predicted Castor 1200 vehicle payload pool evaporation plume direction probability of occurrence observed across the 1751 nighttime balloon sounding cases. It is noted that for nighttime payload pool evaporation scenarios transport of the exhaust plume toward a wide sector from the Northeast clockwise to the South is favored. This is a reflection of prevailing nighttime wind directions near the ground surface.

Table 6-128. LATRA3D Predicted Exhaust Cloud Transport Directions for Nighttime Castor 1200 Payload Pool Evaporation NO_2 Scenarios.

Plume Transport Direction Bin	Count	Probability
337.5 – 22.5 (N)	174	0.09937
22.5 – 67.5 (NE)	332	0.18961
67.5 – 112.5 (E)	269	0.15363
112.5 – 157.5 (SE)	311	0.17761
157.5 – 202.5 (S)	298	0.17019
202.5 – 247.5 (SW)	188	0.10737
247.5 – 292.5 (W)	117	0.06682
292.5 – 337.5 (NW)	62	0.03541

6.4.16 Payload Spill and Pool Evaporation MMH Results

LATRA3D was used to estimate the evaporation rate from a spill of MMH fuel assuming that payload impact ruptures the propellant tanks but does not lead to a fire or explosion. The evaporated oxidizer produces the toxic airborne chemical MMH. The boiling point of MMH is 188.6 F and it has low saturation pressure and therefore evaporates slowly. The total mass of fuel in the payload is assumed to be 1000 pounds (a small to medium sized satellite). Neutral buoyancy dispersion of all 1000 pounds of MMH is evaluated in this scenario. Since this is a neutral buoyancy release there is no “cloud rise” as with the sources that release combustion heat. The neutral buoyancy source forms at ground level where the concentrations of interest are being estimated. The pool evaporation scenarios can have very high concentrations right at the pool location and concentration decreases monotonically moving away from the pool in the downwind direction. For this reason, reporting statistics on the “maximum peak ground level concentration” is not very informative about the size of the toxic hazard corridor. Concentrations of MMH near the evaporating pool are estimated to be in the 200 to 5,000 ppm range, which is extremely hazardous to health. To give a better assessment of the downwind extent of a potential toxic hazard corridor, a threshold of 5 ppm of MMH was selected as a reference value. The 5-ppm hazard zone for MMH could be thought of as a region within which adverse effect would be low (or worst) but not negligible. Solar heating and ground temperature effects generally result in higher predicted evaporation rates during the day than at night, consequently the daytime hazard corridors are somewhat longer than the nighttime hazard corridors.

Table 6-129 presents the estimated 5-ppm hazard corridor distances predicted over a sample set of 4546 WFF daytime balloon soundings that had MMH concentrations above 5-ppm in the LATRA3D calculation grid (132 cases had very short hazard zones that did not reach the first downwind row in LATRA3D concentration grid node array). The predicted daytime 5-ppm MMH maximum hazard zone distances ranged from 170 to 280 meters downwind from the spill site. Table 6-130 presents the estimated 5-ppm hazard corridor distances predicted over a sample set of 1669 WFF nighttime balloon soundings that had MMH concentrations above 5-ppm in the LATRA3D calculation grid (82 cases had very short hazard zones that did not reach the first downwind row in LATRA3D concentration grid node array). The predicted nighttime 5-ppm MMH maximum hazard zone distances ranged from 100 to 240 meters downwind from the spill site.

Table 6-129: Castor 1200 Payload Pool Evaporation 5-ppm MMH Concentration Summary – Daytime Meteorology.

Month	Number of Weather Cases	Reference MMH Concentration [ppm]	Max Distance to Reference MMH Concentration [m]	Bearing to Reference MMH Concentration [deg]
January	309	5.00E+00	207	55
February	336	5.00E+00	169	190
March	380	5.00E+00	195	285
April	367	5.00E+00	225	55
May	396	5.00E+00	257	50
June	391	5.00E+00	264	60
July	417	5.00E+00	266	90
August	409	5.00E+00	276	50
September	411	5.00E+00	260	310
October	424	5.00E+00	219	230
November	365	5.00E+00	204	261
December	341	5.00E+00	169	176

Table 6-130: Castor 1200 Payload Pool Evaporation 5-ppm MMH Concentration Summary – Nighttime Meteorology.

Month	Number of Weather Cases	Reference MMH Concentration [ppm]	Max Distance to Reference MMH Concentration [m]	Bearing to Reference MMH Concentration [deg]
January	81	5.00E+00	104	40
February	141	5.00E+00	115	150
March	144	5.00E+00	148	310
April	156	5.00E+00	186	100
May	159	5.00E+00	217	30
June	153	5.00E+00	229	157
July	152	5.00E+00	237	133
August	162	5.00E+00	222	50
September	161	5.00E+00	197	71
October	125	5.00E+00	146	270
November	122	5.00E+00	141	112
December	113	5.00E+00	108	50

The LATRA3D predicted cloud transport directions for the payload evaporating pool MMH dispersion were also aggregated into bins representing 45-degree arc corridors around the compass (i.e. N, NE, E, SE, S, SW, W, NW). Table 6-131 indicates the predicted Castor 1200 payload evaporating pool plume direction probability of occurrence observed across the 4546 daytime balloon sounding cases that produced predicted ground level MMH concentrations above 5 ppm. It is noted that for the daytime payload pool evaporation scenarios transport of the exhaust plume to the North is favored. This is a reflection of prevailing wind directions near the ground surface.

Table 6-131. LATRA3D Predicted Exhaust Cloud Transport Directions for Daytime Castor 1200 Payload Pool Evaporation MMH Scenarios.

Plume Transport Direction Bin	Count	Probability
337.5 – 22.5 (N)	997	0.21931
22.5 – 67.5 (NE)	704	0.15486
67.5 – 112.5 (E)	558	0.12275
112.5 – 157.5 (SE)	658	0.14474
157.5 – 202.5 (S)	538	0.11835
202.5 – 247.5 (SW)	433	0.09525
247.5 – 292.5 (W)	404	0.08887
292.5 – 337.5 (NW)	254	0.05587

Table 6-132 indicates the predicted Castor 1200 vehicle payload pool evaporation plume direction probability of occurrence observed across the 1669 nighttime balloon sounding cases. It is noted that for nighttime payload pool evaporation scenarios transport of the exhaust plume toward a wide sector from the Northeast clockwise to the South is favored. This is a reflection of prevailing nighttime wind directions near the ground surface.

Table 6-132. LATRA3D Predicted Exhaust Cloud Transport Directions for Nighttime Castor 1200 Payload Pool Evaporation MMH Scenarios.

Plume Transport Direction Bin	Count	Probability
337.5 – 22.5 (N)	168	0.10066
22.5 – 67.5 (NE)	325	0.19473
67.5 – 112.5 (E)	266	0.15938
112.5 – 157.5 (SE)	286	0.17136
157.5 – 202.5 (S)	287	0.17196
202.5 – 247.5 (SW)	166	0.09946
247.5 – 292.5 (W)	111	0.06651
292.5 – 337.5 (NW)	60	0.03595

7. CONCLUSIONS

Approximately 102,000 REEDM and LATRA3D computer simulations have been executed to assess peak ground level concentrations for HCl, AL_2O_3, NO_2 and MMH chemicals that are released either as part of normal launch propellant combustion or from catastrophic breakup of a Castor 1200 based launch vehicle and payload. Tables of maximum predicted ground level concentration values are provide for each chemical release scenario and are parsed into daytime versus nighttime weather cases for each month of the year. Some minor trends can be seen in the monthly data that reflect seasonal weather effects. These are not deemed overly significant. Some diurnal effects are also observed between day and night. Toxic transport and dispersion and the formation of the convective boundary layer are very weather dependent. At night stable air layers can form near the ground and these cases can present the most adverse conditions for rocket emissions leading to high ground level concentrations if toxic plume material gets trapped in the surface stable layer.

Not surprisingly, the normal launch scenario generates relatively benign toxic results due to the limited amount of propellant that is burned while the vehicle is ascending through the atmospheric boundary layer (e.g. lower 10,000 feet of the atmosphere). The vehicle catastrophic solid propellant “conflagration” and liquid propellant “deflagration” modes generate some cases where ground level concentrations are high enough to pose a toxic hazard to humans (and presumably other animals). Many of the conflagration and deflagration cases result in low or zero ground level concentrations, however, there are a large enough percentage of cases with higher concentration predictions that can be used to estimate reasonable bounding conditions both in terms of expected maximum exposure concentrations and maximum hazard distances from the source (e.g. launch pad). Readers are referred to the Executive Summary of this document for a more concise summary of the peak concentrations and maximum hazard zone distances.

8. REFERENCES

[1] Randolph L. Nyman, “Evaluation of Taurus II Static Test Firing and Normal Launch Rocket Plume Emissions”, Report No. 09-640/5-01, ACTA Inc., Torrance, CA, March 18, 2009.

[2] Richard Jeffs, “Stage Descriptions for ACTA 2012-07-25.pptx”, personal communications, ATK PowerPoint Briefing, July 2012.

[3] Randolph L. Nyman, “REEDM Version 7.09 Technical Description Manual”, Report No. 99-400/2.1-02, ACTA Inc., Torrance, CA, September 30, 1999.

[4] Mark Herndon et. Al., “LATRA3D Technical Description Manual” ”, Report No. 10-142/11.3-02, ACTA Inc., Torrance, CA, September 30, 2010.

[5] Hanna, Steven R., David G. Strimaitis, and Jeffrey Weil, *IV&V of LATRA3D Software*, Report No. P122-4, Hanna Consultants, Kennebunkport, ME 04046, March 28, 2010.

[6] Gordon, Sanford and Bonnie J. McBride, “Computer Program for Calculation of Complex Chemical Equilibrium Compositions, Rocket Performance, Incident and Reflected Shocks, and Chapman-Jouguet Detonations”, Interim Revision NASA SP-273, Lewis Research Center, Cleveland OH, March 1976.

[7] Gordon, Sanford and Bonnie J. McBride, “Computer Program for Calculation of Complex Chemical Equilibrium Compositions and Applications, I. Analysis”, NASA Reference Publication 1311, Lewis Research Center, Cleveland OH, October 1994.

Appendix A

Representative Sample Toxic Hazard Corridors and Concentration Isopleths for Castor 1200 Release Scenarios

A. Case 1 - Castor 1200 Worst Case Normal Launch HCl Isopleths

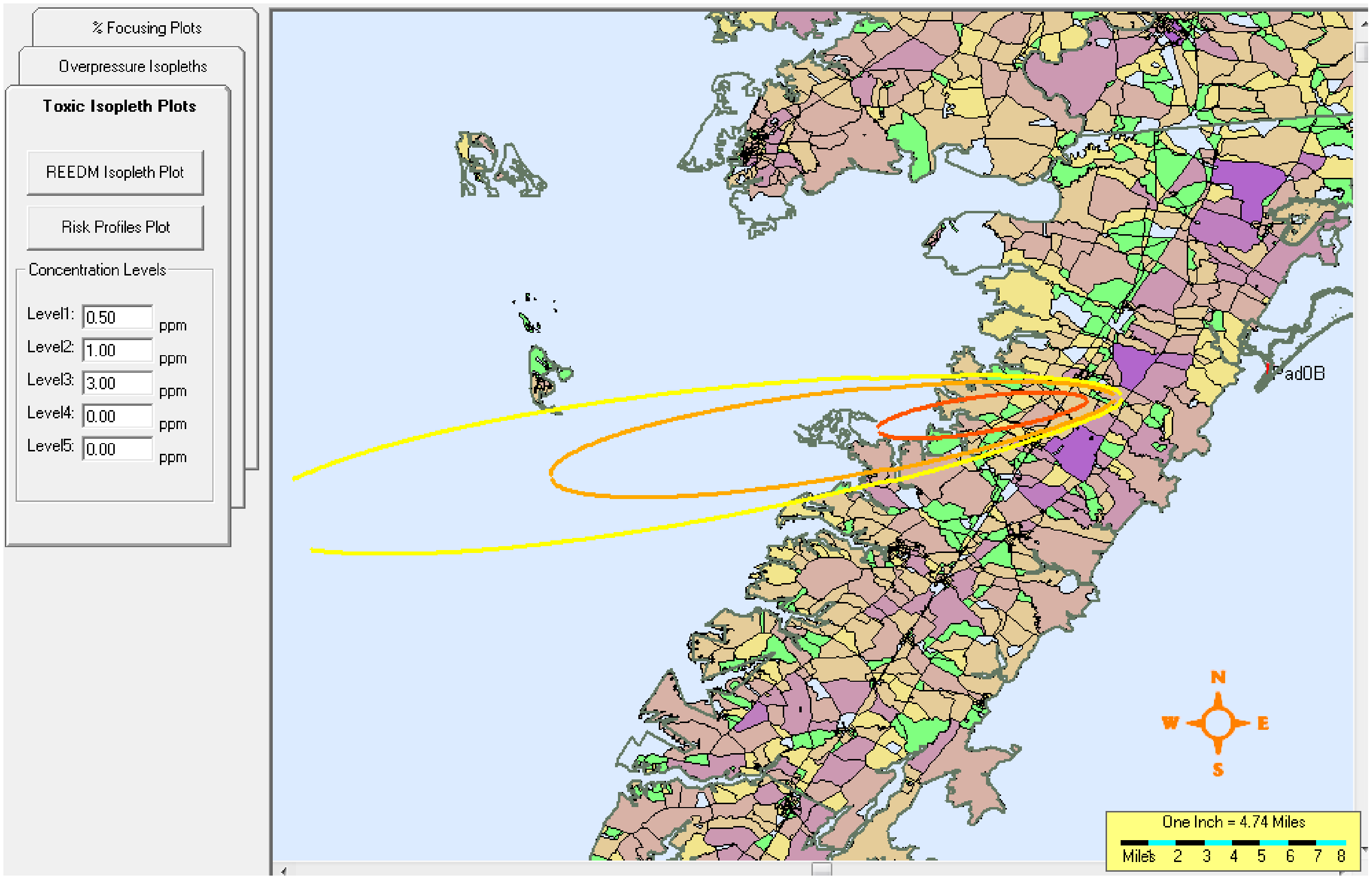

Figure A - 1. Worst Case Hydrogen Chloride Concentration Contours for the Normal Launch of a Castor 1200 from Wallops Flight Facility.

Case 1 Discussion

This example plots the 0.5, 1 and 3 ppm ground level HCl isopleths for the meteorological case that generated the worst case peak HCl concentration prediction of 5.03 ppm out of the 6430 cases evaluated. The analysis code used here was REEDM. The normal launch ground cloud centroid was predicted to stabilize at an altitude of 1138 meters above the ground with the bottom of the cloud positioned 733 meters above the ground. REEDM assigned a mixing layer boundary at 1473 meters, effectively trapping the majority of the ground cloud beneath a reflective upper boundary set at 1473 meters. In this case the winds carry the exhaust cloud inland from the WFF launch site along a bearing of 256 degrees.

The surface concentrations of HCl from a normal launch result from emissions of the rocket first stage during lift-off and ascent. The largest portion of exhaust mass is injected into the ground cloud, which is that portion of the nozzle exit flow that interacts with the launch pad structure and ground surface. The ground cloud could potentially interact with deluge water injected into the motor exhaust flame trench and onto the pad structures. In this study any effect of deluge water has been ignored as that amount of deluge water (if any) is as yet undefined. The composition of the gases leaving the Castor 1200 nozzle exit plane is about 20% hydrogen chloride gas by mass. As the rocket ascends away from the launch pad it accelerates and begins to pitch in the downrange direction leaving a contrail of exhaust gases behind the vehicle. The contrail cloud is also considered when performing HCl normal launch dispersion analyses. In this study a launch azimuth of 115 degrees was applied, but the toxic dispersion model for normal launch emissions is relatively insensitive to launch azimuth since the early phase of liftoff has the vehicle climbing nearly vertically above the launch pad and with only a small downrange velocity component after pitch is initiated.

Both the ground cloud and the contrail cloud are buoyant and rise from the launch site to the stabilization altitude of 1138 meters. Atmospheric turbulence eventually mixes the cloud material back down to the ground level. This is predicted to occur about 8000 meters downwind from the launch site (Pad-OA). The maximum predicted ground level concentration is 5.03 ppm, occurring at 16,000 meters downwind. REEDM HCl concentration versus distance predictions for this case are presented in Table A - 1. Note that the predicted cloud passage time is only a few minutes over any given receptor location.

Table A - 1. REEDM Predicted HCl Concentration Versus Distance for the Normal Launch Worst Case.

----- MAXIMUM CENTERLINE CALCULATIONS -----

** DECAY COEFFICIENT (1/SEC) = 0.00000E+00 **

CONCENTRATION OF HCL AT A HEIGHT OF 0.0
DOWNWIND FROM A CASTOR1200 NORMAL LAUNCH
CALCULATIONS APPLY TO THE LAYER BETWEEN 0.0 AND 1472.8 METERS

RANGE FROM PAD (METERS)	BEARING FROM PAD (DEGREES)	PEAK CONCEN-TRATION (PPM)	CLOUD ARRIVAL TIME (MIN)	CLOUD DEPARTURE TIME (MIN)	
8000.0000	254.7636	0.0017	1.8522	4.1909	
9000.9307	255.3932	0.2098	2.3474	4.6904	
10000.1982	255.8563	1.0785	2.8402	5.1889	
11000.0000	256.2197	2.2862	3.3322	5.6877	
12000.1621	256.5155	3.4056	3.8236	6.1867	
13000.3672	256.6477	4.2454	4.3145	6.6861	
14000.2334	256.5479	4.7665	4.8050	7.1857	
15000.6660	256.7570	5.0076	5.2953	7.6856	
16000.5518	**256.6931**	**5.0327**	**5.7854**	**8.1858**	**←peak concentration**
17000.4551	256.6367	4.9075	6.2754	8.6862	
18000.3730	256.5865	4.6908	6.7652	9.1868	
19000.3047	256.5416	4.4262	7.2549	9.6877	
20000.2461	256.5012	4.1442	7.7446	10.1888	
21000.1953	256.4647	3.8642	8.2342	10.6902	
22000.1543	256.4315	3.5972	8.7237	11.1917	
23000.4570	256.4012	3.3487	9.2127	11.6929	
24000.0898	256.3733	3.1197	9.7027	12.1953	
25000.9570	256.7185	2.9114	10.1921	12.6974	
26000.9199	256.6992	2.7215	10.6815	13.1997	
27000.8867	256.6814	2.5484	11.1709	13.7021	
28000.8535	256.6648	2.3905	11.6602	14.2047	
29000.8242	256.6494	2.2462	12.1495	14.7074	
30000.7969	256.6350	2.1139	12.6389	15.2102	
31000.7715	256.6215	1.9925	13.1282	15.7132	
32000.7480	256.6089	1.8808	13.6175	16.2163	
33000.7266	256.5970	1.7779	14.1067	16.7195	
34000.7031	256.5858	1.6827	14.5960	17.2229	
35000.6836	256.5753	1.5947	15.0853	17.7263	
36000.6641	256.5653	1.5131	15.5745	18.2299	
37000.6484	256.5559	1.4373	16.0638	18.7335	
38000.6289	256.5470	1.3668	16.5530	19.2372	
39000.6133	256.5386	1.3012	17.0422	19.7410	
40000.5977	256.5305	1.2400	17.5315	20.2449	
41000.5820	256.5229	1.1828	18.0207	20.7488	
42000.5703	256.5156	1.1293	18.5099	21.2529	

43000.5547	256.5087	1.0792	18.9991	21.7570
44000.5430	256.5020	1.0323	19.4883	22.2611
45000.5312	256.4957	0.9882	19.9775	22.7654
46000.5195	256.4897	0.9468	20.4667	23.2696
47000.5078	256.4839	0.9078	20.9559	23.7740
48000.5000	256.4783	0.8711	21.4451	24.2784
49000.4883	256.4730	0.8365	21.9343	24.7828
50000.4766	256.4679	0.8038	22.4235	25.2873
51000.4688	256.4630	0.7730	22.9127	25.7918
52000.4609	256.4582	0.7438	23.4019	26.2964
53000.4531	256.4537	0.7162	23.8911	26.8010
54000.4414	256.4493	0.6900	24.3803	27.3057
55000.4336	256.4451	0.6653	24.8695	27.8104
56000.4258	256.4410	0.6417	25.3586	28.3151
57000.4180	256.4371	0.6194	25.8478	28.8199
58000.4141	256.4333	0.5982	26.3370	29.3247
59000.4062	256.4296	0.5780	26.8262	29.8295
60000.3984	256.4261	0.5588	27.3153	30.3343

	RANGE	BEARING
5.033 IS THE MAXIMUM PEAK CONCENTRATION	16000.6	256.7

A. Case 2 - Castor 1200 Worst Case Normal Launch Al_2O_3 Isopleths

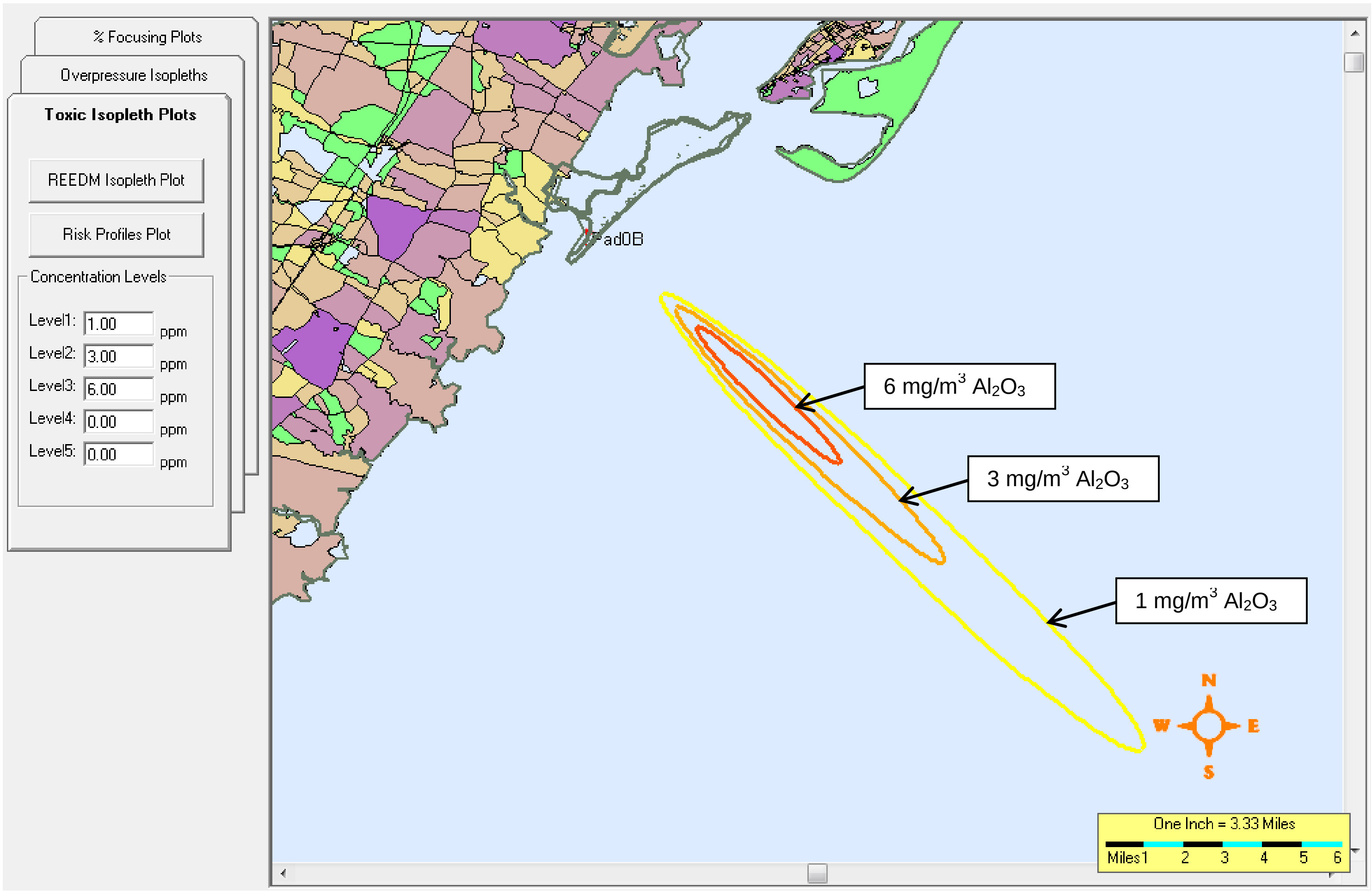

Figure A - 2. Worst Case Aluminum Oxide Particulate Concentration Contours for the Normal Launch of a Castor 1200 from Wallops Flight Facility.

Case 2 Discussion – Normal Launch AL_2O_3

This example plots the 1, 3 and 6 mg/m^3 ground level AL_2O_3 isopleths for the meteorological case that generated the worst case peak AL_2O_3 concentration prediction of 9.07 mg/m^3 out of the 6430 cases evaluated. The analysis code used here was REEDM. The normal launch ground cloud centroid was predicted to stabilize at an altitude of 642 meters above the ground with the bottom of the cloud positioned 419 meters above the ground. REEDM assigned a mixing layer boundary at 314 meters. Although the ground cloud is placed entirely above the mixing boundary layer, the boundary layer is deemed to only prevent gaseous transport across the boundary. Particulate AL_2O_3 is allowed by REEDM to pass through the gaseous boundary due to the influence of gravitational settling. The meteorological profile has light wind speeds and very little wind direction shear, which keeps the cloud from spreading out in the horizontal plane. In this case the winds carry the exhaust cloud offshore from the WFF launch site along a bearing of 136 degrees.

The surface concentrations of AL_2O_3 from a normal launch result from emissions of the rocket first stage during lift-off and ascent. The largest portion of exhaust mass is injected into the ground cloud, which is that portion of the nozzle exit flow that interacts with the launch pad structure and ground surface. The ground cloud could potentially interact with deluge water injected into the motor exhaust flame trench and onto the pad structures. In this study any effect of deluge water has been ignored as that amount of deluge water (if any) is as yet undefined. The composition of the gases leaving the Castor 1200 nozzle exit plane is about 28% aluminum oxide by mass. As the rocket ascends away from the launch pad it accelerates and begins to pitch in the downrange direction leaving a contrail of exhaust gases behind the vehicle. The contrail cloud up to an altitude of 3000 meters is also considered when performing AL_2O_3 normal launch dispersion analyses. In this study a launch azimuth of 115 degrees was applied, but the toxic dispersion model for normal launch emissions is relatively insensitive to launch azimuth since the early phase of liftoff has the vehicle climbing nearly vertically above the launch pad and with only a small downrange velocity component after pitch is initiated.

Both the ground cloud and the contrail cloud are buoyant and rise from the launch site to the stabilization altitude of 642 meters. Atmospheric turbulence eventually mixes the cloud material back down to the ground level. This is predicted to occur about 3000 meters downwind from the launch site (Pad-OA). The maximum predicted ground level concentration is 9.07 mg/m^3, occurring at 10,000 meters downwind. REEDM AL_2O_3 concentration versus distance predictions for this case are presented in Table A - 2. Note that the predicted cloud passage time is only about 10 minutes at the peak concentration point increasing to about 60 minutes at 60,000 meters downwind.

Table A - 2. REEDM Predicted AL_2O_3 Concentration Versus Distance for the Normal Launch Worst Case.

----- MAXIMUM CENTERLINE CALCULATIONS -----

** DECAY COEFFICIENT (1/SEC) = 0.00000E+00 **

CONCENTRATION OF AL2O3 AT A HEIGHT OF 0.0
DOWNWIND FROM A CASTOR1200 NORMAL LAUNCH
CALCULATIONS APPLY TO THE LAYER BETWEEN 0.0 AND 3007.5 METERS

RANGE FROM PAD (METERS)	BEARING FROM PAD (DEGREES)	PEAK CONCEN-TRATION (MILLI G/ M**3)	CLOUD ARRIVAL TIME (MIN)	CLOUD DEPARTURE TIME (MIN)	
3000.0000	134.8997	0.0289	4.3376	5.5857	
4000.0000	134.6230	0.8472	5.9502	7.8461	
5000.0000	134.7638	2.9236	7.2351	10.1874	
6000.0000	135.0241	5.1650	8.4533	12.5314	
7000.0000	135.2521	6.9702	9.4184	14.8774	
8000.0000	135.5624	8.2030	10.3896	17.2228	
9000.0000	135.7263	8.8792	11.4859	19.5704	
10000.0000	**135.8717**	**9.0713**	**12.7690**	**21.9184**	**←Peak Concentration**
11000.0000	135.9805	8.8977	14.0460	24.2716	
12000.0000	136.0801	8.4809	15.3269	26.6205	
13000.0000	136.1547	7.9256	16.6062	28.9703	
14000.0000	136.0536	7.3082	17.8848	31.3204	
15000.0000	136.1093	6.6816	19.1629	33.6706	
16000.0000	136.1581	6.0747	20.4404	36.0210	
17000.0000	136.1705	5.5043	21.7165	38.3728	
18000.0000	136.2082	4.9800	22.9933	40.7235	
19000.0000	136.2424	4.5034	24.2698	43.0742	
20000.0000	136.2727	4.0737	25.5460	45.4251	
21000.0000	136.3005	3.6884	26.8151	47.7843	
22000.0000	136.3254	3.3439	28.0906	50.1357	
23000.0000	136.3482	3.0364	29.3660	52.4871	
24000.0000	136.3687	2.7620	30.6413	54.8386	
25000.0000	136.3879	2.5172	31.9164	57.1901	
26000.0000	136.4056	2.2985	33.1915	59.5416	
27000.0000	136.4219	2.1030	34.4664	61.8932	
28000.0000	136.4367	1.9279	35.7412	64.2448	
29000.0000	136.4509	1.7709	37.0160	66.5964	
30000.0000	136.4642	1.6298	38.2906	68.9481	
31000.0000	136.3198	1.5029	39.5653	71.2997	
32000.0000	136.3311	1.3885	40.8398	73.6514	
33000.0000	136.3423	1.2852	42.1143	76.0031	
34000.0000	136.3523	1.1917	43.3888	78.3548	
35000.0000	136.3622	1.1070	44.6632	80.7065	
36000.0000	136.3716	1.0301	45.9376	83.0582	

37000.0000	136.3799	0.9601	47.2119	85.4100
38000.0000	136.3884	0.8964	48.4862	87.7617
39000.0000	136.3959	0.8383	49.7604	90.1135
40000.0000	136.4035	0.7853	51.0347	92.4652
41000.0000	136.4103	0.7367	52.3089	94.8170
42000.0000	136.4172	0.6922	53.5831	97.1687
43000.0000	136.4233	0.6514	54.8572	99.5205
44000.0000	136.4296	0.6139	56.1314	101.8723
45000.0000	136.4352	0.5794	57.4054	104.2241
46000.0000	136.4406	0.5477	58.6795	106.5759
47000.0000	136.4461	0.5184	59.9536	108.9277
48000.0000	136.4510	0.4913	61.2128	111.2985
49000.0000	136.4561	0.4662	62.4866	113.6507
50000.0000	136.4606	0.4430	63.7603	116.0030
51000.0000	136.4653	0.4214	65.0341	118.3552
52000.0000	136.4695	0.4014	66.3078	120.7074
53000.0000	136.4735	0.3828	67.5815	123.0597
54000.0000	136.4775	0.3654	68.8551	125.4119
55000.0000	136.4814	0.3492	70.1288	127.7642
56000.0000	136.4853	0.3340	71.4025	130.1164
57000.0000	136.4884	0.3199	72.6761	132.4687
58000.0000	136.4921	0.3066	73.9498	134.8209
59000.0000	136.4956	0.2941	75.2235	137.1731
60000.0000	136.4990	0.2824	76.4971	139.5254

	RANGE	BEARING
9.071 IS THE MAXIMUM PEAK CONCENTRATION	10000.0	135.9

A. Case 3 - Castor 1200 Worst Case Conflagration Abort Mode Al_2O_3 Isopleths

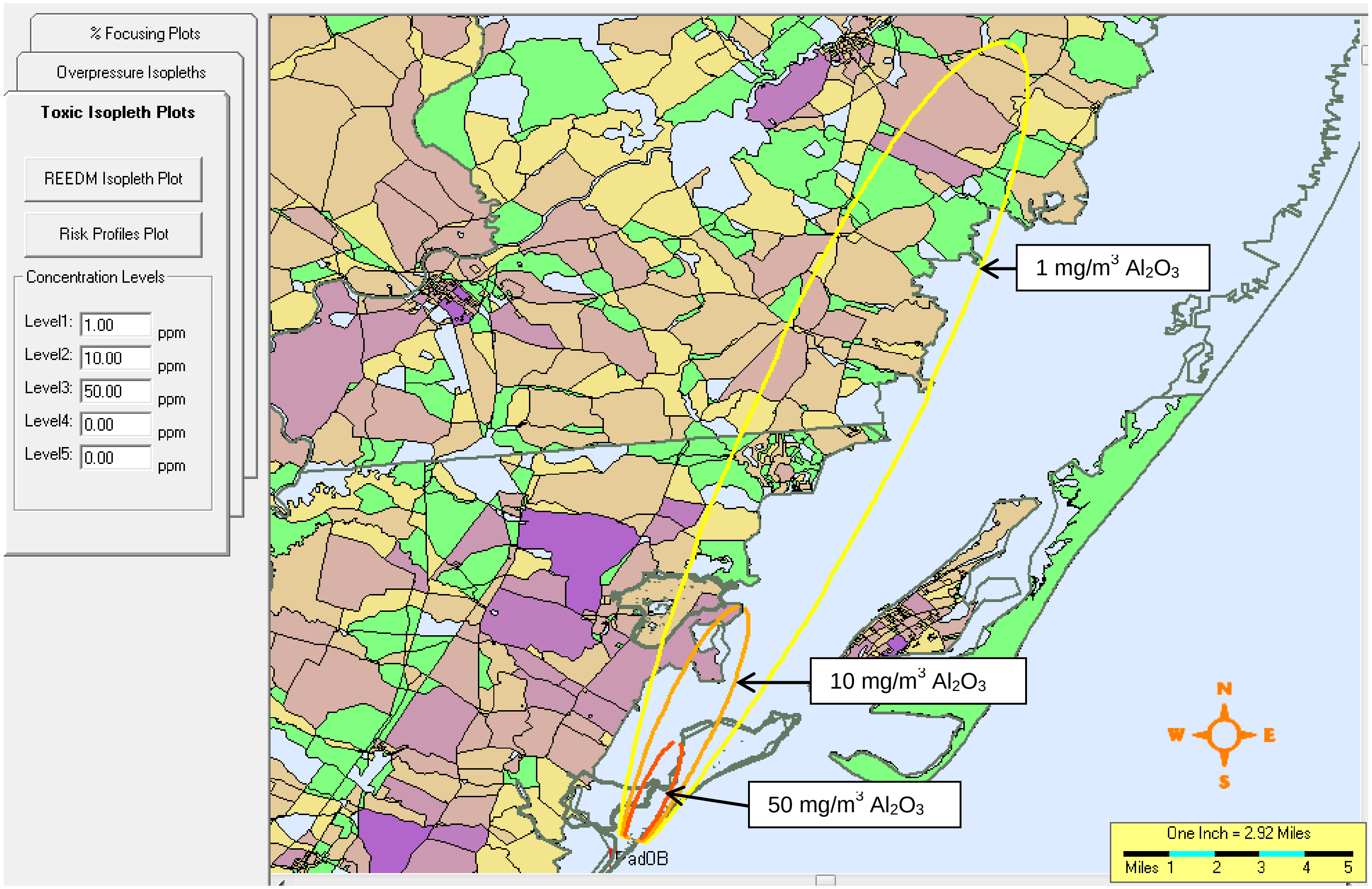

Figure A - 3. Worst Case Aluminum Oxide Particulate Concentration Contours for a Castor 1200 Conflagration Failure at T+8 Seconds from Wallops Flight Facility.

Case 3 Discussion – Conflagration Abort Mode AL_2O_3

This example plots the 1, 10 and 50 mg/m^3 ground level AL_2O_3 isopleths for the meteorological case that generated the worst case peak AL_2O_3 concentration prediction of 423 mg/m^3 given a T+8 second failure time evaluated over 6430 meteorological cases. The analysis code used here was REEDM. The conflagration cloud centroid was predicted to stabilize at an altitude of 48 meters above the ground with the bottom of the cloud contacting the ground. REEDM assigned a mixing layer boundary at 1457 meters. The conflagration cloud stabilized at a low altitude because of the presence of a strong nocturnal stable layer over the lower 130 meters of the atmosphere. The meteorological profile has moderately high wind speeds with very little wind direction shear in the cloud region, which keeps the cloud from spreading out in the horizontal plane. In this case the winds carry the exhaust cloud offshore from the WFF launch site along a bearing of 17 degrees.

The surface concentrations of AL_2O_3 from a conflagration event result from emissions of the solid propellant fragments burning on the ground. The failure at 8 seconds in to flight destroys the Castor 1200 generating an estimated 1221 fragments (including the 3 upper stages) with a propellant weight of just over 1.2 million pounds. Explosion induced velocities range from 10 to 243 feet/second. The debris impact area is approximately circular with an estimated radius of 265 meters centered approximately 55 meters downrange of the launch pad. The estimated burn time of the residual propellant burning on the ground is 275 seconds.

The maximum predicted ground level concentration is 423 mg/m^3 of Al_2O_3, occurring at 1,000 meters downwind. REEDM AL_2O_3 concentration versus distance predictions for this case are presented in Table A - 3. There are actually two parts to this table, one for liquid phase Al_2O_3 (L) and one for solid alpha phase Al_2O_3 (A). The liquid phase is identified by the REEDM internal combustion model as a product of the conflagration burn conditions at adiabatic flame temperature, but this liquid phase will be converted to solid phase as the buoyant plume rises and cools. ACTA summed the two phase concentrations to estimate downwind airborne Al_2O_3 particulate concentrations. Note that the predicted cloud passage time is only few minutes near the source at the peak concentration point and increases to about 16 minutes at 30,000 meters downwind. Even though the wind speed is assumed constant, the cloud passage time increases in the downwind direction because the cloud continues to expand horizontally and vertically as it moves downwind.

Table A - 3. REEDM Predicted AL_2O_3 Concentration Versus Distance the Worst Case T+8 Second Castor 1200 Conflagration Failure.

----- MAXIMUM CENTERLINE CALCULATIONS -----

** DECAY COEFFICIENT (1/SEC) = 0.00000E+00 **

CONCENTRATION OF AL2O3(L) AT A HEIGHT OF 0.0
DOWNWIND FROM A CASTOR1200 CONFLAGRATION LAUNCH
CALCULATIONS APPLY TO THE LAYER BETWEEN 0.0 AND 3016.6 METERS

RANGE FROM PAD (METERS)	BEARING FROM PAD (DEGREES)	PEAK CONCEN-TRATION (MILLI G/ M**3)	CLOUD ARRIVAL TIME (MIN)	CLOUD DEPARTURE TIME (MIN)	
1000.0000	**16.7844**	**395.5367**	**0.0000**	**3.9721**	**←Peak Concentration**
2000.0000	17.1377	346.9832	0.0000	5.3218	
3000.0000	16.7326	167.7236	0.4792	6.6781	
4000.0000	17.1734	96.5501	1.5084	8.0393	
5000.0000	16.8524	62.2361	2.5346	9.4005	
6000.0000	16.8235	43.2066	3.5564	10.7704	
7000.0000	17.1176	31.6245	4.5734	12.1523	
8000.0000	16.9226	24.0447	5.5908	13.5247	
9000.0000	17.0983	18.8346	6.6037	14.9107	
10000.0000	16.8340	15.0932	7.6150	16.2986	
11000.0000	16.9551	12.3443	8.6289	17.6716	
12000.0000	17.0559	10.2545	9.6381	19.0613	
13000.0000	17.1411	8.6349	10.6465	20.4520	
14000.0000	17.2142	7.3604	11.6540	21.8435	
15000.0000	16.8835	6.3489	12.6661	23.2135	
16000.0000	16.9404	5.5365	13.6729	24.6052	
17000.0000	16.9906	4.8765	14.6793	25.9973	
18000.0000	17.0352	4.3354	15.6852	27.3899	
19000.0000	17.0750	3.8877	16.6909	28.7829	
20000.0000	17.1109	3.5137	17.6962	30.1762	
21000.0000	17.1433	3.1979	18.7013	31.5698	
22000.0000	17.1728	2.9284	19.7061	32.9637	
23000.0000	17.1997	2.6960	20.7108	34.3578	
24000.0000	17.2244	2.4935	21.7153	35.7521	
25000.0000	16.8630	2.3157	22.7196	37.1465	
26000.0000	16.8845	2.1583	23.7325	38.5034	
27000.0000	16.9045	2.0175	24.7369	39.8968	
28000.0000	16.9230	1.8906	25.7413	41.2904	
29000.0000	16.9402	1.7754	26.7455	42.6840	
30000.0000	16.9562	1.6705	27.7497	44.0778	

	RANGE	BEARING
395.537 IS THE MAXIMUM PEAK CONCENTRATION	1000.0	16.8

----- MAXIMUM CENTERLINE CALCULATIONS -----

** DECAY COEFFICIENT (1/SEC) = 0.00000E+00 **

CONCENTRATION OF AL2O3(A) AT A HEIGHT OF 0.0
DOWNWIND FROM A CASTOR1200 CONFLAGRATION LAUNCH
CALCULATIONS APPLY TO THE LAYER BETWEEN 0.0 AND 3016.6 METERS

RANGE FROM PAD (METERS)	BEARING FROM PAD (DEGREES)	PEAK CONCEN- TRATION (MILLI G/ M**3)	CLOUD ARRIVAL TIME (MIN)	CLOUD DEPARTURE TIME (MIN)	
1000.0000	**16.7844**	**27.6024**	**0.0000**	**3.9721**	**←Peak Concentration**
2000.0000	17.1377	24.2141	0.0000	5.3218	
3000.0000	16.7326	11.7045	0.4792	6.6781	
4000.0000	17.1734	6.7377	1.5084	8.0393	
5000.0000	16.8524	4.3431	2.5346	9.4005	
6000.0000	16.8235	3.0152	3.5564	10.7704	
7000.0000	17.1176	2.2069	4.5734	12.1523	
8000.0000	16.9226	1.6780	5.5908	13.5247	
9000.0000	17.0983	1.3144	6.6037	14.9107	
10000.0000	16.8340	1.0533	7.6150	16.2986	
11000.0000	16.9551	0.8614	8.6289	17.6716	
12000.0000	17.0559	0.7156	9.6381	19.0613	
13000.0000	17.1411	0.6026	10.6465	20.4520	
14000.0000	17.2142	0.5136	11.6540	21.8435	
15000.0000	16.8835	0.4431	12.6661	23.2135	
16000.0000	16.9404	0.3864	13.6729	24.6052	
17000.0000	16.9906	0.3403	14.6793	25.9973	
18000.0000	17.0352	0.3025	15.6852	27.3899	
19000.0000	17.0750	0.2713	16.6909	28.7829	
20000.0000	17.1109	0.2452	17.6962	30.1762	
21000.0000	17.1433	0.2232	18.7013	31.5698	
22000.0000	17.1728	0.2044	19.7061	32.9637	
23000.0000	17.1997	0.1881	20.7108	34.3578	
24000.0000	17.2244	0.1740	21.7153	35.7521	
25000.0000	16.8630	0.1616	22.7196	37.1465	
26000.0000	16.8845	0.1506	23.7325	38.5034	
27000.0000	16.9045	0.1408	24.7369	39.8968	
28000.0000	16.9230	0.1319	25.7413	41.2904	
29000.0000	16.9402	0.1239	26.7455	42.6840	
30000.0000	16.9562	0.1166	27.7497	44.0778	

	RANGE	BEARING
27.602 IS THE MAXIMUM PEAK CONCENTRATION	1000.0	16.8

A. Case 4 - Castor 1200 Long 1-ppm HCl Isopleth for Conflagration Abort at T+8 Seconds

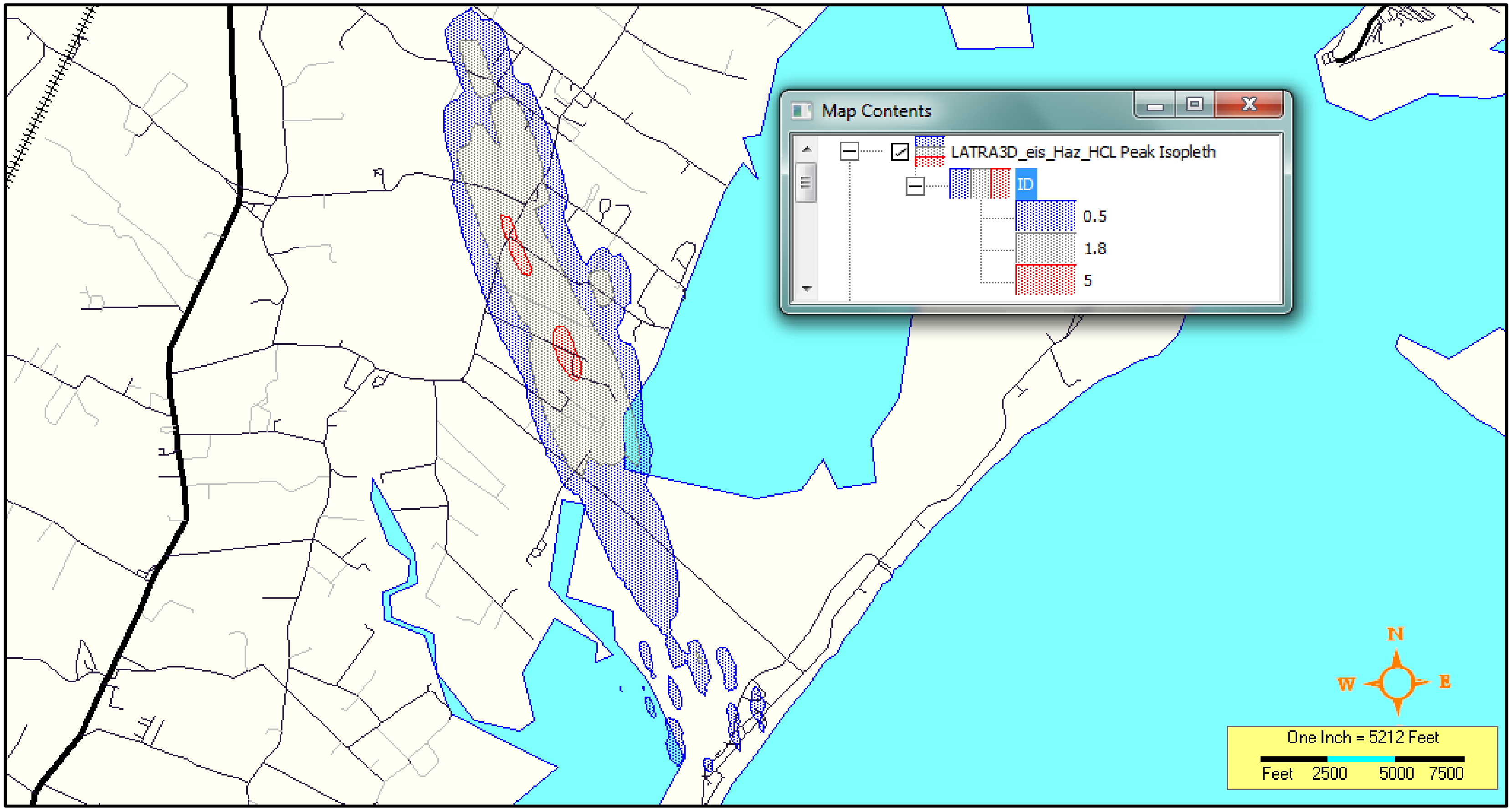

Figure A - 4. HCl Concentration Contours for a Castor 1200 Conflagration Failure at T+8 Seconds for the Case Yielding a Long 1-ppm HCl Hazard Zone from Wallops Flight Facility.

Case 4 Discussion – Conflagration Abort Mode HCl

This example plots the 0.5 1.8 (AEGL-1) and 5 ppm ground level HCl isopleths for the meteorological case that generated the longest downwind distance HCl 1 ppm isopleth that extended 8930 meters downwind. The peak HCl concentration level predicted for this case was 6.1 ppm at a range of 5013 meters and a bearing of 337 degrees. The maximum HCl peak concentration over all 6430 meteorological cases evaluated for a T+8 second failure time was 120 ppm but the peak concentration occurred much closer to the source. The analysis code used here was LATRA3D.

The surface concentrations of HCl from a conflagration event result from emissions from a combination of the normal launch emissions to the failure time (e.g. 8 seconds), emissions from the falling solid propellant fragments, and emissions from the solid propellant fragments burning on the ground. The failure at 8 seconds into flight destroys the Castor 1200 generating an estimated 1221 fragments (including the 3 upper stages) with a propellant weight of just over 1.2 million pounds. Explosion induced velocities range from 10 to 243 feet/second. The debris impact area is approximately circular with an estimated radius of 265 meters centered approximately 55 meters downrange of the launch pad. The estimated burn time of the residual propellant burning on the ground is 275 seconds.

The maximum predicted ground level concentration is 6.1 ppm of HCl, occurring at 5013 meters downwind. LATRA3D HCl concentration versus distance predictions for this case are presented in Table A-4. Note that the predicted cloud passage time is about 29 minutes.

Table A - 4. LATRA3D Predicted HCl Concentration Versus Distance for a Case with a Long 1-ppm Concentration Isopleth Given a T+8 Second Castor 1200 Conflagration Failure.

```
EXPOSURE GRID DEFINITION:
   UTM ZONE:      17.0
   UTM COORDS OF MIN X,Y (M):  980825.4 4210017.5
   SPACING BETWEEN NODES (M):      80.0      80.0
   NUMBER OF X,Y GRID NODES:        122        28
   X AXIS ORIENTATION WRT EAST (DEG):    -68.5
   EXPOSURE CALCULATION HEIGHT (M):        0.0
   TWA CONC AVERAGING PERIOD (SEC):     3600.0
   UTM COORDS OF PAD X,Y (M):  985200.3 4201711.5

 NUMBER OF SPECIES INCLUDED IN EXPOSURE CALCS:  1
 ORDER OF SPECIES:    HCL
```

MAXIMUM CROSSWIND CONCENTRATION LOCATIONS

ALONG WIND NODE	RANGE	BEAR	CONC	PUFF TIME (MIN) ARR	DEP
119	366.	217.	4.08E-01	3	5
118	332.	229.	1.39E-01	3	5
117	30.	146.	3.92E-01	6	7
116	239.	261.	7.71E-01	7	7
115	212.	30.	7.28E-01	4	6
114	269.	17.	8.96E-01	4	6
113	335.	8.	1.36E+00	4	7
112	666.	282.	1.39E+00	4	7
111	663.	26.	1.24E+00	5	7
110	720.	21.	1.33E+00	7	8
109	773.	301.	1.30E+00	3	9
108	837.	304.	8.82E-01	3	9
107	774.	333.	6.95E-01	8	14
106	911.	360.	1.20E+00	4	15
105	982.	320.	1.25E+00	9	12
104	1011.	339.	1.10E+00	8	17
103	1094.	343.	1.28E+00	3	19
102	1174.	343.	1.70E+00	4	20
101	1254.	343.	2.36E+00	4	21
100	1334.	342.	1.71E+00	5	22
99	1419.	332.	1.40E+00	5	21
98	1499.	333.	9.94E-01	5	22
97	1641.	322.	7.38E-01	8	16
96	1659.	344.	7.14E-01	10	26
95	1739.	344.	7.46E-01	11	27
94	1828.	346.	7.85E-01	11	28
93	1907.	346.	8.21E-01	12	29
92	1986.	346.	8.61E-01	12	29
91	2066.	345.	8.98E-01	13	29
90	2145.	345.	9.32E-01	13	29
89	2225.	345.	9.61E-01	14	29
88	2292.	337.	1.04E+00	14	29
87	2372.	337.	1.11E+00	14	29
86	2452.	337.	1.21E+00	14	30
85	2532.	337.	1.30E+00	15	31
84	2612.	337.	1.37E+00	15	32
83	2692.	337.	1.43E+00	16	33
82	2772.	337.	1.49E+00	16	34
81	2852.	337.	1.56E+00	17	35
80	2932.	337.	1.64E+00	17	36
79	3012.	337.	1.63E+00	18	36
78	3092.	337.	1.73E+00	18	37
77	3175.	336.	1.78E+00	19	38
76	3254.	336.	1.59E+00	19	38
75	3334.	336.	1.65E+00	20	39
74	3414.	336.	1.68E+00	20	40

73	3495.	341.	1.85E+00	22	45	
72	3575.	341.	2.33E+00	23	46	
71	3655.	341.	2.70E+00	23	47	
70	3735.	341.	2.83E+00	24	48	
69	3811.	339.	3.22E+00	24	49	
68	3891.	339.	3.55E+00	24	50	
67	3972.	337.	3.98E+00	24	47	
66	4051.	338.	4.09E+00	25	48	
65	4131.	338.	4.30E+00	25	48	
64	4211.	338.	4.69E+00	25	49	
63	4291.	338.	4.70E+00	26	51	
62	4371.	338.	4.83E+00	26	52	
61	4451.	338.	4.77E+00	27	54	
60	4531.	338.	4.78E+00	27	55	
59	4611.	338.	4.82E+00	28	55	
58	4693.	337.	4.95E+00	28	56	
57	4773.	337.	5.44E+00	29	57	
56	4853.	337.	5.77E+00	29	58	
55	4933.	337.	6.04E+00	30	58	
54	**5013.**	**337.**	**6.14E+00**	**30**	**59**	**← Peak Concentration Point**
53	5093.	337.	6.02E+00	31	60	
52	5173.	337.	5.76E+00	31	60	
51	5253.	337.	5.62E+00	32	61	
50	5333.	337.	5.11E+00	33	62	
49	5413.	337.	4.73E+00	33	62	
48	5493.	337.	4.46E+00	34	63	
47	5573.	337.	4.23E+00	39	64	
46	5653.	337.	3.82E+00	40	64	
45	5736.	336.	3.93E+00	40	64	
44	5816.	336.	4.23E+00	40	64	
43	5895.	336.	4.47E+00	40	64	
42	5975.	336.	4.80E+00	40	64	
41	6055.	336.	5.17E+00	41	65	
40	6135.	336.	5.28E+00	41	66	
39	6215.	336.	5.27E+00	42	66	
38	6299.	336.	5.19E+00	42	67	
37	6379.	336.	5.30E+00	42	67	
36	6458.	336.	5.13E+00	43	68	
35	6538.	336.	5.23E+00	43	68	
34	6618.	336.	5.23E+00	44	71	
33	6698.	336.	5.11E+00	44	72	
32	6778.	336.	5.00E+00	45	72	
31	6858.	336.	4.79E+00	45	73	
30	6938.	336.	4.55E+00	46	74	
29	7018.	336.	4.19E+00	46	75	
28	7098.	336.	3.93E+00	47	75	
27	7178.	336.	3.64E+00	48	76	
26	7251.	339.	3.23E+00	55	87	
25	7331.	339.	3.33E+00	56	88	
24	7411.	339.	3.37E+00	57	89	
23	7491.	339.	3.38E+00	58	89	
22	7573.	340.	3.42E+00	60	90	
21	7653.	340.	3.63E+00	61	90	

20	7733.	340.	3.41E+00	65	90
19	7811.	339.	3.24E+00	65	90
18	7891.	339.	2.89E+00	66	90
17	7971.	339.	2.36E+00	66	90
16	8055.	340.	1.29E+00	69	90
15	8131.	339.	2.25E+00	68	92
14	8211.	339.	2.69E+00	69	92
13	8291.	339.	2.82E+00	69	93
12	8371.	339.	2.67E+00	71	93
11	8451.	339.	2.62E+00	71	94
10	8531.	338.	2.57E+00	72	94
9	8611.	338.	2.53E+00	72	95
8	8691.	338.	2.36E+00	74	95
7	8771.	338.	1.85E+00	74	95
6	8851.	338.	1.61E+00	74	95
5	8931.	338.	9.85E-01	74	95
4	9012.	340.	7.04E-01	85	89
3	9092.	340.	5.14E-01	85	89
2	9171.	339.	2.78E-01	86	89
1	9259.	336.	1.03E-01	75	78
0	9339.	336.	9.97E-02	76	78

MAXIMUM HCL   CONC 6.14E+00 AT RANGE 5013. M, BEARING 337. DEG
PUFF ARRIVAL AT   30, DEPARTURE AT   59 MIN

A. Case 5 - Castor 1200 Worst Case Payload Deflagration Abort Mode NO_2 and MMH Isopleths

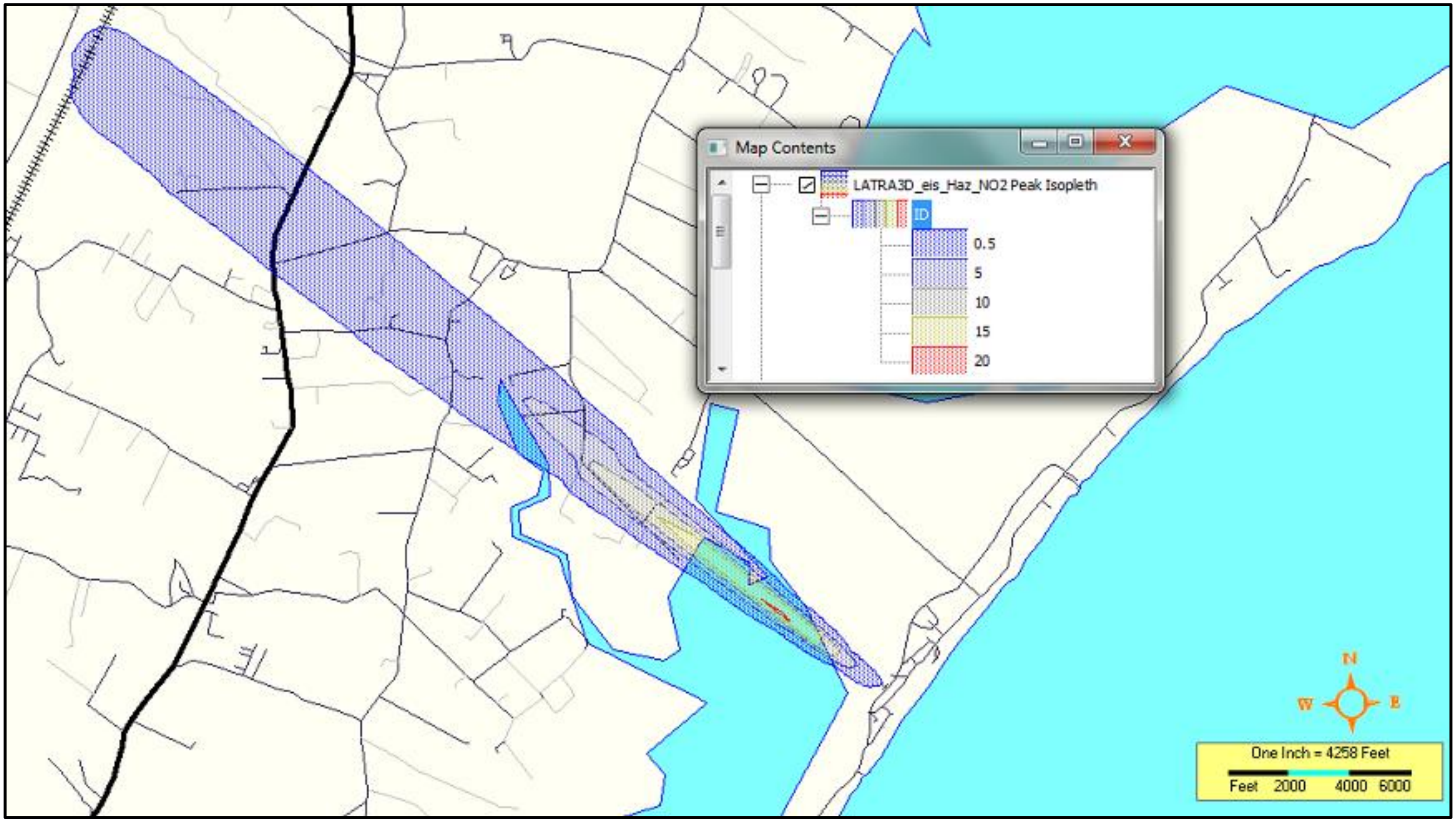

Figure A - 5. NO_2 Concentration Contours for a Castor 1200 Payload Deflagration Failure for a Case Yielding a Long 0.5-ppm NO_2 Hazard Zone from Wallops Flight Facility.

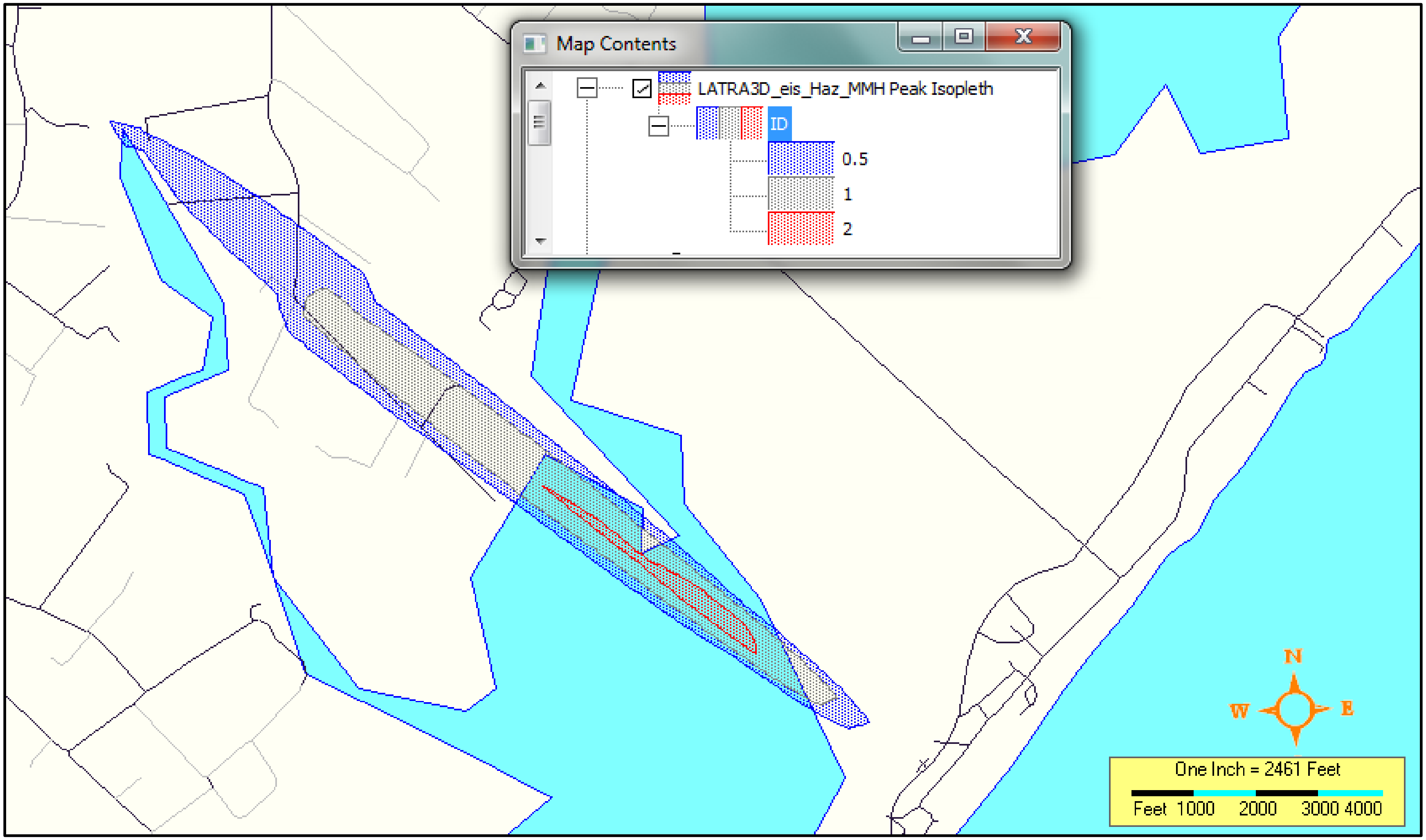

Figure A - 6. MMH Concentration Contours for a Castor 1200 Payload Deflagration Failure for a Case Yielding a Long 0.5-ppm MMH Hazard Zone from Wallops Flight Facility.

Case 5 Discussion – Payload Deflagration Abort Mode Producing NO_2 and MMH.

This example plots the 0.5 5, 10 15 and 20 ppm ground level NO_2 isopleths for the meteorological case that generated the longest downwind distance NO_2 0.5 ppm isopleth that extended 10700 meters downwind. The peak NO_2 concentration level predicted for this case was 20.5 ppm at a range of 1547 meters and a bearing of 305 degrees. The maximum NO_2 peak concentration over all 6430 meteorological cases evaluated for the payload deflagration failure mode was 41.9 ppm. The case presented here represents approximately a 99th percentile case with regard to peak NO_2 concentration. The analysis code used here was LATRA3D. The deflagration cloud is assumed to form when an intact payload ejected for a breakup of the launch vehicle impacts the ground rupturing the Hygergol tanks resulting in propellant mixing and a propellant fireball.

The same event deflagration event produces residual unreacted vapor phase MMH that is assumed to travel downwind in conjunction with the NO_2 cloud. The peak MMH concentration for this case is predicted to be 2.25 ppm located at the same point of maximum concentration as the NO_2 cloud (1547 meters downwind on a bearing of 305 degrees).

LATRA3D NO_2 and MMH concentrations versus distance predictions for this case are presented in Table A-5. Note that the predicted cloud passage time is short, only about 3 minutes, due to the small size of the deflagration cloud.

Table A - 5. LATRA3D Predicted NO_2 and MMH Concentrations Versus Distance for a Case with a Long 0.5-ppm NO_2 Concentration Isopleth Given a Payload Deflagration Failure.

```
EXPOSURE GRID DEFINITION:
   UTM ZONE:       17.0
   UTM COORDS OF MIN X,Y (M):   975876.4 4207721.0
   SPACING BETWEEN NODES (M):       80.0      80.0
   NUMBER OF X,Y GRID NODES:         139        21
   X AXIS ORIENTATION WRT EAST (DEG):     -36.8
   EXPOSURE CALCULATION HEIGHT (M):         0.0
   TWA CONC AVERAGING PERIOD (SEC):        90.0
   UTM COORDS OF PAD X,Y (M):   985200.3 4201711.5

 NUMBER OF SPECIES INCLUDED IN EXPOSURE CALCS:  2
 ORDER OF SPECIES:    MMH       NO2
```

MAXIMUM CROSSWIND CONCENTRATION LOCATIONS

ALONG WIND NODE	RANGE	BEAR	CONC	PUFF TIME (MIN) ARR	DEP	RANGE	BEAR	CONC	ARR	DEP	
137	110.	323.	9.49E-03	1	1	110.	323.	8.65E-02	1	1	
136	189.	316.	2.71E-02	1	2	189.	316.	2.47E-01	1	2	
135	268.	313.	7.25E-02	1	2	268.	313.	6.61E-01	1	2	
134	347.	312.	1.55E-01	2	3	347.	312.	1.41E+00	2	3	
133	427.	311.	2.79E-01	2	4	427.	311.	2.54E+00	2	4	
132	507.	310.	4.43E-01	2	4	507.	310.	4.03E+00	2	4	
131	587.	310.	6.36E-01	3	5	587.	310.	5.80E+00	3	5	
130	667.	309.	8.47E-01	3	5	667.	309.	7.72E+00	3	5	
129	747.	309.	1.06E+00	4	6	747.	309.	9.67E+00	4	6	
128	827.	309.	1.27E+00	4	6	827.	309.	1.16E+01	4	6	
127	907.	309.	1.46E+00	4	7	907.	309.	1.33E+01	4	7	
126	987.	309.	1.62E+00	5	7	987.	309.	1.48E+01	5	7	
125	1067.	304.	1.81E+00	5	8	1067.	304.	1.65E+01	5	8	
124	1147.	304.	1.96E+00	6	9	1147.	304.	1.79E+01	6	9	
123	1227.	304.	2.08E+00	6	9	1227.	304.	1.89E+01	6	9	
122	1307.	305.	2.17E+00	7	10	1307.	305.	1.97E+01	7	10	
121	1387.	305.	2.22E+00	7	10	1387.	305.	2.02E+01	7	10	
120	1467.	305.	2.25E+00	7	11	1467.	305.	2.05E+01	7	11	
119	**1547.**	**305.**	**2.25E+00**	**8**	**11**	**1547.**	**305.**	**2.05E+01**	**8**	**11**	**←Peak Conc.**
118	1627.	305.	2.24E+00	8	12	1627.	305.	2.04E+01	8	12	
117	1707.	305.	2.21E+00	9	12	1707.	305.	2.01E+01	9	12	
116	1787.	305.	2.17E+00	9	13	1787.	305.	1.98E+01	9	13	
115	1867.	305.	2.12E+00	10	13	1867.	305.	1.93E+01	10	13	
114	1947.	305.	2.11E+00	10	14	1947.	305.	1.92E+01	10	14	
113	2027.	305.	2.13E+00	10	15	2027.	305.	1.93E+01	10	15	
112	2107.	305.	2.13E+00	11	15	2107.	305.	1.94E+01	11	15	

111	2187.	305.	2.12E+00	11	16	2187.	305.	1.93E+01	11	16
110	2267.	306.	2.10E+00	12	16	2267.	306.	1.91E+01	12	16
109	2347.	306.	2.08E+00	12	17	2347.	306.	1.89E+01	12	17
108	2427.	306.	2.04E+00	13	17	2427.	306.	1.86E+01	13	17
107	2507.	306.	2.00E+00	13	18	2507.	306.	1.82E+01	13	18
106	2587.	306.	1.96E+00	13	18	2587.	306.	1.78E+01	13	18
105	2667.	306.	1.91E+00	14	19	2667.	306.	1.74E+01	14	19
104	2747.	306.	1.86E+00	14	19	2747.	306.	1.69E+01	14	19
103	2827.	306.	1.81E+00	15	20	2827.	306.	1.65E+01	15	20
102	2907.	306.	1.76E+00	15	20	2907.	306.	1.60E+01	15	20
101	2987.	306.	1.71E+00	16	21	2987.	306.	1.55E+01	16	21
100	3067.	306.	1.66E+00	16	21	3067.	306.	1.51E+01	16	21
99	3147.	306.	1.61E+00	16	22	3147.	306.	1.46E+01	16	22
98	3227.	306.	1.56E+00	17	22	3227.	306.	1.42E+01	17	22
97	3307.	306.	1.51E+00	17	23	3307.	306.	1.37E+01	17	23
96	3387.	306.	1.46E+00	18	24	3387.	306.	1.33E+01	18	24
95	3467.	306.	1.42E+00	18	25	3467.	306.	1.29E+01	18	25
94	3547.	306.	1.37E+00	19	25	3547.	306.	1.25E+01	19	25
93	3626.	306.	1.33E+00	19	26	3626.	306.	1.21E+01	19	26
92	3706.	306.	1.29E+00	20	26	3706.	306.	1.17E+01	20	26
91	3786.	306.	1.25E+00	20	27	3786.	306.	1.13E+01	20	27
90	3866.	306.	1.22E+00	20	27	3866.	306.	1.10E+01	20	27
89	3946.	306.	1.19E+00	21	28	3946.	306.	1.08E+01	21	28
88	4026.	307.	8.95E-01	21	29	4026.	307.	8.11E+00	21	29
87	4106.	307.	8.53E-01	22	29	4106.	307.	7.74E+00	22	29
86	4186.	307.	8.14E-01	22	30	4186.	307.	7.38E+00	22	30
85	4266.	307.	7.77E-01	23	30	4266.	307.	7.04E+00	23	30
84	4346.	307.	7.44E-01	23	31	4346.	307.	6.75E+00	23	31
83	4426.	307.	7.12E-01	24	31	4426.	307.	6.45E+00	24	31
82	4506.	307.	6.81E-01	24	32	4506.	307.	6.17E+00	24	32
81	4586.	307.	6.52E-01	24	32	4586.	307.	5.91E+00	24	32
80	4666.	307.	6.25E-01	25	33	4666.	307.	5.66E+00	25	33
79	4746.	307.	5.99E-01	25	33	4746.	307.	5.43E+00	25	33
78	4826.	307.	5.75E-01	25	34	4826.	307.	5.21E+00	25	34
77	4906.	307.	5.52E-01	26	35	4906.	307.	5.00E+00	26	35
76	4986.	307.	5.30E-01	26	35	4986.	307.	4.80E+00	26	35
75	5066.	307.	5.08E-01	27	36	5066.	307.	4.60E+00	27	36
74	5146.	307.	5.26E-01	27	36	5146.	307.	4.76E+00	27	36
73	5226.	307.	5.11E-01	28	37	5226.	307.	4.63E+00	28	37
72	5306.	307.	4.96E-01	28	37	5306.	307.	4.49E+00	28	37
71	5386.	307.	4.82E-01	28	38	5386.	307.	4.36E+00	28	38
70	5466.	307.	4.69E-01	29	38	5466.	307.	4.24E+00	29	38
69	5546.	307.	4.56E-01	29	39	5546.	307.	4.12E+00	29	39
68	5626.	307.	4.43E-01	30	39	5626.	307.	4.01E+00	30	39
67	5706.	307.	4.31E-01	30	40	5706.	307.	3.90E+00	30	40
66	5786.	307.	4.21E-01	31	40	5786.	307.	3.81E+00	31	40
65	5866.	307.	4.13E-01	31	41	5866.	307.	3.73E+00	31	41
64	5946.	307.	4.04E-01	32	41	5946.	307.	3.66E+00	32	41
63	6026.	307.	3.96E-01	32	42	6026.	307.	3.58E+00	32	42
62	6106.	306.	3.90E-01	33	42	6106.	306.	3.53E+00	33	42
61	6186.	306.	3.85E-01	33	43	6186.	306.	3.48E+00	33	43
60	6266.	306.	3.79E-01	33	43	6266.	306.	3.43E+00	33	43
59	6346.	307.	3.79E-01	34	44	6346.	307.	3.43E+00	34	44

58	6426.	307.	3.86E-01	34	44	6426.	307.	3.49E+00	34	44
57	6506.	307.	3.78E-01	35	45	6506.	307.	3.42E+00	35	45
56	6586.	307.	3.70E-01	35	45	6586.	307.	3.35E+00	35	45
55	6666.	307.	3.63E-01	36	46	6666.	307.	3.28E+00	36	46
54	6746.	306.	3.56E-01	36	46	6746.	306.	3.21E+00	36	46
53	6826.	306.	3.49E-01	37	47	6826.	306.	3.15E+00	37	47
52	6906.	306.	3.42E-01	37	47	6906.	306.	3.09E+00	37	47
51	6986.	306.	3.37E-01	37	48	6986.	306.	3.05E+00	37	48
50	7066.	306.	3.31E-01	38	48	7066.	306.	2.99E+00	38	48
49	7146.	306.	3.25E-01	39	49	7146.	306.	2.93E+00	39	49
48	7226.	306.	3.18E-01	39	49	7226.	306.	2.88E+00	39	49
47	7306.	306.	3.12E-01	40	50	7306.	306.	2.82E+00	40	50
46	7386.	306.	3.06E-01	40	50	7386.	306.	2.77E+00	40	50
45	7466.	306.	3.00E-01	40	51	7466.	306.	2.71E+00	40	51
44	7546.	306.	2.94E-01	41	51	7546.	306.	2.66E+00	41	51
43	7626.	307.	2.91E-01	41	52	7626.	307.	2.62E+00	41	52
42	7706.	306.	2.88E-01	42	52	7706.	306.	2.60E+00	42	52
41	7786.	306.	2.83E-01	42	53	7786.	306.	2.55E+00	42	53
40	7866.	306.	2.78E-01	42	53	7866.	306.	2.50E+00	42	53
39	7946.	306.	2.72E-01	43	54	7946.	306.	2.46E+00	43	54
38	8026.	306.	2.67E-01	43	54	8026.	306.	2.41E+00	43	54
37	8106.	306.	2.62E-01	44	55	8106.	306.	2.36E+00	44	55
36	8186.	306.	2.57E-01	44	55	8186.	306.	2.32E+00	44	55
35	8266.	307.	2.52E-01	45	56	8266.	307.	2.27E+00	45	56
34	8346.	307.	2.47E-01	45	56	8346.	307.	2.23E+00	45	56
33	8426.	307.	2.44E-01	46	57	8426.	307.	2.20E+00	46	57
32	8506.	306.	2.43E-01	46	57	8506.	306.	2.19E+00	46	57
31	8586.	306.	2.39E-01	47	58	8586.	306.	2.15E+00	47	58
30	8666.	306.	2.35E-01	47	58	8666.	306.	2.12E+00	47	58
29	8746.	306.	2.31E-01	48	59	8746.	306.	2.08E+00	48	59
28	8826.	306.	2.27E-01	48	59	8826.	306.	2.05E+00	48	59
27	8906.	306.	2.25E-01	49	60	8906.	306.	2.03E+00	49	60
26	8986.	307.	2.20E-01	49	60	8986.	307.	1.98E+00	49	60
25	9066.	307.	2.17E-01	50	61	9066.	307.	1.95E+00	50	61
24	9146.	306.	2.14E-01	50	61	9146.	306.	1.93E+00	50	61
23	9226.	306.	2.12E-01	51	61	9226.	306.	1.91E+00	51	61
22	9306.	306.	2.09E-01	51	62	9306.	306.	1.88E+00	51	62
21	9386.	306.	2.05E-01	51	62	9386.	306.	1.84E+00	51	62
20	9466.	306.	2.01E-01	52	63	9466.	306.	1.81E+00	52	63
19	9546.	306.	1.97E-01	52	63	9546.	306.	1.77E+00	52	63
18	9626.	306.	1.93E-01	53	64	9626.	306.	1.74E+00	53	64
17	9706.	306.	1.93E-01	53	64	9706.	306.	1.74E+00	53	64
16	9786.	306.	1.96E-01	54	65	9786.	306.	1.76E+00	54	65
15	9866.	306.	1.98E-01	54	65	9866.	306.	1.78E+00	54	65
14	9946.	306.	1.93E-01	55	65	9946.	306.	1.73E+00	55	65
13	10026.	306.	1.86E-01	55	66	10026.	306.	1.67E+00	55	66
12	10106.	307.	1.74E-01	56	66	10106.	307.	1.57E+00	56	66
11	10186.	307.	1.64E-01	56	67	10186.	307.	1.48E+00	56	67
10	10266.	307.	1.47E-01	57	67	10266.	307.	1.32E+00	57	67
9	10346.	307.	1.22E-01	57	67	10346.	307.	1.10E+00	57	67
8	10426.	307.	1.10E-01	58	67	10426.	307.	9.89E-01	58	67
7	10507.	307.	9.84E-02	59	67	10507.	307.	8.85E-01	59	67
6	10587.	307.	8.52E-02	59	67	10587.	307.	7.66E-01	59	67

5	10667.	307.	6.43E-02	60	67	10667.	307.	5.78E-01	60	67
4	10748.	308.	4.80E-02	60	67	10748.	308.	4.32E-01	60	67
3	10828.	308.	3.25E-02	61	67	10828.	308.	2.92E-01	61	67
2	10908.	308.	1.85E-02	62	67	10908.	308.	1.66E-01	62	67
1	10989.	308.	1.28E-02	65	67	10989.	308.	1.15E-01	65	67

MAXIMUM MMH CONC 2.25E+00 AT RANGE 1547. M, BEARING 305. DEG
PUFF ARRIVAL AT 8, DEPARTURE AT 11 MIN

MAXIMUM NO2 CONC 2.05E+01 AT RANGE 1547. M, BEARING 305. DEG
PUFF ARRIVAL AT 8, DEPARTURE AT 11 MIN

A. Case 6 - Castor 1200 Worst Case Payload Deflagration Abort Mode NO_2 and MMH Isopleths

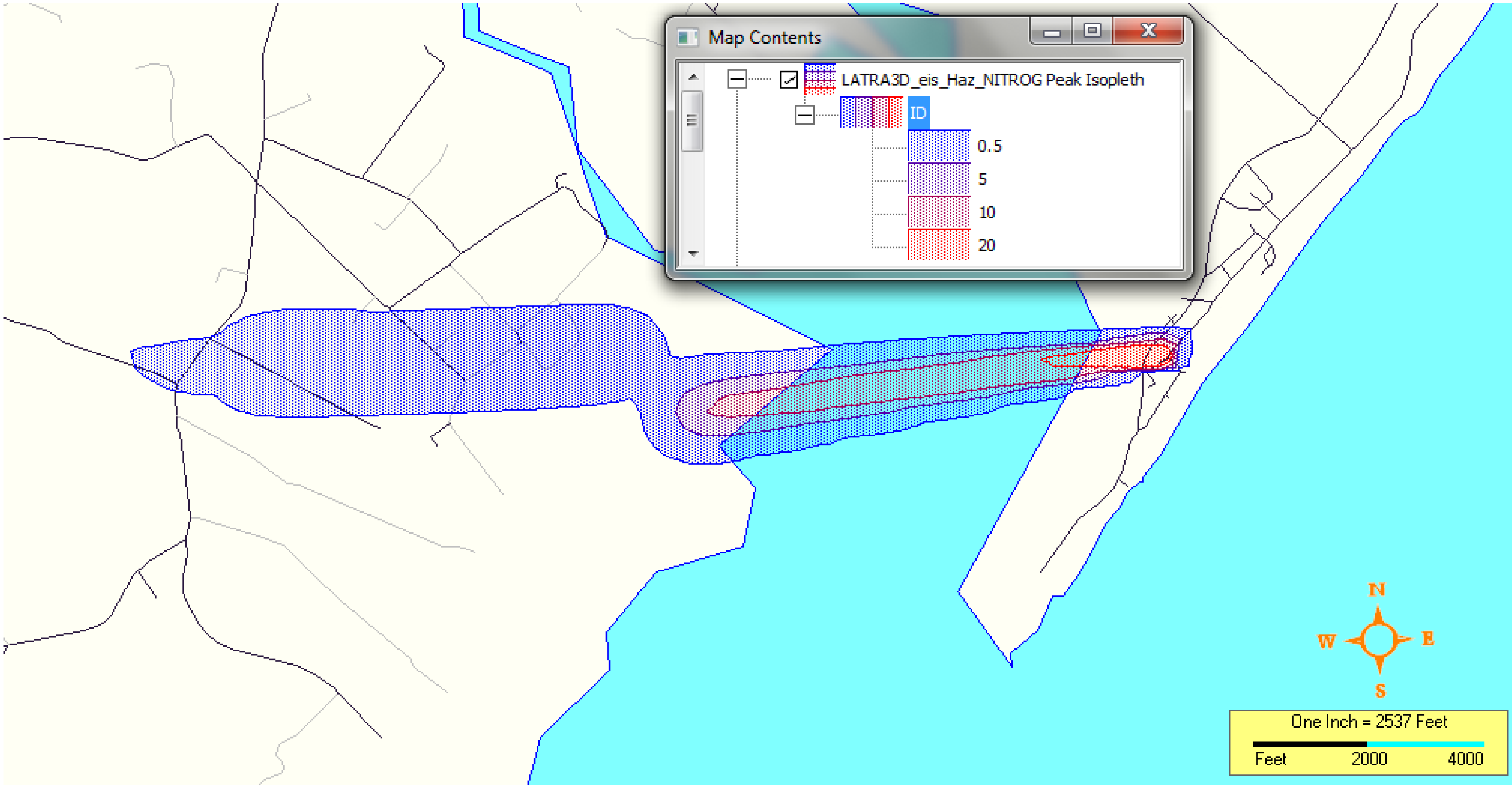

Figure A - 7. NO_2 Concentration Contours for a Castor 1200 Payload Pool Evaporation Scenario for a Case Yielding a Long 0.5-ppm NO_2 Hazard Zone from Wallops Flight Facility.

Case 6 Discussion – Payload Pool Evaporation Mode Producing NO_2.

This example plots the 0.5 5, 10 and 20 ppm ground level NO_2 isopleths for the meteorological case that generated the longest downwind distance NO_2 5 ppm isopleth that extended 2800 meters downwind. The peak NO_2 concentration level predicted for this case was 62.7 ppm at a range of 257 meters and a bearing of 255 degrees. The maximum NO_2 peak concentration near the evaporating pool should be much higher (in the hundreds of ppm range). In this run LATRA3D was set up with an 80 meter by 80 meter concentration grid spacing input. The original source puffs formed at the evaporating pool are small; on the order of 5 meters diameter. The 80 meter grid spacing is too coarse to accurately capture the high concentrations in the source puffs. At 10 meter by 10 meter grid would have been better for the pool evaporation scenario, but this highly resolved grid would have created thousands of grid point calculations far downwind where the puffs have grown large and would have negatively impacted the computer run time to process all 6430 cases. The analysis code used here was LATRA3D. The evaporating pool is assumed to form when an intact payload ejected for a breakup of the launch vehicle impacts the ground rupturing the hygergol tanks causing them to spill their contents but without generating a fire or explosion.

The same event payload impact event produces an evaporating pool of MMH that is assumed to travel downwind in conjunction with the NO_2 plume, at least initially. The downwind distance of the MMH corridor is approximately 1/10th as long as the NO_2 corridor due to the slow evaporation rate of MMH compared to N_2O_4.

LATRA3D NO_2 concentration versus distance predictions for this case are presented in Table A-6. Note that the predicted cloud passage time on the order of 45 minutes, due primarily to the time required to evaporate the entire pool.

Table A - 6. LATRA3D Predicted NO_2 Concentration Versus Distance for a Case with the Longest 5-ppm NO_2 Concentration Isopleth Given a Payload Pool Evaporation Scenario.

```
EXPOSURE GRID DEFINITION:
   UTM ZONE:      17.0
   UTM COORDS OF MIN X,Y (M):  979462.5 4200892.0
   SPACING BETWEEN NODES (M):      80.0      80.0
   NUMBER OF X,Y GRID NODES:         74        12
   X AXIS ORIENTATION WRT EAST (DEG):      2.9
   EXPOSURE CALCULATION HEIGHT (M):        0.0
   TWA CONC AVERAGING PERIOD (SEC):       90.0
   UTM COORDS OF PAD X,Y (M):  985200.3 4201711.5

 NUMBER OF SPECIES INCLUDED IN EXPOSURE CALCS:  1
 ORDER OF SPECIES:    NITROG
```

MAXIMUM CROSSWIND CONCENTRATION LOCATIONS

ALONG WIND NODE	RANGE	BEAR	CONC	PUFF TIME (MIN) ARR	DEP
71	96.	284.	6.05E+00	1	45
70	179.	250.	4.25E+01	2	47
69	257.	255.	6.27E+01	3	49
68	336.	258.	5.83E+01	4	50
67	415.	260.	4.89E+01	5	52
66	494.	261.	4.02E+01	6	53
65	574.	262.	3.33E+01	7	55
64	654.	263.	2.79E+01	8	56
63	733.	263.	2.37E+01	10	58
62	813.	263.	2.04E+01	11	59
61	901.	259.	1.91E+01	12	61
60	980.	259.	1.96E+01	13	63
59	1060.	260.	1.96E+01	14	64
58	1139.	260.	1.93E+01	16	65
57	1219.	261.	1.86E+01	17	67
56	1298.	261.	1.78E+01	18	68
55	1378.	262.	1.68E+01	19	70
54	1458.	262.	1.58E+01	20	71
53	1537.	262.	1.48E+01	22	73
52	1625.	260.	1.40E+01	23	74
51	1705.	260.	1.43E+01	24	76
50	1784.	260.	1.43E+01	25	77
49	1864.	261.	1.42E+01	27	79
48	1943.	261.	1.40E+01	28	80
47	2023.	261.	1.36E+01	29	81
46	2102.	261.	1.32E+01	30	83
45	2182.	262.	1.27E+01	32	84
44	2262.	262.	1.21E+01	33	86
43	2341.	262.	1.16E+01	34	87
42	2429.	260.	1.15E+01	35	89
41	2509.	260.	1.14E+01	37	89
40	2588.	261.	1.10E+01	38	89
39	2668.	261.	9.75E+00	39	89
38	2747.	261.	7.45E+00	40	89
37	2827.	261.	4.54E+00	42	89
36	2906.	261.	2.06E+00	43	89
35	2972.	268.	1.99E+00	47	94
34	3052.	268.	3.26E+00	47	95
33	3132.	268.	4.23E+00	47	97
32	3212.	268.	4.67E+00	47	98
31	3292.	268.	4.76E+00	47	99
30	3372.	268.	4.68E+00	47	101
29	3452.	268.	4.58E+00	48	102
28	3532.	268.	4.48E+00	50	103
27	3612.	268.	4.37E+00	51	104

26	3692.	268.	4.27E+00	52	106
25	3772.	268.	4.18E+00	53	107
24	3852.	268.	4.07E+00	54	108
23	3932.	268.	3.97E+00	56	110
22	4012.	268.	3.87E+00	57	111
21	4092.	268.	3.78E+00	58	112
20	4172.	268.	3.69E+00	59	114
19	4252.	266.	3.60E+00	61	115
18	4332.	266.	3.56E+00	62	116
17	4412.	266.	3.51E+00	63	118
16	4492.	267.	3.56E+00	64	119
15	4572.	267.	3.65E+00	65	120
14	4652.	267.	3.72E+00	67	121
13	4732.	267.	3.72E+00	68	122
12	4812.	267.	3.57E+00	69	122
11	4892.	267.	3.28E+00	70	124
10	4972.	267.	3.00E+00	71	125
9	5052.	267.	2.57E+00	73	126
8	5132.	267.	2.16E+00	74	127
7	5212.	267.	1.79E+00	75	128
6	5292.	267.	1.23E+00	79	129
5	5372.	267.	1.19E+00	79	130
4	5452.	267.	1.04E+00	80	131
3	5533.	268.	8.02E-01	81	131
2	5613.	268.	7.02E-01	82	132
1	5693.	268.	5.64E-01	83	132
0	5773.	268.	4.09E-01	84	132

MAXIMUM NITROG CONC 6.27E+01 AT RANGE 257. M, BEARING 255. DEG
PUFF ARRIVAL AT 3, DEPARTURE AT 49 MIN